

**UNIVERSIDADE FEDERAL DE SANTA CATARINA
CENTRO TECNOLÓGICO
PROGRAMA DE PÓS-GRADUAÇÃO EM ENGENHARIA DE
ALIMENTOS**

Nathália Buss da Silva

**Predictive Modelling for the Growth of *Bacillus cereus* in
Reconstituted Infant Formula and Culture Medium at Population
and Single Cell Levels**

Tese apresentada ao Programa de Pós-Graduação em Engenharia de Alimentos do Centro Tecnológico da Universidade Federal de Santa Catarina como requisito para obtenção do título de Doutor em Engenharia de Alimentos.

Orientador:

Prof. Dr. Bruno Augusto Mattar
Carciofi

Coorientadores:

Prof. Dr. József Baranyi

Dr^a. Mariem Ellouze

Florianópolis
2019

Ficha de identificação da obra elaborada pelo autor
através do Programa de Geração Automática da Biblioteca Universitária
da UFSC.

Buss da Silva, Nathália

Predictive Modelling for the Growth of *Bacillus cereus* in Reconstituted Infant Formula and Culture Medium at Population and Single Cell Levels / Nathália Buss da Silva ; orientador, Bruno Augusto Mattar Carciofi ; coorientador, József Baranyi, coorientadora, Mariem Ellouze. 2019.

257 p.

Tese (doutorado) – Universidade Federal de Santa Catarina, Centro Tecnológico, Programa de Pós-Graduação em Engenharia de Alimentos, Florianópolis, 2019.

Inclui referências.

1. Engenharia de alimentos. 2. Microbiologia preditiva. 3. *Bacillus cereus*. I. Carciofi, Bruno Augusto Mattar. II. Baranyi, József. III. Ellouze, Mariem. IV. Universidade Federal de Santa Catarina. Programa de Pós-Graduação em Engenharia de Alimentos. V. Título.

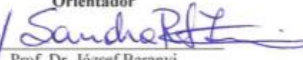
**“PREDICTIVE MODELLING FOR THE GROWTH OF
BACILLUS CEREUS IN RECONSTITUTED INFANT
FORMULA AND CULTURE MEDIUM AT POPULATION
AND SINGLE CELL LEVELS”**

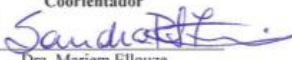
Por

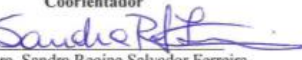
Nathália Buss da Silva

Tese julgada para obtenção do título de **Doutor em Engenharia Alimentos**, área de Concentração de **Desenvolvimento de Processos da Indústria de Alimentos**, e aprovada em sua forma final pelo Programa de Pós-graduação em Engenharia de Alimentos da Universidade Federal de Santa Catarina.


Prof. Bruno Augusto Mattar Carciofi
Orientador

p/ 
Prof. Dr. József Baranyi
Coorientador

p/ 
Dra. Mariem Ellouze
Coorientador



Profa. Dra. Sandra Regina Salvador Ferreira
Coordenadora

Banca Examinadora:


Prof. Dr. Bruno A M Carciofi


Profa. Dra. Bernadette D. G. M. Franco

p/ 
Prof. Dr. Daniel A. Longhi
(videoconferência)


Prof. Dr. André Wüst Zibetti

Florianópolis, 18 de março de 2019.

ABSTRACT

Bacillus cereus is a spore-forming and a toxin-producing bacteria; it is therefore an emerging concern for the food industry. The objective of this study was to investigate the growth of *B. cereus* and provide appropriate predictive models taking into account the medium, temperature, strains, and thermal stress. To do so, a quantitative methodology was developed to follow *B. cereus* development after a heat stress in two growth media (Reconstituted Infant Formulae (RIF) and culture medium (BHI)) at population and individual cell level by means of direct (viable counts) and indirect (turbidity) measurements. In viable counts experiments, growth rates were higher in BHI when compared to RIF, and a strain-dependent bias factor could be estimated. The heat stress caused a 2 log (CFU/mL) reduction on average, but did not significantly affect the subsequent growth of survival cells. As for cardinal values estimations, the growth boundaries of three *B. cereus* strains (B596, B594 and B626) from the Nestlé Pathogen Culture Collection were successfully determined in terms of temperature, pH, and a_w . These were compared to other two strains from emetic group, analysing intra-group and pair-wise differences. B594 strain differed more from the all the others strains in terms of their cardinal parameters and strains B596 and B626 are equal in all parameters. The predictions of *B. cereus* growth in RIF made with the cardinal parameter values determined by turbidity in culture medium were good, especially when using bias factor to estimate optimal growth rate in RIF. Confronted with literature data from different sources and from a variety of dairy products, the proposed general secondary model for emetic *B. cereus* showed reasonably good performance with more than 85% of the collected growth rates within the confidence boundaries. Additionally, no significant difference on the probability of growth of heated and unheated individual cells for all investigated temperatures could be inferred and also no significant difference on the average individual cells lag time, denying the initial hypothesis that says heated cells would need an extra adaptation period in a new environment. This result is aligned with the one at population level. Recommendations on target value of average number of cells per wells were given in order to optimize single-cell probability of growth experiments using turbidity measurements. The findings constitute an important insight about

different features of *B. cereus* behaviour that can be applied by the food industry to improve processing and/or to give guidance on decisions based on Quantitative Risk Assessment.

Key words: *Bacillus cereus*; heat stress; growth matrix; population level; single cell level.

RESUMO

Bacillus cereus é uma bactéria formadora de esporos e produtora de toxinas, sendo, portanto, uma preocupação emergente para a indústria de alimentos. O objetivo deste estudo foi investigar o crescimento de *B. cereus* e fornecer modelos preditivos apropriados, levando em consideração o meio de crescimento, a temperatura, as cepas e o estresse térmico. Para isso, uma metodologia quantitativa foi desenvolvida para acompanhar o desenvolvimento de *B. cereus* após determinado estresse térmico em dois meios de crescimento (Fórmula Infantil Reconstituída (RIF) e meio de cultura (BHI)) a nível populacional e de célula individual por meio de contagem direta (contagem de células viáveis em placas) e indireta (turbidez). Nos experimentos de contagem direta, as velocidades de crescimento foram maiores em BHI quando comparado ao RIF, e um fator *bias* pôde ser estimado para cada cepa investigada. O estresse térmico causou uma redução de 2 log (UFC/mL) em média, mas não afetou significativamente o crescimento subsequente das células sobreviventes. Quanto às estimativas de valores cardinais, os limites de crescimento de três cepas de *B. cereus* (B596, B594 e B626) da Coleção de Culturas de Patógenos da Nestlé foram determinados com sucesso em termos de temperatura, pH e a_w . Estes foram comparados com outras duas cepas pertencentes ao grupo emético, analisando as diferenças entre o grupo e par a par. A cepa B594 diferiu mais de todas as outras em termos dos seus parâmetros cardinais e as cepas B596 e B626 são iguais em todos os parâmetros. As predições de crescimento de *B. cereus* em RIF feitas utilizando os parâmetros cardinais determinados em meio de cultura foram boas, especialmente quando se utiliza o fator *bias* para estimar a velocidade de crescimento ótima em RIF. Confrontado com dados de literatura de diferentes fontes e de uma variedade de produtos lácteos, o modelo secundário proposto para o grupo emético de *B. cereus* apresentou um desempenho razoavelmente bom, com mais de 85% das taxas de crescimento coletadas dentro dos limites de confiança do modelo. Além disso, nenhuma diferença significativa na probabilidade de crescimento de células individuais estressadas e não estressadas para todas as temperaturas investigadas foi inferida e também nenhuma diferença significativa na duração da fase lag das células individuais, negando a hipótese inicial de que as células estressadas precisariam de um período de adaptação extra quando inoculadas em um novo ambiente.

Este resultado está alinhado com o que foi observado a nível populacional. Recomendações sobre o número ideal de células por poço foram dadas a fim de otimizar experimentos de medida indireta (turbidez) que objetivem estimar a probabilidade de crescimento de células individuais. As descobertas constituem uma compreensão importante sobre as diferentes características do comportamento de *B. cereus* que podem ser aplicadas pela indústria de alimentos para melhorar o processamento e/ou dar orientações sobre decisões baseadas na Avaliação Quantitativa de Riscos.

Palavras-chave: *Bacillus cereus*; estresse térmico; meio de crescimento; nível populacional; nível de célula individual.

RESUMO EXPANDIDO

Introdução

Bacillus cereus é uma bactéria patogênica comumente encontrada em matérias-primas e alimentos processados (CEUPPENS et al, 2011; WIJNANDS et al, 2006). Pode suportar processos de pasteurização, resistir à secagem por pulverização e sobreviver em produtos industrializados (McAULEY et al, 2014). Além disso, as diferentes cepas de *B. cereus* são altamente variáveis em termos de seus limites de crescimento. Dada a tolerância térmica de *B. cereus*, é de extrema importância investigar o efeito do estresse térmico sobre o comportamento cinético desse microorganismo a níveis populacional e unicelular, bem como investigar como ele pode afetar o potencial de crescimento de células individuais. Convencionalmente, a modelagem preditiva é realizada por meio de um procedimento de identificação em duas etapas. Uma série de experimentos é realizada a várias temperaturas (constantes), e para cada temperatura a curva de crescimento/sobrevivência produzida é modelada por um modelo primário, cujos parâmetros incluem a velocidade de crescimento (primeiro passo). Em seguida, um modelo secundário é ajustado às estimativas dos parâmetros primários obtidos. Por exemplo, as velocidades de crescimento em função de um ou mais fatores ambientais, mais comumente a temperatura (segundo passo). Esta tese investiga o poder preditivo de modelos encontrados na literatura e amplamente utilizados pela comunidade de microbiologia preditiva ao modelar o crescimento de *Bacillus cereus* a nível populacional e de célula individual.

Objetivos

O objetivo desta tese de doutorado é fornecer um melhor entendimento do comportamento cinético de *B. cereus* em Fórmulas Infantis Reconstituídas (RIF) e em meio de cultura (BHI) a nível populacional e avaliar a probabilidade de crescimento e os tempos de adaptação (fase lag) de células individuais de *B. cereus* antes e depois um tratamento térmico estressante. Além disso, os objetivos específicos são:

- Construir um planejamento experimental apropriado e gerar dados sobre o crescimento de diferentes cepas de *B. cereus* por meio de contagem direta de células viáveis (contagem de placas) e medições de turbidez a nível de população e de célula individual;
- Utilizar um modelo matemático primário para descrever os dados de crescimento experimental obtidos pelo método de contagem de placas e

avaliar o efeito da temperatura, estresse e meio de crescimento nos parâmetros primários;

- Estimativa do fator *bias* como medida de discrepância entre os dois meios testados (RIF e BHI) para quatro cepas (B596; B626; B635 e B577) e propor uma função-*link* que o torna independente da temperatura;
- Estimar velocidades específicas de crescimento por meio de medidas de turbidez para três cepas (B594, B596 e B626); avaliar seus valores cardinais em termos de temperatura, pH e atividade de água, ajustando os respectivos modelos cardinais às velocidades estimadas e comparar os parâmetros obtidos com outras cepas do mesmo grupo filogenético;
- Validar modelos cardinais propostos em termos de temperatura a serem utilizados para cenários alimentares com dados deste estudo (validação interna) e com dados da literatura (validação externa), considerando duas abordagens de estimativa da velocidade de crescimento ótima em RIF;
- Avaliar o desempenho de modelos cardinais e suposições feitas para o estado fisiológico das células (h_0) e a população máxima atingida (N_{\max}) ao prever a concentração bacteriana ao longo do tempo em RIF (validação interna de modelos primários);
- A nível de célula individual, avaliar e comparar a probabilidade de crescimento e os tempos de adaptação (*lag*) individuais antes e depois do tratamento térmico para a cepa B577 por meio de medições de turbidez;
- Propor uma rotina otimizada para experimentos de turbidez com o objetivo de estimar a probabilidade de crescimento de células bacterianas individuais.

Metodologia

Dois técnicas são amplamente utilizadas para medir o crescimento de microrganismos com o tempo e foram aplicadas ao longo da tese: (i) contagem de placas, método direto que estima a concentração bacteriana e (ii) medidas de densidade óptica, método indireto que estima a turbidez que as células produzem ao se multiplicarem. O método de contagem de placas tem a vantagem de poder abranger várias ordens de grandeza de concentrações bacterianas e pode ser aplicado em várias matrizes de crescimento, enquanto medições de turbidez podem ser utilizadas apenas com meio de cultura e medem somente o final da fase exponencial da curva de crescimento. No entanto, o último método tem a vantagem de poder produzir várias curvas de crescimento simultaneamente em condições idênticas. Por meio de experimentos de contagem de placas, estimou-se o fator *bias* e o efeito de tratamento térmico no crescimento subsequente das células. Através das medidas de turbidez, velocidades específicas de crescimento foram estimados e valores cardinais para

temperatura, pH e atividade de água foram determinados para as cepas B594, B596 e B626.

Não é claro se os resultados dos dois métodos de medição podem ser transformados uns nos outros, tornando-se importante compará-los para validar sua aplicabilidade em diferentes níveis. Aqui, o procedimento de validação pretendeu comparar (e em certo nível, mesclar) informações provenientes dos dois métodos de medição descritos acima e comparar previsões com dados produzidos por este trabalho (validação interna) e dados provenientes de várias fontes (validação externa).

A nível de célula individual, a probabilidade de crescimento e a duração da fase lag da cepa B577 foram estudada em condições de estresse e de não-estresse por meio de medidas de turidez. Além disso, um procedimento experimental otimizado foi sugerido para a obtenção de respostas para células individuais utilizando medidas de turbidez.

Resultados e Discussão

O único fator que afeta os parâmetros h_0 (estado fisiológico) e N_{max} (máxima população atingida) é o meio de crescimento, enquanto o estresse térmico parece não ter impacto significativo sobre eles. A raiz quadrada das velocidades de crescimento foi modelada em função da temperatura utilizando o modelo de Ratkowsky (1982) e sua estimativa de T_{min} (temperatura teórica mínima para o crescimento) não é significativamente diferente para os modelos em BHI e RIF para uma mesma cepa, o que dá suporte à avaliação do fator *bias*. Além disso, o fator *bias* entre as velocidades de crescimento em BHI e RIF foi estimado para cada cepa usando a função-*link* da raiz quadrada, uma vez que seu resíduo não apresentou correlação com a temperatura.

As taxas de crescimento específico por turbidez foram estimadas de acordo com os critérios de qualidade especificados e os modelos cardinais de temperatura, pH e atividade de água foram ajustados aos dados experimentais para cada cepa separadamente com R^2 maior que 0,938 para modelos de temperatura; R^2 maior que 0,845 para atividade de água e 0,814 para pH. De fato, o modelo cardinal para pH foi o que apresentou pior desempenho quando ajustado aos dados, provavelmente porque estimar as velocidades de crescimento em condições desfavoráveis de pH aumenta a incerteza das estimativas e consequentemente a variabilidade entre as repetições.

Com base nas estimativas apresentadas ao longo do capítulo para as cepas eméticas investigadas, μ_{opt} varia de 2,68 a 3,67 h^{-1} ; T_{min} entre 5,95 e 8,82;

T_{opt} entre 36,74 e 41,44; T_{max} desde 47,57 a 48,44; pH_{min} de 4,59 a 4,75; pH_{opt} de 6,43 a 7,08; aw_{min} de 0,929 a 0,950 e aw_{opt} de 0,990 a 0,994.

Diferenças significativas nos parâmetros estimados puderam ser identificadas e uma concordância de 61,2% foi obtida quando cepas foram comparadas aos pares. A concordância foi de 100% para pH_{min} e aw_{opt} . Os parâmetros estimados para a cepa B594 parecem diferir mais de todas as outras cepas. As cepas B596 e B626 são iguais em todos os parâmetros.

As predições do crescimento de *B. cereus* em RIF feitas com os valores cardinais e com base no fator bias foram satisfatórias. A criação de um modelo geral para cepas eméticas de *B. cereus* foi desenvolvida usando temperaturas cardinais obtidas para as diferentes cepas investigadas e velocidade ótima de crescimento em RIF estimada de acordo com a metodologia sugerida por Pinon et al (2004). Confrontado com dados da literatura de diferentes fontes e de uma variedade de produtos lácteos, o modelo proposto mostrou bom desempenho com 88% das velocidades de crescimento coletadas dentro dos limites de confiança.

Para células individuais, é difícil adquirir dados suficientemente precisos, especialmente quando a técnica escolhida pode dar respostas apenas a nível populacional. Esta é provavelmente uma das razões pelas quais nenhuma diferença significativa na probabilidade de crescimento de células estressadas e não estressadas foi observada para todas as temperaturas testadas. Juntamente com a grande incerteza da avaliação do número médio de células por poço (devido ao número limitado de repetições), o resultado final pode ser interpretado como células estressadas e não estressadas são igualmente e totalmente (probabilidade igual a 100%) capazes de crescer sob temperaturas que variam de 15 °C a 47 °C. Quanto à avaliação da fase *lag*, nenhuma diferença significativa entre células individuais estressadas e não estressadas pode ser observada a partir dos dados experimentais.

A fim de aumentar a confiança dos pesquisadores, as recomendações propostas podem fornecer um meio para lidar com os desafios mencionados e podem ser usadas para otimizar projetos experimentais ao avaliar a probabilidade de crescimento de células individuais por medições de turbidez.

Considerações Finais

Ficam aqui algumas sugestões para desenvolvimento futuro:

* Células individuais: experimentos de citometria de fluxo (*flow cytometry*) para identificar a fração de células mortas, vivas e danificadas e sua capacidade individual de crescimento; verificar principalmente se

células injuriadas e células vivas têm a mesma probabilidade de se dividirem como a probabilidade de crescimento usando medidas de turbidez sugere.

* A nível populacional: investigar se as células sobreviventes são mais tolerantes a subseqüentes estresses térmicos. Isto pode ser observado através de uma redução da fase *lag* devido ao tratamento térmico ou nenhuma diferença entre as médias de h_0 .

* Produção de toxinas por cepas eméticas de *B. cereus*: com delineamento experimental semelhante, avaliar o efeito do estresse, meio e temperatura na produção de toxina. Qual fator a influencia mais e qual(is) pode(m) ser considerado(s) insignificante(s)?

Palavras-chave: *Bacillus cereus*; estresse térmico; meio de crescimento; nível populacional; nível de célula individual.

Acknowledgments

This work was carried out in close collaboration between Nestlé Research Centre (NRC) in Lausanne/Switzerland and the Federal University of Santa Catarina (UFSC) in Florianópolis/Brazil with a cooperation of a third part - Institute of Food Research (IFR) in Norwich/UK - for a shorter period. It would have not been possible to make it without the active support from all involved parts. A very special thank you goes to CAPES for providing my PhD grant along the last four years, to Programa de Pós-Graduação em Engenharia de Alimentos (PPGEAL/UFSC) for hosting me as a PhD student and to NRC for allowing me to develop my PhD research within one of their projects and for the financial support with my internship and experiments.

All my gratitude to my three supervisors Bruno, József and Mariem for their patience and support in giving me numerous advice and for helping me overcoming obstacles during this research. Bruno, thanks for your endless patience, for believing in my work and supporting my ideas since undergrad times. Your insightful comments and questions incited me to widen my perspective on this piece of research. József, you have taught me more than I could ever give you credit for here. You have shown me, by your own example (or should I say “non-traditional methods?”), what a good scientist (and person) should be. Mariem, your encouragement, guidance and trust were essential during all steps of the PhD, especially during my time in Switzerland. You became a role model for me and my admiration towards you increases at every conversation we have.

A great thanks to IFR and NRC, in special the Computational Microbiology Research and Food Safety Microbiology Groups that hosted me so warmly and provided me an opportunity to join their teams. You will always have a special place in my memories. It was fantastic to have the opportunity to work a great part of my research in your facilities. To Susie who patiently and joyfully taught me a lot in the lab, Amanda for the nice conversations and for “holding the fort” with the experiments during my short absence and to Yuqi and Beatriz, who made my days much lighter, fun and sweet (in all possible manners).

To my family, whose love and guidance are with me in whatever I pursue, thanks for making me feel I have a nest to fly back whenever I need. To Marc who truly supports me in everything, thanks for showing

me how small the world can be and that for the important things it is worth being patient. To my friends Amanda and Paula for the lasting friendship, good moments, laughs and advice when you knew me better than myself.

I am grateful to all of those with whom I have had the pleasure to work and get to know during the last years. I had the amazing opportunity to meet many interesting people coming from all around the world and develop myself in ways I couldn't imagine four years ago.

For all your encouragement, thank you!

SUMMARY

1. Introduction	29
1.1 General Objective.....	31
1.2 Specific objectives.....	31
2. Literature review	33
2.1 <i>Bacillus cereus</i>	33
2.2 Predictive Microbiology.....	34
2.2.1 Primary models	36
2.2.1.1 Baranyi and Roberts model	37
2.2.2 Secondary Models	39
2.2.2.1 Ratkowsky model.....	40
2.2.2.2. Cardinal models.....	40
2.2.3 Bias factor	43
2.2.4 Effect of stress on microorganisms growth at population level	45
2.2.5 Effect of stress on microorganisms response at single-cell level.....	46
3. <i>B. CEREUS</i> GROWTH IN RECONSTITUTED INFANT FORMULAE (RIF) AND CULTURE MEDIUM AT SUBOPTIMAL TEMPERATURES	51
3.1 Introduction	51
3.2 Material and Methods.....	52
3.2.1 <i>Bacillus cereus</i> growth in RIF and BHI.....	52
3.2.1.1 Strain preparation	52
3.2.1.2 Temperature control	53
3.2.1.3 Determining heat up and cool down times	53
3.2.1.4 Inoculum preparation	53
3.2.1.5 Stress characterization.....	54

3.2.1.6	Temperature effect on <i>B. cereus</i> growth.....	54
3.2.1.7	Experimental design.....	55
3.2.1.8	Primary and secondary modelling procedure.....	56
3.2.1.9	Bias factor.....	56
3.3	Results and Discussion.....	57
3.3.1	Growth of <i>B. cereus</i> in RIF and BHI.....	57
3.3.1.1	Primary parameters.....	57
3.3.1.1.1	The physiological state (h_0).....	58
3.3.1.1.2	Maximum population density (N_{\max}).....	62
3.3.1.1.3	Growth rate.....	64
3.3.1.1.3.1	Secondary modelling.....	64
3.3.1.1.3.2	Bias factor.....	66
3.4	Conclusions and Considerations.....	70
3.5	References.....	71
4.	CARDINAL VALUES ASSESSMENT OF EMETIC <i>B. CEREBUS</i> STRAINS IN TERMS OF TEMPERATURE, PH AND WATER ACTIVITY.....	73
4.1	Introduction.....	73
4.2	Material and Methods.....	75
4.2.3	Cardinal parameters estimation.....	75
4.2.3.1	Strains.....	75
4.2.3.2	Media preparation.....	75
4.2.3.3	Inoculum preparation.....	75
4.2.3.4	Turbidity experiments.....	75
4.2.3.5	Growth rates estimation.....	76
4.2.3.6	Estimation of cardinal values and confidence intervals....	77
4.3	Results and Discussion.....	81
4.3.1	Growth rates estimation.....	81

4.3.2 Cardinal parameters estimation	81
4.3.3 Validation of cardinal parameters	89
4.4 Conclusions	94
4.5 References	95
5. PRIMARY AND SECONDARY MODELS VALIDATION.....	97
5.1 Introduction	97
5.2 Material and Methods.....	99
5.2.1 Internal validation	99
5.2.1.1 Secondary models	99
5.2.1.1.1 Approach-A:.....	99
5.2.1.1.2 Approach-B	100
5.2.1.1.3 Secondary models performance analysis.....	101
5.2.1.2 Primary models	102
5.2.2 External validation	102
5.2.2.1 Secondary models	102
5.3 Results and Discussion.....	104
5.3.1 Internal validation	104
5.3.1.1 Secondary models	104
5.3.1.1.1 Approach-A.....	104
5.3.1.1.2 Approach-B	106
5.3.1.1.3 Comparison between Approaches-A and -B	108
5.3.1.2 Primary model	108
5.3.1.2.1 Using Approach-A to predict growth rates in RIF	108
5.3.1.2.2 Using Approach-B to predict growth rates in RIF	113
5.3.2 External validation	116
5.3.2.1 Secondary models	116
5.4 Conclusions	119

5.5 References.....	120
6. PROBABILITY OF GROWTH OF <i>B. CEREBUS</i> INDIVIDUAL CELLS AFTER PRE-INOCULATION STRESS	123
6.1 Introduction.....	123
6.2 Material and Methods	126
6.2.1 Probability of growth of stressed and non-stressed <i>B. cereus</i> individual cells	126
6.2.1.1 Inoculum preparation	126
6.2.1.1.1 Unheated cells	126
6.2.1.1.2 Heated cells	126
6.2.1.1.3 Single cells inoculum	126
6.2.1.2 Population growth rate for heated and unheated cells	127
6.2.1.3 Plate design	127
6.2.1.4 Calibration curve.....	128
6.2.1.5 Data analysis	128
6.2.2 Optimization of turbidity experiments to estimate the probability of growth for individual bacterial cells.....	128
6.2.2.1 A-priori estimation using plate count method.....	128
6.2.2.3 Estimating the probability of growth	130
6.3 Results and Discussion.....	132
6.3.1 Probability of growth of stressed and non-stressed <i>B. cereus</i> individual cells	132
6.3.2 Optimization of turbidity experiments to estimate the probability of growth for individual bacterial cells.....	133
6.3.3 Individual lag times.....	136
6.4 Conclusions.....	140
6.5 References.....	141
7. Conclusions.....	143
8. Suggestions for future development.....	147

9. References	149
ANNEX A	159
ANNEX B	215
ANNEX C	225
ANNEX D	243
ANNEX E	253
ANNEX F	251

List of figures

Figure 2.0.1 - Characteristic curve of microbial growth along the time. From: Swinnen et al. (2004).....	37
Figure 2.0.2 - (A) influence of pH on cardinal model for temperature and (B) influence of temperature on cardinal model for pH. Adapted from Rosso et al (1995).....	42
Figure 2.0.3 - Viable counts for <i>Salmonella spp.</i> in culture medium with 3% salt. From: Zhou et al. (2012).	46
Figure 2.0.4 - Probability density functions of individual cell lag times for different NaCl concentrations. From: Kutalik et al (2005A).....	48
Figure 3.0.1 - Fitted growth curves obtained for B635 strain in BHI at different temperatures: 30 °C in blue, 25 °C in grey, 22 in green, 18 °C in orange, 15 °C in yellow and 12 °C in red.....	57
Figure 3.0.2 - All h_0 values obtained for strains B577 (in blue), B594 (in grey), B596 (in orange), B626 (in yellow) and B635 (in green) in RIF (stars) and BHI (circles) at different temperatures.	59
Figure 3.0.3 - h_0 values for BHI (first two rows) and RIF (last two rows) at different temperatures. B577 strain in blue, B594 in grey, B596 in orange, B626 in yellow and B635 in green.	61
Figure 3.0.4 - Maximum population density (N_{\max} [log CFU/ml]) as a function of temperature obtained in BHI for strains B577 (in blue), B596 (in orange) B626 (in yellow) and B635 (green).	63
Figure 3.0.5 - Maximum population density (N_{\max} [log CFU/ml]) as a function of temperature obtained in RIF for strains B577 (in blue), B594 (in grey), B596 (in orange) B626 (in yellow) and B635 (in green).....	64
Figure 3.0.6 - Ratkowsky model fittings in BHI and RIF with strains B577 in blue, B594 in grey, B596 in orange, B626 in yellow and B635 in green strains.	65
Figure 3.0.7 - B-line showing the correlation between b and T_{\min} parameters from Ratkowsky model. In black, data and trend published by Baranyi et al (2017). In red, four strains (B577, B596, B626 and B635) from this work.	66
Figure 3.0.8 - Absolute residuals for square root link function. BHI in full dots and RIF in empty dots.	68
Figure 3.0.9 -Square-root (maximum specific growth rates) vs. temperature data and fitted models for medium variability observation	

and bias factor assessment for B577, B596, B626 and B635 strains in RIF (squares; dashed line) and BHI (circles; continuous line).	69
Figure 4.0.1 - Bioscreen plate design for cardinal values estimates – O.D. experiments. Diluted subculture inoculated into red wells and binary dilutions performed down in each column.....	76
Figure 4.0.2 - how to estimate generation time from O.D. curves. From: Rukundu (2015).	77
Figure 4.0.3 - Example of estimating the specific growth rate from O.D. curves. Broken line at left represents the detection level at O.D. = 0.4.	81
Figure 4.0.4 - Cardinal models (continuous line) for temperature fitted to data from this study (squares) for B594, B596 and B626 strains and fitted to data taken from Carlin et al (2013) (dots) for B577, B635 and F837/76 strains. Dashed lines: confidence limits.	84
Figure 4.0.5 - Cardinal models (continuous line) for water activity fitted to data from this study (squares) for B594, B596 and B626 strains and fitted to data taken from Carlin et al (2013) (dots) for B577, B635 and F837/76 strains. Dashed lines: confidence limits.	85
Figure 4.0.6 - Cardinal models (continuous line) for pH fitted to data from this study (squares) for B594, B596 and B626 strains and fitted to data taken from Carlin et al (2013) (dots) for B577, B635 and F837/76 strains. Dashed lines: confidence limits.	86
Figure 4.0.7 - Predicted vs. observed specific growth rate based on cardinal model fittings presented in Figures 4.4 - 4.6. Strain B594 in circles, B596 in triangles and B626 in stars.	88
Figure 4.0.8 - Cardinal parameters and their confidence interval for the models in terms of water activity and pH for B594, B596, B626, B577, and F837/76 strains. *Raw data taken from Carlin et al (2013) and re-fitted according to procedure proposed in this study.	90
Figure 4.0.9 - Cardinal parameters and their confidence intervals for the models in terms of temperature for B594, B596, B626, B577, and F837/76 strains. *Raw data taken from Carlin et al (2013) and re-fitted according to procedure proposed in this study.	91
Figure 5.0.1 - Secondary models validation. Continuous line: cardinal model in RIF according to Approach-A. Dashed lines: confidence limits. Dots: specific growth rates observed in RIF.	105
Figure 5.0.2 - Secondary models validation. Continuous line: cardinal model in RIF according Approach-B. Dashed lines: confidence limits. Dots: specific growth rates observed in RIF.	107

Figure 5.0.3 – Examples of primary model validation using Approach-A from secondary model to estimate growth rates. Simulated growth curve (continuous line); experimental data (dots).....	110
Figure 5.0.4 - Observed vs. predicted logcounts for all studied strains using Approach-A to simulate growth rates coupled with h_0 and N_{max} assumptions. In red: heated cells. In black: unheated cells.	112
Figure 5.0.5 - Example of primary model validation using Approaches-A (continuous line) and -B (dashed line) from growth rate secondary model to illustrate improvement resulting from Approach-B. Experimental data (dots).	114
Figure 5.0.6 - Observed vs. predicted logcounts for all studied strains using Approach-B to simulate growth rates coupled with h_0 and N_{max} assumptions. In red: heated cells. In black: unheated cells.	115
Figure 5.0.7 - External validation of secondary model for emetic strains. Continuous line: predictive model. Dashed lines: C.I. In blue: literature data in RIF. In red: Combase data in milk. In purple: Nestlé data for dairy products.....	118
Figure 6.0.1 - Bioscreen plate design for probability of growth experiments. In red, the wells dedicated to population level; in blue they were dedicated to single cell level.....	127
Figure 6.0.2 - Comparison between average number of cells per well according to method 1 (dots) and method 2 (squares) for each replicate of the experiments with heated cells at 15 °C (top) and for unheated cells (bottom).	133
Figure 6.0.3 - Accuracy of the estimators ρ (A) and its modification ρ' (B). Continuous blue: $w=50$; dash-dotted orange: $w=100$; dotted green: $w=200$; dashed yellow: $w=400$	134
Figure 6.0.4 - Efficiency of the ρ' estimator quantified by its relative deviation for different number of wells. Continuous blue: $w=50$; dash-dotted orange: $w=100$; dotted green: $w=200$; dashed yellow: $w=400$	135
Figure 6.0.5 - Average lag time for individual cells unheated (in blue), heated (in red) and population lag time (in empty orange) coming from viable counts experiments.	138

List of tables

Table 3.0.1 - Experimental design for <i>B. cereus</i> growth experiments in RIF and BHI.....	55
Table 3.0.2 - Average of h_0 values for each heated and unheated strain at each medium and average of h_0 values for all heated and unheated strains at each medium.....	58
Table 3.0.3 - Average of h_0 values for each strain at different temperatures for each medium and average of h_0 values for each strain at each medium.....	59
Table 3.0.4 – Parameters, confidence intervals (between brackets) and the coefficient of determination from fitting of Ratkowsky model for B577, B594, B596, B626 and B635 in RIF and BHI.....	65
Table 3.0.5 - p-values from analysis of correlation of absolute residuals with temperature.....	68
Table 3.0.6 – Bias factors between BHI and RIF media estimated for each strain with square-root (μ_{\max}) link function.....	69
Table 4.0.1 - Cardinal values and respective confidence intervals between brackets for temperature, pH and water activity for B594, B596, B626, B577 (F4810/72), F837/76 and B635 strains.....	82
Table 4.0.2 - Pair-wise analysis of significant differences for the cardinal parameters of different emetic strains.....	92
Table 5.0.1 – Estimated optimal specific growth rates in RIF according to Approach-A.....	104
Table 5.0.2 - RMSE values for predictive performance evaluation of Approach-A.....	106
Table 5.0.3 – Optimal growth rates in RIF estimated by means of Approach-B.....	107
Table 5.0.4 - RMSE values for predictive performance evaluation of Approach-B.....	108
Table 5.0.5 - Summary of parameters used in simulations of growth curves; growth rates estimated according to Approach-A of secondary models.....	109
Table 5.0.6 - RMSE values for predictive performance evaluation of Approach-A when applied together with h_0 and N_{\max} assumptions to simulate primary growth curves.....	111

Table 5.0.7 - RMSE values for predictive performance evaluation of Approach-B when applied together with h_0 and N_{\max} assumptions to simulate primary growth curves.....	115
Table 5.0.8 - Cardinal values used for creation of general model for <i>B. cereus</i> emetic strains	117
TABLE 6.0.1 - NOMENCLATURE AND MEANING OF SYMBOLS AND ASSUMPTIONS.	124
Table 6.0.2 - Recommendations on target optimal value of ρ . At these values, both the accuracy coefficient and efficiency of the ρ' estimator are optimal.	135
Table 6.0.3 - Detection levels used to calculate detection times and respective concentration of cells used to calculate individual lag times.....	139

1. Introduction

Bacillus cereus is a pathogenic bacterium commonly found in raw materials and processed foods (CEUPPENS et al, 2011; WIJNANDS et al, 2006). It can endure high temperature short time (HTST) pasteurization, resist spray drying and survive in final products (McAULEY et al, 2014). Additionally, *B. cereus* strains are highly variable in terms of their growth limits, characteristic mainly dependent on their phylogenetic group (CARLIN et al, 2013). Emetic strains of *B. cereus* are of concern since they are toxin producers and it is not possible to eliminate the toxin (cereulide) once preformed in the food.

Given *B. cereus* thermo tolerance, it is of extreme importance to investigate the effect of heat stress(es) on the kinetic behaviour of this microorganism at population and single-cell levels as well as investigating how can it affect the growth potential of individual cells. That's where predictive microbiology can be useful and make the difference when analysing experimental data.

Predictive Microbiology is a multidisciplinary area making use of mathematics and statistics in food microbiology since 1980s when the increase in public awareness of the need for safe food supply came together with the fact that traditional methods for assessing microbiological quality and safety were limited by the time to obtain results and the poor predictive and reproducible value. Since then, the area has deeply developed, constituting important instrument for safety assurance within the food industry.

Conventionally, predictive modelling is carried out via a two-step identification procedure. A series of experiments is performed at various (constant) temperatures, and for each temperature the produced growth / survival curve is modelled by a so-called primary model, whose parameters includes the maximum specific growth rate (first step). Then a secondary model is fitted to the obtained primary parameter estimates, most importantly the maximum specific growth rate estimates, as a function of one or more environmental factors, most commonly the temperature (second step).

By comparing secondary models that describe how growth rates vary with temperature using two different growth media, it is possible to assess the medium effect on the growth rate and create a link between

them that, based on certain assumptions, can be extrapolated to a wider range of the environmental factor. Commonly, this link is measured between culture medium and a given food. Namely, it is desirable to use culture medium-based models to predict the bacterial behaviour in food matrices since more literature data are available for the former.

From a population kinetic perspective, two main techniques are widely used to measure the microorganism growth with time: plate count, a direct method, which estimates the bacterial concentration, and optical density (OD-) measurements, an indirect method, which estimates the turbidity that the cells cause. Plate counts method have the advantage that they can span through orders of magnitude of bacterial concentrations and that they can be applied to several growth matrices, while turbidity measurements can be used only with culture medium, and only for the late exponential phase of the growth curve. However, the latter method has the advantage that it can produce several OD-curves simultaneously, under identical conditions. It is not obvious whether the results from the two measurement methods can be transformed into each other, making it important to compare/merge them to validate their applicability at different levels.

By validation, it is meant checking if the chosen models and assumptions made are valid and can predict the microorganism behaviour correctly. Here, the validation procedure intends to compare (and at a certain level, merge) information coming from both measurement methods described above and compare predictions to data produced by this work (internal validation) and data coming from various sources (external validation).

Lately, predictive microbiology research has begun to focus on the understanding of the microorganism behaviour at single cell or even molecular level. This approach needs to take into account the complexity of intracellular mechanisms and their intrinsic variability. This is important because food poisoning outbreaks may be initiated by contamination with just a few pathogenic cells if they are able grow in the food to reach an infective dose. Quantitative Microbial Risk Assessment studies frequently need to estimate the probability that a few contaminating cells multiply to a population level above a tolerance limit (BARANYI et al, 2009). To analyse this, one needs to identify the probability of growth and distribution of the lag times of single cells coming from similar population. Turbidity measurements can also be

useful here with a standard procedure where cultures are diluted to a level until the majority of the inoculated wells will receive zero or one cell. The disadvantage is that, using an automated turbidimeter, many wells will be empty and, for a statistically robust estimation, it is desirable to have as many positive wells as possible, revealing the urgent need of an experimental optimization for this technique aiming at single cells probability of growth assessment.

Taking all this information into account, the thesis was divided into four main chapters, where the three first ones refer to population level and the last one to single-cell level: (i) to provide a better understanding on the kinetic behaviour of different strains of *B. cereus* in RIF and culture medium by means of viable counts, analysing how to properly estimate the bias factor between the two media; (ii) to characterize the cardinal values for temperature, pH and a_w for a selection of emetic *B. cereus* strains by means of turbidity measurements, (iii) to validate the proposed kinetic models by assessing how applicable are the cardinal values - coupled with two different approaches of estimating optimal growth rate (μ_{opt}) in RIF - to food scenarios and (iv) to study the impact of heat treatment on the probability of growth and individual lag times of a reference strain of *B. cereus* and propose an experimental optimization for assessment of probability of growth of individual cells using turbidity measurements.

1.1 General Objective

The objective of this PhD thesis is to provide a better understanding on the kinetic behaviour of *B. cereus* in Reconstituted Infant Formulae and culture medium at population level and to evaluate the probability of growth and individual lag times of *B. cereus* individual cells before and after a stressful heat treatment.

1.2 Specific objectives

- Build an appropriate experimental design and generate data on the growth of different strains of *B. cereus* by means of viable counts and turbidity measurements at population and single cell level;
- Use a mathematical primary model to describe the experimental growth data obtained by plate count method and assess the effect

of temperature, stress and growth medium on the primary parameters;

- Estimate bias factor as a measure of discrepancy between the two tested media (Reconstituted Infant Formulae and broth) for four strains (B596; B626; B635 and B577) and propose a link-function that makes it temperature-independent;
- Estimate specific growth rates by means of turbidity measurements for three strains (B594, B596 and B626); assess their cardinal values in terms of temperature, pH and water activity by fitting the respective cardinal models to estimated rates and compare the obtained parameters with other strains from the same phylogenetic group;
- Validate proposed cardinal models in terms of temperature to be used to food scenarios with data from this study (internal validation) and with data from literature (external validation), considering two approaches of estimating μ_{opt} in RIF;
- Evaluate the performance of cardinal models and assumptions made for the physiological state of the cells (h_0) and the maximum population reached (N_{max}) when predicting bacterial concentration along time in RIF (primary models internal validation);
- At single cell level, assess and compare probability of growth and individual lag times before and after heat treatment for B577 strain by means of turbidity measurements;
- Propose an optimized routine for turbidity experiments to estimate the probability of growth for individual bacterial cells to obtain recommendations concerning experimental design.

2. Literature review

2.1 *Bacillus cereus*

B. cereus sensu stricto (*B. cereus* in short) is an opportunistic foodborne pathogen included into *Bacillus cereus sensu lato* bacterial group, which consists of *B. anthracis*, *B. cereus*, *B. cytotoxicus*, *B. mycoides*, *B. pseudomycoides*, *B. thuringiensis*, and *B. weihenstephanensis*. (CEUPPENS et al, 2013). *B. cereus* is able to produce toxins such as cereulide, cytotoxin K, hemolysin BL (HBL) and non-hemolytic enterotoxin (NHE) (ROWAN & ANDERSON, 1998; EHLING-SCHULZ et al, 2005). It is mainly associated with gastrointestinal disorders and with a multitude of other infections, such as severe eye infections, periodontitis, necrotizing fasciitis, endocarditis, nosocomial acquired bacteraemia, osteomyelitis, sepsis, liver abscess, pneumonia and meningitis, particularly in postsurgical patients, immunosuppressed individuals, intravenous drug abusers and neonates (YANG et al, 2016).

B. cereus might come from farm lands, it is able to endure ultrahigh-temperature (UHT) pasteurization and concentration, survive from spray drying tower and appear in final products (McAULEY et al, 2014). Shaheen et al. (2006) suggested that the *B. cereus* pathogens should be intensively monitored in infant formula. According to De Jonghe et al. (2008), *B. cereus* should be controlled and might be a suitable microbiological safety indicator for food products, especially for infant formula. It is considered as one of high-risk foods on account of its high protein contents and its vulnerable consumers (YANG et al, 2016).

Bacillus cereus is now attracting interest among researchers because it is not only associated with foodborne outbreaks but also responsible for spoilage of food products. It produces various extracellular enzymes which can be able to decrease the organoleptic quality of milk and dairy products. Also, *B. cereus* can be introduced into the dairy environment from various sources during production, handling and processing, mainly from improperly cleaned and sanitized equipment (KUMARI & SARKAR, 2016). It is still a challenging task to effectively control these bacteria in dairy products and processing environment, because as spore-forming bacteria are ubiquitous in nature, contamination has been shown to occur along the whole processing line (ENEROTH et al, 2001).

According to a review published by the European Food Safety Agency, *B. cereus sensu lato* are particularly interesting because their genetic background confers variable tolerance to temperature. Indeed, the global evolution of *B. cereus sensu lato* is not anarchic but seems to be strongly determined by ecological adaptations. This genetic diversification associated with modifications of temperature tolerance limits is a first example of the genetic adaptive faculty of *B. cereus sensu lato*. There is a speculation that the emergence of more cold-adapted populations or more warm-adapted populations is due to the colonization of new or different environments for which *B. cereus* organisms had to adapt. Global warming may also push towards a homogenization of the actual populations to a thermo tolerant status. (CARLIN et al, 2010)

A good indicative of adaptive skills of *B. cereus* is that many strains isolated from food poisoning cases have a tendency rather to be more thermo tolerant. In addition, global food trade presumably makes the *B. cereus* population in foods less dependent from the local environment. For example, dry ingredients can be an important source of *B. cereus* in processed foods (GUINEBRETIERE et al, 2003), and these ingredients can be imported from remote countries.

The risk of survival of vegetative pathogens and spoilage organisms are decreased considerably due to the high temperature applied during pasteurisation, but this is not always the case for *B. cereus*. To control the level of contamination with this organism, a low initial count, cooling after pasteurisation, and limiting storage time should be considered (ZWIETERING et al, 1996).

Although some thermic processes are not very efficient to inactivate *B. cereus*, one question not very well investigated is the effect of these processes, as a stress condition, on the subsequent behaviour of survival cells at population and single-cell level. This is where Predictive Microbiology can play a role and help Food Microbiologists to better understand what in fact happens.

2.2 Predictive Microbiology

Predictive microbiology can be defined as a research area that uses mathematical models to describe the population dynamics (growth and survival) of microorganisms undergoing complex physical, chemical and biological changes during processing, transportation, distribution and storage of food (HUANG, 2014). Predictive microbiology is a

multidisciplinary area, since it applies mathematics, engineering, chemistry and biology knowledge to provide microbial predictions in certain foods under defined conditions (SCHAFFNER & LABUZA, 1997; McDONALD & SUN, 1999).

The beginning of the use of mathematical models in food microbiology was at around 1920, revolutionizing the canning industry with the development of methods to calculate the thermal inactivation time of microorganisms (GOLDBLITH et al, 1961). However, only from 1983, the potential of predictive microbiology began to attract research and funding interest, mainly in the United States, United Kingdom, Australia and Europe (ROSS & McMEEKIN, 1994).

According to Ross and McMeekin (1994), the interest in predictive models occurred for two reasons: the increase of food poisoning cases during the 1980s, leading to an enhanced public awareness of the need for safe food supply and the fact that traditional methods for assessing microbiological quality and safety were limited by the time to obtain results and the poor predictive and reproducible value.

According to Tijssens et al (2001), the practical applications of predictive microbiology began to materialize only in the 1980s because of an important tool used today, the computer. According to Whiting (1995), with the advent of personal computers, microbial modelling has become an area of great interest, since the models could easily be used by food microbiologists and technologists.

Whiting and Buchanan (1993) suggested the following classification for mathematical models used in predictive microbiology that will be further discussed during next sections:

Primary models: describe the response of the microorganism along the time, for a set of fixed conditions. The microbial response can be directly measured by the population density (plate count, microscopy, etc.), indirectly (absorbance, impedance, etc.) or by products of microbial metabolism (acid production, toxin synthesis, etc.).

Secondary models: describe the primary model parameters as a function of culture conditions, such as temperature, pH, water activity etc.

Tertiary models: are applications of one or more secondary models to provide predictions to non-modelers by means of user-friendly software packages.

Even though this classification is widely used until the present days, Baranyi et al (2017) proposed a new way of classifying tertiary

models. The authors propose that the name “tertiary modeling” should be used for researches logically derived from the concepts of “primary” and “secondary” modeling. Such investigations may then reveal, for example, biological relationships between kinetic parameters within a group of strains following the same rationale that secondary models reveal relationships between kinetic parameters of the primary models.

2.2.1 Primary models

A standard introduction to primary modelling must start with the case when the specific growth rate is constant and the maximum population can be achieved, as shown in Equation (2.1).

$$\frac{dx(t)}{dt} = \mu_{max}x(t) \quad (2.1)$$

where $x(t)$ is the size of the population at that time and μ_{max} is the specific growth rate.

This is the pure exponential growth model (Malthus’ model) and the solution for the differential Equation (2.1), at the given initial population size x_0 , is:

$$x(t) = x_0 e^{\mu_{max}t} \quad (2.2)$$

or, expressed by $y(t) = \ln(x(t))$, the natural logarithm of the cell concentration:

$$y(t) = y_0 + \mu_{max} t = \ln x_0 + \mu_{max} t \quad (2.3)$$

where $x(0)=x_0$ and $y(0)=y_0$ are the initial values for the differential equation. The $\log x(t)$ concentration preferred by food microbiologists can be obtained by using the conversion factor $\ln(10) \approx 2.3$, keeping in mind that this is the factor between the natural and the 10-based logarithm.

$$\log x(t) = \log x_0 + \mu t \quad (2.4)$$

where $\mu = \mu_{max} / 2.3$. That is the slope of the growth curve on the log scale, μ , differs from the specific growth rate, μ_{max} by the factor 2.3.

Primary models describe the bacterial curve a constant environment. This curve is meant as the variation of log cell concentration

with time. If the environment supports growth, then the bacterial curve is of sigmoid shape, as shown in FIGURE 2.0.1.

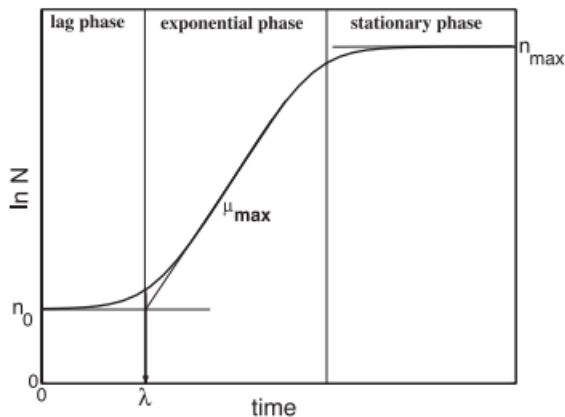


Figure 2.0.1 - Characteristic curve of microbial growth along the time. From: Swinnen et al. (2004).

In population dynamics, sigmoid growth curves are obtained when the size of the population is described as a function of time. In microbiology, however, the log-population follows sigmoid pattern with time and this is why Baranyi and Roberts (1994) introduced a new model, instead of using classical sigmoid functions, such as that of Gompertz (GOMPERTZ, 1893) or Logistic (VERHULST, 1845). The rationale behind this model will be summarized in the next section.

2.2.1.1 Baranyi and Roberts model

The primary model published by Baranyi and Roberts (1994) can be summarized as

$$\frac{dx(t)}{dt} = \frac{q(t)}{1 + q(t)} \mu_{max} x(t) \left(1 - \left(\frac{x(t)}{x_{max}} \right)^m \right) \quad (2.5)$$

where $q(t)$ is described by Equations 2.6a and 2.6b. It has the advantage that it has an algebraic solution if the parameters are constant with time. In dynamic situations, however, it should be solved by numerical methods.

$$\frac{dq}{dt} = vq \quad (2.6a)$$

$$q(0) = q_0 \quad (2.6b)$$

The simplification $v = \mu$ has some mechanistic background and makes the model more suitable for practical curve fitting procedures, too.

The following reparameterizations of q_0 have biological interpretations and advantageous numerical/statistical properties that are useful when using the model for curve fitting:

$$\alpha_0 = \frac{q_0}{(1 + q_0)} \quad (2.7)$$

$$h_0 = -\ln(\alpha_0) \quad (2.8)$$

The solution of the differential Equation 2.5 can be expressed in terms of $y(t)$, the natural logarithm of the cell concentration:

$$y(t) = y_0 + \mu_{max}A(t) - \frac{1}{m} \ln \left(1 + \frac{e^{m\mu_{max}A(t)} - 1}{e^{m(y_{max}-y_0)}} \right) \quad (2.9)$$

in which $A(t)$, the integral of $\alpha(t)$, can be considered as a gradually delayed measure of time:

$$A(t) = t - \lambda + \frac{\ln(1 - e^{vt} + e^{-v(t-\lambda)})}{v} \quad (2.10)$$

The four parameters of this model (y_0 , y_{max} , μ_{max} , and λ) can be categorised as follows:

μ_{max} : The maximum specific growth rate is a so-called autonomous parameter, characterising purely the ability of the bacteria to grow in the current environment, independently of the history of the cells. This reflects the belief that the cells sooner or later grow at a specific rate determined by the actual growth environment, after a possible adjustment to it.

y_{max} (or N_{max} along this thesis): The final cell concentration is also an autonomous (history-independent) parameter, but much less important, from application point of view, than the maximum specific

growth rate since food microbiology focuses on low level of cell concentrations.

y_0 (or N_0 along this thesis): The initial cell concentration is obviously purely history dependent. In fact, in experiments, it is set up by the experimenter, and can be relatively easily estimated. In real food, however, its estimation can be complicated, which can cause difficulties when estimating the error of predictions of bacterial concentration in the actual environment.

The most difficult parameter, from modelling point of view, is the lag parameter (λ), because both the history and the actual environment affect it. To overcome this difficulty, Baranyi and Roberts (1995) reparameterised the system and introduced the $h_0 = \mu_{max} \cdot \lambda$ quantity. If the lag and the maximum specific growth rate are inversely proportional (equivalently: if the relative lag defined as the ratio lag time by generation time of the exponential phase is constant, which is observed by many researchers), then the parameter h_0 is constant and can quantify the work to be done during the lag phase. A rescaling of the h_0 parameter, $\alpha_0 = \exp(-h_0)$ is a sort of “suitability” parameter, between 0 and 1, quantifying how much the history of the cells suitable to the actual environment. $\alpha_0 = 1$ means optimum history, when there is no lag at all ($\lambda = 0$); and $\alpha_0 = 0$ marks the infinitely long lag situation. Therefore, the system has two initial values: y_0 and α_0 (or h_0). With this concept, the lag obviously depends on both history and the actual environment shown by the simple Equation (2.11):

$$\lambda = h_0 / \mu_{max} = -\ln(\alpha_0) / \mu_{max} \quad (2.11)$$

It can be also shown that the $\alpha_0 = \exp(-\mu_{max} \cdot \lambda)$ quantity expresses the fraction of cells that would have been able to grow into the same curve without lag. Therefore, for example, $\alpha_0 = 0.04$ means that if only 4% of the cells grow, they would reach a certain (high) concentration level at the same time as the actual growth curve, if those 4% can grow without lag.

2.2.2 Secondary Models

Any equation that represents the variation of the parameters of the primary model as a function of the environment variable (temperature, for example) can be classified as a secondary model. There are some pre-

established secondary models widely used in the literature and two of them – the Ratkowsky Model and the Cardinal Model - will be briefly described here due to their importance to the development of this thesis.

2.2.2.1 Ratkowsky model

When temperature is the primary factor of interest, Ratkowsky et al (1982) suggested a linear relationship between the square root of growth rate and this environmental factor as presented in Equation 2.12.

$$\sqrt{\mu_{max}} = b(T - T_{min}) \quad (2.12)$$

where b is the regression coefficient and T_{min} is a hypothetical temperature which is an intrinsic property of the organism, also considered the theoretical minimum temperature for growth. The proposed model – also known as “square-root model” was found to be applicable to the growth of a wide range of bacteria and it is valid for suboptimal temperatures of growth for the investigated organism.

2.2.2.2. Cardinal models

Rosso et al (1995) proposed a new modelling approach in which the maximum microbial specific growth rate (μ_{max}) is described as a function of pH and temperature (Equation 2.15) for the whole range of environmental factor(s) where growth is observed. The seven parameters of this model are the three cardinal pH parameters (the pH below which no growth occurs (pH_{min}), the pH above which no growth occurs (pH_{max}), and the pH at which the μ_{max} is optimal (pH_{opt})), the three cardinal temperature parameters (the temperature below which no growth occurs (T_{min}), the temperature above which no growth occurs (T_{max}), and the temperature at which the μ_{max} is optimal (T_{opt})), and the specific growth rate at the optimum temperature and optimum pH (μ_{opt}). The combined model presented in Equations 2.13 - 2.15 was constructed by using the hypothesis that the temperature and pH effects on the μ_{max} are independent.

$$\mu_{max} = \begin{cases} T < T_{min}, 0 \\ T_{min} < T < T_{max}, \mu_{opt} * \tau(T) \\ T > T_{max}, 0 \end{cases}$$

(2.13)

 $\tau(T)$

$$= \frac{(T - T_{max})(T - T_{min})^2}{(T_{opt} - T_{min})[(T_{opt} - T_{min})(T - T_{opt}) - (T_{opt} - T_{max})(T_{opt} + T_{min} - 2T)]}$$

$$\mu_{max} = \begin{cases} pH < pH_{min}, 0 \\ pH_{min} < pH < pH_{max}, \mu_{opt} * \rho(pH) \\ pH > pH_{max}, 0 \end{cases}$$

$$\rho(pH) = \frac{(pH - pH_{min})(pH - pH_{max})}{(pH - pH_{min})(pH - pH_{max}) - (pH - pH_{opt})^2}$$

(2.14)

$$\mu_{max}(T, pH) = \mu_{opt} \tau(T) \rho(pH)$$

(2.15)

FIGURE 2.0.2 shows the shape of Equations 2.13 and 2.14 and the interpretation of the cardinal temperatures and cardinal pHs. Note that the influence of pH on cardinal model for temperature (Figure 2.0.2A) and the influence of temperature on cardinal model for pH (Figure 2.0.2B) affects only μ_{opt} parameter (maximum μ_{max} reached for each one of the curves), but does not influence the cardinal temperatures and pHs.

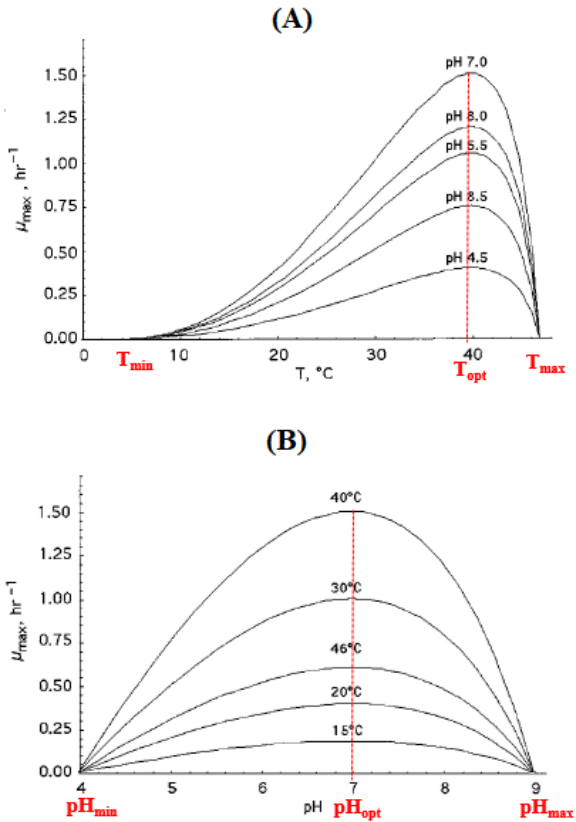


Figure 2.0.2 - (A) influence of pH on cardinal model for temperature and (B) influence of temperature on cardinal model for pH. Adapted from Rosso et al (1995).

Later, Rosso and Robinson (2001) suggested an analogous cardinal model for the effect of water activity on the growth rate of moulds, presented in Equation (2.16), and since then has been generalized to be used for a wide range of microorganisms.

$$\mu_{max} = \begin{cases} aw < aw_{min}, 0 \\ aw_{min} < aw < aw_{max}, \mu_{opt} * \alpha(aw) \\ aw > aw_{max}, 0 \end{cases}$$

$$\alpha(aw) = \frac{(aw - aw_{max})(aw - aw_{min})^2}{(aw_{opt} - aw_{min})[(aw_{opt} - aw_{min})(aw - aw_{opt}) - (aw_{opt} - aw_{max})(aw_{opt} + aw_{min} - 2aw)]} \quad (2.16)$$

Note that the proposed model for water activity has the same structure as the cardinal model for temperature described in Equation 2.13. The three independent models (Equations 2.13; 2.14 and 2.16) combined can be used to predict growth rates and while there is influence of each of the factors on it, there is no interaction between the factors. This methodology is called gamma approach (ZWIETERING et al, 1996), and can be summarized by Equation 2.17.

$$\mu_{max}(T, pH, aw) = \mu_{opt} \tau(T) \rho(pH) \alpha(aw) \quad (2.17)$$

The authors also suggest that the gamma concept can be extended to a wide range on environmental factors affecting the microorganism growth.

2.2.3 Bias factor

The bias factor, proposed by Ross (1996) and shown in Equation 2.18, is an index largely used to evaluate predictive models performance and to validate its predictions, once it assess the level of reliability the user can have in the predictions of the model and whether the model shows any bias which could lead to ‘fail-dangerous’ predictions, when the growth of the microorganism is underestimated or the inactivation is overestimated.

$$\text{bias factor} = 10^{(\sum(\log(GT_{\text{predicted}}/GT_{\text{observed}})/n))} \quad (2.18)$$

where $GT_{\text{predicted}}$ is the generation time predicted, GT_{observed} is the observed generation time and n is the number of observations. The generation time

values can be substituted by growth rates or inactivation rates in the equation, depending on the evaluation, since the log transformation makes it indifferent whether a variable or its reciprocal is used in its argument.

Ross (1996) suggested that this index can also be used to characterize the discrepancy between food and broth models for growth rate dependency with temperature. Since predictions (μ_{pred}) of commonly used software packages are often based on experiments carried out in culture medium broth, while practical observations (μ_{obs}) refer to food, the above expectation can be translated to

$$\text{bias factor} = 10^{(\sum(\log(\mu_{\text{food}}/\mu_{\text{broth}})/n))} \quad (2.19)$$

When the average of the $\ln(\mu_{\text{food}}) - \ln(\mu_{\text{pred}})$ values is taken, it is implicitly assumed that the probability distribution of this difference is independent of the temperature and possibly other environmental factors (MELLEFONT et al, 2003; NEUMAYER et al, 1997; BUCHANAN & BAGI, 1997; GILL & PHILIPS, 1985); otherwise it would not be very useful to take their average as a function of the conditions. The temperature-independence of the bias-factor is a reasonable assumption in case of the temperature, conceiving that all affecting biochemical reactions speeding up or slowing down at the same proportion when temperature changes. The assumption of temperature-independent bias factor is equivalent to the existence of a minimum growth temperature for the studied organism that is the same for the model and for the matrix on which the model is tested as shown in Equation 2.20a and 2.20b. This assumption has been made by quite a few authors (MILES et al, 1997; CARLIN et al, 2013; ARYANI et al, 2015; ARYANI et al, 2016; BUSS DA SILVA et al, 2017). Therefore, if Ratkowsky model is used to model growth rate dependency with temperature, the bias factor can be calculated by means of Equation 2.21.

$$\sqrt{\mu_{\text{broth}}} = b_{\text{broth}}(T - T_{\text{min}}) \quad (2.20a)$$

$$\sqrt{\mu_{\text{food}}} = b_{\text{food}}(T - T_{\text{min}}) \quad (2.20b)$$

$$\text{bias factor} = \left(b_{\text{food}} / b_{\text{broth}} \right)^2 \quad (2.21)$$

where T_{\min} is the medium-independent theoretical minimum temperature for growth; b_{food} is the regression coefficient (slope) for Ratkowsky model in food and b_{broth} is the regression coefficient (slope) for Ratkowsky model in culture medium.

2.2.4 Effect of stress on microorganisms growth at population level

As mentioned before, one of the major unsolved problems of Predictive Microbiology is modelling the lag period preceding the exponential growth phase of bacteria. Unlike the maximum specific growth rate, the lag time depends on the cells history, not only on the actual growth environment. The issue is even more complex when the cells have gone through a sub lethal stress environment, such as high temperature, low pH, and high salt concentration; In this case, the cells would need an extra adaptation period to the new environment compared to the case when they were not stressed at all.

A frequent observed bacterial growth pattern under stress conditions, so-called “phoenix phenomenon”, was first described by Collee et al (1961) for *Clostridium perfringens* grown at 50°C. This phenomenon was characterized by a decrease in viable-cell numbers immediately after inoculation, followed by an increase to the level of the initial count and a subsequent continued increase beyond the inoculum-level count. In later work (PARKHILL et al, 2000) the initial decrease and increase in count were shown to be caused by an injury-and-recovery process that could be eliminated by using strictly anaerobic conditions during dilution and plating. (KELLY et al, 2003).

Similar behaviour was observed by Zhou et al. (2012) when evaluating *Salmonella* growth from different osmotic histories in low water activity conditions. Cell cultures were successfully diluted and grown in batch, without and with NaCl, several times and from different inoculum levels. The viable count curves present the phoenix phenomenon, as shown in FIGURE 2.0.3. What is more, the results suggest that periodic, systematic “training” can improve the adaptation capability of the organism to the stress condition, without resulting in a higher growth rate.

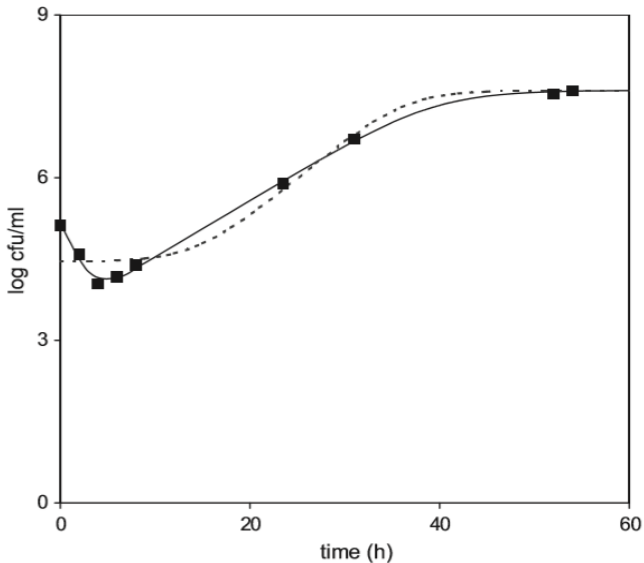


Figure 2.0.3 - Viable counts for *Salmonella spp.* in culture medium with 3% salt. From: Zhou et al. (2012).

In some other studies, the effect of stress on the growth is revealed by simply a longer lag phase with no prior decline on the population counts, like reported by Augustin et al (2000) when studying *Listeria monocytogenes*. In their research, it was found that the more severe is the stress, the longer is the adaptation needed to the microorganism start dividing.

2.2.5 Effect of stress on microorganisms response at single-cell level

Bacterial growth is traditionally seen as the result of symmetrical cell division generating a genetically identical progeny. However, it has long been documented that within isogenic populations, bacterial cells can present different phenotypes (VEENING et al, 2008). This microbial cell individuality or phenotypic variation is getting increased attention because of its relevance for cellular differentiation and implications for the treatment of bacterial infections (SMITS et al, 2006). Amazingly, many documented cases of phenotypic variability relate to responses to environmental stresses, suggesting that phenotypic variation supports the

survival of cells under adverse conditions and therefore may be a gradually developed feature.

In some cases, the described heterogeneity is manifested by the bifurcation into distinct subpopulations, being this phenomenon called “*bistability*” (DUBNAU & LOSICK, 2006). Such behaviour has been reported by many authors (KOIRALA et al, 2014; MAISONNEUVE & GERDES, 2014; VEENING et al, 2008; DUBNAU & LOSICK, 2006) at phenotypic and genotypic levels, but so far, no study has been performed on the effect of a heat stress on the kinetic behaviour of survival single cells of *B. cereus*.

Similarly to the population level, it is expected that a stressful environment (or a pre-stress) would increase the single cell lag times and influence also the probability of growth of the survival (but maybe injured) cells. Kotalik et al (2005A) studied how different NaCl concentrations influence the individual lag times. As can be seen in FIGURE 2.0.4, for *Salmonellae*, an increase on NaCl concentration in the growth medium results in a larger mean (individual) lag time and wider spread in distribution. The same result was found previously by Robinson et al. (2001) and by Augustin et al (2000) when investigating the effect of the inoculum size on the lag times of *Listeria monocytogenes*.

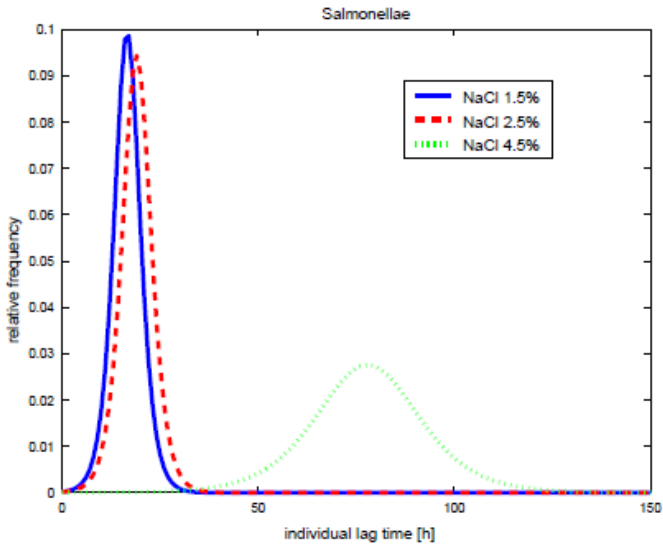


Figure 2.0.4 - Probability density functions of individual cell lag times for different NaCl concentrations. From: Kutalik et al (2005A).

Lately, more and more studies concentrate on single cell lag times (ELFWING et al 2004; FRANÇOIS et al 2005; KUTALIK et al 2005B; PRATS et al 2008; PIN & BARANYI, 2008; BARANYI et al, 2009; ASPRIDOU et al, 2018). The reason for this is that, in practice, pathogenic contamination is frequently caused by a few cells only.

An easy way to assess single cell lag times is by means of turbidity measurements, while there is no easy way to sort single cells into the wells of the Bioscreen microtitre plates. The usual procedure is that cultures are diluted to a level such that a sample in a well should contain only a few cells. With a sufficiently high dilution factor, the majority of the wells will receive zero or one cell (BARANYI et al, 2009). The disadvantage is that many wells will be empty and, for a statistically robust distribution estimation, it is desirable to have as many positive wells as possible, a minimum of about one hundred (BACANOVA, 2004).

The same experimental design described above can be used to calculate the probability of growth of single cells (or fraction of cells able to divide) and compare these values for stressed and non-stressed cells.

This procedure described above have not been used so far with the purpose of investigating differences on the probability of growth of stressed and non-stressed single cells under growth-supporting conditions, so this is one of the objectives of this study, using *B. cereus* as a model organism and a pre heat-treatment as stress condition.

3. *B. CEREUS* GROWTH IN RECONSTITUTED INFANT FORMULAE (RIF) AND CULTURE MEDIUM AT SUBOPTIMAL TEMPERATURES

3.1 Introduction

Bacillus cereus can endure ultrahigh-temperature (UHT) pasteurization, resist spray drying and survive in final products (MCAULEY et al., 2014). What is more, according to a review published by the European Food Safety Agency (EFSA, 2005), *B. cereus* strains are highly variable in terms of their tolerance to high temperatures and their ability to grow. This is mainly dependent on their phylogenetic group (CARLIN et al. 2013). Mathematical modelling can be a valuable tool to assess and quantify this variability. Understanding how this microorganism behaves after going through a heat stress in different matrices is vital for the food industry. As mentioned in the Literature Review (Chapter 2), a heat stress could affect the adaptation period of the microorganism to the new environment, the lag phase, while a different growing matrix must have an effect on the growth rate of the microorganism. Moreover, establishing an approach to obtain a constant correction factor between food and culture medium-based models that can be somehow generalized to other foods and microorganisms would be valuable for the food industry, since developing and validating a new model to predict microbial behaviour during the manufacturing or the shelf life of a food commodity require extensive experimental work.

To quantify the similarity between prediction in culture medium and observation in food matrices, the accuracy and bias factors, Af and Bf , of Ross (1996) are commonly used for practical applications. A bias factor $Bf = 1$ means that, in a studied region, on average, the model predictions in culture medium are neither over-estimating nor under-estimating the growth rate compared to the observations in the food matrix. However, this could happen in such a way, too, that the predictions are underestimations in one part of the region while they are overestimations in the other part. It would be desirable that, for a certain matrix, the bias factor is independent of the environmental conditions, primarily of the temperature, at least in the normal physiological growth region of the organism in question. In this case, culture-medium-based predictions, could be readily applied to the food in question. Since culture media

provide optimal substrate for the organism, the bias factor should normally be less than 1.

This chapter presents the results of plate counts measurements of *Bacillus cereus* growing in RIF and BHI under suboptimal temperatures after going through or not a heat stress. The main objective is to evaluate the effect, if any, of the growth factors - such as matrix and stress - on the growth parameters and also to study how to better apply culture-medium-based models to food scenarios. The paper published as part of this PhD thesis entitled “From Culture-Medium Based Models to Food Based Models: Application to Predict *B. cereus* Growth in Reconstituted Infant Formulae” enclosed in ANNEX F is a significant part of this investigation and gave support to the assumptions and investigations made during this chapter.

3.2 Material and Methods

The experiments described below were performed in two different laboratories and every time there were different practices among them the respective text is identified as *IFR* (Institute of Food Research, Norwich, UK) and/or *NRC* (Nestlé Research Center, Lausanne, Switzerland).

3.2.1 *Bacillus cereus* growth in RIF and BHI

3.2.1.1 Strain preparation

IFR: Three strains of *Bacillus cereus* were studied (B594, B596 and B577). After streaking each strain onto TSAye (Trypticase Soy Agar with 0.6% Yeast Extract) and incubating for 24 h at 37 °C (to check for purity), one isolated colony was picked into BHI (Brain Heart Infusion) broth and incubated for 24 h at 37 °C. Then, 1 mL of the culture was added to 1 mL of sterile 80% glycerol and 100 µL of this mixture was put into sterile screw cap tubes and stored at -80 °C. One tube was used for each experiment.

NRC: Stock cultures for five strains of *B. cereus* (B594, B596, B626, B635 and B577) were used in these experiments. To prepare the cryotubes, one cryobead of each strain from the Nestlé Pathogen Culture Collection (NPCC) was placed into a BHI (Oxoid™, Hampshire, UK) tube using a sterile needle and incubated for 8h at 37°C. After performing a second culture for 18h at the same temperature, the purity of the suspension was checked by streaking 10 µl of the suspension on a TSAye plate (Oxoid™, Hampshire, UK and Merck, Kenilworth, USA) to

achieve isolated colonies. If the suspension is pure, well-isolated colonies (until the loop is filled with colonies) were taken with a sterile plastic loop and put into a cryotube. After 1 minute of shaking, the tube was left for an additional minute, then the cryoprotectant was removed and the cryotube stored at -18°C until used. Two working tubes were prepared for each strain and stored at -18°C .

3.2.1.2 Temperature control

IFR: The water baths probes readings were checked against certificated thermometer to set up the required temperatures for the storage experiments. The probes were put into bottles containing 50 mL of water to represent samples. Temperature was measured every ten minutes and the average temperature for each experiment was considered in the analysis.

NRC: Incubators were used and their temperature measured each five minutes using a specific probe. The average temperature for each experiment was considered in the analysis.

3.2.1.3 Determining heat up and cool down times

To determine the heat up and the cool down times, a heating process was simulated and, with a probe sealed inside a tube containing 10 mL of water (at the same initial temperature of the milk ($\sim 45^{\circ}\text{C}$)), the temperature was measured at each 0.5 s. The heat up time is the time needed to the water to reach 72°C and the cool down time is the necessary time to cool it down to 22°C . This process was repeated three times to check reproducibility.

3.2.1.4 Inoculum preparation

IFR: One tube of frozen stock culture was taken out and put into 10 mL of BHI and incubated for 24h at 30°C . Then 100 μL of this culture was put into another 10 mL of BHI and incubated for 18h at 30°C .

NRC: Under aseptic conditions, the cryotube of the strain of interest was opened and one of the beads was removed using a disposable plastic needle and placed into a BHI tube. The vial was quickly re-capped and returned immediately to the freezer. The BHI tube was incubated for 8h at 30°C . A second culture was then performed taking 100 μL of the previous and inoculating another BHI tube stored for 18 hours at 30°C to achieve a final concentration of 10^8 CFU/mL. In order to prepare the inoculum, 0.1 mL of the final subculture was diluted into 100mL of the

targeted medium (BHI or Reconstituted Infant Formulae (RIF)) to achieve a concentration of 10^5 CFU/mL for the inoculum.

3.2.1.5 Stress characterization

The subculture was enumerated on selective media (Bacara, bioMérieux) to assess the concentration prior to stress. The tube containing 10 ml of BHI was preheated at 72 °C according to the heating up time, the pressure was released with a sterile needle and 100 μ L of the subculture was injected into preheated tube. After 25 seconds, the tube was removed from the waterbath and cooled down to 22 °C during the pre-established cooling down time. The culture was then enumerated on Bacara plates to assess the concentration after stress. The log reduction due to the heat stress was then calculated. The procedure was repeated three times to B577, B594 and B596 strains.

3.2.1.6 Temperature effect on *B. cereus* growth

In laminar flow cabinet, infant formulae powder was weighted into sterile bottle and warm ($\sim 50^\circ\text{C}$); sterile water was added and then mixed to dissolve. The reconstituted infant formula (RIF) was dispensed into sterile tubes of 10 ml for heat treatment and sterile bottles of 50 ml for storage experiments. Initial pH was measured. Two bottles, one inoculated and one control, at each temperature were pre-incubated to reach the storage temperature by the moment of inoculation. A tube of RIF was preheated at 72 °C for 3.5 minutes and the pressure was released when hot. The subculture (100 μ l) was injected and after 25 seconds the tube was removed to cool down for 20 seconds in a mixture of ice and water. At each storage bottle, 0.5 ml of the heated milk was added and samples for viable counts were taken (in triplicate) during a pre-establish time. For B577 and B596 strains, seven storage temperatures were studied: 9, 12, 15, 18, 22, 25, and 30 °C. For the B594 strain, the five investigated temperatures were: 9, 12, 15, 18, and 22 °C. For B626 and B635 strains, six temperatures were studied: 12, 15, 18, 22, 25, and 30 °C. For the storage experiments with unheated cells, the subculture was diluted (1/100) and 0.5 mL of the dilution was added to the 50mL bottle of RIF and stored at 22 °C. Selective medium plates (Bacara, bioMérieux) were used for the plate counts during the storage experiments. The pH of the control bottle of milk was measured in the beginning and in the end of the experiment for all the temperature conditions and for the F4810/72,

B626 and B635 strains, the pH of the inoculated bottles was measured along the storage time as well. The same procedure was used for experiments performed in culture medium (BHI (Oxoid™, Hampshire, UK)).

3.2.1.7 Experimental design

The experimental design of the performed experiments is presented in Table 3.0.1. It is important to notice that only B577 strain has curves in both matrices with heated and unheated cells and, since it is also the reference strain for the emetic group of *B. cereus*, it was chosen to characterize the effect of these factors on growth parameters. B594 strain has no growth curves in culture medium, making it unmanageable to assess any link between the two matrices for this specific strain.

Table 3.0.1 - Experimental design for *B. cereus* growth experiments in RIF and BHI.

Strain	Matrix	Stress	Number of growth curves at different temperatures
B577	BHI	Heated	5
		Unheated	12
	RIF	Heated	15
		Unheated	10
B594	BHI	Heated	0
		Unheated	0
	RIF	Heated	12
		Unheated	2
B596	BHI	Heated	0
		Unheated	6
	RIF	Heated	12
		Unheated	9
B626	BHI	Heated	0
		Unheated	12
	RIF	Heated	0
		Unheated	12
B635	BHI	Heated	0
		Unheated	12
	RIF	Heated	0
		Unheated	12

3.2.1.8 Primary and secondary modelling procedure

The primary growth model parameters were obtained through the fitting the model of Baranyi and Roberts (1994) described by Equation 2.5 to isothermal *B. cereus* growth data by the DMFit Excel Add-in downloadable from the ComBase web site (www.combase.cc). As for the quality of fitting assessment, (standard error $(\mu_{\max})/\mu_{\max}$)<0.60 was kept as the only criteria and it was based on visual observation of data against fitted curves. Then, the square-root model of Ratkowsky (1982) presented in Equation 2.12 was used to describe the effect of temperature on the growth rate. For the h_0 parameter, the estimations and their standard deviations were compared to analyse significant differences between strains and medium. For the logarithm of the maximum population density (N_{\max}), as this parameter is generally taken as a constant, only some features related to temperature effect were investigated. An ANOVA analysis was used to identify effect of medium and stress on these two parameters (h_0 and N_{\max}). Strain variability analysis is presented in Chapter 4.

3.2.1.9 Bias factor

The bias factor of Ross (1996) was used to assess the difference between culture medium-based model and food model, following the methodology suggested by Buss da Silva et al (2017), paper published as part of this thesis. For more details, see item 2.2.3 of Literature Review and ANNEX F, where the paper entitled “*From Culture-Medium-Based Models to Applications to Food: Predicting the Growth of B. cereus in Reconstituted Infant Formulae*” is enclosed. In summary, the Ratkowsky model (Equation 2.12) with natural logarithm (\ln) link function and square-root link function was used to regress growth rates against temperature and their differences were investigated. The bias factor will be estimated for each strain based on the link function presenting better performance.

3.3 Results and Discussion

3.3.1 Growth of *B. cereus* in RIF and BHI

The effect of the applied heat stress prior to the *B. cereus* inoculation on the respective population number was 2.00 ± 0.44 log CFU/mL reduction on average. This value is valid for all strains and for both studied media (BHI and RIF). The initial inoculum level was calculated taking this value into account, showing reproducible levels.

3.3.1.1 Primary parameters

FIGURE 3.0.5 gives an example of the results obtained for the growth experiments. Each curve represents the fitted growth curve to the experimental data at a different incubation temperature for B635 strain in BHI.

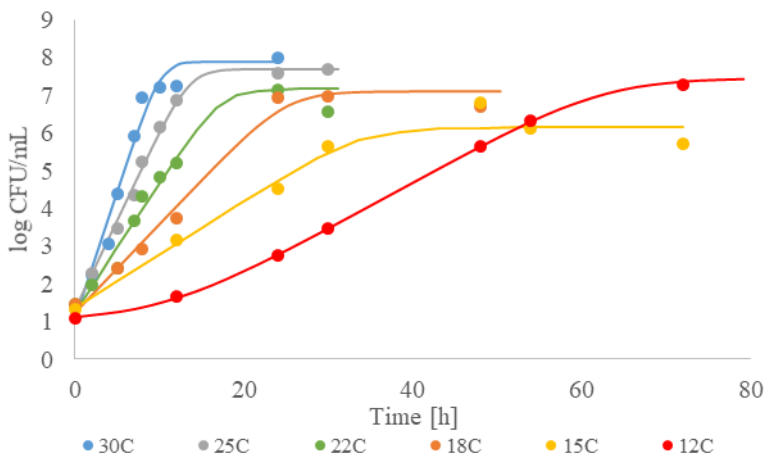


Figure 3.0.5 - Fitted growth curves obtained for B635 strain in BHI at different temperatures: 30 °C in blue, 25 °C in grey, 22 °C in green, 18 °C in orange, 15 °C in yellow and 12 °C in red.

The raw data (log counts vs. time) are presented in ANNEX A and the fittings of Baranyi and Roberts model (1994) to the experimental data performed according to the experimental design (available in TABLE 3.0.1) are in ANNEX B. The primary parameters were analysed separately to investigate the effects of the medium, strain and temperature on them. The physiological state (h_0) allows an assessment of the lag phase and the raw estimates will be used in this analysis, as well as for the maximum population density (N_{\max}), which expresses the upper

asymptote of the growth curve. The specific growth rate parameter (μ_{\max}) was further evaluated through the secondary parameters obtained when fitting the Ratkowsky (1982) model to the different estimates at the studied temperatures. Based on quality of fitting criteria, only one growth curve was excluded from the following analysis. It is important to mention that only B635 strain was able to grow at the temperature of 10 °C (turbidity observation of an inoculated BHI tube), therefore all the other strains tested at 9 °C were not able to produce a growth curve, making these experiments not considered for further analysis.

3.3.1.1.1 The physiological state (h_0)

The lag phase of the different experiments performed will be investigated through h_0 parameter ($h_0 = \text{lag} * \mu_{\max}$). As explained in the Literature Review (Chapter 2), a previous-to-inoculation stress could have an effect on the lag phase, so that was the first assumption investigated through h_0 . Merging temperature (assuming it does not have an influence on h_0 , as its own definition says), but keeping stress and medium factors separately and running an ANOVA analysis on these data for B577 strain (which is the reference strain for the emetic group and the only one with experiments performed with all possible combinations of stress and medium), it is possible to observe there is no significant difference ($p=0.35$) among heated and unheated cells, but there is an effect of medium ($p=0.00044$), with h_0 values bigger in BHI than in RIF. Since no significant longer lag time was identified for heated cells, heated and unheated data can be merged for further analysis. It is possible that the microbiological variability is bigger than the effect of stress on h_0 , making it not possible to observe the significant difference. Or even the heat treatment was not strong enough to change the cells physiological state. TABLE 3.0.2 was built to identify trends in terms of stress effect on h_0 and it can be seen that, on average, h_0 values are bigger for heated cells, even though the uncertainty (here characterized by the standard error) is quite big, being up to two times the actual h_0 value.

Table 3.0.2 - Average of h_0 values for each heated and unheated strain at each medium and average of h_0 values for all heated and unheated strains at each medium.

Strain	BHI				RIF			
	heated		unheated		heated		unheated	
	h_0	st dev(h_0)	h_0	st dev(h_0)	h_0	st dev(h_0)	h_0	st dev(h_0)
B577	2.83	0.52	2.27	1.74	1.67	0.61	0.44	0.88
B594	x	x	x	x	1.26	0.42	0.63	0.89

B577	2.64	3.56	2.63	1.75	1.82	2.8	2.53	0.75
B596	2.68	0	2.71	1.92	1.33	1.93	1.76	1.01
B626	2.16	2.89	3.74	1.43	1.08	2.15	2.24	1.08
B635	0.69	0	0.76	0	0.67	0.67	0.46	0.38
B594	x	x	x	x	x	x	x	x

RIF

Strain	12 °C	15 °C	18 °C	22 °C	25 °C	30 °C	average	st. dev.
B577	1.67	1.91	0.86	1.22	1.37	0	1.17	0.68
B596	1.72	2.14	1.48	1.35	0.76	1.63	1.51	0.46
B626	1.34	1.16	1.44	1.5	0.43	1.52	1.23	0.41
B635	0	0	0	0	0	0	0.11	0
B594	0.48	1.06	1.41	1.5	x	x	1.11	0.46

x = no available data.

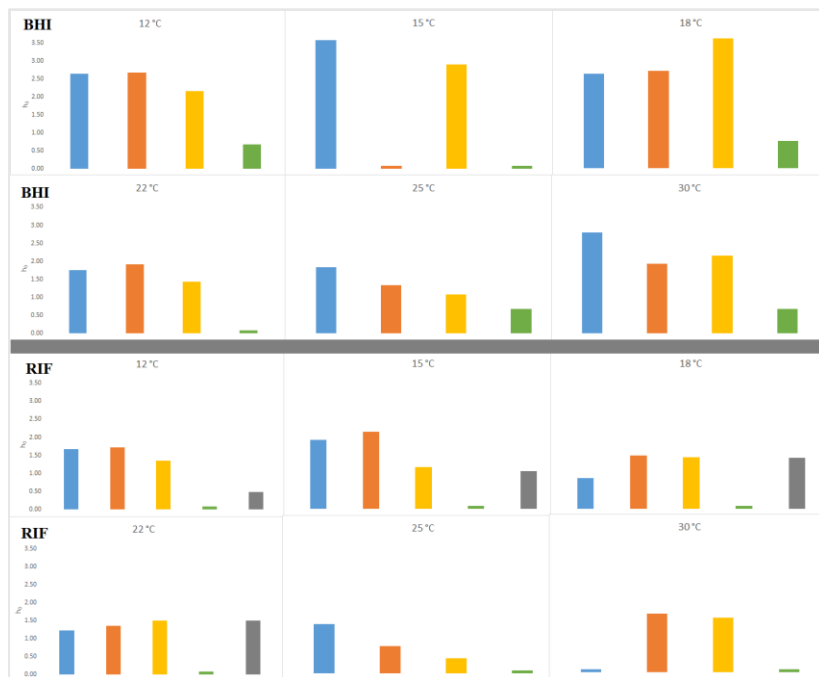


Figure 3.0.7 - h_0 values for BHI (first two rows) and RIF (last two rows) at different temperatures. B577 strain in blue, B594 in grey, B596 in orange, B626 in yellow and B635 in green.

Looking at the histograms presented in FIGURE 3.0.7 built with h_0 data presented in TABLE 3.0.3 it is possible to see the lower tendency on the h_0 values for RIF when compared to BHI and also the B635 lower h_0 values (most of the times equal to zero) for the same factor. As for the temperature influence on the h_0 values, it is possible to say that higher h_0 values come from the three lowest temperature investigated (18, 15, and 12 °C). Grouping h_0 data for BHI and for RIF for all strains, replicates and temperatures, we obtain an average \pm standard deviation of 1.79 ± 1.39 and 1.17 ± 0.80 for BHI and RIF respectively. For a statistical analysis (t-Test: Two-Sample Assuming Unequal Variances, in Excel), one can conclude again that RIF and BHI are significantly different for this factor (p-value = 0.0089). This was already expected, once the inoculation medium in different and h_0 parameter is affected by both the history of cells and the current growing environment. Also, growth rates in RIF are lower than in BHI, as it will be analysed in section 3.3.1.1.3.2,

and the h_0 value is obtained by the multiplication of the growth rate and the lag time for the condition in question.

3.3.1.1.2 Maximum population density (N_{\max})

Taking into account the estimated N_{\max} coming from the fitting of the primary model (ANNEX B), the following observations could be derived.

FIGURE 3.0.8 shows that for strains B577, B594, B626 and B596 there is an increasing trend when temperature increases in BHI medium, while in RIF the maximum population reached does not show any visual relationship with temperature for conditions above 15 °C (FIGURE 3.0.9). This might be explained by the presence of a probiotic strain within the RIF (KENT & DOHERTY, 2014). Thus, in a monoculture in BHI medium the temperature dependency was easier to observe, however, when co-cultured with another micro-organism in RIF matrix, the N_{\max} reached by the *B. cereus* strains did not show any temperature dependency in non-refrigerated temperatures. It is also possible to say that at 12 °C there is a bigger variability on the estimated N_{\max} values for the different strains, due to the fact this condition is closer to the boundaries for growth when compared to the others. A previous study (LIANOU & KOUTSOUMANIS, 2011) already suggested that variability among microbiological growth data was larger when the growth conditions became unfavourable.

Based on the ANOVA analysis output, there is no effect of stress ($p=0.39$), significant effect of medium ($p=0.00053$) and no interaction between these factors ($p=0.24$) on N_{\max} . In general, this parameter can be considered constant (not expressively different between strains and replicates) for temperatures ranging from 15 to 30 °C, being equal to 7.18 ± 0.58 for BHI and 8.08 ± 0.31 for RIF. For B635 strain, no visual pattern for N_{\max} with the temperature could be concluded, either in RIF or BHI.

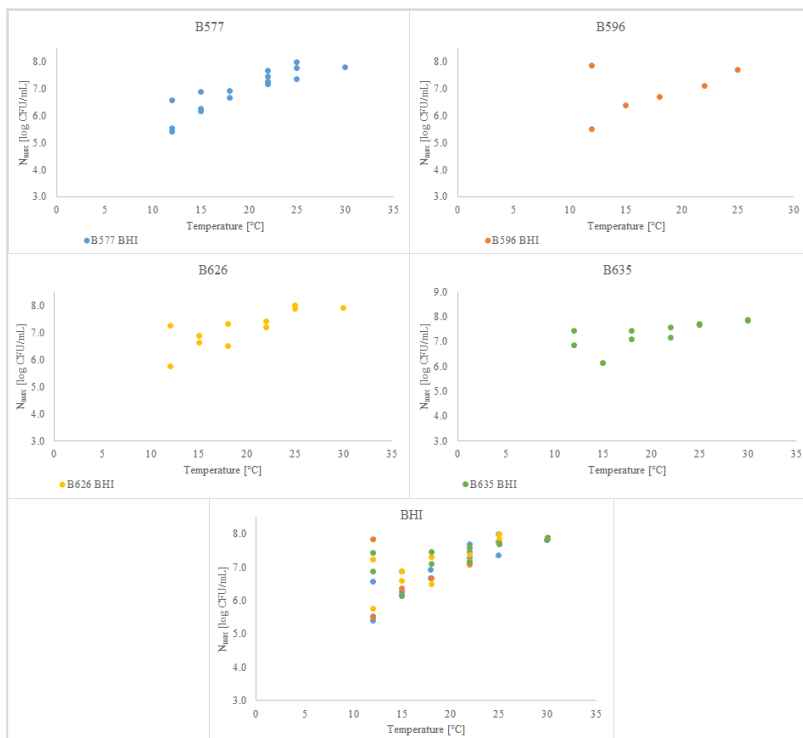


Figure 3.0.8 - Maximum population density (N_{max} [log CFU/ml]) as a function of temperature obtained in BHI for strains B577 (in blue), B596 (in orange) B626 (in yellow) and B635 (green).

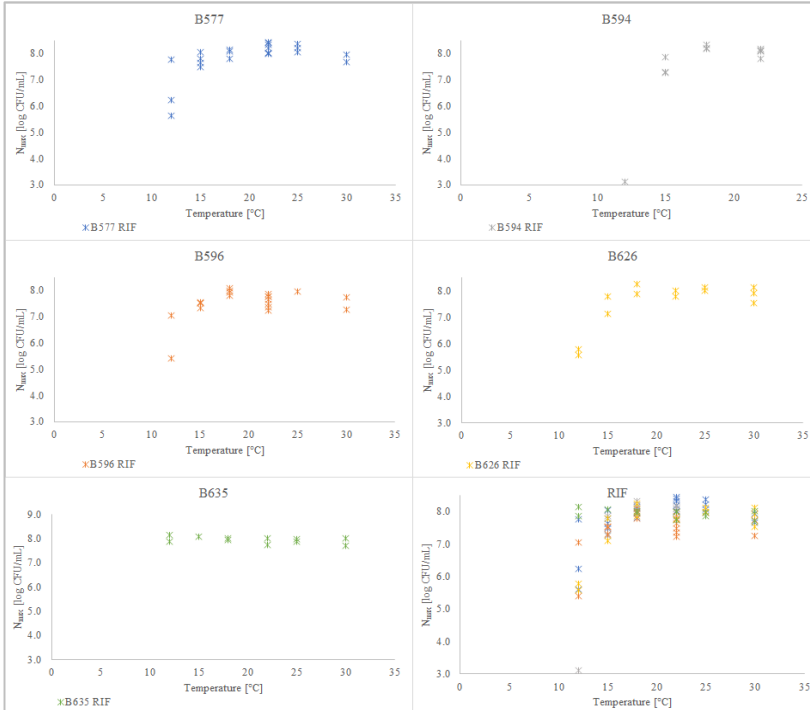


Figure 3.0.9 - Maximum population density (N_{max} [log CFU/ml]) as a function of temperature obtained in RIF for strains B577 (in blue), B594 (in grey), B596 (in orange) B626 (in yellow) and B635 (in green).

3.3.1.1.3 Growth rate

In the same way as h_0 and N_{max} , the growth rate was estimated by fitting the Baranyi and Roberts model (Equation 2.5) to the raw data for each experiment performed and its features will be analysed by means of the secondary parameters when studying the dependency of the growth rate with the temperature.

3.3.1.1.3.1 Secondary modelling

As for the growth rate dependency with temperature, to perceive medium and strain variability, the parameters of Ratkowsky model (Equation 2.12) were estimated for the five strains investigated and the results are presented in Table 3.0.4. At this stage, all growth rates from stressed and non-stressed cells were considered since there was no significant difference among them (p -value > 0.05).

Table 3.0.4 – Parameters, confidence intervals (between brackets) and the coefficient of determination from fitting of Ratkowsky model for B577, B594, B596, B626 and B635 in RIF and BHI.

Medium	Strain	b [CI] ($\text{h}^{-1/2}/^\circ\text{C}$)	T_{\min} [CI] ($^\circ\text{C}$)	R^2
BHI	B577	0.0569[0.0483;0.0655]	4.27[1.87;6.67]	0.9220
BHI	B596	0.0544[0.0468;0.062]	4.13[1.69;6.57]	0.9757
BHI	B626	0.0535[0.0461;0.0609]	3.00[0.48;5.52]	0.9502
BHI	B635	0.0472[0.0406;0.0538]	2.15[-0.55;4.85]	0.9479
RIF	B577	0.0467[0.0419;0.0515]	5.25[3.63;6.87]	0.9381
RIF	B594	0.065[0.054;0.076]	9.44[7.80;11.08]	0.9256
RIF	B596	0.0527[0.0471;0.0583]	6.53[5.13;7.93]	0.9449
RIF	B626	0.0545[0.0501;0.0589]	5.23[3.91;6.55]	0.9798
RIF	B635	0.0395[0.0347;0.0443]	0.919[-1.661;3.499]	0.9628

Assuming a normal distribution for the sample, the confidence intervals were calculated from the estimates plus or minus two times the associated standard errors. It is important to notice that there are no significant differences between T_{\min} from BHI and RIF for each strain once their confidence intervals overlap.

The plots in FIGURE 3.0.10 show the square root of the growth rate against temperature and although the growth rates estimate looks similar to each other, the trends are different among the strains. For example, in RIF, B635 has the highest rates in lower temperatures and lower rates at higher temperatures when compared to the other strains trend, while the B626 strain show the opposite pattern, with the highest rates in high temperatures.

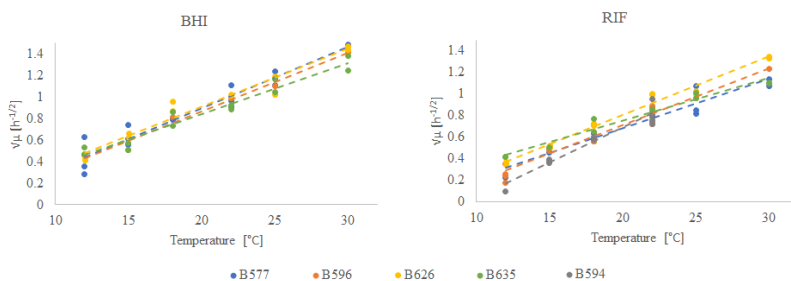


Figure 3.0.10 - Ratkowsky model fittings in BHI and RIF with strains B577 in blue, B594 in grey, B596 in orange, B626 in yellow and B635 in green strains.

A simple and very visual way to compare these estimated secondary parameters with others strains of *B. cereus* is by means of the so-called b-line (BARANYI et al., 2017). In their study, the authors found a biological relationship between the parameters b and T_{\min} for twelve strains of *B. cereus sensu lato* divided into six different phylogenetic groups, presented in Figure 3.0.11 as black dots. The four strains (B577, B596, B626 and B635) to which it was possible to build a model in BHI are shown in red dots in the same in Figure 3.0.11 and the interesting fact is that they are in great accordance with the trend defined by the b-line. This is a thought-provoking finding, because it means the kinetic parameters of a *B. cereus* strain do not arbitrarily scatter in the 4D-space. This finding was evident for the cardinal temperatures, but has so far been unknown for the b parameter.

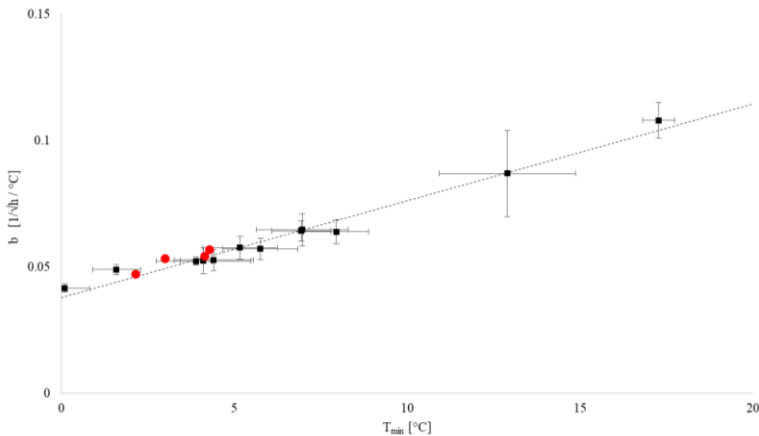


Figure 3.0.11 - B-line showing the correlation between b and T_{\min} parameters from Ratkowsky model. In black, data and trend published by Baranyi et al (2017). In red, four strains (B577, B596, B626 and B635) from this work.

3.3.1.1.3.2 Bias factor

The maximum specific growth rate of the strains B577, B596, B626 and B635 were measured in both RIF and BHI, providing a good opportunity to investigate the bias between food and culture medium models.

The main concern about the bias factor estimation is regarding which link function would make it constant with the temperature, without adding a tendency to it.

A first investigation was already published as part of this thesis (see ANNEX F) and here in this section the subject will be further studied once more data was produced since then. As in the referred publication, the two link functions investigated are the square-root and the natural logarithm of the parameter, once they are known as functions that stabilize the variance around the model, feature required to have a constant-with-temperature bias factor.

Plots with square-root of the growth rates against temperature were prepared for each strain separately differentiating between the estimates in RIF and BHI and Ratkowsky model (Equation 2.12) was fitted to the data. The same procedure was repeated using the natural logarithm link-function. It is important to remember that the only assumption made so far is that each strain has the same T_{\min} in both media (DELIGNETTE-MULLER & ROSSO, 2000), and in fact it was already confirmed by the confidence interval analysis on the previous section: the estimated T_{\min} in BHI and RIF for the same strain were not different at 95% significance level.

For both link functions, the absolute residuals were analysed to check if any trend with temperature can be inferred and a summary of the statistical analysis is shown in TABLE 3.0.5. The link function that showed better performance in stabilizing the data variance around the model seems to be the square-root(μ_{\max}), once there was no correlation of the residuals with temperature at 95% significance level (p-value>0.05) for all strains and media (see Figure 3.0.12). For this reason, the square-root link function was selected to estimate the bias factor in the present work and the respective values are presented in Table 3.0.6.

This finding is not in accordance with the findings published in Buss da Silva (2017). In that publication, the natural logarithm link function seemed to be more appropriate for that data-set. Based on those *B. cereus* data, the logarithm link function was more suitable to be applied to the observed maximum specific growth rates when regressing them against temperature to obtain the discrepancy between growth media. It is important to notice that the authors had data coming from different sources and taken from different measurement methods and also the bigger scatter of the data (and consequently the major difference between the two link functions residuals) occurred at low temperatures, just as it is observed here. At these conditions it is not easy to keep the environment constant for the required long time to reach the stationary phase, therefore the environmental effects (ex. pH decrease in the medium) rather than biological ones (linked to strain variability for example) can dominate the

variance of the observed maximum specific growth rates (BUSS DA SILVA et al, 2017).

Table 3.0.5 - p-values from analysis of correlation of absolute residuals with temperature.

Strain	Square-root link function		Natural logarithm link function	
	BHI	RIF	BHI	RIF
B577	0.055	0.473	<i>0.04*</i>	<i>0.032*</i>
B596	0.137	0.341	0.163	<i>0.024*</i>
B626	0.885	0.899	0.933	0.06
B635	0.673	0.323	0.383	0.863

*In italics, conditions where there was correlation between the absolute model residuals and temperature at 95% significance level ($p < 0.05$).

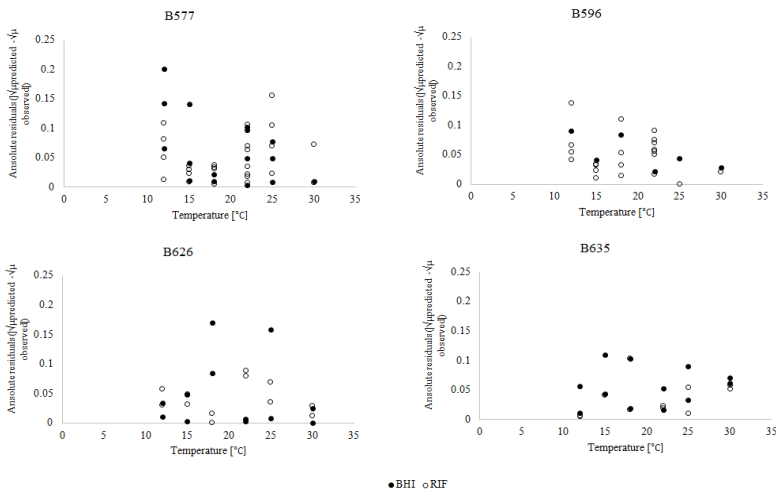


Figure 3.0.12 - Absolute residuals for square root link function. BHI in full dots and RIF in empty dots.

Observing the plots presented in Figure 3.0.13, for all the strains there is a gap between the growth rates in RIF and the ones in culture medium, the latter one being always bigger, as expected. For the different strains, different *bias factors* were obtained using the square-root link function, suggesting this factor is strain dependent. It is important to

comment that the biggest bias factor was obtained for B626 strain, to which the smallest gap between BHI and RIF curves can be observed as well. A bigger bias factor (closer to 1) indicates a smaller disagreement between growth medium and food growth rates.

Table 3.0.6 – Bias factors between BHI and RIF media estimated for each strain with square-root (μ_{\max}) link function.

Strain	bias factor
B577	0.60
B596	0.70
B626	0.81
B635	0.79

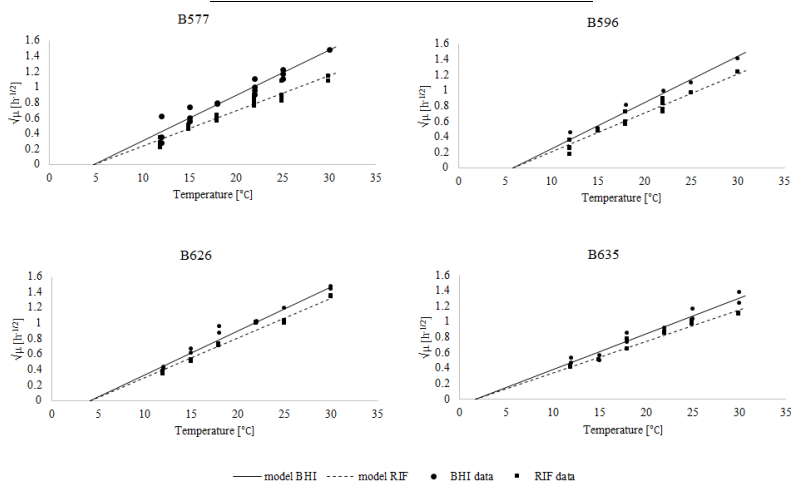


Figure 3.0.13 -Square-root (maximum specific growth rates) vs. temperature data and fitted models for medium variability observation and bias factor assessment for B577, B596, B626 and B635 strains in RIF (squares; dashed line) and BHI (circles; continuous line).

3.4 Conclusions and Considerations

In this chapter, the analysis considered viable count measurements, focusing on evaluating the effect of two factors (stress and growing medium) on the physiological state of the cells (h_0) and on the maximum reached population (N_{\max}), assessing the effect of temperature on growth rates and how to use them to find a correlation between culture medium based models and food models.

The only factor affecting h_0 and N_{\max} parameters is the growth medium, while the heat stress seems to have no significant impact on them. The square-root of the growth rates were regressed against temperature using the Ratkowsky model (1982) and their T_{\min} estimate is not significant different for BHI and RIF models for the same strain, finding that gives support to the bias factor assessment.

Moreover, the bias factor between BHI and RIF growth rates was estimated for each strain using the square-root link function once its residual showed no correlation with temperature.

Strain variability will be discussed in more details during next chapter with a more complete discussion on the boundaries for growth of emetic strains.

3.5 References

BARANYI J.; ROBERTS, T. A. A dynamic approach to predicting bacterial growth in food. **International Journal of Food Microbiology**, v. 23. p. 277-280. 1994.

BARANYI, J.; BUSS DA SILVA, N; ELLOUZE, M. Rethinking Tertiary Models: Relationships between growth parameters of *Bacillus cereus* strains. **Frontiers in Microbiology**, v.8:1890, 2017.

BUSS DA SILVA, N; BARANYI, J; CARCIOFI, B. A. M; ELLOUZE, M. From culture-medium-based models to applications to food: Predicting the growth of *B. cereus* in Reconstituted Infant Formulae. **Frontiers in Microbiology**, v.8:1799, 2017.

CARLIN, F.; ALBAGNAC, C.; RIDA A.; GUINEBRETIÈRE M. H.; COUVERT, O.; NGUYEN-THE, C. Variation of cardinal growth parameters and growth limits according to phylogenetic affiliation in the *Bacillus cereus* Group. Consequences for risk assessment. **Food Microbiology** v. 33, p. 69-76. 2013.

EFSA [European Food Safety Authority]. Opinion of the scientific panel on biological hazards on *Bacillus cereus* and other *Bacillus spp.* in foodstuffs. **The EFSA Journal**,175, 1-48, 2005.

KENT, R. M.; DOHERTY, S. B. Probiotic bacteria in infant formula and follow-up formula: Microencapsulation using milk and pea proteins to improve microbiological quality. **Food Research International**, v.64, p.567–576, 2014.

LIANOU, A.; KOUTSOUMANIS, K. P. Effect of the growth environment on the strain variability of *Salmonella enterica* kinetic behavior. **Food Microbiology**, v. 28, p.828-837, 2011.

RATKOWSKY D.; OLLEY, J.; MCMEEKIN, T. A; BALL, A. Relationship between temperature and growth rate of bacterial cultures. **Journal of Bacteriology**, 149, 1-5, 1982.

ROSS, T. Indices for performance evaluation of predictive models in food microbiology. **Journal of Applied Microbiology**, v.81, p.501–508, 1996.

MCAULEY, C.M.; MCMILLAN, K.; MOORE, S.C.; FEGAN, N.; FOX, E.M. Prevalence and characterization of foodborne pathogens from Australian dairy farm environments. **Journal of Dairy Science**, v.97, p.7402-7412, 2014.

4. CARDINAL VALUES ASSESSMENT OF EMETIC *B. CEREUS* STRAINS IN TERMS OF TEMPERATURE, PH AND WATER ACTIVITY

4.1 Introduction

The *B. cereus sensu lato* phylogenetic construction was recently divided in seven major phylogenetic groups showing clear differences in their ability to grow at low or high temperatures and to cause food poisoning (GUINEBRETIERE et al, 2008, 2010). Part of this broad ability was already shown and discussed during Chapter 3 when mentioning the b-line (BARANYI et al, 2017).

Growth limits for temperature, pH or water activity are major characteristics of foodborne pathogenic bacteria and important determinants of food safety hazards. Numerous approaches have been suggested to predict microbial growth in food and among those Cardinal Parameter Models (CPM) (ROSSO et al, 1995) offer the advantage of being suitable to simulate the effects of different environmental conditions on growth kinetics. CPM parameters have a direct biological interpretation, once they provide minimum, maximum and optimal conditions for growth as well as the maximum growth rate expected from a specific microorganism or strain. To obtain these parameters, it is desirable to have growth rates estimates embracing all the growth range (or as much as possible) for each analysed environmental factor of the microorganism in question. The simplest and recommended way to obtain these growth rates are by mean of turbidity measurements, where the increase of inoculated culture medium optical density (O.D.) with time is associated to bacterial growth and translated into specific growth rates. It is simple to modify broth pH and water activity by adding acid, base or salt and possible to run turbidity measurements at different temperatures by means of an automated turbidimeter making it an appropriate technique to simulate the diverse environmental scenarios.

The aim of this chapter is to determine whether strains from the same phylogenetic affiliation reveal similar cardinal growth parameters and how are these related to growth limits of other emetic strains. Strain variability will be investigated when discussing how the strains differ in terms of their boundaries for growth. This chapter concentrates on assessing specific growth rates by means of turbidity measurements with the objective of estimating the cardinal values for three uncategorized

strains of Nestlé Pathogen Culture Collection (NPCC) (B594, B596, B626) in terms of temperature, pH and water activity and comparing these estimations with references strains of the same phylogenetic group. The application of the determined cardinal parameters for growth predictions will be discussed in the next chapter which is focused on the validation of the proposed models and assumptions made along this thesis.

4.2 Material and Methods

4.2.3 Cardinal parameters estimation

4.2.3.1 Strains

Three of the working strains, B594, B596 and B626 were characterized for their cardinal values for temperature, pH and water activity. For this, turbidity experiments using Bioscreen equipment, (Oy curves, Finland) were performed at different conditions to estimate the respective growth rates.

4.2.3.2 Media preparation

To obtain the growth rates at different pH and a_w conditions, different BHI solutions were prepared.

The range of investigated pH was 4.23 to 9.66. It was obtained by adding HCl or NaOH to BHI and then filtering the solution to make it sterile.

The range of investigated water activity was from 0.927 to 0.997. It was obtained by adding NaCl to the BHI solutions to obtain the targeted a_w and then sterilizing the solutions in autoclave. The water activity of the sterilized solutions was then again measured. Both pH and a_w experiments were run at the temperature of 37 °C.

The range of investigated temperature was from 13 to 48 °C. Regular BHI was used for temperature experiments at optimal pH and a_w . For temperatures below 20 °C, it was necessary to keep the equipment in a controlled cold room at 10 °C.

4.2.3.3 Inoculum preparation

Under aseptic conditions, one cryobead of the studied strain was removed using a disposable plastic needle and placed into a BHI tube. The vial was quickly re-capped and returned immediately to the freezer. The BHI tube was incubated for 8 h at 30 °C and then a subculture of 0.1 ml was introduced in a BHI tube for an additional 18 h at 30 °C to achieve a final concentration of 10^8 CFU/ml.

Two ten-fold dilutions of the subculture were prepared using BHI broth adjusted to the experimental conditions to reach a concentration of 10^6 CFU/ml in the initial Bioscreen wells.

4.2.3.4 Turbidity experiments

For temperature experiments, each well of the microplates was prefilled with 200 μ L of regular BHI broth, except the first wells (colored in red in FIGURE 4.0.1) dedicated to the inoculum. To obtain the specific

growth rates at different pH and water activity levels, each well of the microplates is prefilled with 200 μL BHI broth with the targeted pH or water activity. 400 μL of the inoculum are placed on the empty wells, then binary dilutions are performed down in the column of inoculated wells.

The filled microplate(s) are placed in the Bioscreen automate turbidity reader and incubated at 37 $^{\circ}\text{C}$ to study the pH and a_w and at several temperatures ranging from 12 to 48 $^{\circ}\text{C}$ to study the effect of temperature. O.D. readings were performed at 600 nm each 10 minutes with shaking. The Bioscreen C was run with continuous and medium shaking for a pre-established period.

At the end of each experiment, purity checks of the final well of each Bioscreen plate column was performed by streaking 10 μL of the remaining dilution on TSAYe plates and incubating at 30 $^{\circ}\text{C}$ for 24 hours to observe pure colonies.

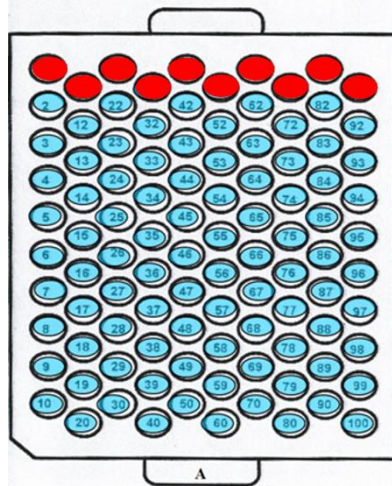


Figure 4.0.1 - Bioscreen plate design for cardinal values estimates – O.D. experiments. Diluted subculture inoculated into red wells and binary dilutions performed down in each column.

4.2.3.5 Growth rates estimation

If the inoculum goes through binary dilutions, then the difference between the detection time (t_d), defined as the time needed to reach a pre-defined O.D. threshold for two successive curves, should be close to the doubling time of the population, as can be seen in FIGURE 4.0.2. The μ_{\max} was calculated as the negative reciprocal slope of the linear regression between t_d and the natural logarithm of the initial bacterial concentration ($\ln C$) of the inoculated wells.

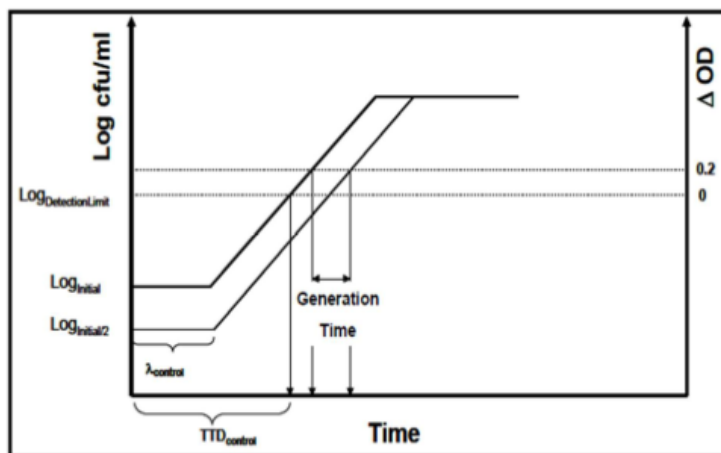


Figure 4.0.2 - How to estimate generation time from O.D. curves. From: Rukundu (2015).

Quality criteria for the estimated growth rates were defined as: a) for temperature, R^2 bigger than 0.98 and, at least, seven dilutions considered; b) for pH and a_w , R^2 bigger than 0.95 and, at least, four dilutions for a single rate estimate. The difference among the quality criteria is due to the fact that the range on which growth is observed is wider for temperature than for water activity or pH, to which growth boundaries can be easily reached with 6-7 levels of the factor.

4.2.3.6 Estimation of cardinal values and confidence intervals

Once the growth rates were estimated for each condition and each strain, MATLAB software (Version R2016a, Mathworks, Natick, MA) was used to fit the respective cardinal model (described by Equations 4.1, 4.2 and 4.3) (ROSSO et al, 1995) to these data. In particular, the nonlinear least squares curve fitting toolbox was used, with trust-region algorithm. Before fitting, the response parameter, μ_{max} , was rescaled by the square root link function.

$$\sqrt{\mu_{max}} = \begin{cases} T < T_{min}, 0 \\ T_{min} < T < T_{max}, \sqrt{\mu_{opt} * \tau(T)} \\ T > T_{max}, 0 \end{cases}$$

$$\tau(T) = \frac{(T - T_{max})(T - T_{min})^2}{(T_{opt} - T_{min})[(T_{opt} - T_{min})(T - T_{opt}) - (T_{opt} - T_{max})(T_{opt} + T_{min} - 2T)]} \quad (4.1)$$

$$\sqrt{\mu_{max}} = \begin{cases} aw < aw_{min}, 0 \\ aw_{min} < aw < aw_{max}, \sqrt{\mu_{opt} * \alpha(aw)} \\ aw > aw_{max}, 0 \end{cases} \quad (4.2)$$

$$\alpha(aw) = \frac{(aw - aw_{max})(aw - aw_{min})^2}{(aw_{opt} - aw_{min})[(aw_{opt} - aw_{min})(aw - aw_{opt}) - (aw_{opt} - aw_{max})(aw_{opt} - aw_{min})]}$$

$$\sqrt{\mu_{max}} = \begin{cases} pH < pH_{min}, 0 \\ pH_{min} < pH < pH_{max}, \sqrt{\mu_{opt} * \rho(pH)} \\ pH > pH_{max}, 0 \end{cases}$$

$$\rho(pH) = \frac{(pH - pH_{min})(pH - pH_{max})}{(pH - pH_{min})(pH - pH_{max}) - (pH - pH_{opt})^2} \quad (4.3)$$

The cardinal parameters X_{min} and X_{max} represent the value of X_i factor below and above which no growth occurs (μ_{max} is equal to 0), and X_{opt} the value at which μ_{max} is equal to μ_{opt} and reaches a maximum (ROSS & DALGAARD, 2004).

The gamma concept introduced by Zwietering et al (1996) and described by Equation 4.4 considers the effect of the three factors when assessing the maximum specific growth rate. Along this study, when one factor is taken as a variable, the other two are considered constant and at their optimal values, since they were not deliberately modified. It means that the effect of each factor is always investigated separately.

$$\mu_{max} = \mu_{opt} \tau(T) \alpha(aw) \rho(pH) \quad (4.4)$$

To be able to compare the estimated parameters and their confidence intervals with the ones obtained by Carlin et al (2013) for emetic strains, the same procedure was reproduced on the data from this study and data produced by those authors. The raw data of Carlin et al (2013) used in the present work are available in the Supplementary Material of that publication. For pH, once the authors only have suboptimal data for this factor, the assumption ($pH_{max} = 2(pH_{opt}) - pH_{min}$) made by the

authors was considered here (AUGUSTIN & CARLIER, 2000), to decrease the number of parameters to be estimated to only three (μ_{opt} , pH_{min} , and pH_{opt}) and to increase the degree of freedom in the regression. For temperature, four parameters were estimated (μ_{opt} , T_{min} , T_{opt} , and T_{max}). For water activity the maximum value (aw_{max}) was fixed as 1 (CARLIN et al, 2013) and three parameters were estimated (μ_{opt} , aw_{min} , and aw_{opt}).

The confidence intervals were estimated by means of ten thousand Monte Carlo simulations for each strain and each environmental factor (T, a_w or pH) using the estimated parameters and root-mean-square error (RMSE) for each factor ($RMSE_{global}$), defined by Equation 4.5 and assuming a normal distribution for the $\sqrt{\mu_{max}}$ around the model (RATKOWSKY et al, 1982; ARYANI et al, 2015):

$$RMSE_{global} = \sqrt{\sum_{i=1}^N \frac{(\sqrt{\mu_{maxPRED(i)}} - \sqrt{\mu_{maxOBS(i)}})^2}{N}} \quad (4.5)$$

where N is the number of data points for all strains and the same environmental factor; $\sqrt{\mu_{maxPRED(i)}}$ is the square-root of i specific growth rates predicted by the individual models for each strain at the specific environmental factor and $\sqrt{\mu_{maxOBS(i)}}$ is the square-root of i specific growth rates measured for each strain at the specific environmental factor.

This $RMSE_{global}$ quantified the error around the model in a consistent manner. It is known that data variability increases with the amount of collected data and having a single RMSE for all the strains and the same factor would compensate the fact that the number of collected growth rates for each strain is different even for the same factor. Once the measurement procedure is the same, the strains belong to the same species and even the same phylogenetic group, it is reasonable to assume the scatter of the data around the model (characterized by RMSE) is the same. For the data of Carlin (2013), the individual RMSE values were considered, once the amount of data is lower, the data collection was slightly different and performed in a different lab.

4.2.3.7 Validation of cardinal parameters

The cardinal parameters determined in the present work were compared to the ones obtained from Carlin et al (2013) for the same phylogenetic group, F4810/72 (B577 in the present study) and F837/76. The difference with other cardinal parameters was considered as non-significant when confidence intervals at 95% of the cardinal parameters of the compared strains were overlapping.

4.3 Results and Discussion

4.3.1 Growth rates estimation

FIGURE 4.0.3 shows an example of the estimate of the specific growth rate from the O.D. curves coming from Bioscreen. Plotting the different detection times (obtained by setting the detection level for O.D. = 0.4) vs. the respective dilutions (plate design in FIGURE 4.0.1), a straight line with a negative value for the slope is expected. The specific growth rate for the investigated condition is the absolute value of this slope.

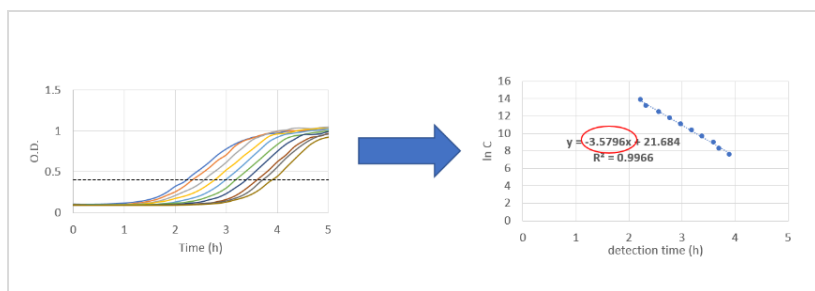


Figure 4.0.3 - Example of estimating the specific growth rate from O.D. curves. Broken line at left represents the detection level at O.D. = 0.4.

ANNEX C presents all the specific growth rates estimated by means of procedure presented in FIGURE 4.0.3 for the three strains (B594, B596 and B626) at each temperature, pH, and water activity values used in this study.

4.3.2 Cardinal parameters estimation

The respective cardinal model for each environmental factor (Equations 4.1 – 4.3) was fitted for each strain set of estimated specific growth rates and the parameters with their confidence intervals are presented in TABLE 4.0.1. The plots with the fittings and confidence intervals are presented in Figures 4.4 – 4.6.

Table 4.0.1 - Cardinal values and respective confidence intervals between brackets for temperature, pH and water activity for B594, B596, B626, B577 (F4810/72), F837/76 and B635 strains.

Estimated parameter	B594	B596	B626	B577*	F837/76**	B635***
μ_{opt} (h ⁻¹)	2.73[2.63; 2.84]	3.67[3.54; 3.8]	3.42[3.29; 3.55]	2.88[2.62; 3.15]	2.68[2.38; 3.01]	2.23[2.07; 2.38]
T_{min} (°C)	8.82[7.85; 9.86]	6.95[5.92; 7.95]	5.95[4.79; 7.08]	7.10[4.40; 9.21]	8.25[5.11; 10.83]	0.24[-1.05; 1.37]
T_{opt} (°C)	36.74[36.10; 37.32]	40.89[40.42; 41.33]	41.44[40.94; 41.93]	39.6[38.19; 40.90]	39.44[37.79; 40.98]	37.55[36.62; 38.31]
T_{max} (°C)	47.57[47.42; 47.79]	48.40[48.35; 48.49]	48.44[48.34; 48.58]	48.00[47.99; 48.04]	47.99[47.98; 48.09]	41.00[40.64; 41.93]
R² (Temperature)	0.9866	0.9758	0.9862	0.9649	0.9375	0.9634
RMSE (Temperature)	0.0526	0.0745	0.0535	0.1073	0.1407	0.0898
μ_{max} (h ⁻¹) (37 °C; pH _{opt} ; aw _{broth})	2.35[2.09; 2.61]	2.19[1.91; 2.46]	2.5[2.2; 2.79]	2.43[2.29; 2.56]	2.4[2.2; 2.59]	2.09[1.94; 2.24]
pH_{min}	4.59[4.33; 4.75]	4.69[4.45; 4.8]	4.75[4.57; 4.81]	4.63[4.56; 4.68]	4.64[4.55; 4.69]	4.68[4.62; 4.7]
pH_{opt}	7.05[6.93; 7.16]	7.08[6.97; 7.18]	7.08[6.99; 7.15]	6.82[6.79; 6.85]	6.43[6.38; 6.47]	6.58[6.54; 6.62]
R² (pH)	0.8140	0.8384	0.8588	0.9292	0.8326	0.887
RMSE (pH)	0.2242	0.249	0.256	0.1136	0.1523	0.1261

μ_{max} (h^{-1}) (37 °C; $a_{w_{opt}}$; pH_{broth})	3.14[3.01; 3.27]	3.00[2.85; 3.14]	3.38[3.24; 3.54]	2.51[2.27; 2.85]	2.32[2.09; 2.78]	2.19[1.95; 2.67]
$a_{w_{min}}$	0.950[0.94 9;0.952]	0.929[0.92 6;0.932]	0.932[0.92 9;0.934]	0.934[0.93 ;0.939]	0.933[0.93 ;0.937]	0.940[0.93 5;0.994]
$a_{w_{opt}}$	0.990[0.98 9;0.991]	0.992[0.99 1;0.993]	0.992[0.99 1;0.992]	0.992[0.98 9;0.995]	0.994[0.99 1;0.998]	0.993[0.99 0;0.997]
R² (a_w)	0.8972	0.9484	0.9494	0.9023	0.9250	0.8448
RMSE (a_w)	0.1605	0.0744	0.0781	0.1493	0.1191	0.1605

*Raw data taken from Carlin et al. (2013), strain referred as F4810/72 in that publication; **Raw data taken from Carlin et al, 2013, strain referred as F837/76 in that publication; ***Raw data taken from Carlin, 2013, strain referred to as RIVM BC120 in that publication; Text in italics: unknown μ_{opt} conditions (not mentioned in Carlin (2013) what were the environmental conditions in which they performed these experiments)

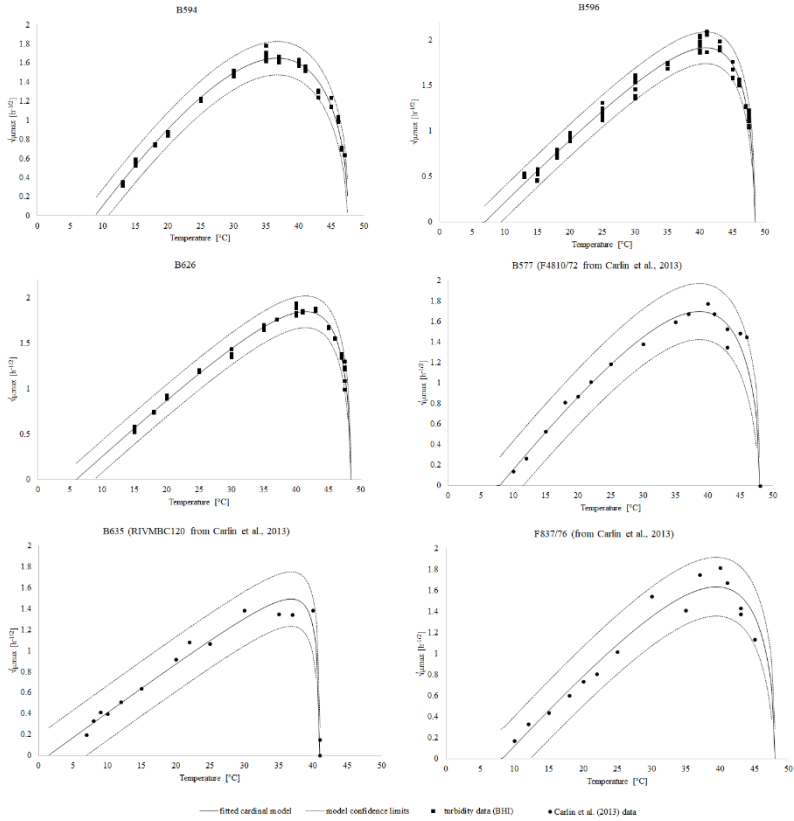


Figure 4.0.4 - Cardinal models (continuous line) for temperature fitted to data from this study (squares) for B594, B596 and B626 strains and fitted to data taken from Carlin et al (2013) (dots) for B577, B635 and F837/76 strains. Dashed lines: confidence limits.

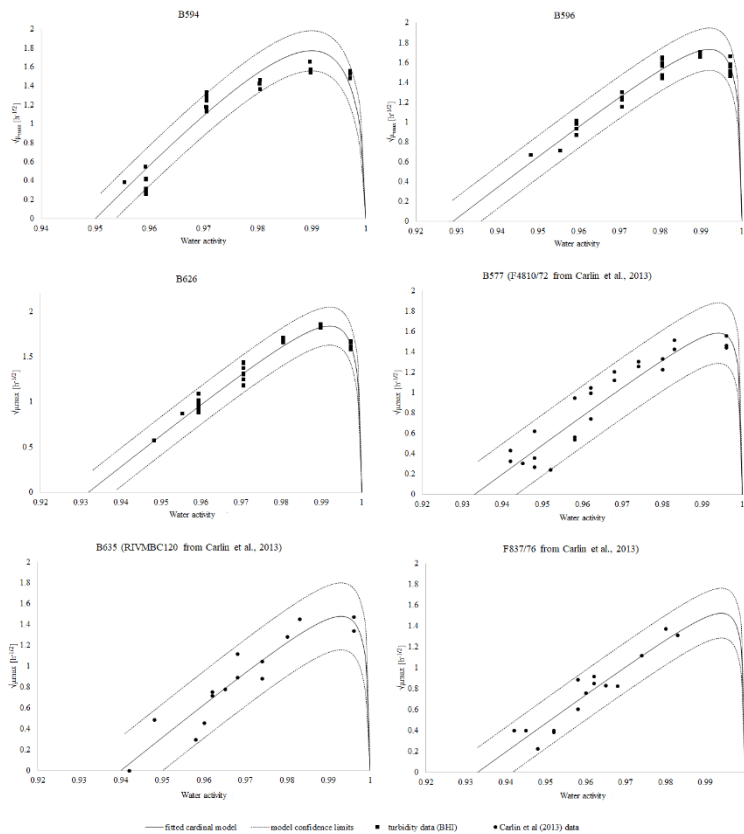


Figure 4.0.5 - Cardinal models (continuous line) for water activity fitted to data from this study (squares) for B594, B596 and B626 strains and fitted to data taken from Carlin et al (2013) (dots) for B577, B635 and F837/76 strains. Dashed lines: confidence limits.

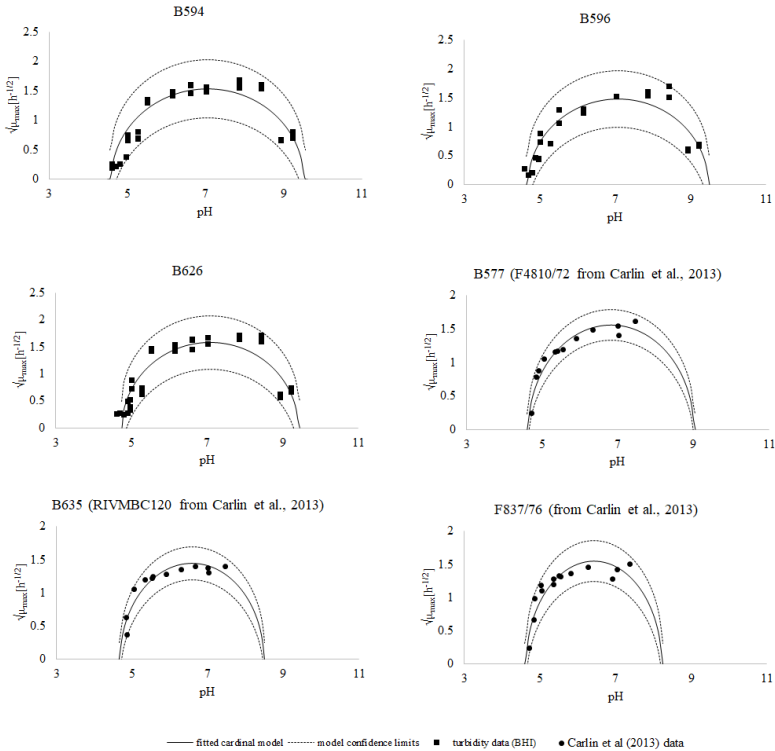


Figure 4.0.6 - Cardinal models (continuous line) for pH fitted to data from this study (squares) for B594, B596 and B626 strains and fitted to data taken from Carlin et al (2013) (dots) for B577, B635 and F837/76 strains. Dashed lines: confidence limits.

Looking at Figures 4.0.4 – 4.0.6 one can notice the difference on the number of replicates for each factor level for strains of the present study and the ones coming from the literature. For strains B594, B596 and B626, μ_{max} replicates were obtained every time they were in accordance with the quality criteria, while for strains B577, B635 and F837/76 there is a much reduced number of μ_{max} replicates. This might have an impact on the uncertainty linked to the parameters estimation. FIGURE 4.0.6 shows a flatter shape for strains coming from this work than from strains coming from Carlin et al (2013) work, probably because of the difference

on the temperature the experiments were performed by the present study and by those authors. In the present study, the temperature values were more far away from the optimal temperature for growth.

To build the prediction confidence interval, the assumption that the square root rates normally distributed around the model (RATKOWSKY et al, 1982; ARYANI et al, 2015) was taken. That being the case, it is possible to assume the confidence will be the predicted value plus and minus two times the standard error of fit (or RMSE in this study). For strains B594, B596 and B626, to which the growth rates data were directly assessed, a general RMSE for each condition was considered (0.088 for temperature, 0.1061 for water activity, and 0.2467 for pH), once the number of observations for each strain is different it is reasonable to consider their scatter to be the same (once all the experimental procedure was the same and they come from the same emetic group of *B. cereus*). For B577, B635 and F837/76 strains, the growth rates data were extracted from Carlin et al (2013) and the individual RMSE for each fitting was considered (see values in Table 4.1).

It is important to notice that each of the cardinal models presented in Equations 4.1 to 4.3 estimate μ_{opt} value, what means that each strain would have three different estimates for this parameter. The μ_{opt} considered was the one coming from the estimation of cardinal temperatures (Eq. 4.1), once the experiments were run with pure BHI which is known as having the ideal pH and water activity and the optimal temperature for growth will be properly identified by the fitting to the collected data. The other estimates are presented in TABLE 4.0.1 as μ_{max} at certain pH, a_w and temperature conditions.

All data points fall within temperature prediction confidence limits for all the strains. Regarding water activity, B594 strain has a few data points outside the confidence limits due to its individual RMSE being bigger than the general RMSE for water activity. The same is true for B596 strain regarding its pH model.

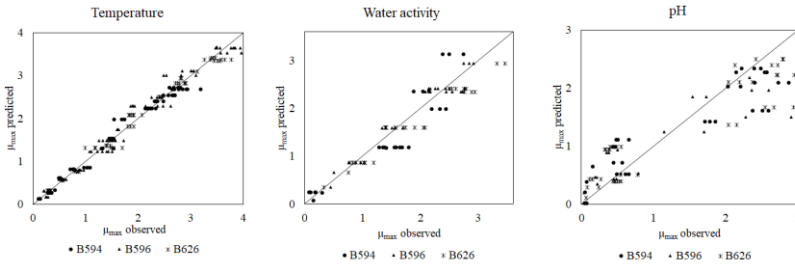


Figure 4.0.7 - Predicted vs. observed specific growth rate based on cardinal model fittings presented in Figures 4.4 - 4.6. Strain B594 in circles, B596 in triangles and B626 in stars.

The residual plots presented in FIGURE 4.0.7 show the discrepancy between predicted and observed specific growth rates where the straight diagonal line represents the case where predicted values are equal to observed data. For all strains, residues were homogeneously distributed on both sides of the line of perfect agreement for temperature and water activity (to a less extend) models. For temperature the data were very close to the identity line, while for water activity there was a distribution from both sides of the line and for pH areas of over and underestimation were observed. As expected, knowing RMSE values, the factor with bigger and smaller dissimilarity are pH and temperature respectively. For water activity as the considered environmental factor, the only noticeable trend is that for B594 strain the bigger μ_{\max} observed data are overestimated. It is also possible to notice that the bigger discrepancy for pH data occurs at bigger μ_{\max} estimates with the model underestimating the real μ_{\max} values. The opposite happens for smaller μ_{\max} values, where the model overestimates its real value. Biesta-Peters et al (2010) also observed a bigger uncertainty when assessing *B. cereus* growth rates by means of turbidity measurements for different pH values, especially at low values close to the growth boundary, resulting in higher RMSE values when fitting the cardinal model due to unrealistic μ_{\max} estimates.

In general, for temperature the data scatter around the model is small compared to the other factors and fairly constant with the increase of μ_{\max} . Analysing the plots presented in FIGURE 4.0.4, it is perceptible that the bigger scatter of the data for a single temperature measurement

occurs close to the optimum temperature for growth, where μ_{\max} reaches its maximum values and where the expected data variability would be smaller due to the good development of the microorganism (BIESTA-PETERS et al., 2010; CARLIN et al, 2013). A simple assumption to explain this unexpected behaviour would be the fact that the detection time (necessary time to reach the O.D. detection limit) for the higher concentration wells is smaller than the O.D. measurement time interval, making the slope from which specific growth rates are determined influenced by interpolation.

4.3.3 Validation of cardinal parameters

By means of the estimated parameters and their confidence interval it is possible to compare the boundaries of growth for five emetic strains (B594, B596 and B626 from NPCC and other two from group III of emetic strains published by Carlin et al (2013) (F4810/72 and F837/76). Parameters estimated for B635 strain (RIVM BC120 in Carlin et al (2013)) are also presented in TABLE 4.0.1 once this information is required in the next chapter, even though no comparison among this strain and the others was prepared because it belongs to other phylogenetic group what makes its parameters projected in a different range.

The comparison between the main cardinal parameters and their confidence interval for the five emetic strains considered in this work are presented in FIGURE 4.0.8 and FIGURE 4.0.9.

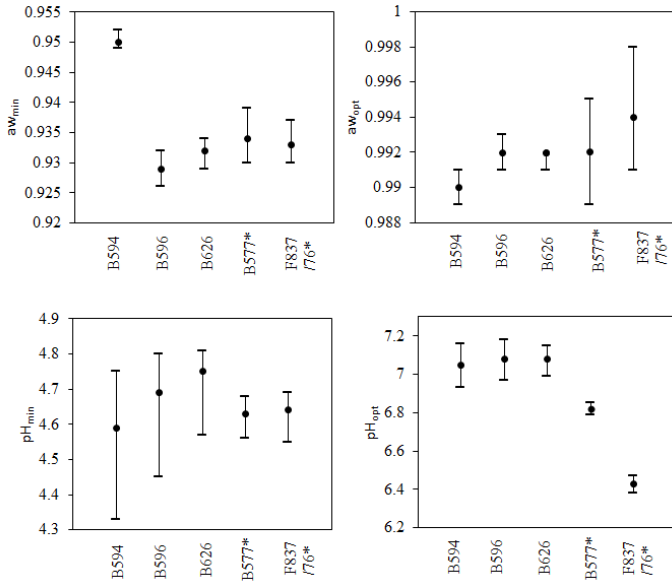


Figure 4.0.8 - Cardinal parameters and their confidence interval for the models in terms of water activity and pH for B594, B596, B626, B577, and F837/76 strains. *Raw data taken from Carlin et al (2013) and re-fitted according to procedure proposed in this study.

$T_{\text{opt}} [^{\circ}\text{C}]$	≠	≠	≠	≠	=	=	=	≠	=	=
$T_{\text{max}} [^{\circ}\text{C}]$	≠	≠	≠	≠	=	≠	≠	≠	≠	=
pH_{min}	=	=	=	=	=	=	=	=	=	=
pH_{opt}	=	=	=	≠	=	≠	≠	≠	≠	≠
a_{wmin}	≠	≠	≠	≠	=	=	=	=	=	=
a_{wopt}	=	=	=	=	=	=	=	=	=	=

Based on Table 4.0.2 there was no statistical difference (p -value > 0.05) between the cardinal values in 49 out of 80 pairs of compared data, i.e. an agreement in 61.2% of the cases. When comparing his results with the literature, Carlin et al (2013) obtained a similar agreement of 58%. The higher percentage of agreement equal to 90% (9 out of 10 pairs of compared data with no significant difference) was obtained for T_{min} parameter. This high agreement was favoured by large confidence intervals on T_{min} for estimates for Carlin et al (2013) strains, which do not exist for the other cardinal temperatures for instance. The agreement was particularly high for pH_{min} and a_{wopt} (100% of pairs of compared data with no significant difference). The agreement was lower than 50% for μ_{opt} , T_{max} and pH_{opt} . The smaller confidence interval of T_{max} parameter can be responsible for this low percentage of agreement between the strains for this parameter. For pH_{opt} parameter, there was no significant difference among strains of this study, but all the possible combinations involving Carlin et al (2013) strains were significantly different, suggesting that the experimental design can influence the parameters estimates.

Strain B594 seems to differ from the all the others in terms of T_{opt} , T_{max} and a_{wmin} . This might have been affected by the fitting quality of the water activity model for B594 strain, which was the one showing the least satisfactory performance compared to the other strains. Strains B596 and B626 are equal in all parameters.

An intra-group variability was also observed by Guinebretière et al (2008) and Carlin et al (2013) when analysing boundaries of growth in terms of pH, a_{w} and temperature for different *B. cereus* group of strains.

It is very interesting to notice that there is no significant difference between all the strains for the T_{min} parameter, except for B594/B626 pair. For the plate counts data, there is no significant

difference between all the strains (see TABLE 3.0.4) when the Ratkowsky model was used. The confidence intervals of T_{\min} as a Ratkowsky parameter are generally bigger than the ones from T_{\min} as a cardinal parameter, what could justify the fact that there is no difference between B594/B626 pair. In that analysis, just suboptimal temperatures for growth were studied (up to 30 °C), being a different model fitted to the data, what could have had an influence on this observation, as well as the influence of the only two parameters (b and T_{\min}) of the suboptimal model have on each other, for example a higher b (slope) would somehow leads to a higher T_{\min} (point where the line crosses the x axis). For the cardinal model fitting, the whole range of conditions in which growth was observed was considered for the parameters estimation. Also, the bacteria concentration was assessed using plate counts in Chapter 3, while here in Chapter 4 the optical density was used for the cardinal values assessment.

4.4 Conclusions

The specific growth rates by means of turbidity were estimated according to the specified quality criteria and the cardinal models for temperature, pH and water activity were fitted to the experimental data for each strain separately with R^2 bigger than 0.938 for temperature models; R^2 bigger than 0.845 for water activity and 0.814 for pH. Indeed, the cardinal model for pH was the one that showed worst performance when fitted to the data, probably because estimating growth rates at unfavourable pH conditions increases the estimates uncertainty and consequently the variability between replicates.

Based on the estimates presented along the chapter for the investigated emetic strains, μ_{opt} varies from 2.68 to 3.67 h^{-1} ; T_{min} from 5.95 °C to 8.82 °C; T_{opt} from 36.74 °C to 41.44 °C; T_{max} from 47.57 °C to 48.44 °C; pH_{min} from 4.59 to 4.75; pH_{opt} from 6.43 to 7.08; $a_{w_{\text{min}}}$ from 0.929 to 0.950 and $a_{w_{\text{opt}}}$ from 0.990 to 0.994.

Significant differences on the estimated parameters could be identified and an agreement of 61.2% was obtained when comparing the strains by pairs. The agreement was 100% for pH_{min} and $a_{w_{\text{opt}}}$. B594 estimated parameters seem to differ more from the all the other strains. Strains B596 and B626 are equal in all parameters.

Knowing the big diversity of *B. cereus* species, it is clear that there is a correlation between the cardinal parameters for strains coming from the same phylogenetic group in terms of the three environmental factors investigated. Foodborne poisonings caused by the emetic group will likely be a consequence of storage at abuse temperature and although able to multiply in some refrigeration conditions, these strains represent a much lower risk of food poisoning in this case. Thus, these cardinal parameters could be used to generate predictions and assess the different growth abilities of *B. cereus* emetic strains and, together with other studies, be applied to *B. cereus* quantitative risk assessment.

4.5 References

AUGUSTIN, J.-C.; CARLIER, V. Mathematical modelling of the growth rate and lag time for *Listeria monocytogenes*. **International Journal of Food Microbiology**, v.56, p.29–51, 2000.

BARANYI, J.; BUSS DA SILVA, N; ELLOUZE, M. Rethinking Tertiary Models: Relationships between growth parameters of *Bacillus cereus* strains. **Frontiers in Microbiology**, v.8:1890, 2017.

BIESTA-PETERS, E.G.; REIJ, M.W.; JOOSTEN, H.; GORRIS, L.G.; ZWIETERING, M.H. Comparison of two optical-density-based methods and a plate count method for estimation of growth parameters of *Bacillus cereus*. **Applied and Environmental Microbiology**, v.76, p.1399-1405, 2010.

CARLIN, F.; ALBAGNAC, C.; RIDA A.; GUINEBRETIERE M. H.; COUVERT, O.; NGUYEN-THE, C. Variation of cardinal growth parameters and growth limits according to phylogenetic affiliation in the *Bacillus cereus* Group. Consequences for risk assessment. **Food Microbiology** v. 33, p. 69-76. 2013.

GUINEBRETIERE, M.H.; THOMPSON, F.L.; SOROKIN, A.; NORMAND, P.; DAWYNDT, P.; EHLING-SCHULZ, M.; SVENSSON, B.; SANCHIS, V.; NGUYEN-THE, C.; HEYNDRICKX, M.; DE VOS, P. Ecological diversification in the *Bacillus cereus* group. **Environmental Microbiology**, v.10, p.851-865, 2008.

GUINEBRETIERE, M.H.; VELGE, P.; COUVERT, O.; CARLIN, F.; DEBUYSER, M.L.; NGUYEN-THE, C. Ability of *Bacillus cereus* group strains to cause food poisoning varies according to phylogenetic affiliation (Groups I to VII) rather than species affiliation. **Journal of Clinical Microbiology**, v. 48, p.3388-3391, 2010.

ROSSO, L; LOBRY, J. R.; BAJARD,S; FLANDROIS, J.P. Convenient Model To Describe the Combined Effects of Temperature and pH on Microbial Growth. **Applied and Environmental Microbiology**, v.61, n.2, p. 610-616, 1995.

WIJTZES, T.; ROMBOUTS, F. M.; KANT-MUERMANS, M. L. T.; VAN'T RIET, K; ZWIETERING, M. H. Development and validation of a combined temperature, water activity, pH model for bacterial growth rate of *Lactobacillus curvatus*. **International Journal of Food Microbiology**, v.63 p.57–64, 2001.

ZWIETERING, M.H.; DE VIT, J.C.; NOTERMANS, Application of predictive microbiology to estimate the number of *Bacillus cereus* in pasteurised milk at the point of consumption. **International Journal of Food Microbiology**, v.30, p.55-70, 1996.

5. PRIMARY AND SECONDARY MODELS VALIDATION

5.1 Introduction

Given the importance of predictive microbiology models to food industry, impacting on HACCP, shelf-life determination, product formulation, process enhancement, and so on; it is essential to evaluate their performance and limitations in order to define a model's viability for use in an operational setting.

As explained along the previous chapter, data used to obtain cardinal values are acquired in laboratory media. However, the predictions agree more or less successfully with observations of food products (CASTILLEJO-RODRIGUEZ et al, 2002; WALLS & SCOTT, 1996). Therefore, validation of the model proves to be required.

Such evaluation can be made by means of internal and/or external validation of primary and secondary models. A confrontation of the predictions with the data used to build part of it can be understood by internal validation, while for external validation a new set of data needs to be produced or literature data taken to confirm and test the ability of the models to predict microbiological behaviour in the food/group of foods of interest.

In this chapter, the main idea is to integrate information from previous chapters in order to show how the collected information, proposed models and analysis made so far can be applied to real food scenarios. The objective is to validate the suggested models and modelling approaches with data produced in this work and also originating from the literature. Since temperature is the major factor of interest in the food industry (McDONALD & SUN, 1999), the studies stated focus on that aspect. This will be performed through internal validation of the secondary and the primary models, then through an external validation of the secondary model.

For the secondary model internal validation, two approaches will be tested and their main difference is on how to estimate μ_{opt} in RIF, being the cardinal temperatures considered the same as for culture medium (DELIGNETTE-MULLER & ROSSO, 2000) for both approaches.

For the primary model internal validation, both secondary model validation approaches will be used to estimate the growth rate at specific conditions together with h_0 and N_{max} to generate predictions in terms of

log counts vs. time and the viable counts in RIF will be tested against the prediction to evaluate models predictive ability for each strain.

As for the secondary model external validation, a general model for growth of emetic strains of *Bacillus cereus* will be proposed and validated with literature data from various individual strains and cocktails of strains growing at different temperatures in a range of dairy products.

5.2 Material and Methods

5.2.1 Internal validation

5.2.1.1 Secondary models

In order to evaluate the prediction ability of the cardinal model for temperature when applied to food scenarios, cardinal parameters in terms of temperature estimated in Chapter 4 (see Table 4.0.1) will be used and considered the same for RIF, as they are considered specific for the studied strain but independent from the medium. The only parameter that needs to be adjusted to adapt the model to the RIF is μ_{opt} , once it is medium dependent. Estimation of μ_{opt} in RIF was performed by means of μ_{max} values in RIF from viable counts experiments (Approach-A) or by means of bias factor (Approach-B), as described below.

5.2.1.1.1 Approach-A:

Here, in this Approach-A, μ_{opt} in RIF (μ_{opt}^{RIF}) estimation follows a modified version of the methodology proposed by Pinon et al (2004). In their study, the authors used the cardinal temperatures estimated in culture medium, once $\tau(T)$ in Equation 5.1 is medium independent, and a set of viable counts experiments in the new medium of interest at different temperatures as a way to estimate μ_{opt}^{RIF} . For each μ_{max_i} estimation from the i kinetics (or growth curves; these presented in TABLE 3.0.1), a $\mu_{opt_i}^{RIF}$ is estimated for that medium by means of

$$\mu_{opt_i}^{RIF} = \frac{\mu_{max_i}}{\tau(T)} \quad (5.1)$$

where $\mu_{opt_i}^{RIF}$ is the estimation of μ_{opt} in RIF for each i kinetic; μ_{max_i} is the estimated μ_{max} for each i kinetic by means of fitting the primary model of Baranyi and Roberts (1994) to the experimental data and $\tau(T)$ is the factor presented in Equation 4.1. To estimate the optimal specific growth rate (μ_{opt}^{RIF}), an average between the i estimations is made for each strain by means of Equation 5.2.

$$\mu_{opt}^{RIF} = \frac{\sum_{i=1}^k \mu_{opt_i}^{RIF}}{k} \quad (5.2)$$

where k is equal to the number of growth kinetics in RIF for each strain.

Note that according to this methodology, only the cardinal temperatures (T_{\min} , T_{opt} , T_{\max}) are considered, and no use of μ_{opt} in culture medium was made.

The model confidence limits were calculated in the same way and considered the same wide as the original model built in broth, meaning that the same $\text{RMSE}_{\text{global}}$ (Equation 4.5) was considered. Doing so, it is guaranteed that there is no overestimation of the model confidence limits, once food data are generally more erratic making predictive models in food to have a bigger uncertainty around the estimates (BARANYI et al, 2014).

Approach-A of estimating μ_{opt} in RIF focus on calculating this parameter for each of the strains from independent growth curves of *B. cereus* in the food of concern. Coupled with cardinal temperatures (from fitting of cardinal model to culture medium turbidity data), a cardinal model in terms of temperature for RIF is built for each strain and such predictive model is compared with RIF growth rates. A simplified step-by-step procedure is described below:

- 1) Determine the maximum specific growth rates in RIF from fitting Baranyi and Roberts model at different temperatures for each strain
- 2) Estimate $\mu_{\text{opt}_i}^{\text{RIF}}$ by means of Equation 5.1;
- 3) Use Equation 5.2 to estimate $\mu_{\text{opt}}^{\text{RIF}}$ as an average of $\mu_{\text{opt}_i}^{\text{RIF}}$ for each strain;
- 4) Take cardinal temperatures (T_{\min} , T_{opt} , T_{\max}) estimated by means of turbidity experiments in culture medium for each strain (TABLE 4.0.1);
- 5) Create cardinal model for the growth of each strain in RIF with $\mu_{\text{opt}}^{\text{RIF}}$, T_{\min} , T_{opt} and T_{\max} ;
- 6) Estimate model confidence limits considering $\text{RMSE}_{\text{global}}$ for temperature equal to 0.088.

5.2.1.1.2 Approach-B

In this methodology, μ_{opt} in RIF will be estimated by means of bias factor (see respective values in Table 3.0.6), according to Equation 5.3 below:

$$\mu_{\text{opt}}^{\text{RIF}} = \mu_{\text{opt}}^{\text{BHI}} * \text{bias factor} \quad (5.3)$$

where μ_{opt}^{RIF} is the maximum specific growth rate in RIF at T_{opt} and μ_{opt}^{BHI} is the maximum specific growth rate in BHI at T_{opt} coming from fitting of cardinal model to turbidity data (see Table 4.0.1).

The model confidence limits were calculated in the same way proposed in Approach-A and deliberated the same wide as the original model built in broth, meaning that the same $RMSE_{global}$ (Equation 4.5) was used for the calculations.

The internal validation of the secondary model estimating μ_{opt}^{RIF} by means of the bias factor followed the simplified step-by-step procedure:

- 1) Take cardinal values (μ_{opt}^{BHI} , T_{min} , T_{opt} , T_{max}) estimated by means of turbidity experiments in culture medium for each strain (TABLE 4.0.1);
- 2) Take bias factor estimated by means of the quantified dissimilarity between growth rates obtained by viable counts in BHI and RIF (TABLE 3.0.6);
- 3) Estimate μ_{opt}^{RIF} by means of Equation 5.3;
- 4) Create cardinal model for the growth of each strain in RIF with μ_{opt}^{RIF} , T_{min} , T_{opt} and T_{max} ;
- 5) Estimate model confidence limits considering $RMSE_{global}$ for temperature equal to 0.088.

5.2.1.1.3 Secondary models performance analysis

In order to evaluate the performance of the proposed secondary models to food scenarios the Root Mean Square Error was adopted here to compare among-strains performance and both Approach-A and -B of secondary model validation.

$$RMSE = \sqrt{\frac{\sum_{i=1}^n (\sqrt{\mu_{max_{PRED}}} - \sqrt{\mu_{max_{OBS}}})^2}{n}} \quad (5.4)$$

where $\mu_{max_{PRED}}$ is the predicted maximum specific growth rate [h^{-1}], $\mu_{max_{OBS}}$ is the observed maximum specific growth rate [h^{-1}] obtained by fitting the Baranyi and Roberts (1994) primary model to log counts data and n is the number of observations for each growth curve.

Root mean square error (RMSE) is a widely used measure of the goodness-of-fitting. The larger the RMSE value, the less accurate is the

agreement between predicted and observed growth rates and it may be used as a simple measure of the level of confidence one may have in the model's predictions.

5.2.1.2 Primary models

The two approaches suggested for secondary model validation were used to predict growth rates in RIF for every strain of this study at different temperatures. Together with h_0 estimates per strain and stress (see values in Table 3.0.2), N_{\max} average per medium ($N_{\max} = 8.08$ log(CFU/mL) for RIF; see item 3.3.1.1.2) and N_0 fixed as the initial observed log counts for each kinetic, it is possible to simulate growth curves (log counts vs. time) using the primary model of Baranyi and Roberts (1994) (Equation 2.5). The simulations were performed with DMFit Excel Add-in downloadable from the ComBase web site (www.combase.cc). The simulations were then one-by-one compared to the experimental data in RIF.

In order to compare the predictive ability of growth rate secondary model approaches and the assumptions made for h_0 and N_{\max} , $RMSE_{\text{prediction}}$ will be calculated for each strain as shown in Equation 5.5.

$$RMSE_{\text{prediction}} = \sqrt{\sum_{i=1}^n \frac{(\logcounts_{\text{PRED}_i} - \logcounts_{\text{OBS}_i})^2}{n}} \quad (5.5)$$

where $\logcounts_{\text{PRED}_i}$ are the i predicted log counts [log(CFU/mL)]; $\logcounts_{\text{OBS}_i}$ are the i observed log counts [log(CFU/mL)] and n is the number of observations used in the calculation.

5.2.2 External validation

5.2.2.1 Secondary models

The external validation of the secondary model was performed taking into account strain variability, meaning that once literature data comes from a variety of strains or cocktails of strains, a general model for the growth of emetic strains in RIF was created using the information obtained from the cardinal values estimation and $\mu_{\text{opt}}^{\text{RIF}}$ estimated according to Approach-A (see Equations 5.1 and 5.2). The aim was to check whether this general model can be extrapolated and is suitable to

predict growth rates for the growth of a diversity/mix of strains of *B. cereus* in dairy products.

To create the model, an average of the cardinal values (μ_{opt}^{RIF} , T_{min} , T_{opt} , and T_{max}) among five strains of this study (B577, B594, B596, B626, and B635) was performed and these average estimates used to create an expected trend. The confidence limits of such trend were calculated using confidence limits of the individual models for each strain, considering as the lower limit the one of the strain that presents the higher T_{min} and lower T_{opt} , μ_{opt}^{RIF} , and T_{max} and, as the upper confidence limit, the one of the strain that presents the lower T_{min} and higher T_{opt} , μ_{opt}^{RIF} , and T_{max} .

5.3 Results and Discussion

5.3.1 Internal validation

5.3.1.1 Secondary models

5.3.1.1.1 Approach-A

The estimated μ_{opt}^{RIF} are presented in Table 5.0.1 Coupled with cardinal temperatures showed in TABLE 4.0.1, a cardinal model for the growth of each strain in RIF is built using Equation 4.1 and shown in Figure 5.0.1.

Table 5.0.1 – Estimated optimal specific growth rates in RIF according to Approach-A.

Strain	μ_{opt}^{RIF} [h ⁻¹]
B594	1.46
B596	2.36
B626	2.97
B635	1.68
B577	2.36

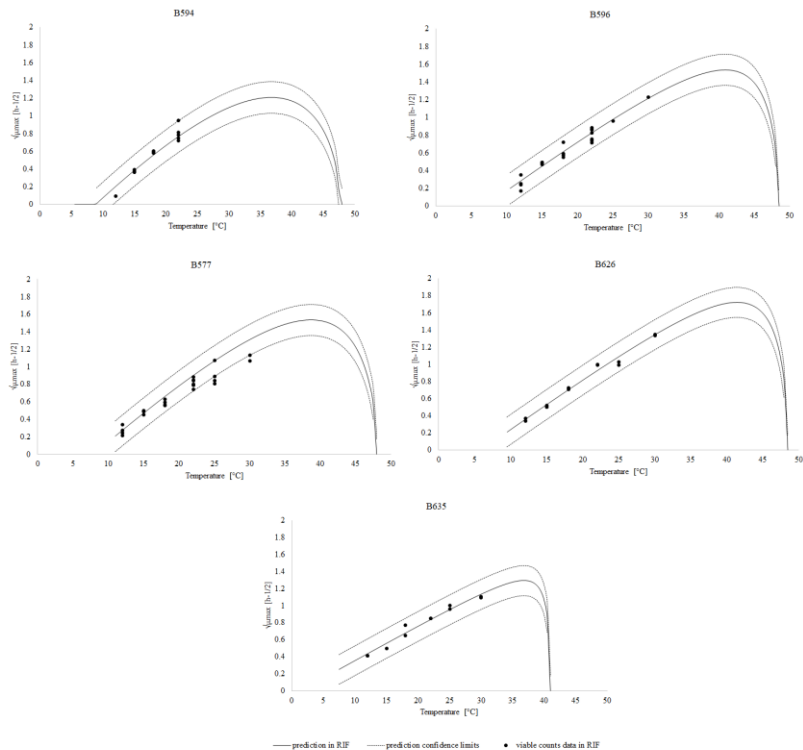


Figure 5.0.1 - Secondary models validation. Continuous line: cardinal model in RIF according to Approach-A. Dashed lines: confidence limits. Dots: specific growth rates observed in RIF.

As a general trend, it is sensible to say that the proposed model can, in general, predict the growth rates within the confidence limits range. Only for B577 strain, three out of twenty-five growth rates (12%) fall out of the model confidence limits, even if the proposed model is a proper generalization of the strain growth rates, it would only allow 5% of the data to be not represented. It is important to notice that the model confidence limits were built using RMSE values coming from fitting of turbidity data in culture medium, describing a scenario where the data variability is generally smaller compared to the log counts data. This could influence the model predictive ability when confronted with data from food matrices. Also, looking at the estimates of the cardinal values

for B577 (T_{\min} , T_{opt}), they have larger confidence intervals than the other strains, probably due to different experimental designs and lower number of μ_{\max} replicates per temperature level. This uncertainty around the T_{\min} , for example, will have an impact on the estimation of the $\mu_{\text{opt}}^{\text{BHI}}$ and, at the validation step, on the simulations. The proposed model for this strain shows an inclination to overestimate the growth rates, especially for temperatures above 18 °C, once the observed growth rates are all below the estimated trend line. Another possible explanation for this is that for temperatures close to the optimum, *B. cereus* is metabolically very active, as a consequence an acidification of the medium could be observed. As we move away from the optimum pH, then the growth rate becomes smaller because of the dynamic evolution of the pH, then the apparent growth rate at a given temperature is smaller than the one we would have obtained, for example, if the experiment was performed in a pH regulated medium.

Table 5.0.2 brings RMSE values calculated according to Equation 5.4. These values can be used to compare the model in terms of their agreement with the observed data for each of the strains, but also to compare both approaches of secondary model internal validation. The last one will be done after presenting Approach-B results. As a main inference, the poorest agreement between predicted and observed growth rates occur for B577 strain, due to a probable overestimation of $\mu_{\text{opt}}^{\text{RIF}}$ when following the technique investigated here.

Table 5.0.2 - RMSE values for predictive performance evaluation of Approach-A.

Strain	RMSE
B594	0.067
B596	0.059
B626	0.043
B577	0.102
B635	0.041
ALL	0.073

5.3.1.1.2 Approach-B

Estimated $\mu_{\text{opt}}^{\text{RIF}}$ for each strain are presented in Table 5.0.3 and in Figure 5.0.2 the models and experimental data are shown.

Table 5.0.3 – Optimal growth rates in RIF estimated by means of Approach-B.

Strain	μ_{opt}^{BHI} [h ⁻¹]	Bias factor	μ_{opt}^{RIF} [h ⁻¹]
B596	3.67	0.70	2.57
B626	3.42	0.81	2.77
B635	2.23	0.79	1.76
B577	2.88	0.60	1.73

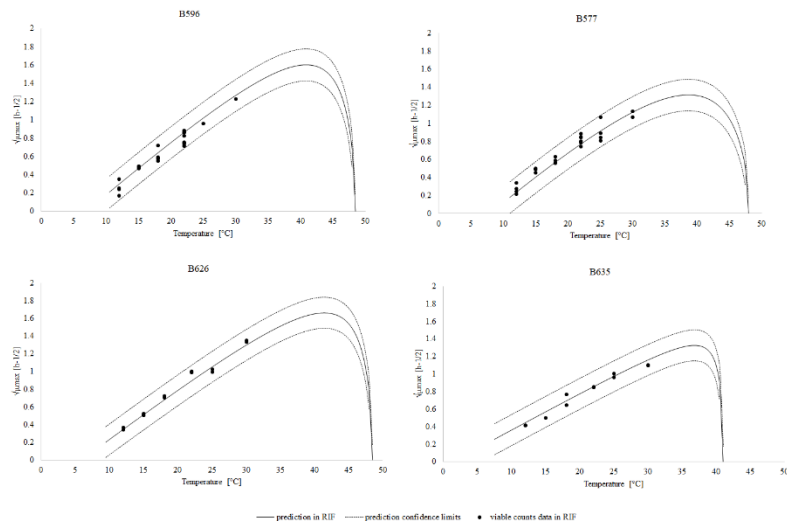


Figure 5.0.2 - Secondary models validation. Continuous line: cardinal model in RIF according Approach-B. Dashed lines: confidence limits. Dots: specific growth rates observed in RIF.

The proposed model can predict the growth rates within the confidence limits range for all studied strains. This result indicates that the model gives correct predictions for the effect of temperature on growth rate for RIF. RMSE values presented in Table 5.0.4 indicate values smaller than 0.07, endorsing that the individual RMSE values are smaller than $RMSE_{global}$ used to build the confidence limits. This observation confirms the fact that all data sets fall within the model confidence interval. Moreover, the hypothesis of the food-independent T_{min} , T_{opt} , and T_{max} was confirmed by the good predictive ability of the models.

Table 5.0.4 - RMSE values for predictive performance evaluation of Approach-B.

Strain	RMSE
B596	0.048
B626	0.051
B577	0.070
B635	0.045
ALL	0.057

5.3.1.1.3 Comparison between Approaches-A and -B

Estimated μ_{opt}^{RIF} for each strain are presented Table 5.0.1 (Approach-A) and Table 5.0.3 (Approach-B). For B596, B626 and B635 strains the estimations differ in less than 10%, while for B577 strain Approach-B estimation is 27% lower than Approach-A. This higher estimation for Approach-A can be a feasible explanation for the overestimation of growth rates above 18°C for that method resulting in a higher RMSE (=0.102) when compared to Approach-B (RMSE=0.070). No possible conclusion can be derived for μ_{opt}^{RIF} estimates of B594 strain, once its bias factor was not estimated.

When grouping all data, Approach-B has a RMSE 22% smaller than Approach-A (0.057 compared to 0.073). Smaller individual RMSE for B577, B596 and B626 strains were also observed. Only for B635 strain, Approach-A proved to be slightly better (RMSE=0.043 compared to 0.045 for approach B). In general, it can be inferred that Approach-B is more suitable to be applied when using cardinal models to predict growth rates of *B. cereus* in food matrices.

This result can be a reaction to the fact that $\mu_{opt_i}^{RIF}$ estimates are not independent of temperature ($0.00075 < p\text{-value} < 0.0012$) for all studied strains, making their average value (μ_{opt}^{RIF}) not consistent, while the bias factor estimates proved to be independent of the temperature (as analysed during Chapter 3). The predictive power of both approaches is presented when evaluating primary model validation.

5.3.1.2 Primary model

5.3.1.2.1 Using Approach-A to predict growth rates in RIF

Table 5.0.5 summarizes the parameters used to simulate growth curves for every strain at each temperature and stress condition. The μ growth rate is the scale-transformed specific growth rate estimated from

the cardinal models in RIF for each strain by means of the logarithm base conversion ($\mu = \mu_{\max}/2.3$), h_0 estimates come from its analysis made during Chapter 3 (section 3.3.1.1.1) by means of which the lag time can be estimated ($lag = h_0/\mu$), and N_{\max} average comes from the RIF N_{\max} estimates for all strains (see 3.3.1.1.2 for more details).

Table 5.0.5 - Summary of parameters used in simulations of growth curves; growth rates estimated according to Approach-A of secondary models.

Strain	T [°C]	heated				unheated							
		μ [logCFU/h]	h_0	lag [h]	N_{\max} [log(CFU/mL)]	μ [logCFU/h]	h_0	lag [h]	N_{\max} [log(CFU/mL)]				
B577	12	0.03	1.67	50.71	8.08	0.03	0.44	13.36	8.08				
	15	0.10	1.67	17.34	8.08	0.10	0.44	4.57	8.08				
	18	0.19	1.67	8.83	8.08	0.19	0.44	2.33	8.08				
	22	0.35	1.67	4.75	8.08	0.35	0.44	1.25	8.08				
	25	0.49	1.67	3.38	8.08	0.49	0.44	0.89	8.08				
	30	0.75	1.67	2.24	8.08	0.75	0.44	0.59	8.08				
B594	15	0.06	1.26	19.53	8.08	0.06	0.63	9.77	8.08				
	18	0.13	1.26	9.33	8.08	0.13	0.63	4.67	8.08				
	22	0.26	1.26	4.92	8.08	0.26	0.63	2.46	8.08				
B596	12	0.04	2.06	58.83	8.08	0.04	0.94	26.85	8.08				
	15	0.09	2.06	23.45	8.08	0.09	0.94	10.70	8.08				
	18	0.16	2.06	12.63	8.08	0.16	0.94	5.76	8.08				
	22	0.30	2.06	6.98	8.08	0.30	0.94	3.18	8.08				
	30	0.41	2.06	4.97	8.08	0.41	0.94	2.27	8.08				
B626	12	No experiments with heated cells for B626 and B635 strains				0.06	1.23	22.33	8.08				
	15					0.12	1.23	10.08	8.08				
	18					0.21	1.23	5.75	8.08				
	22					0.37	1.23	3.31	8.08				
	25					0.51	1.23	2.39	8.08				
	30					0.79	1.23	1.57	8.08				
B635	12					No experiments with heated cells for B626 and B635 strains				0.08	0.00	0.00	8.08
	15									0.13	0.00	0.00	8.08
	18									0.20	0.00	0.00	8.08
	22									0.30	0.00	0.00	8.08
	25	0.39	0.00	0.00	8.08								
	30	0.56	0.00	0.00	8.08								

Some aspects and limitations of the elected predictive approach can be identified when confronting simulated growth curves with the experimental data. Some examples are shown in Figure 5.0.3, where (A) and (D) shows good agreement between predictions and observations due to accurate prediction of lag time, growth rate and maximum population

reached at two specific conditions for B577 and B596 strains; (B) prediction underestimates lag time and overestimates growth rate as a consequence of having h_0 as an average and knowing the secondary model for B577 overestimates the growth rate at this temperature (see FIGURE 5.0.1); (C) presents reasonably good estimation of lag time and growth rate at initial stage of growth, but the small difference between N_{\max} and N_0 (small increase of log counts with time) makes the model overestimate the final observed bacterial concentration. Since a simple average was taken to obtain N_{\max} in RIF for all strains, this overestimation of the maximum concentration reached is also observed for other strains (except B635) at lower temperatures and was already expected as commented in along Chapter 3. In this case, the fact that observations continue to increase while the prediction is already at its maximum suggest the need to improve both N_{\max} and μ_{\max} predictions.

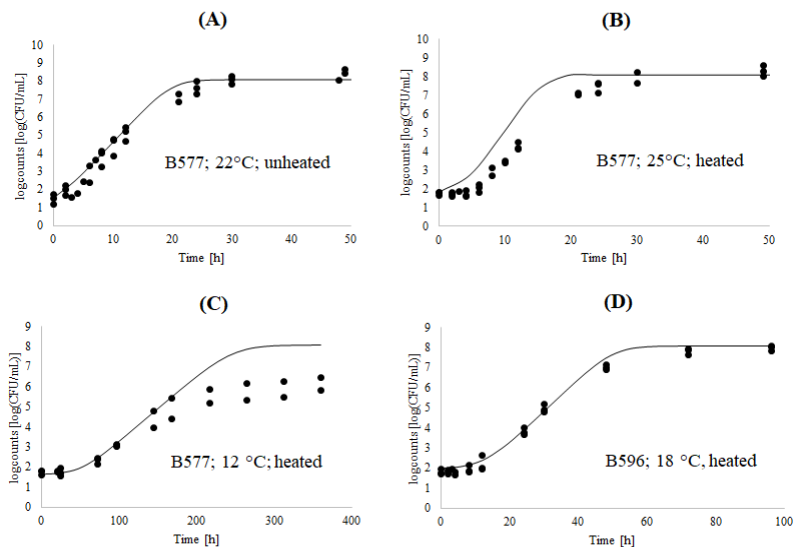


Figure 5.0.3 – Examples of primary model validation using Approach-A from secondary model to estimate growth rates. Simulated growth curve (continuous line); experimental data (dots).

In order to evaluate how agreeable the predictions are with the whole collection of observed data, $RMSE_{\text{prediction}}$ (Equation 5.5) was

calculated for each strain and presented in Table 5.0.6. Plots with predicted vs. observed log counts for each strain are shown in FIGURE 5.0.4.

Table 5.0.6 - RMSE values for predictive performance evaluation of Approach-A when applied together with h_0 and N_{\max} assumptions to simulate primary growth curves.

Strain	RMSE _{prediction}	RMSE _{prediction}	RMS _{Eprediction}
	total	unheated	heated
B577	0.752	0.529	0.836
B596	0.463	0.425	0.488
B594	0.328	0.321	0.329
B626	0.390	0.390	x
B635	0.250	0.250	x
ALL	0.580	0.433	0.682

x=no available data.

The secondary model limitations are reflected on the simulated growth curves and consequently on RMSE values and on the plots of predicted vs. observed log counts. For this reason, a bigger scatter around the equivalence line as well as a tendency to overestimate the observed data is observed for B577 strain. Smaller RMSE and better agreement between predicted and observed log counts are observed for B635 strain, followed by B594, B626 and B596 strains.

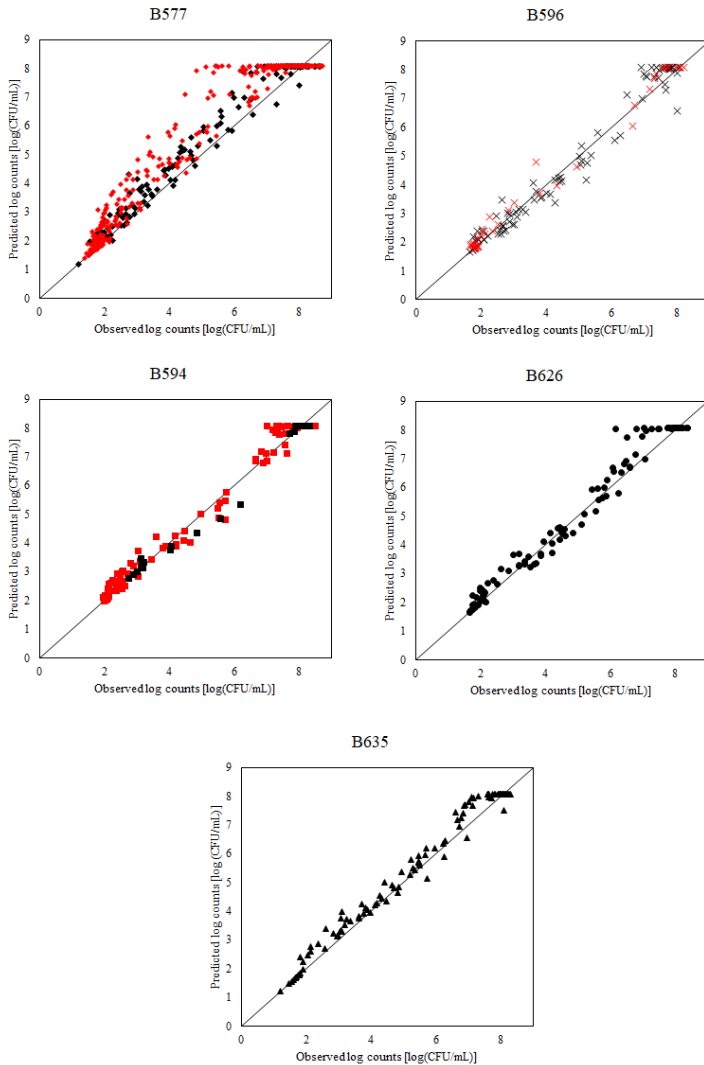


Figure 5.0.4 - Observed vs. predicted logcounts for all studied strains using Approach-A to simulate growth rates coupled with h_0 and N_{\max} assumptions. In red: heated cells. In black: unheated cells.

5.3.1.2.2 Using Approach-B to predict growth rates in RIF

In the same way as described along Approach-A validation analysis, Approach-B of secondary model for growth rate together with h_0 and N_{\max} assumptions were used to simulate growth curves and confront them with experimental data. To illustrate the main improvement from modelling point of view using Approach-B, FIGURE 5.0.5 was built and shows how a correct prediction of the growth rate can also improve the estimation of the lag phase by means of h_0 ($\text{lag}=h_0/\mu$). As expected, it is very clear the improvement of the log counts prediction for this strain at temperatures above 18 °C due to more precise estimation of the growth rate, influencing the prediction of lag time as well. The prediction of maximum population reached did not change from Approach-A to Approach-B, once it was considered as a fixed value for both cases.

The time needed to reach the safety threshold contamination level of 5 log(CFU/mL) for *B. cereus* (EFSA, 2005) according to both approaches will differ in about five hours: 10h for Approach-A and 15h for Approach-B and, while from a modelling perspective Approach-B predicts log counts is a much more reliable way, Approach-A is more conservative for this single example, making the predictions fail-safe. Independent of the selected predictive approach for the application it is important to know their limitations and make use of a (so far arbitrary) buffer time in order to give safer predictions.

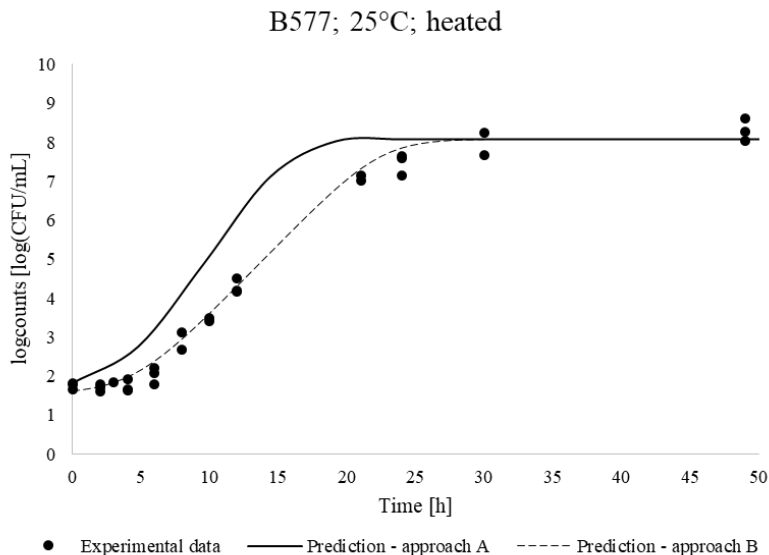


Figure 5.0.5 - Example of primary model validation using Approaches-A (continuous line) and -B (dashed line) from growth rate secondary model to illustrate improvement resulting from Approach-B. Experimental data (dots).

Table 5.0.7 presents $RMSE_{\text{prediction}}$ (Equation 5.5) values for each strain and stress condition as a measure of how agreeable the predictions are with the observed data. The respective plots with predicted vs. observed log counts for each strain are shown in FIGURE 5.0.6. It is interesting to notice that for both approaches of estimating growth rate the biggest RMSE values are attributed to B577 strain. This strain is also the reference strain for emetic *B. cereus* and the one with the bigger amount of collected log counts data, probably reflecting in quite a realistic way the real data variability expected for the phylogenetic group. Here in Approach-B, the data are scattered around the equivalence line indicating a tendency to not overestimate or underestimate the log counts, differently from what happens in Approach-A. This is also valid for all the other investigated strains.

Table 5.0.7 - RMSE values for predictive performance evaluation of Approach-B when applied together with h_0 and N_{\max} assumptions to simulate primary growth curves.

Strain	RMSE _{prediction} total	RMSE _{prediction} unheated	RMSE _{prediction} heated
B577	0.465327	0.496226	0.449541
B596	0.493465	0.457304	0.516778
B626	0.33784	0.33784	x
B635	0.423911	0.423911	x
ALL	0.453379	0.436324	0.471137

x = no available data.

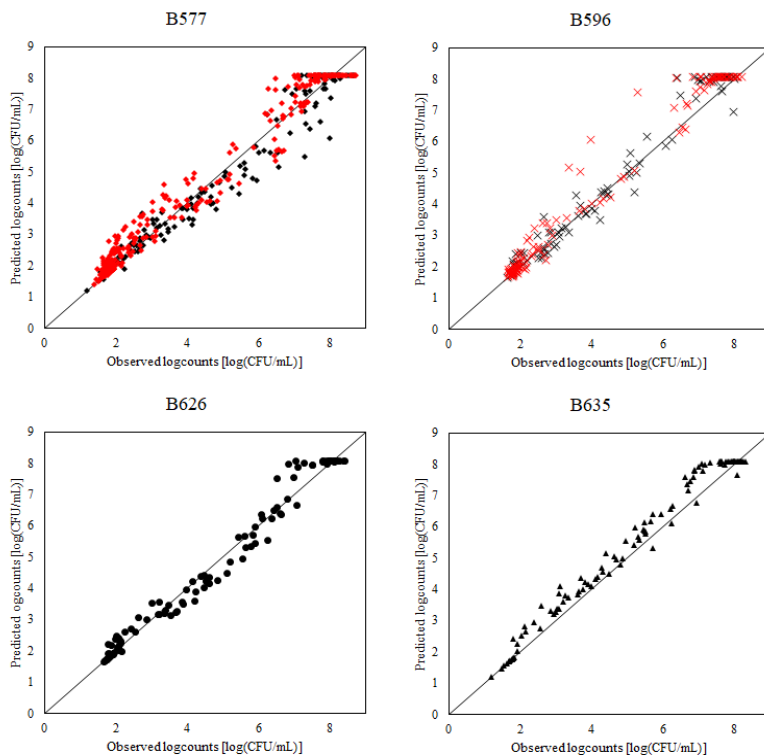


Figure 5.0.6 - Observed vs. predicted logcounts for all studied strains using Approach-B to simulate growth rates coupled with h_0 and N_{\max} assumptions. In red: heated cells. In black: unheated cells.

As already suggested during secondary model validation, Approach-B proposes a more robust model for growth rates estimation that together with h_0 and N_{\max} produces predictions more in accordance with the observations and seemed to be more suitable to be applied when predicting the behaviour of *B. cereus* in food matrices. The biggest limitation of this method is that a prior estimation of bias factor is needed for each of the matrices of interest (and perhaps each of the strains), what can increase the laboratory workload and costs for the food industry, once the ideal is to have a wide range and same number of replicates of measured growth rates for both culture medium and food matrix to obtain a robust bias factor estimation.

5.3.2 External validation

5.3.2.1 Secondary models

For the external validation of secondary models, Approach-A was selected to estimate μ_{opt}^{RIF} once it presented a wider range for this parameter estimates considering the strains investigated. The creation of a general secondary model for emetic strains was prepared using the average cardinal values (T_{\min} , T_{opt} , T_{\max} , and μ_{opt}^{RIF}) between all emetic strains (B577, B594, B596 and B626) with upper boundary built with model confidence limits for B626 strain once it presented the minimum T_{\min} , maximums T_{opt} , T_{\max} and μ_{opt}^{RIF} and with lower boundary built with (lower) model confidence limit for B594 strain, once it has maximum T_{\min} and minimums T_{opt} , T_{\max} and μ_{opt}^{RIF} . The values are summarized and presented in TABLE 5.0.8. Comparing the predictions to external *B. cereus* growth rates data coming from literature gives an idea of how the model can be considered as generic. Selected literature data were: in RIF (BURSOVÁ et al, 2018), Combase data in milk (DUFRENNE et al, 1995; FSA-FMBRA/UK; HARMON & KAUTTER et al, 1991; IZS-BS; MANSOUR & MILLIÈRE et al, 2001; MIKOLAJCIK et al, 1973; MEER et al, 1991; PENNA et al, 2002; RODRIQUEZ & BARRETT, 1986; STU; WONG et al, 1988) and Nestlé data in dairy products for different strains. As implemented before, here the square-root transformation was used to stabilize μ_{\max} variance; the same transformation was used by Aryani et al (2015) when validating secondary models for *Listeria monocytogenes* after testing different link functions.

Table 5.0.8 - Cardinal values used for creation of general model for *B. cereus* emetic strains

Parameter	Average	Lower boundary (B594 strain)	Upper boundary (B626 strain)
μ_{opt}^{RIF} [h ⁻¹]	2.29	1.46	2.97
Tmin [°C]	7.40	8.82	5.95
Topt [°C]	39.44	36.74	41.44
Tmax [°C]	48.10	47.57	48.44

Note that the actual upper boundary is equal to the predicted $\sqrt{\mu_{max}}$ for B626 strain using cardinal values presented in TABLE 4.0.1 plus two times RMSE_{global} for temperature (=0.088). The lower boundary is built analogously, being equal to the predicted $\sqrt{\mu_{max}}$ for B594 strain minus two times RMSE_{global} for temperature.

According to Guillier (2016), for the validation of secondary models for growth or inactivation, more and more studies are based on data extracted from existing literature data. The modelling of data from different studies raises particular difficulties. Datasets should not be selected just because they lead to favourable results for the model. Similarly, one should not exclude a dataset just because it represents disagreements to the simulated values. It is therefore necessary to define the criteria for inclusion of data and take into account the fact that validation is also the place to check the range of application (food types) of the model. In this context, the model proposed here should be suitable to be applied to a range of dairy products with pH and water activity within the optimal development range for *B. cereus*. FIGURE 5.0.7 presents the proposed secondary model with its confidence limits and the collected data from literature.

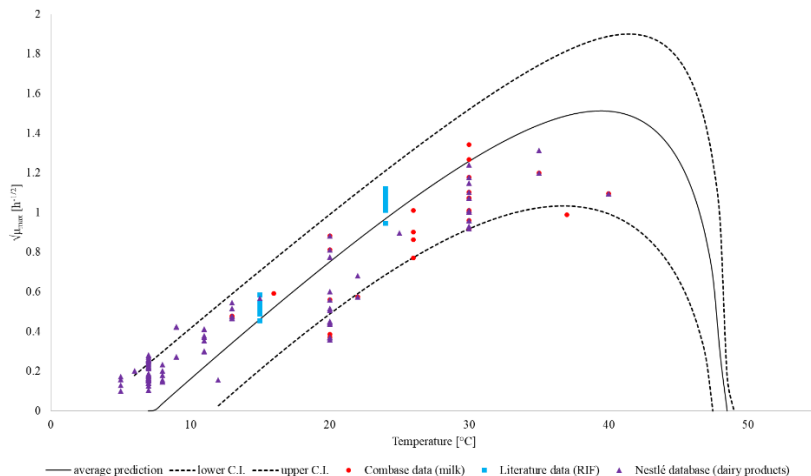


Figure 5.0.7 - External validation of secondary model for emetic strains. Continuous line: predictive model. Dashed lines: C.I. In blue: literature data in RIF. In red: Combase data in milk. In purple: Nestlé data for dairy products.

FIGURE 5.0.7 shows the variability of the external data collected over a temperature range from 5 to 30°C. Very few points are collected at temperatures above 30°C. This means that the validation of the model in the high temperature region will be not possible.

Overall, the proposed model presents a good predictive performance, once the vast majority of the literature growth rates data are within the model suggested boundaries. More precisely, the model predictive accuracy for growth rates is 88% (with only 16 out of 130 collected data out of C.I.). Two main limitations of the validation procedure are the fact that it is not always possible to find data in the literature for a specific phylogenetic group of *B. cereus* and, as mentioned before, this is a species with wide behaviour in terms of temperature and the fact that it is difficult to find data for the specific media the model was built for (RIF in this case). These two factors combined increase the data variability considerably and despite them, the proposed model seems to be suitable for practical application.

5.4 Conclusions

The objective of this chapter was to evaluate the predictive performance of models and assumptions made along Chapters 3 and 4 when applied to food scenarios.

The predictions of *B. cereus* in RIF made with the cardinal parameter values using turbidity experiments in culture medium combined with challenge test data and based on the bias factor, were satisfactory. Considering the cardinal temperatures are medium-independent, Approach-A, which took an average of individual μ_{opt}^{RIF} as this parameter estimate, seemed to overestimate this parameter for one of the strains (B577), what resulted in a clear overestimation of log counts when primary growth curves were simulated. On the other hand, Approach-B, using bias factor to estimate μ_{opt}^{RIF} showed much more reliable predictions for all strains. The assumptions made for h_0 and N_{max} seemed to respond well for most of the cases, confirming the statement that a simple average is enough.

The creation of a general model for emetic strains of *B. cereus* was developed using cardinal temperatures obtained for the different strains investigated and μ_{opt}^{RIF} estimated according to Approach-A. Confronted with literature data from different sources and from a variety of dairy products, the proposed model showed good performance with 88% of the collected growth rates within the confidence boundaries.

5.5 References

ARYANI, D. C.; DEN BESTEN H. M. W.; HAZELEGER, W. C.; ZWIETERING, M. H. Quantifying strain variability in modeling growth of *Listeria monocytogenes*. **International Journal of Food Microbiology**, v. 208, p.19-29, 2015.

BARANYI, J.; CSERNUS, O.; BECZNER, J. Error analysis in predictive modelling demonstrated on mould data. **International Journal of Food Microbiology**, v.170, p.78–82, 2014.

CASTILLEJO-RODRIGUEZ, A. M.; GIMENO, R. M. G.; COSANO, G. Z.; ALCALA, E. B.; PEREZ, M. R. R. Assessment of mathematical models for predicting *Staphylococcus aureus* growth in cooked meat products. **Journal of Food Protection**, v.65, p.659–665, 2002.

DELIGNETTE-MULLER, M. L.; ROSSO, L. Biological variability and exposure assessment. **International Journal of Food Microbiology**, v.58, p.203–212, 2000.

DUFRENNE, J.; BIJWAARD, M.; TE GIFFEL, M.; BEUMER, R.; NOTERMANS, S. Characteristics of some psychotropic *Bacillus cereus* isolates. **International Journal of Food Microbiology**, v.27, n.2, p.175-183, 1995.

IZS – BS: Dipartimento di sicurezza alimentare, Istituto Zooprofilattico Sperimentale della Lombardia e dell'Emilia Romagna, Brescia, Italia.

FSA-FMBRA: Food Standards Agency funded data generated at the former FMBRA, Chorleywood (today Champden and Chorleywood Food Research Association), UK.

GUILLIER, L. Predictive microbiology models and operational readiness. **Procedia Food Science**, v.7, p.133 – 136, 2016.

HARMON, S. M.; KAUTTER, D. A. Incidence and growth potential of *Bacillus cereus* in ready-to-serve foods. **Journal of Food Protection**, v.54, n.5, p.372–374, 1991.

MANSOUR, M.; MILLIÈRE, J-B. An inhibitory synergistic effect of a nisin-monolaurin combination on *Bacillus sp.* vegetative cells in milk. **Food Microbiology**, v.18, p.87-94, 2001.

MCDONALD, K.; SUN, D. W. Predictive food microbiology for the meat industry: a review. **International Journal of Food Microbiology**, v.52, p.1–27, 1999.

MEER, R. R.; BAKER, J.; BODYFELT, F. W.; GRIFFITHS, M. W. Psychrotrophic *Bacillus spp.* in fluid milk products: A review. **Journal of Food Protection**, v.54, n.12, p.969–979, 1991.

MIKOLAJCIK et al. Fate of *Bacillus cereus* in cultured and direct acidified skim milk and Cheddar cheese. **Journal of Milk and Food Technology** v.36, n.6, p.317–320, 1973.

PENNA, H. C. V.; MORAES, D. A.; FAJARDO, D. N. The effect of nisin on growth kinetics from activated *Bacillus cereus* spores in cooked rice and in milk. **Journal of Food Protection**, v.65, n.2, p.419-422, 2002.

PINON, A.; ZWIETERING, M.; PERRIER, L.; MEMBRÉ, J-M.; LEPORQ, B.; METTLER, E.; THUAULT, D.; COROLLER, L.; STAHL, V.; VIALETTE; M. Development and validation of experimental protocols for use of cardinal models for prediction of microorganism growth in food products. **Applied and Environmental Microbiology**, v.70, n.2, p.1081–1087, 2004.

RODRIGUEZ, M. H.; BARRETT, E. L. Changes in microbial population and growth of *Bacillus cereus* during storage of reconstituted dry milk. **Journal of Food Protection** v.49, n.9, p.680–686, 1986.

ROSS, T. Indices for performance evaluation of predictive models in food microbiology. **Journal of Applied Bacteriology**, v.81, p.501-508, 1996.

STU: Slovak Technical University, Bratislava, Slovakia.

WALLS, I.; SCOTT, V. N. Validation of predictive mathematical models describing the growth of *Escherichia coli* O157:H7 in raw ground beef. **Journal of Food Protection**, v.59, p.1331–1335, 1996.

WONG, H. C.; CHEN, Y. L.; CHEN, C. L. F. Growth, germination and toxigenic activity of *Bacillus cereus* in milk products. **Journal of Food Protection** v.51, n.9, p.707–710, 1988.

6. PROBABILITY OF GROWTH OF *B. CEREBUS* INDIVIDUAL CELLS AFTER PRE-INOCULATION STRESS

6.1 Introduction

One of the most important areas of quantitative microbiology is bacterial kinetics. It can be described by rates, such as the number of cell divisions or cell deaths in a unit time, or the production rate of a specified metabolite. However, for a single cell, it is difficult to interpret and measure these quantities directly. At low levels of cell concentrations, the probability of division (or death) of a single cell becomes the main parameter, from which the respective population level parameters can be inferred. A simple example for this is the probability whether a single cell can generate an exponentially growing subpopulation.

Any system or equipment able to identify the turbidity in a culture broth can be used to detect bacterial growth (turbid / no-turbid after an experimental time). A popular example is the Bioscreen C (Oy Growth Curves Ab Ltd, Helsinki, Finland). This equipment allows to monitor many bacterial cultures simultaneously and it is frequently used in growth probability assessments (LÖWDIN et al, 1993; LEE et al, 2011; AHMAD et al, 2015). Its working principle is based on the following idea: A homogeneous cell population is distributed over a large number of wells (typically 50, 100, 200 or even 400, if several equipment can be used), targeting an inoculation of one cell *per* well concentration. However, it is difficult to guarantee that the inoculum level is exactly one cell per well, and the number of inoculated cells is normally just expected to be low. Besides, the turbidity readings refer to the generated growing subpopulation of the inoculated cells, and not to those initial cells directly.

Despite these difficulties, the probability of growth of an inoculated cell can be estimated efficiently and reliably by turbidity measurements. To achieve this, the number of cells *per* well before and after running the experiment is assessed by:

- i) plate counts of a sample of the culture prepared for inoculating the wells (an *a-priori* estimator denoted by \hat{r});
- ii) means of the proportion of wells not becoming turbid during the experiment (an *a-posteriori* estimator denoted by \hat{p}).

These can then be used to estimate the probability of growth for a single cell by $\hat{g} = \hat{\rho}/\hat{r}$. Finally, the accuracy of this probability estimate is assessed by the respective accuracies of the counter and the denominator.

This study aims to identify the difference, if any, between the probability of growth of stressed and non-stressed *B. cereus* cells and increase the confidence of experimenters in using the turbidity methods to assess this probability.

TABLE 6.0.1 - NOMENCLATURE AND MEANING OF SYMBOLS AND ASSUMPTIONS.

Notation	Meaning
E(), Var(), $\sigma()$	Expected value, variance and deviation (square-root of variance) of a random variable
c, \hat{c}, m_c	<p>Number of colonies on a plate, its estimator and its expected value $m_c = E(c)$. If $E(\hat{c})=m_c$ then the estimator is unbiased. Typically, $50 < m_c < 200$.</p> <p>Since the total number of cells in the primary culture is typically 10^7 or more, \hat{c} follows the Poisson distribution, therefore its expected value is equal to its variance:</p> $E(\hat{c}) = \text{Var}(\hat{c}) = m_c$
r, \hat{r}, m_r	<p>Number of cells inoculated in a well, its estimator, and its expected value. \hat{r} is calculated from \hat{c} by means of a small, constant factor $a < 1$. Its value depends on the used dilution, which is a linear operation, so \hat{r} is unbiased, too.</p> $m_r = E(\hat{r}) = E(a \cdot \hat{c}) = a \cdot m_c \quad \text{and} \quad \text{Var}(\hat{r}) = \text{Var}(a \cdot \hat{c}) = a^2 \cdot m_c = a \cdot m_r$
w	<p>Total number of wells; a constant. Typical values are 50, 100, 200 or 400. Each well is inoculated by a random number of cells following the Poisson distribution.</p>
$\rho, \hat{\rho}, m_\rho$	<p>Number of cells per well, its estimator and its expected value $E(\rho) = m_\rho$.</p>
w_0	<p>Number of wells showing no growth (negative wells). The random variable $w-w_0$ follows the Bernoulli distribution with the success probability z, where success is if a well is positive (i.e. it shows growth). Then $E(w_0/w) = 1-z$</p>

If $\hat{\rho} = -\ln(w_0/w)$, then, as it turns out, $m_\rho < E(\hat{\rho})$ ($\hat{\rho}$ is a biased estimator).

$\hat{\rho}'$	Modified estimator for ρ , to make the estimation close-to-unbiased in the studied region. $\hat{\rho}' = -\ln(w_0/(w-2))$
g, \hat{g}, m_g	No growth / growth indicator; a $\{0, 1\}$ binary event for a single inoculated cell, its estimator, and its expected value: the probability of growth for a single cell). No-growth is defined here by the event that the well containing the cell remains non-turbid (that is, within the experimental time, the inoculated cell does not generate OD-detectable cell population). The estimator for g is: $\hat{g} = \hat{\rho}' / \hat{\rho}$
$re[E(\hat{\rho})]$	Accuracy coefficient for $\hat{\rho}$ (or relative error for $E(\hat{\rho})$): $re[E(\hat{\rho})] = (E(\hat{\rho}) - m_\rho) / m_\rho$
$rd(\hat{\rho})$	Efficiency coefficient (relative deviation) of the $\hat{\rho}$ estimator: $rd(\hat{\rho}) = \sigma(\hat{\rho}) / E(\hat{\rho})$

6.2 Material and Methods

6.2.1 Probability of growth of stressed and non-stressed *B. cereus* individual cells

The aim of this part on probability of growth experiments is to evaluate the effect of the heat stress on the subsequent growth of single cells at different temperatures. Thus, the potential of growth of both non-stressed and stressed cells could be investigated and compared as well as their individual lag times. In this part, just the reference strain B577 for the emetic group was used and the following temperatures were investigated: 15, 22, 25, 40, and 47 °C to evaluate if the temperature of the recovery medium after the stress had an impact on the individual behaviour of stressed and non-stressed cells and on their probability of growth.

6.2.1.1 Inoculum preparation

The same inoculum was used to prepare heated and unheated cells, to be studied at a population and single cell level.

6.2.1.1.1 Unheated cells

Under aseptic conditions, one cryobead of B577 strain was removed using a disposable plastic needle and placed into a BHI tube. The vial was quickly re-capped and returned immediately to the freezer. The BHI tube was incubated for 8 h at 30 °C and then a subculture of 0.1 ml was introduced in a BHI tube for an additional 18 h at 30 °C to achieve a final concentration of 10⁸ CFU/ml.

To fill the wells dedicated to population level (coloured in red in FIGURE 6.0.1), two ten-fold dilutions of the subculture were prepared using BHI broth adjusted to the experimental conditions to reach a concentration of 10⁶ CFU/ml in the initial Bioscreen wells.

6.2.1.1.2 Heated cells

To obtain heat-stressed cells, a 10 mL BHI tube is preheated for 3.5 min at 72 °C, then 100 µl of the 18 h subculture (prepared as described in 3.1.1 section of Chapter 3) is injected into it and heated at 72 °C for 25 seconds and quickly removed from the water bath to be cooled to 22 °C during 20 seconds in a mixture of ice and water.

6.2.1.1.3 Single cells inoculum

The methodology suggested by Guillier and Augustin (2006) was used in this part of the work and can be briefly described as following. The Poisson distribution, with 0.42 cells/well allows to have in 80% of

the wells showing growth a maximum of one single cell per well and no more than 35% of the inoculated wells were expected to show growth. Therefore this 0.42 cells/well is a suitable target.

6.2.1.2 Population growth rate for heated and unheated cells

To obtain the growth rates for heated and unheated cells from the wells dedication to population kinetics, the same method was used as when estimating growth rates for the cardinal values estimation (described in section 4.2.3.5 of Chapter 4).

6.2.1.3 Plate design

The plate design used for the probability of growth experiments is shown in FIGURE 6.0.1 where the first 90 wells were dedicated to single cell studies (to assess the number of growing wells and the correspondent individual lag time in those wells) and the last 10 wells to assess the growth rate at population level. The wells 1 to 100 (first plate) were always used for unheated cells and wells 101 to 200 (second plate) for heated cells.

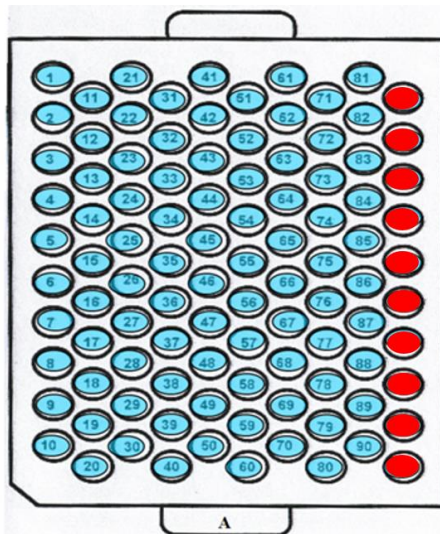


Figure 6.0.1 - Bioscreen plate design for probability of growth experiments. In red, the wells dedicated to population level; in blue they were dedicated to single cell level.

6.2.1.4 Calibration curve

To be able to calculate the concentration on the bacteria at the chosen threshold, a calibration curve with B577 strain was performed by measuring the O.D. for different concentrations of the inoculum. It is presented in ANNEX E.

6.2.1.5 Data analysis

In case of a low inoculum (wells 1 to 90 dedicated for single cells), from the distribution of the detection times, the individual lag times can be estimated, according to Equation (6.1) (METRIS et al., 2003).

$$\tau_i = t_{d_i} - \left(\frac{\ln N_d - \ln N_0}{\mu_{\max}} \right) \quad (6.1)$$

where t_{d_i} = detection times; τ_i = individual lag times; N_d = number of cells in the well at detection level; N_0 = initial number of cells in the well (1 CFU); μ_{\max} = maximum specific growth rate.

The probability of growth will be estimated according to \hat{g} estimator (Equation (6.11)), which will be presented along 6.2.2.3 section. The probability of growth estimator compares two methods of assessing the average number of cells per well: method 1 as the *a-priori* estimator (see 6.2.2.1) and method 2 as the *a-posteriori* estimator (see 6.2.2.2)

6.2.2 Optimization of turbidity experiments to estimate the probability of growth for individual bacterial cells

6.2.2.1 *A-priori* estimation using plate count method

A basic assumption behind plate count methods is that one cell in the sample produces one colony. The number of colonies on a plate is a random number, \hat{c} that follows the Poisson distribution (WIMMER & ALTMANN, 1996) since the colonies are from a population orders of magnitude bigger than the sample from which the colonies were plated. Its expected value is in the order of 100, so, for the optimization studies, the region where $50 < c = E(\hat{c}) < 200$ will be considered. Due to the Poisson assumption, the variance of \hat{c} is the same as its expected value. Furthermore, when estimating the expected number of initial cells in a well, a factor a can be calculated from the used dilutions. This factor is typically around the reciprocal of c once the theoretical aim is a single

cell inoculated in a well. From these, the accuracy of the \hat{r} estimator can be assessed by its relative deviation as shown by Equation (6.4).

$$r = E(\hat{r}) = E(a \cdot \hat{c}) = a \cdot c \quad (6.2)$$

$$\text{Var}(\hat{r}) = \text{Var}(a \cdot \hat{c}) = a^2 \cdot c = a \cdot r \quad (6.3)$$

$$rd(\hat{r}) = \frac{\sqrt{\text{Var}(\hat{r})}}{r} = \sqrt{\frac{a}{r}} \quad (6.4)$$

6.2.2.2 *A-posteriori* estimation using turbidity results

When inoculating the plate for turbidity observation (e.g. Bioscreen), a diluted culture consisting of N cells is distributed among w wells, where $w \ll N$. As described in the previous section, the number of initial cells producing detectable turbidity follows the Poisson distribution, with the expected value ρ . An estimator for ρ can be obtained by using the number of the so-called negative wells, in which either no cells were inoculated, or the cells did not produce turbidity. Let this (random) number of negative wells be denoted by w_0 . The expected value of the fraction w_0/w is $z=e^{-\rho}$, from which an estimator for ρ is (BARANYI et al., 2009):

$$\hat{\rho} = -\ln\left(\frac{w_0}{w}\right) \quad (6.5)$$

Here the properties of this estimator are investigated for small values of ρ when the occurrence of non-turbid wells is very likely.

Consider the event for a well that does not become turbid as the success in a Bernoulli trial. The size of the trial is w and $z = e^{-\rho}$ is the probability of success, while the w_0 number of successes follows the binomial distribution.

$$\text{Prob}(w_0 = i) = \binom{z}{i} z^i (1 - z)^{n-i} \quad (i = 0 \dots w) \quad (6.6)$$

The estimator cannot interpret the $w_0 = 0$ and $w_0 = w$ situations, which in effect means that the experiments where all the wells are positive, or all the wells are negative are discarded. This results in the conditional distribution with b_i probabilities:

$$\begin{aligned} \text{Prob}(w_0 = i) = b_i &= \frac{\binom{n}{i} z^i (1-z)^{n-i}}{1 - [(1-z)^n + z^n]} \quad (i \\ &= 1, \dots, w-1) \end{aligned} \quad (6.7)$$

The (conditional) expected value of the estimator is therefore

$$E(\hat{\rho}) = - \sum_{i=1}^{w-1} \ln\left(\frac{i}{w}\right) b_i \quad (6.8)$$

It is desirable that the estimator is at least close-to-unbiased, i.e., its expected value is close to the parameter it intends to estimate. Besides, the smaller the relative deviation of the estimator, the more efficient it is. First, concentrating on the accuracy of the estimator, defined by its relative error from the parameter it intends to estimate

$$re[E(\hat{\rho})] = \frac{E(\hat{\rho}) - \rho}{\rho} \quad (6.9)$$

Secondly, the efficiency of the estimator is studied, which can be quantified by

$$rd[\hat{\rho}] = \frac{\sqrt{\text{Var}(\hat{\rho})}}{E(\hat{\rho})} \quad (6.10)$$

Notice that Eq. (6.9) is a comparison with the real value ρ , while Eq. (6.10) is the relative deviation of the estimator (which is a random variable). In summary, Eq. (6.9) is about the accuracy of the expected value of the estimator, and Eq. (6.10) is about the scatter of the estimator.

6.2.2.3 Estimating the probability of growth

A way to estimate the probability of growth of single cells is to compare the *a-priori* and the *a-posteriori* estimators for the number of cells per well, described in sections 6.2.2.1 and 6.2.2.2 respectively. This approach was proposed by Baranyi et al (2009) and it is presented in Eq. (6.11).

$$\hat{g} = \hat{\rho} / \hat{r} \quad (6.11)$$

For stability reasons, it is reasonable to consider its logarithm instead:

$$\ln(\hat{g}) = \ln(\hat{\rho}) - \ln(\hat{r}) \quad (6.12)$$

Remember that the two estimators are independent (so are their logarithm values), therefore the variance of their sum is the sum of the respective variances, i.e.,

$$\text{Var}(\ln(\hat{g})) = \text{Var}(\ln(\hat{\rho})) + \text{Var}(\ln(\hat{r})) \quad (6.13)$$

This gives an opportunity to estimate the error of the $\ln(\hat{g})$ estimator based on the approximation that small relative error of a variable is close to the error in its natural logarithm.

6.3 Results and Discussion

6.3.1 Probability of growth of stressed and non-stressed *B. cereus* individual cells

As mentioned before, the probability of growth of individual cells is inferred comparing *a-priori* ($\hat{\rho}$) and *a-posteriori* (\hat{r}) methods of assessing the average number of cells per well (see Equation 6.11). If the actual *a-posteriori* concentration is significantly lower than the *a-priori* concentration, the fraction of cells able to divide in the wells during the experiment time is less than 100%. For this, it is important to have rigorously defined assumptions and proper confidence limit calculations.

The input data needed by Method 1 are the triplicate plate counts and the dilution factor; for method 2, the only information needed is the total amount of inoculated wells (w) and the number of negative wells observed after running the experiments (w_0). The confidence limits were obtained by assuming a normal distribution of the number of cells in the plates for method 1 and, for method 2, the Poisson distribution of the cells in the wells (WIMMER & ALTMANN, 1996).

Thus, with this information for every replicate at the different tested conditions, it is possible to compare method 1 and method 2 of assessing the average number of cells per well for heated and unheated cells. As can be seen in FIGURE 6.0.2 there is no significant difference between the average number of cells per well assessed by means of method 1 and method 2 for each of the replicates. The same behaviour is observed for all the replicates at all temperature conditions (see ANNEX D for all the other respective plots). This result means that at some extent all the replicates have 100% probability of growth, not leading to any conclusive significant difference between the potential of growth of heated and unheated cells for all the tested conditions (temperatures between 15 °C and 47 °C). This can be an interesting result, once the assumption was an underestimation of the potential of growth of these stressed cells. Now, in fact, it is known that as much care as with non-stresses cells need to be taken into account. Regarding the methods confidence interval, the *a-posteriori* estimator is always bigger due to the bigger uncertainty of the method.

Next section of the results was built with the idea of analysing the properties of \hat{r} estimator and consequently optimizing probability of growth experiments.

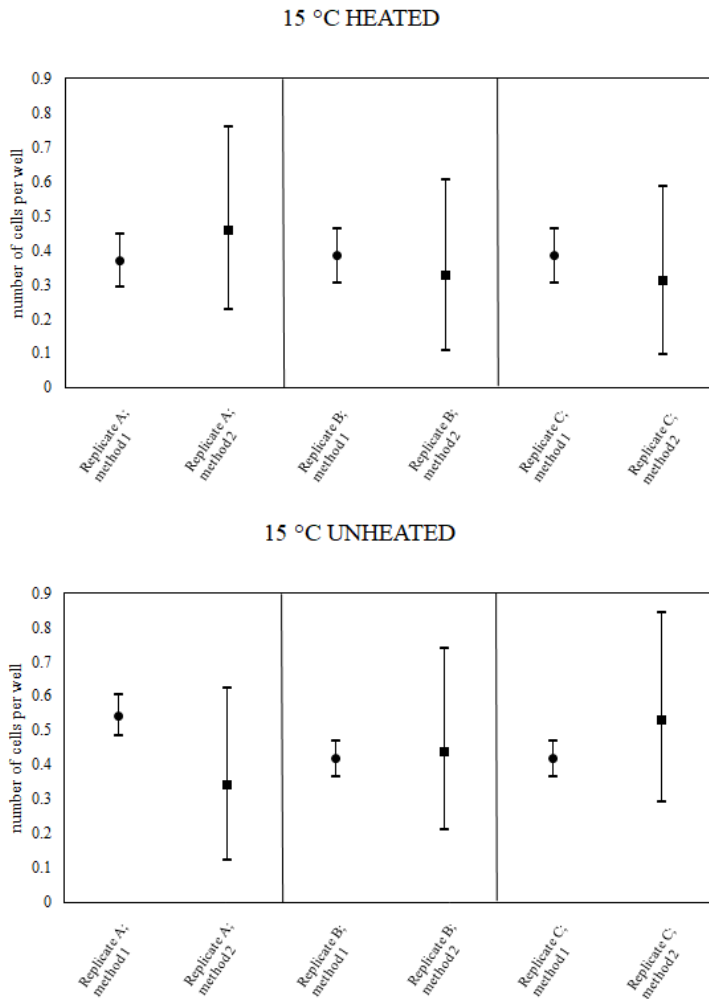


Figure 6.0.2 - Comparison between average number of cells per well according to method 1 (dots) and method 2 (squares) for each replicate of the experiments with heated cells at 15 °C (top) and for unheated cells (bottom).

6.3.2 Optimization of turbidity experiments to estimate the probability of growth for individual bacterial cells

To decrease the uncertainty in assessing the growth probability, this optimization is performed to increase the number of wells where

growth can be observed (higher than 35% of wells showing growth provided by the Poisson distribution) while making sure that not too many cells (less than 3 cells) are present in the wells showing growth.

Considering the pragmatic 50 to 200 colonies on a plate (*a-priori estimation*), the relative error of the *a-priori* estimator will be less than 10%. For the *a-posteriori* estimation, if $0.5 < \rho < 3$, then the expected fraction of negative wells is between 5 and 60%, the expected value of the $\hat{\rho}$ estimator is always smaller than ρ , as shown in FIGURE 6.0.3(A). Therefore, this estimator is biased. To make it at least close-to-unbiased, the estimator was modified according to Equation (6.14).

$$\hat{\rho}' = -\ln\left(\frac{w_0}{w-2}\right) \quad (6.14)$$

FIGURE 6.0.3 (B) shows the effect of this modification. For any w number of wells, the ideal value of ρ , where the estimator is unbiased, is *ca.* $\rho = 1.6$ cell per well, corresponding to *ca.* 20% negative wells ($w_0 = 0.2w$). For the studied $w = 50, 100, 200,$ and 400 , the expected value of the estimator approximates the ρ parameter within $\varepsilon = 3\%$ accuracy in intervals that increase with w . The accuracy of the estimators is characterized by the relative difference between the expected value of the estimator and the parameter it intends to estimate.

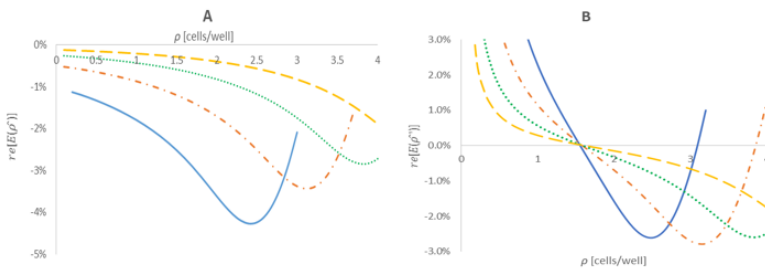


Figure 6.0.3 - Accuracy of the estimators $\hat{\rho}$ (A) and its modification $\hat{\rho}'$ (B). Continuous blue: $w=50$; dash-dotted orange: $w=100$; dotted green: $w=200$; dashed yellow: $w=400$.

Combining the 5% accuracy and maximum efficiency of the estimator $\hat{\rho}'$ (FIGURE 6.0.3 (B) and FIGURE 6.0.4, respectively), a desirable range is presented in

TABLE 6.0.2. For this, a simple criterion was established based on visual observation of the graph: for each w , take the global minimum value of $rd[\hat{\rho}'] + 1.5\%$, which corresponds to the region where $rd[\hat{\rho}']$ has a local minimum for all w values (FIGURE 6.0.4). Maximum efficiency of the estimator coincides with its minimum relative error region, corresponding to the case when *ca.* 10-40% of the wells are negative. This simultaneous analysis of accuracy and efficiency of the estimator $\hat{\rho}'$ indicates a local optimum efficiency of the estimator that coincides with its optimal accuracy region, corresponding to the case when *ca.* 5-40% of the wells are negative.

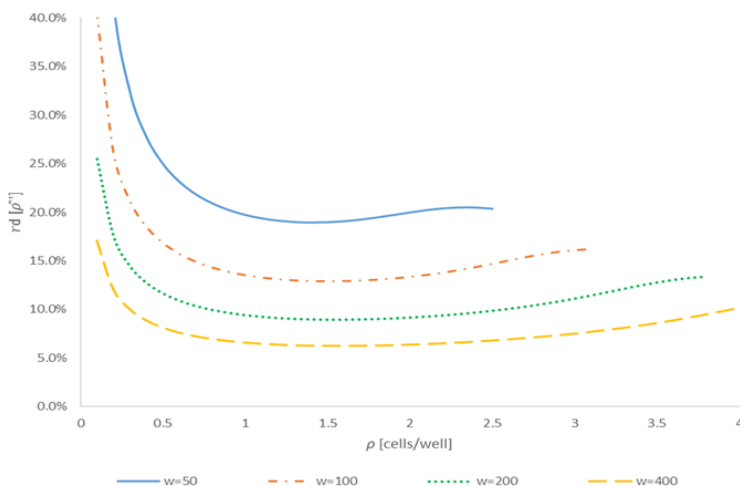


Figure 6.0.4 - Efficiency of the $\hat{\rho}'$ estimator quantified by its relative deviation for different number of wells. Continuous blue: $w=50$; dash-dotted orange: $w=100$; dotted green: $w=200$; dashed yellow: $w=400$.

Table 6.0.2 - Recommendations on target optimal value of ρ . At these values, both the accuracy coefficient and efficiency of the $\hat{\rho}'$ estimator are optimal.

w [number of wells]	Ideal range of ρ [cells/well]
50	0.9 – 2.0
100	0.9 – 2.2
200	0.9 – 3.0
400	0.8 – 3.0

Previous studies (GUILLIER & AUGUSTIN, 2006), have recommended to obtain a number lower than our finding for the *cell-per-well* inoculum level. However, those authors aimed to analyse individual cell lag times, which is out of the scope of the present study. Note that Metris et al (2003), while also investigating single-cell lag times, prepared the inoculation so that the fraction of negative wells was between 12.5% and 37.5%. Based on the Poisson distribution and assuming, that all cells produced growing subpopulations, this means that the mean number of initial cells in a well that would grow to detectably turbid level was between 1 and 2 cell *per well* in all experiments, in accord with the recommendations given here.

As can be seen, it can easily be achieved that the efficiency of the unbiased *a-priori* estimator is less than 10% in the studied region. However, the *a-posteriori* estimator has 10% or less efficiency only for $w > 200$ (Figure 2). In that case, based on Eq. 12, the scatter of the $\ln(\hat{g})$ estimator is about 0.1-0.2, which means that the method offers a way to measure the probability of growth with one digit accuracy and, for this, all the 200 wells of the Bioscreen plate, are desirable.

A consequence is that it is not feasible to identify changes in the probability of growth if it is close to 1, and only changes greater than about 10% are detectable. This level, however, can be still useful, considering that the probability of growth rapidly changes with environmental factors like temperature or water activity; that is, relatively small changes in the conditions can induce detectable changes in the single cell probability of growth provided by our method.

Remember that, strictly speaking, probability of growth for a single cell means the probability that an inoculated single cell generates a progeny that grows over the optical density detection level. In stress conditions (e.g. at low water activity), it is possible that the single cell produces a growing subpopulation which however does not grow over the detection level. This possibility needs to be considered when interpreting the results.

6.3.3 Individual lag times

For the individual lag times estimation (using Equation 6.1), the concentration of the bacteria at the detection level needs to be assessed, so a calibration curve with B577 strain was used (ANNEX E).

TABLE 6.0.3 shows the detection level used to calculate the detection times for each experiment with their respective concentration of *B. cereus* at that level (these coming from the calibration curve). The detection level for each experiment was chosen to be equal to the base line (which depends on the Bioscreen equipment) + 0.1, that is why they may differ from one experiment to another.

Table 6.0.3 - Detection levels used to calculate detection times and respective concentration of cells used to calculate individual lag times.

Experiment	Detection level [O.D.]	Number of cells/well at O.D. level (N_d)
15A	0.20	1.8×10^6
15B	0.40	3.4×10^6
15C	0.30	2.6×10^6
22A	0.20	1.8×10^6
22B	0.20	1.8×10^6
22C	0.20	1.8×10^6
25A	0.20	1.8×10^6
25B	0.20	1.8×10^6
25C	0.20	1.8×10^6
40A	0.20	1.8×10^6
40B	0.20	1.8×10^6
40C	0.20	1.8×10^6
47A	0.31	2.7×10^6
47B	0.31	2.7×10^6
47C	0.20	1.8×10^6

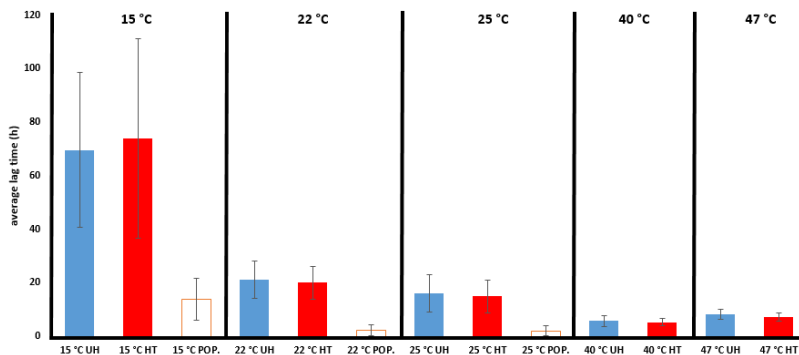


Figure 6.0.5 - Average lag time for individual cells unheated (in blue), heated (in red) and population lag time (in empty orange) coming from viable counts experiments.

From the plots shown in FIGURE 6.0.5 it can be seen that there is no significant difference between the individual lag times of heated and unheated cells for all the temperatures. This goes against the initial idea since the heat stress should increase the lag phase duration of the cells. An interesting fact is that this is in agreement with the findings described in Chapter 3 of this thesis, when the evaluation of h_0 suggests no difference between the physiological states of the heated and unheated cells (and consequently between their the lag times, once the stress does not affect the growth rates either), assuming that the cells grow in the same medium to a population level.

Heterogeneity at the individual cell level can be masked in conventional microbial culturing techniques that depend on data estimated from population level observation, which is the case here using turbidity measurements, once the obtained curves picture only the late exponential phase onwards and the single-cell parameters are estimated by means of these curves.

Furthermore, the population lag time (coming from the viable counts experiments with B577 strain growing in BHI) is always significantly lower than the individual lag times (derived from the single cells lag times), meaning that the fastest growers in the population will control the growth, while the effect of slowest growers can be detected only at single cell level. Also, as expected, the lag time is lower at temperatures close to optimum (at around 40 °C in this case) and increases

as temperature gets higher or lower. This can be understood from the h_0 parameter ($h_0 = \mu * \text{lag} = \text{constant}$). Under close to optimal temperature, the growth rate is high and the lag is low, while at sub/super optimal conditions the growth rate is lower and the lag higher, keeping the parameter more or less constant, once the cells have the same history prior-inoculation.

6.4 Conclusions

For individual cells, it is difficult to acquire sufficiently accurate data, especially when the chosen technique can give responses only at population level. This is probably one of the reasons why no significant difference on the probability of growth of heated and unheated cells could be observed for all tested temperatures. Coupled with the big uncertainty of the assessment of the average number of cells per well (due to the limited number of replicates), the final result can be interpreted as stressed and non-stressed cells are equally and fully (probability equal to 100%) able to grow at temperatures ranging from 15 to 47 °C. As for the individual lag times assessment, no significant difference between heated and unheated individual cells can be read from the experimental data.

In order to increase the confidence of experimenters, the proposed recommendations may provide a means to deal with the mentioned challenges and can be used to optimize experimental designs when assessing the probability of growth for single cells by turbidity measurements.

6.5 References

- AHMAD A.; ZACHARIASEN C.; CHRISTIANSEN L. E.; GRÆSBØLL K.; TOFT N.; MATTHEWS L.; DAMBORG P.; AGERSØ Y.; OLSEN J. E.; NIELSEN S. S. Pharmacodynamic modelling of in vitro activity of tetracycline against a representative, naturally occurring population of porcine *Escherichia coli*. **Acta Veterinaria Scandinavica**, v.57, p.79, 2015.
- BARANYI J.; GEORGE S. M.; KUTALIK Z. Parameter estimation for the distribution of single cell lag times. **Journal of Theoretical Biology**, v.259, p. 24–30, 2009.
- FELLER, W. An introduction to probability theory and its applications. Wiley, 1970.
- GEORGE S. M.; METRIS A.; BARANYI J. Integrated kinetic and probabilistic modeling of the growth potential of bacterial populations. **Applied and Environmental Microbiology**, v.81, n.9, p.3228-3234, 2015.
- GUILLIER L.; AUGUSTIN J-C. Modelling the individual cell lag time distributions of *Listeria monocytogenes* as a function of the physiological state and the growth conditions. **International Journal of Food Microbiology**, v.111, p.241–251, 2006.
- KENT, R. M.; DOHERTY, S. B. Probiotic bacteria in infant formula and follow-up formula: Microencapsulation using milk and pea proteins to improve microbiological quality. **Food Research International**, v.64, p.567–576, 2014.
- LEE Y. H.; KINGSTON A. W.; HELMANN J. D. Glutamate dehydrogenase affects resistance to cell wall antibiotics in *Bacillus subtilis*. **Journal of Bacteriology**, v.194, p.993–1001, 2011.
- LÖWDIN E.; ODENHOLT-TORNQVIST I.; BENGTSSON S.; CARS O. A new method to determine postantibiotic effect and effects of subinhibitory antibiotic concentrations. **Antimicrobial Agents and Chemotherapy**, v.37, p.2200–2205, 1993.

MÉTRIS A.; GEORGE S. M.; PECK M. W.; BARANYI J. Distribution of turbidity detection times produced by single cell-generated bacterial populations. **Journal of Microbiological Methods**, v.55, p.821– 827, 2003.

WIMMER G.; ALTMANN G. The multiple Poisson distribution, its characteristics and a variety of forms. **Biometrical Journal**, v.38, n.8, p.995-1011, 1996.

7. Conclusions

In this thesis, an extensive analysis on the behaviour of *B. cereus* at population and single cell levels was made, constituting an important finding that can be applied to real scenarios by the industry, academy or regulatory agencies when in the need of developing/validating new processes or to give guidance in any food safety matter.

At population level, three main investigations were performed with the aim of providing proper kinetic analysis and predictions. Having different measurement methods to quantify bacterial concentration along time and a few factors (such as growing medium, temperature, heat stress) that could affect the bacteria behaviour, the main conclusions can be summarized as follows:

(i) Considering viable count measurements, the focus was on evaluating the effect of two factors - stress and growing medium - on the physiological state of the cells (h_0) and on the maximum reached population (N_{\max}) and also assessing the effect of temperature on growth rates and how to use them to find a correlation between culture medium based models and food models. The results show that the only factor affecting h_0 and N_{\max} parameters is the growth medium, while the heat stress seems to have no significant impact on them. The square-root of the growth rates were regressed against temperature and their theoretical minimum temperature for growth (T_{\min}) estimate is not significant different for BHI and RIF models for the same strain, what supported the bias factor assessment. The bias factor between BHI and RIF growth models was then estimated for each strain using the square-root link function once, based on these data, it seems to make growth rate data temperature-independent.

(ii) By means of turbidity measurements, the specific growth rates by means of turbidity were estimated according to the specified quality criteria and the cardinal models for temperature, pH and water activity were fitted to the experimental data for each strain. The cardinal model for pH was the one that showed worst performance when fitted to the data, probably because estimating growth rates at unfavourable pH conditions increases the estimates uncertainty and consequently the variability between replicates. Significant differences on the estimated parameters could be identified and an agreement of 61.2% was obtained when comparing the strains by pairs. The agreement was 100% for pH_{\min} and

aw_{opt} parameters. B594 estimated parameters seem to differ more from the all the others strains. Strains B596 and B626 are equal in all parameters. The cardinal values proposed in this work respect differences between the same phylogenetic group and have been able to give acceptable predictions in foods, as shown along the validation chapter. These cardinal parameters could then be used in predictive models to estimate the different growth potentials of *B. cereus* strains, and more generally in *B. cereus* quantitative risk assessment.

(iii) A validation analysis to evaluate the predictive performance of models, assumptions and results obtained previously (items i and ii) when applied to food scenarios was performed. Despite some limitations, the predictions of *B. cereus* in RIF made with the cardinal parameter values estimated in culture medium combined with challenge test data in RIF were satisfactory. Considering the cardinal temperatures are medium-independent, the approach which took an average of individual μ_{opt}^{RIF} as this parameter estimate seemed to overestimate this parameter for one of the strains (B577), what resulted in a clear overestimation of log counts when primary growth curves were simulated, while the approach that used the bias factor to estimate μ_{opt}^{RIF} showed much more reliable predictions for all strains. Both approaches are likely to result in reliable predictions when applied to other scenarios (different microorganism, food, etc.), and the decision on which of them to use mainly depends on the available information and data. The assumptions made for h_0 and N_{max} seemed to respond well for most of the cases, confirming the statement that a simple average is enough. The creation of a general model for emetic strains of *B. cereus* was developed using cardinal temperatures obtained for the different strains investigated and an average of individual μ_{opt}^{RIF} as this parameter estimate. When compared to literature data from different sources and from a variety of dairy products, the proposed model showed good performance with 88% of the collected growth rates within the confidence boundaries, showing this can be a feasible way to create a general model for a species/group of microorganisms.

At individual cell level, the focus was on estimating and comparing the probability of growth of stressed and non-stressed cells and optimizing the experimental design for this kind of investigation using turbidity measurements. For individual cells, it is difficult to acquire sufficiently accurate data, especially when the chosen technique can give

responses only at population level. This is probably one of the reasons why no significant difference on the probability of growth of heated and unheated cells could be observed for all tested temperatures. Coupled with the big uncertainty of the assessment of the average number of cells per well (due to the limited number of replicates), the final result can be interpreted as stressed and non-stressed cells are equally and fully (probability equal to 100%) able to grow at temperatures ranging from 15 to 47 °C. As for the individual lag times assessment, no significant difference between heated and unheated individual cells can be read from the experimental data. In order to increase the confidence of experimenters, the proposed recommendations for the targeted concentration of cells in the wells may provide a means to deal with the mentioned challenges and can be used to optimize experimental designs when assessing the probability of growth for single cells by turbidity measurements.

8. Suggestions for future development

→Single cell level: Flow cytometry experiments to identify the fraction of dead, live and injured cells and their individual ability to grow; mainly if injured and live cells have the same probability to divide as the probability of growth using turbidity measurements suggest.

→Population level: Investigate if survival cells are more thermo tolerant with subsequent heat stresses. This could be read as a smaller log reduction due to heat treatment or no difference between h_0 averages.

→Toxin production by emetic strains of *B. cereus*: with similar experimental design, evaluate the effect of stress, medium, temperature and strain on toxin (cereulide) production. What factor influences it the most and which one(s) can be considered insignificant?

9. References

- ARYANI, D. C.; DEN BESTEN H. M.; HAZELEGER W. C.; ZWIETERING, M. H. Quantifying strain variability in modeling growth of *Listeria monocytogenes*. **International Journal of Food Microbiology**, v. 208. p. 19-29. 2015.
- ARYANI, D. C.; ZWIETERING, M. H.; DEN BESTEN, H. M. W. The effect of different matrices on the growth kinetics and heat resistance of *Listeria monocytogenes* and *Lactobacillus plantarum*. **International Journal of Food Microbiology**, v. 238, p.326–337, 2016.
- ASPRIDOU, Z.; AKRITIDOU, T.; KOUTSOUMANIS, K. P. Simultaneous growth, survival and death: the trimodal behavior of *Salmonella* cells under osmotic stress giving rise to “phoenix phenomenon”. **International Journal of Food Microbiology**, v.285, p.103–109, 2018.
- AUGUSTIN, J.-C.; BROUILLAUD-DELATTRE, A.; ROSSO, L.; CARLIER, V. Significance of inoculum size in the lag time of *Listeria monocytogenes*. **Applied and Environmental Microbiology**, v.66, n.4, p.1706–1710, 2000.
- AUGUSTIN J. C.; BERGIS H.; MIDELET-BOURDIN, G.; CORNU, M.; COUVERT, O.; DENIS, C.; HUCHET, V.; LEMONNIER, S.; PINON, A.; VIALETTE, M.; ZULIANI, V.; STAHL, V. Design of challenge testing experiments to assess the variability of *Listeria monocytogenes* growth in foods. **Food Microbiology**, v. 28. p. 746 -754, 2011.
- BACANOVA, 2005. Final report on the EU-QLRT-2000-01145: optimisation of safe food processing methods based on accurate characterisation of bacterial lag time using analysis of variance techniques, **BACANOVA**.
- BAKER, D.A.; GENIGEORGIS, C. Predicting the safe storage of fresh fish under modified atmospheres with respect to *Clostridium botulinum* toxigenesis by modelling length of lag phase of growth. **Journal of Food Protection**, v.53, p131–140, 1990.

BARANYI, J. Comparison of stochastic and deterministic concepts of bacterial lag. **Journal of Theoretical Biology**, v. 192. p. 403-408. 1998.

BARANYI, J.; CSERNUS, O.; BECZNER, J. Error analysis in predictive modelling demonstrated on mould data. **International Journal of Food Microbiology**, v.170, p.78–82, 2014.

BARANYI. J.; PIN, C; ROSS,T. Validating and comparing predictive models. **International Journal of Food Microbiology**, v.48, p.159-166, 1999.

BARANYI, J.; PIN C. Estimating bacterial growth parameters by means of detection times. **Applied and Environmental Microbiology**, v. 65, p. 732. 1999.

BARANYI, J; ROBERTS, T.A. Mathematics of predictive food microbiology. **International Journal of Food Microbiology**, v.26, p.199-218, 1995.

BARANYI J.; ROBERTS, T. A. A dynamic approach to predicting bacterial growth in food. **International Journal of Food Microbiology**, v. 23. p. 277-280. 1994.

BERNAERTS, K; GYSEMANS, K.P.; NHAN MINH, T.; VAN IMPE, J. F. Optimal experiment design for cardinal values estimation: guidelines for data collection. **International Journal of Food Microbiology**, v. 100. p. 153-158. 2005.

BUCHANAN, R. L.; BAGI, L. K. Effect of water activity and humectant identity on the growth kinetics of *Escherichia coli* O157:H7. **Food Microbiology**, v.14, p.413–423, 1997.

CARLIN, et al. Adaptation of *Bacillus cereus*, an ubiquitous worldwide-distributed foodborne pathogen, to a changing environment. **Food Research International**, v.43, p. 1885-1894, 2010.

CARLIN, F.; ALBAGNAC, C.; RIDA A.; GUINEBRETIERE M. H.; COUVERT, O.; NGUYEN-THE, C. Variation of cardinal growth parameters and growth limits according to phylogenetic affiliation in the

Bacillus cereus Group. Consequences for risk assessment. **Food Microbiology** v. 33, p. 69-76. 2013.

CEUPPENS, S.; RAJKOVIC, A.; HEYNDRICKX, M.; TSILIA, V.; VAN DE WIELE, T.; BOON, N.; UYTTENDAELE, M. Regulation of toxin production by *Bacillus cereus* and its food safety implications. **Critical Reviews in Microbiology**, v.37, p.188-213, 2011.

CEUPPENS, S.; BOON, N.; UYTTENDAELE, M. Diversity of *Bacillus cereus* group strains is reflected in their broad range of pathogenicity and diverse ecological lifestyles. **FEMS Microbiology Ecology**, v. 84, p.433-450, 2013.

COLLEE, J. G.; KNOWLDEN, J.A.; HOBBS, B.C. Studies on the growth, sporulation and carriage of *Clostridium welchii* with special reference to food poisoning strains. **Journal of Applied Microbiology**, v.24, p.326–339, 1961.

ComBase. www.combase.cc

CORRADINI, M. G., PELEG, M. Estimating non-isothermal bacterial growth in foods from isothermal experimental. **Journal of Applied Microbiology**, v. 99, p. 187-200, 2005.

CORRADINI, M. G. Modeling and predicting non-isothermal microbial growth using general purpose software. **International Journal of Food Microbiology**, v.106, p.223-226, 2006.

COUVERT, O.; PINON, A.; BERGIS, A.; BOURDICHON, F.; CARLIN, F.; CORNU, M.; DENIS, C.; GNANOU BESSE, N.; GUILLIERD, L.; JAMET, E.; METTLER, E.; STAHL, V.; THUAULT, D.; ZULIANI, V.; AUGUSTIN J.C. Validation of a stochastic modelling approach for *Listeria monocytogenes* growth in refrigerated foods. **International Journal of Food Microbiology**, v. 144. p. 236-240. 2010.

DE JONGHE, V.; COOREVITS, A.; VANDROEMME, J.; HEYRMAN, J.; HERMAN, L.; DE VOS, P.; HEYNDRICKX, M. Intraspecific genotypic diversity of *Bacillus* species from raw milk. **International Dairy Journal**, v.18, p.496-505, 2008.

DUBNAU, D.; LOSICK, R. Bistability in bacteria. **Molecular Microbiology**, v.61, n.3, p.564–572. 2006.

EFSA [Europe Food Safety Authority]. Opinion of the scientific panel on biological hazards on *Bacillus cereus* and other *Bacillus spp.* in foodstuffs. **The EFSA Journal**, v.175, p.1-48, 2005.

EHLING-SCHULZ, M., et al. 2005. Emetic toxin formation of *Bacillus cereus* is restricted to a single evolutionary lineage of closely related strains. **Microbiology**, v. 15, p. 183-197, 2005.

ELFWING, A.; LEMARC, Y.; BARANYI, J.; BALLAGI, A. Observing the growth and division of large number of individual bacteria using image analysis. **Applied and Environmental Microbiology**, v.70, p.675–678, 2004.

ENEROTH, A., SVENSSON, B., MOLIN, G., & CHRISTIANSSON, A. Contamination of pasteurized milk by *Bacillus cereus* in the filling machine. **Journal of Dairy Research**, v.68, p.189-196, 2001.

FRANÇOIS, K.; DEVLIEGHERE, F.; SMET, K.; STANDAERT, A. R.; GEERAERD, A. H.; VAN IMPE, J. F.; DEBEVERE, J. Modelling the individual cell lag phase: effect of temperature and pH on the individual cell lag distribution of *Listeria monocytogenes*. **International Journal of Food Microbiology**, v.100, p.41–53, 2005.

GEORGE S.; METRIS, A.; BARANYI, J. Integrated kinetic and probabilistic modeling of the growth potential of bacterial populations. **Applied and Environmental Microbiology**, v. 81, p. 3228. 2015.

GILL, C. O.; PHILLIPS, D. M. The effect of media composition on the relationship between temperature and growth rate of *Escherichia coli*. **Food Microbiology** v.2, p.285–290, 1985

GOLDBLITH, S.A.; JOSLYN, M.A.; NICKERSON, J.T.R. Introduction to thermal processing of foods: an anthology of food science, v. 1, **AVI Publishing Company**, 1961.

GOMPERTZ, B. On the nature of the function expressive of the law of human mortality, and on a new mode of determining the value of life

contingencies. **Philosophical Transactions of the Royal Society of London**, v.123, p.513-585, 1832.

GUINEBRETIERE, M.H.; GIRARDIN, H.; DARGAIGNARATZ, C.; CARLIN, F.; NGUYEN-THE, C. Contamination flows of *Bacillus cereus* and spore-forming aerobic bacteria in a cooked, pasteurized and chilled zucchini puree processing line. **International Journal of Food Microbiology**, v.82, p.223–232, 2003.

GUINEBRETIERE, M.H.; THOMPSON, F.L.; SOROKIN, A.; NORMAND, P.; DAWYNDT, P.; EHLING-SCHULZ, M.; SVENSSON, B.; SANCHIS, V.; NGUYEN-THE, C.; HEYNDRIKX, M.; DE VOS, P. Ecological diversification in the *Bacillus cereus* group. **Environmental Microbiology** v.10, p.851-865, 2008.

GUINEBRETIERE, M.H.; VELGE, P.; COUVERT, O.; CARLIN, F.; DEBUYSER, M.L.; NGUYEN-THE, C. Ability of *Bacillus cereus* group strains to cause food poisoning varies according to phylogenetic affiliation (Groups I to VII) rather than species affiliation. **Journal of Clinical Microbiology**, v.48, p.3388-3391, 2010.

HUANG, L. A comprehensive data analysis tool for predictive microbiology. **International Journal of Food Microbiology**, v.171, p.100-107, 2014.

KELLY, A.F; MARTINEZ-RODRIGUEZ, A.; BOVILL, R.A.; MACKAY, B.M. Description of a “phoenix” phenomenon in the growth of *Campylobacter jejuni* at temperatures close to the minimum for growth. **Applied and Environmental Microbiology**, v.69, n.8, p. 4975–4978, 2003.

KHURI, A. I.; CORNELL, J.A. Response Surfaces: Designs and Analyses. **CRC Press**, New York, 1996.

KOIRALA, S.; MEARS, P.; SIM, M.; GOLDING, I.; CHEMLA, Y. R.; ALDRIDGE, P. D.; RAOA, C. V. A nutrient-tunable bistable switch controls motility in *Salmonella enterica* serovar Typhimurium. **mBio**, v.5, n.5 p.1611-1614, 2014.

KUMARI, S.; SARKAR, P.K. *Bacillus cereus* hazard and control in industrial dairy processing environment. **Food Control**, v. 69, p. 20-29, 2016.

KUTALIK, Z.; RAZAZ, M.; BARANYI, J. Connection between stochastic and deterministic modelling of microbial growth. **Journal of Theoretical Biology**, v.232, p.285–299, 2005A.

KUTALIK, Z.; RAZAZ, M.; ELFWING, A.; BALLAGI, A.; BARANYI, J. Stochastic modelling of individual cell growth using flow chamber microscopy images. **International Journal of Food Microbiology**, v.105, p.177–190, 2005B.

LE MARC, Y.; SKANDAMIS, P. N.; BELESSI C. I. A.; MERKOURI, S. I.; GEORGE, S. M.; GOUNADAKI, A. S.; SCHVARTZMAN, S.; JORDAN, K.; DROSINOS E. H.; BARANYI, J. modeling the effect of abrupt acid and osmotic shifts within the growth region and across growth boundaries on adaptation and growth of *Listeria monocytogenes*. **Applied and Environmental Microbiology**, v.76. p. 6555-6560. 2010.

LONGHI, D. A. Avaliação da capacidade preditiva de diferentes modelos matemáticos para o crescimento microbiano em condições não-isotérmicas. **Dissertação (Mestrado em Engenharia de Alimentos)**, Universidade Federal de Santa Catarina. Florianópolis, SC, 2012.

MAISONNEUVE, E.; GERDES, K. Molecular mechanisms underlying bacterial persisters: A review. **Cell**, n.157, p.539-548, 2014.

MCAULEY, C.M.; MCMILLAN, K.; MOORE, S.C.; FEGAN, N.; FOX, E.M., 2014. Prevalence and characterization of foodborne pathogens from Australian dairy farm environments. **Journal of Dairy Science**, v.97, p.7402-7412, 2014.

MELLEFONT L.; MCMEEKIN T. A.; ROSS, T. The effect of abrupt osmotic shifts on the lag phase duration of physiologically distinct populations of *Salmonella typhimurium*. **International Journal of Food Microbiology**, v. 92. p. 111. 1996.

MELLEFONT, L. A.; MCMEEKIN, T. A.; ROSS, T. Performance evaluation of a model describing the effects of temperature, water

activity, pH and lactic acid concentration on the growth of *Escherichia coli*. **International Journal of Food Microbiology** v.82, p.45–58, 2003.

MICHAELIS, L.; MENTEN, M.L. Die Kinetik der Invertinwirkung. **Biochem** v.49, p. 333–369, 1913.

MILES, D. W.; ROSS, T.; OLLEY, J.; MCMEEKIN, T. A. Development and evaluation of a predictive model for the effect of temperature and water activity on the growth rate of *Vibrio parahaemolyticus*. **International Journal of Food Microbiology**, v.38, p.133–142, 1997.

McDONALD, K.; SUN, D. Predictive food microbiology for the meat industry: a review. **International Journal of Food Microbiology**, v.52, p. 1-27, 1999.

MCMEEKIN, T. A.; OLLEY, J.; ROSS, T. Predictive Microbiology; Theory and Application. **John Wiley & Sons**, UK. 1993.

NEUMEYER, K.; ROSS, T.; THOMSON, G; MCMEEKIN, T. A. Validation of a model describing the effects of temperature and water activity on the growth of psychotropic *pseudomonads*. **International Journal of Food Microbiology**, v.38, p.55–63, 1997.

PARKHILL, J., B. W. et al. The genome sequence of the foodborne pathogen *Campylobacter jejuni* reveals hypervariable sequences. **Nature** v. 403, p.665–668, 2000.

PIN, C.; BARANYI, J. Single-cell and population lag times as a function of cell age. **Applied and Environmental Microbiology**, v.74, p.2534–2536, 2008.

PRATS, C.; GIRÓ, A.; FERRER, J.; LÓPEZ, D.; VIVES-REGO, J. Analysis and IBM simulation of the stages in bacterial lag phase: basis for an updated definition. **Journal of Theoretical Biology**, v.252, p.56–68, 2008.

RATKOWSKY D.; OLLEY, J.; MCMEEKIN, T. A; BALL A. Relationship between temperature and growth rate of bacterial cultures. **Journal of Bacteriology**, v. 149, p. 1-5, 1982.

RICHARDS, F. J. A flexible growth function for empirical use. **Journal of Experimental Botany**, v.10 n.2, p.290–300, 1959.

ROBINSON, T.; ABOABA, O.; KALOTI, A.; OCIO, M.; BARANYI, J.; MACKEY, B. The effect of inoculum size on the lag phase of *Lysteria monocytogenes*. **International Journal of Food Microbiology**, v.70, p.163–173, 2001.

ROSS, T.; McMEEKIN, T. A. Predictive Microbiology. **International Journal of Food Microbiology**, v.23, p.41-264, 1999.

ROSSO, L.; LOBRY, J. R.; BAJARD,S; FLANDROIS, J.P. Convenient Model To Describe the Combined Effects of Temperature and pH on Microbial Growth. **Applied and Environmental Microbiology**, v.61, n.2, p. 610-616, 1995.

ROSSO, R.; ROBINSON T. A cardinal model to describe the effect of water activity on the growth of moulds. **International Journal of Food Microbiology**, v. 63, p. 265-273. 2001.

ROWAN, N.J.; ANDERSON, J.G., 1998. Diarrhoeal enterotoxin production by psychotropic *Bacillus cereus* present in reconstituted milk-based infant formulae (MIF). **Letters in Applied Microbiology**, v. 26, p.161-165, 1998.

SCHAFFNER, D. W.; LABUZA, T. P. Predictive microbiology: where are we and where are we going? **Food Technology**, v. 51, p. 95-99. 1997.

SHAHEEN, R.; ANDERSSON, M.A.; APETROAIE, C.; SCHULZ, A.; EHLING-SCHULZ, M.; OLLILAINEN, V.M.; SALKINOJA-SALONEN, M.S. Potential of selected infant food formulas for production of *Bacillus cereus* emetic toxin, cereulide. **International Journal of Food Microbiology**, v.107, p.287-294, 2006.

SMITS, W. K.; KUIPERS O. P.; VEENING J. W. Phenotypic variation in bacteria: the role of feedback regulation. **Nature Reviews Microbiology**, v.4, p.259–71, 2006.

SWINNEN, I.A.M., BERNAERTS, E.J.J., DENS, A.H., GEERAED, J.F., VAN IMPE, J.F. Predictive modeling of the microbial lag phase: a

review. **International Journal of Food Microbiology**, v.94, p.137-159, 2004.

TIJSKENS, L. M. M.; HERTOOG, M. L. A. T. M.; NICOLAÏ, B. M. Food Process Modelling. Woodhead Publishing Limited, Cambring, England, 2001.

VERHULST, P. F. Recherches mathématiques sur la loi d'accroissement de la population" [Mathematical Researches into the Law of Population Growth Increase]. **Nouveaux Mémoires de l'Académie Royale des Sciences et Belles-Lettres de Bruxelles**, v.18, p.1–42, 1845

YANG, Y et al. Multilocus sequence type profiles of *Bacillus cereus* isolates from infant formula in China. **Food Microbiology**, v. 62, p.46-50, 2016.

WHITING, R.; BUCHANAN, R. A classification of models in predictive microbiology - reply. **Food Microbiology**, v. 10, n. 2, p. 175-177, 1993.

WHITING, R. C. Microbial modelling in foods. **Critical Reviews in Food Science and Nutrition**, v.35, p. 467-494, 1995.

WIJNANDS, L. M.; DUFRENNE, J. B.; ROMBOUTS, F. M.; in 't VELD, P.H.; van LEUSDEN, F. M. Prevalence of Potentially Pathogenic *Bacillus cereus* in Food Commodities in The Netherlands, **Journal of Food Protection**, v.69, p.2587-2594, 2006.

WIJTZES, T.; ROMBOUTS, F. M.; KANT-MUERMANS, M. L. T.; VAN 'T RIET, K.; ZWIETERING, M. H. Development and validation of a combined temperature, water activity, pH model for bacterial growth rate of *Lactobacillus curvatus*. **International Journal of Food Microbiology**, v.63, p.57–64, 2001.

ZHOU, K.; GEORGE, S.; LI, P.I.; BARANYI, J. Effect of periodic fluctuation in the osmotic environment on the adaptation of *Salmonella*. **Food Microbiology**, v. 30, p. 298-302, 2012.

ZWIETERING, M.H; VAN GERWEN, S.J.C. Sensitivity analysis in quantitative microbial risk assessment. **International Journal of Food Microbiology**, v.51, p.213-221, 2000.

ZWIETERING, M.H.; DE VIT, J.C.; NOTERMANS, Application of predictive microbiology to estimate the number of *Bacillus cereus* in pasteurised milk at the point of consumption. **International Journal of Food Microbiology**, v.30, p.55-70, 1996.

ANNEX A – Viable counts measurements

Strain	LAB	Temperature [°C]	Medium	Replicate	Treatment	time [h]	logC [log CFU/ml]	pH
B577	NRC	29.8	BHI	A	unheated	0	1.99	7.39
B577	NRC	29.8	BHI	A	unheated	2	2.07	
B577	NRC	29.8	BHI	A	unheated	4	2.63	
B577	NRC	29.8	BHI	A	unheated	5	4.37	7.22
B577	NRC	29.8	BHI	A	unheated	6	4.67	
B577	NRC	29.8	BHI	A	unheated	7	5.96	7.27
B577	NRC	29.8	BHI	A	unheated	8	6.78	
B577	NRC	29.8	BHI	A	unheated	10	7.12	6.87
B577	NRC	29.8	BHI	A	unheated	12	7.38	
B577	NRC	29.8	BHI	A	unheated	24	8.28	6.15
B577	NRC	29.8	BHI	A	unheated	30	8.18	6.56
B577	NRC	24.7	BHI	A	unheated	0	1.94	7.39
B577	NRC	24.7	BHI	A	unheated	2	1.99	
B577	NRC	24.7	BHI	A	unheated	5	2.43	7.24
B577	NRC	24.7	BHI	A	unheated	7	4.38	
B577	NRC	24.7	BHI	A	unheated	8	4.64	7.24
B577	NRC	24.7	BHI	A	unheated	10	5.97	
B577	NRC	24.7	BHI	A	unheated	12	6.79	7.16
B577	NRC	24.7	BHI	A	unheated	24	7.37	
B577	NRC	24.7	BHI	A	unheated	30	7.40	6.26
B577	NRC	22.0	BHI	A	unheated	0	1.97	7.39

B577	NRC	22.0	BHI	A	unheated	2	1.96	
B577	NRC	22.0	BHI	A	unheated	5	2.32	7.23
B577	NRC	22.0	BHI	A	unheated	7	3.50	
B577	NRC	22.0	BHI	A	unheated	8	4.03	7.24
B577	NRC	22.0	BHI	A	unheated	10	4.63	
B577	NRC	22.0	BHI	A	unheated	12	5.46	7.24
B577	NRC	22.0	BHI	A	unheated	24	6.78	
B577	NRC	22.0	BHI	A	unheated	30	7.19	6.7
B577	NRC	22.0	BHI	A	unheated	48	7.52	6.24
B577	NRC	18.0	BHI	A	unheated	0	1.97	7.39
B577	NRC	18.0	BHI	A	unheated	5	1.94	
B577	NRC	18.0	BHI	A	unheated	8	2.23	7.24
B577	NRC	18.0	BHI	A	unheated	12	3.39	
B577	NRC	18.0	BHI	A	unheated	24	6.19	
B577	NRC	18.0	BHI	A	unheated	30	7.04	6.91
B577	NRC	18.0	BHI	A	unheated	48	6.15	
B577	NRC	18.0	BHI	A	unheated	54	6.61	6.94
B577	NRC	18.0	BHI	A	unheated	72	6.12	
B577	NRC	18.0	BHI	A	unheated	96	7.40	6.42
B577	NRC	14.8	BHI	A	unheated	0	2.01	7.39
B577	NRC	14.8	BHI	A	unheated	12	1.95	7.24
B577	NRC	14.8	BHI	A	unheated	24	2.78	
B577	NRC	14.8	BHI	A	unheated	30	4.07	7.2
B577	NRC	14.8	BHI	A	unheated	48	6.36	
B577	NRC	14.8	BHI	A	unheated	54	6.82	7.08
B577	NRC	14.8	BHI	A	unheated	72	5.92	

B577	NRC	14.8	BHI	A	unheated	96	6.10	
B577	NRC	14.8	BHI	A	unheated	167	6.09	6.22
B577	NRC	12.3	BHI	A	unheated	0	1.92	7.39
B577	NRC	12.3	BHI	A	unheated	24	1.85	
B577	NRC	12.3	BHI	A	unheated	48	3.01	
B577	NRC	12.3	BHI	A	unheated	72	3.89	
B577	NRC	12.3	BHI	A	unheated	96	5.03	
B577	NRC	12.3	BHI	A	unheated	167	6.03	6.93
B577	NRC	12.3	BHI	A	unheated	192	5.94	
B577	NRC	12.3	BHI	A	unheated	216	5.53	6.91
B577	NRC	12.3	BHI	A	unheated	240	5.60	6.55
B577	NRC	12.3	BHI	A	unheated	264	4.75	6.02
B577	NRC	12.3	BHI	A	unheated	335	4.50	5.62
B577	NRC	29.8	RIF	A	unheated	0	1.59	6.75
B577	NRC	29.8	RIF	A	unheated	2	2.02	
B577	NRC	29.8	RIF	A	unheated	4	3.03	
B577	NRC	29.8	RIF	A	unheated	5	4.29	6.79
B577	NRC	29.8	RIF	A	unheated	6	4.69	
B577	NRC	29.8	RIF	A	unheated	7	5.62	6.83
B577	NRC	29.8	RIF	A	unheated	8	6.00	
B577	NRC	29.8	RIF	A	unheated	10	6.52	6.63
B577	NRC	29.8	RIF	A	unheated	12	6.94	
B577	NRC	29.8	RIF	A	unheated	24	8.00	5.76
B577	NRC	29.8	RIF	A	unheated	30	7.60	5.64
B577	NRC	24.7	RIF	A	unheated	0	1.61	6.75

B577	NRC	24.7	RIF	A	unheated	2	1.91	
B577	NRC	24.7	RIF	A	unheated	5	2.79	6.81
B577	NRC	24.7	RIF	A	unheated	7	4.18	
B577	NRC	24.7	RIF	A	unheated	8	4.66	6.88
B577	NRC	24.7	RIF	A	unheated	10	5.60	
B577	NRC	24.7	RIF	A	unheated	12	6.32	6.83
B577	NRC	24.7	RIF	A	unheated	24	8.06	
B577	NRC	24.7	RIF	A	unheated	30	8.05	6.16
B577	NRC	22.0	RIF	A	unheated	0	1.73	6.75
B577	NRC	22.0	RIF	A	unheated	2	2.02	
B577	NRC	22.0	RIF	A	unheated	5	2.47	6.83
B577	NRC	22.0	RIF	A	unheated	7	3.63	
B577	NRC	22.0	RIF	A	unheated	8	4.05	6.89
B577	NRC	22.0	RIF	A	unheated	10	4.74	
B577	NRC	22.0	RIF	A	unheated	12	5.26	6.89
B577	NRC	22.0	RIF	A	unheated	24	8.03	
B577	NRC	22.0	RIF	A	unheated	30	8.30	6.27
B577	NRC	22.0	RIF	A	unheated	48	8.07	6.82
B577	NRC	18.0	RIF	A	unheated	0	1.78	6.75
B577	NRC	18.0	RIF	A	unheated	5	2.10	
B577	NRC	18.0	RIF	A	unheated	8	2.51	6.89
B577	NRC	18.0	RIF	A	unheated	12	3.46	
B577	NRC	18.0	RIF	A	unheated	24	5.83	
B577	NRC	18.0	RIF	A	unheated	30	6.54	6.6
B577	NRC	18.0	RIF	A	unheated	48	7.90	
B577	NRC	18.0	RIF	A	unheated	54	8.09	6.29

B577	NRC	18.0	RIF	A	unheated	72	8.22	
B577	NRC	18.0	RIF	A	unheated	96	8.28	5.32
B577	NRC	14.8	RIF	A	unheated	0	1.67	6.75
B577	NRC	14.8	RIF	A	unheated	12	2.26	6.88
B577	NRC	14.8	RIF	A	unheated	24	3.48	
B577	NRC	14.8	RIF	A	unheated	30	4.19	6.81
B577	NRC	14.8	RIF	A	unheated	48	5.95	
B577	NRC	14.8	RIF	A	unheated	54	6.57	6.74
B577	NRC	14.8	RIF	A	unheated	72	7.45	
B577	NRC	14.8	RIF	A	unheated	96	7.82	
B577	NRC	14.8	RIF	A	unheated	167	7.84	5.68
B577	NRC	12.3	RIF	A	unheated	0	1.78	6.75
B577	NRC	12.3	RIF	A	unheated	24	2.00	
B577	NRC	12.3	RIF	A	unheated	48	2.43	
B577	NRC	12.3	RIF	A	unheated	72	3.13	
B577	NRC	12.3	RIF	A	unheated	96	3.98	
B577	NRC	12.3	RIF	A	unheated	167	7.30	5.88
B577	NRC	12.3	RIF	A	unheated	192	8.00	
B577	NRC	12.3	RIF	A	unheated	216	7.75	5.45
B577	NRC	12.3	RIF	A	unheated	240	7.59	5.38
B577	NRC	12.3	RIF	A	unheated	264	7.32	5.43
B577	NRC	12.3	RIF	A	unheated	335	8.09	5.52
B577	NRC	30.1	RIF	B	unheated	0	1.78	6.84
B577	NRC	30.1	RIF	B	unheated	2	2.16	
B577	NRC	30.1	RIF	B	unheated	4	2.74	

B577	NRC	30.1	RIF	B	unheated	5	4.32	
B577	NRC	30.1	RIF	B	unheated	7	5.59	
B577	NRC	30.1	RIF	B	unheated	8	5.93	
B577	NRC	30.1	RIF	B	unheated	10	6.26	6.54
B577	NRC	30.1	RIF	B	unheated	12	6.74	
B577	NRC	30.1	RIF	B	unheated	24	8.07	
B577	NRC	30.1	RIF	B	unheated	30	7.95	
B577	NRC	30.1	RIF	B	unheated	48	7.96	5.37
B577	NRC	30.1	BHI	B	unheated	0	1.70	7.28
B577	NRC	30.1	BHI	B	unheated	2	2.06	
B577	NRC	30.1	BHI	B	unheated	4	2.57	7.26
B577	NRC	30.1	BHI	B	unheated	5	4.34	
B577	NRC	30.1	BHI	B	unheated	7	5.96	7.22
B577	NRC	30.1	BHI	B	unheated	8	6.72	
B577	NRC	30.1	BHI	B	unheated	10	6.67	6.98
B577	NRC	30.1	BHI	B	unheated	12	7.01	
B577	NRC	30.1	BHI	B	unheated	24	8.10	6.68
B577	NRC	30.1	BHI	B	unheated	30	8.16	
B577	NRC	30.1	BHI	B	unheated	48	8.13	6.42
B577	NRC	24.7	BHI	B	unheated	0	1.88	7.28
B577	NRC	24.7	BHI	B	unheated	2	2.06	
B577	NRC	24.7	BHI	B	unheated	5	2.40	7.28
B577	NRC	24.7	BHI	B	unheated	7	4.32	
B577	NRC	24.7	BHI	B	unheated	8	4.49	7.12
B577	NRC	24.7	BHI	B	unheated	10	5.18	
B577	NRC	24.7	BHI	B	unheated	12	6.40	7.04

B577	NRC	24.7	BHI	B	unheated	24	7.26	
B577	NRC	24.7	BHI	B	unheated	30	7.11	
B577	NRC	24.7	BHI	B	unheated	48	7.43	6.51
B577	NRC	18.0	BHI	B	unheated	0	1.82	7.28
B577	NRC	18.0	BHI	B	unheated	5	1.87	
B577	NRC	18.0	BHI	B	unheated	8	1.89	
B577	NRC	18.0	BHI	B	unheated	12	2.00	7.24
B577	NRC	18.0	BHI	B	unheated	24	5.81	
B577	NRC	18.0	BHI	B	unheated	30	7.12	7.12
B577	NRC	18.0	BHI	B	unheated	48	6.23	7
B577	NRC	18.0	BHI	B	unheated	54	6.20	6.88
B577	NRC	18.0	BHI	B	unheated	72	6.12	6.43
B577	NRC	14.7	BHI	B	unheated	0	1.53	7.28
B577	NRC	14.7	BHI	B	unheated	7	1.76	
B577	NRC	14.7	BHI	B	unheated	12	1.91	7.31
B577	NRC	14.7	BHI	B	unheated	24	3.08	
B577	NRC	14.7	BHI	B	unheated	30	4.15	
B577	NRC	14.7	BHI	B	unheated	48	5.95	7.24
B577	NRC	14.7	BHI	B	unheated	54	6.74	7.12
B577	NRC	14.7	BHI	B	unheated	72	6.15	
B577	NRC	14.7	BHI	B	unheated	144	5.72	6.56
B577	NRC	12.5	BHI	B	unheated	0	1.73	7.28
B577	NRC	12.5	BHI	B	unheated	24	1.79	7.26
B577	NRC	12.5	BHI	B	unheated	48	3.19	
B577	NRC	12.5	BHI	B	unheated	54	3.65	

B577	NRC	12.5	BHI	B	unheated	72	4.48	7.12
B577	NRC	12.5	BHI	B	unheated	144	5.73	6.98
B577	NRC	12.5	BHI	B	unheated	167	5.82	6.72
B577	NRC	12.5	BHI	B	unheated	216	4.99	6.34
B635	NRC	29.9	BHI	A	unheated	0	1.51	7.17
B635	NRC	29.9	BHI	A	unheated	2	2.26	
B635	NRC	29.9	BHI	A	unheated	4	3.06	
B635	NRC	29.9	BHI	A	unheated	5	4.40	
B635	NRC	29.9	BHI	A	unheated	7	5.92	
B635	NRC	29.9	BHI	A	unheated	8	6.95	
B635	NRC	29.9	BHI	A	unheated	10	7.20	6.95
B635	NRC	29.9	BHI	A	unheated	12	7.26	
B635	NRC	29.9	BHI	A	unheated	24	7.99	
B635	NRC	29.9	BHI	A	unheated	30	8.11	6.16
B635	NRC	29.9	BHI	A	unheated	48	8.03	6.57
B635	NRC	24.7	BHI	A	unheated	0	1.48	7.17
B635	NRC	24.7	BHI	A	unheated	2	2.29	
B635	NRC	24.7	BHI	A	unheated	5	3.46	
B635	NRC	24.7	BHI	A	unheated	7	4.34	
B635	NRC	24.7	BHI	A	unheated	8	5.25	
B635	NRC	24.7	BHI	A	unheated	10	6.14	7.24
B635	NRC	24.7	BHI	A	unheated	12	6.86	
B635	NRC	24.7	BHI	A	unheated	24	7.58	
B635	NRC	24.7	BHI	A	unheated	30	7.69	6
B635	NRC	24.7	BHI	A	unheated	48	7.79	6.09
B635	NRC	21.9	BHI	A	unheated	0	1.45	7.17

B635	NRC	21.9	BHI	A	unheated	2	1.96	
B635	NRC	21.9	BHI	A	unheated	5	2.40	
B635	NRC	21.9	BHI	A	unheated	7	3.68	
B635	NRC	21.9	BHI	A	unheated	8	4.32	
B635	NRC	21.9	BHI	A	unheated	10	4.82	7.25
B635	NRC	21.9	BHI	A	unheated	12	5.20	
B635	NRC	21.9	BHI	A	unheated	24	7.14	
B635	NRC	21.9	BHI	A	unheated	30	6.58	6.05
B635	NRC	21.9	BHI	A	unheated	48	7.77	5.97
B635	NRC	18.0	BHI	A	unheated	0	1.48	7.17
B635	NRC	18.0	BHI	A	unheated	5	2.43	
B635	NRC	18.0	BHI	A	unheated	8	2.93	
B635	NRC	18.0	BHI	A	unheated	12	3.72	7.23
B635	NRC	18.0	BHI	A	unheated	24	6.93	
B635	NRC	18.0	BHI	A	unheated	30	6.99	6.88
B635	NRC	18.0	BHI	A	unheated	48	6.70	6.62
B635	NRC	18.0	BHI	A	unheated	54	6.85	
B635	NRC	18.0	BHI	A	unheated	72	7.67	6.06
B635	NRC	14.8	BHI	A	unheated	0	1.34	7.17
B635	NRC	14.8	BHI	A	unheated	12	3.15	7.25
B635	NRC	14.8	BHI	A	unheated	24	4.52	
B635	NRC	14.8	BHI	A	unheated	30	5.63	7.22
B635	NRC	14.8	BHI	A	unheated	48	6.79	6.94
B635	NRC	14.8	BHI	A	unheated	54	6.11	
B635	NRC	14.8	BHI	A	unheated	72	5.71	6.86

B635	NRC	14.8	BHI	A	unheated	96	5.93	6.81
B635	NRC	12.4	BHI	A	unheated	0	1.34	7.17
B635	NRC	12.4	BHI	A	unheated	24	2.88	
B635	NRC	12.4	BHI	A	unheated	30	3.43	
B635	NRC	12.4	BHI	A	unheated	48	5.54	7.2
B635	NRC	12.4	BHI	A	unheated	54	6.28	
B635	NRC	12.4	BHI	A	unheated	72	6.90	6.86
B635	NRC	12.4	BHI	A	unheated	96	5.60	6.84
B635	NRC	12.4	BHI	A	unheated	167	6.49	6.79
B635	NRC	12.4	BHI	A	unheated	216	7.40	
B635	NRC	12.4	BHI	A	unheated	240	7.59	6.19
B635	NRC	12.4	BHI	A	unheated	264	7.49	
B635	NRC	12.4	BHI	A	unheated	335	6.53	5.64
B635	NRC	29.9	RIF	A	unheated	0	1.76	6.81
B635	NRC	29.9	RIF	A	unheated	2	2.38	
B635	NRC	29.9	RIF	A	unheated	4	3.11	
B635	NRC	29.9	RIF	A	unheated	5	4.28	
B635	NRC	29.9	RIF	A	unheated	7	5.51	
B635	NRC	29.9	RIF	A	unheated	8	5.95	
B635	NRC	29.9	RIF	A	unheated	10	6.67	6.64
B635	NRC	29.9	RIF	A	unheated	12	7.01	
B635	NRC	29.9	RIF	A	unheated	24	7.64	
B635	NRC	29.9	RIF	A	unheated	30	7.92	5.55
B635	NRC	29.9	RIF	A	unheated	48	8.00	5.08
B635	NRC	24.7	RIF	A	unheated	0	1.68	6.81
B635	NRC	24.7	RIF	A	unheated	2	2.05	

B635	NRC	24.7	RIF	A	unheated	5	3.36	
B635	NRC	24.7	RIF	A	unheated	7	4.32	
B635	NRC	24.7	RIF	A	unheated	8	4.86	
B635	NRC	24.7	RIF	A	unheated	10	5.51	6.81
B635	NRC	24.7	RIF	A	unheated	12	6.23	
B635	NRC	24.7	RIF	A	unheated	24	7.81	
B635	NRC	24.7	RIF	A	unheated	30	7.93	5.58
B635	NRC	24.7	RIF	A	unheated	48	8.12	5.15
B635	NRC	21.9	RIF	A	unheated	0	1.79	6.81
B635	NRC	21.9	RIF	A	unheated	2	1.82	
B635	NRC	21.9	RIF	A	unheated	5	3.10	
B635	NRC	21.9	RIF	A	unheated	7	3.76	
B635	NRC	21.9	RIF	A	unheated	8	4.11	
B635	NRC	21.9	RIF	A	unheated	10	4.70	6.85
B635	NRC	21.9	RIF	A	unheated	12	5.34	
B635	NRC	21.9	RIF	A	unheated	24	7.62	
B635	NRC	21.9	RIF	A	unheated	30	7.76	6
B635	NRC	21.9	RIF	A	unheated	48	7.99	5.52
B635	NRC	18.0	RIF	A	unheated	0	1.72	6.81
B635	NRC	18.0	RIF	A	unheated	5	2.57	
B635	NRC	18.0	RIF	A	unheated	8	3.08	
B635	NRC	18.0	RIF	A	unheated	12	3.83	6.87
B635	NRC	18.0	RIF	A	unheated	24	6.28	
B635	NRC	18.0	RIF	A	unheated	30	6.85	6.62
B635	NRC	18.0	RIF	A	unheated	48	7.95	6.02

B635	NRC	18.0	RIF	A	unheated	54	7.97	
B635	NRC	18.0	RIF	A	unheated	72	8.32	5.5
B635	NRC	14.8	RIF	A	unheated	0	1.68	6.81
B635	NRC	14.8	RIF	A	unheated	12	3.04	6.89
B635	NRC	14.8	RIF	A	unheated	24	4.65	
B635	NRC	14.8	RIF	A	unheated	30	5.48	6.86
B635	NRC	14.8	RIF	A	unheated	48	6.89	6.55
B635	NRC	14.8	RIF	A	unheated	54	7.18	
B635	NRC	14.8	RIF	A	unheated	72	8.00	6.04
B635	NRC	14.8	RIF	A	unheated	96	8.21	5.78
B635	NRC	12.4	RIF	A	unheated	0	1.56	6.81
B635	NRC	12.4	RIF	A	unheated	24	3.20	
B635	NRC	12.4	RIF	A	unheated	48	5.30	6.84
B635	NRC	12.4	RIF	A	unheated	54	5.67	
B635	NRC	12.4	RIF	A	unheated	72	6.79	6.61
B635	NRC	12.4	RIF	A	unheated	96	7.32	6.23
B635	NRC	12.4	RIF	A	unheated	167	8.17	5.59
B635	NRC	12.4	RIF	A	unheated	216	7.99	
B635	NRC	12.4	RIF	A	unheated	240	7.63	5.26
B635	NRC	12.4	RIF	A	unheated	264	7.59	
B635	NRC	12.4	RIF	A	unheated	335	7.61	4.89
B635	NRC	30.0	BHI	B	unheated	0	1.20	7.41
B635	NRC	30.0	BHI	B	unheated	2	2.11	
B635	NRC	30.0	BHI	B	unheated	4	3.07	
B635	NRC	30.0	BHI	B	unheated	5	4.28	
B635	NRC	30.0	BHI	B	unheated	7	5.62	

B635	NRC	30.0	BHI	B	unheated	8	6.53	
B635	NRC	30.0	BHI	B	unheated	10	7.53	
B635	NRC	30.0	BHI	B	unheated	12	7.72	
B635	NRC	30.0	BHI	B	unheated	24	8.01	6.22
B635	NRC	30.0	BHI	B	unheated	30	8.07	
B635	NRC	30.0	BHI	B	unheated	48	7.77	6.04
B635	NRC	24.7	BHI	B	unheated	0	1.30	7.41
B635	NRC	24.7	BHI	B	unheated	2	1.82	
B635	NRC	24.7	BHI	B	unheated	5	2.95	
B635	NRC	24.7	BHI	B	unheated	7	4.26	
B635	NRC	24.7	BHI	B	unheated	8	4.63	
B635	NRC	24.7	BHI	B	unheated	10	6.16	
B635	NRC	24.7	BHI	B	unheated	12	6.74	
B635	NRC	24.7	BHI	B	unheated	24	7.72	6.07
B635	NRC	24.7	BHI	B	unheated	30	7.77	
B635	NRC	24.7	BHI	B	unheated	48	8.21	5.88
B635	NRC	22.0	BHI	B	unheated	0	1.08	7.41
B635	NRC	22.0	BHI	B	unheated	2	1.72	
B635	NRC	22.0	BHI	B	unheated	5	2.67	
B635	NRC	22.0	BHI	B	unheated	7	3.36	
B635	NRC	22.0	BHI	B	unheated	8	3.64	
B635	NRC	22.0	BHI	B	unheated	10	4.98	
B635	NRC	22.0	BHI	B	unheated	12	5.38	
B635	NRC	22.0	BHI	B	unheated	24	7.40	6.4
B635	NRC	22.0	BHI	B	unheated	30	7.74	

B635	NRC	22.0	BHI	B	unheated	48	8.06	6.18
B635	NRC	18.0	BHI	B	unheated	0	1.34	7.41
B635	NRC	18.0	BHI	B	unheated	5	1.86	
B635	NRC	18.0	BHI	B	unheated	8	2.23	
B635	NRC	18.0	BHI	B	unheated	10	3.43	
B635	NRC	18.0	BHI	B	unheated	12	3.51	
B635	NRC	18.0	BHI	B	unheated	24	7.06	7.22
B635	NRC	18.0	BHI	B	unheated	30	7.41	
B635	NRC	18.0	BHI	B	unheated	48	7.49	
B635	NRC	18.0	BHI	B	unheated	54	7.51	
B635	NRC	18.0	BHI	B	unheated	72	7.51	6.33
B635	NRC	14.8	BHI	B	unheated	0	1.34	7.41
B635	NRC	14.8	BHI	B	unheated	10	2.20	
B635	NRC	14.8	BHI	B	unheated	24	4.38	7.37
B635	NRC	14.8	BHI	B	unheated	30	5.49	
B635	NRC	14.8	BHI	B	unheated	48	7.16	
B635	NRC	14.8	BHI	B	unheated	54	6.76	
B635	NRC	14.8	BHI	B	unheated	72	5.78	
B635	NRC	14.8	BHI	B	unheated	144	5.85	5.82
B635	NRC	12.4	BHI	B	unheated	0	1.08	7.41
B635	NRC	12.4	BHI	B	unheated	12	1.68	
B635	NRC	12.4	BHI	B	unheated	24	2.74	7.37
B635	NRC	12.4	BHI	B	unheated	30	3.46	
B635	NRC	12.4	BHI	B	unheated	48	5.64	
B635	NRC	12.4	BHI	B	unheated	54	6.32	
B635	NRC	12.4	BHI	B	unheated	72	7.28	

B635	NRC	12.4	BHI	B	unheated	144	7.52	
B635	NRC	12.4	BHI	B	unheated	167	7.61	
B635	NRC	12.4	BHI	B	unheated	192	7.15	
B635	NRC	12.4	BHI	B	unheated	216	7.03	6.32
B635	NRC	30.0	RIF	B	unheated	0	1.48	6.83
B635	NRC	30.0	RIF	B	unheated	2	2.15	
B635	NRC	30.0	RIF	B	unheated	4	3.26	
B635	NRC	30.0	RIF	B	unheated	5	4.18	
B635	NRC	30.0	RIF	B	unheated	7	4.96	
B635	NRC	30.0	RIF	B	unheated	8	5.48	
B635	NRC	30.0	RIF	B	unheated	10	6.72	
B635	NRC	30.0	RIF	B	unheated	12	7.13	
B635	NRC	30.0	RIF	B	unheated	24	7.99	5.87
B635	NRC	30.0	RIF	B	unheated	30	8.06	
B635	NRC	30.0	RIF	B	unheated	48	8.03	5.22
B635	NRC	24.7	RIF	B	unheated	0	1.20	6.83
B635	NRC	24.7	RIF	B	unheated	2	1.91	
B635	NRC	24.7	RIF	B	unheated	5	3.00	
B635	NRC	24.7	RIF	B	unheated	7	3.99	
B635	NRC	24.7	RIF	B	unheated	8	4.49	
B635	NRC	24.7	RIF	B	unheated	10	5.72	
B635	NRC	24.7	RIF	B	unheated	12	6.26	
B635	NRC	24.7	RIF	B	unheated	24	7.85	6.03
B635	NRC	24.7	RIF	B	unheated	30	8.08	
B635	NRC	24.7	RIF	B	unheated	48	8.24	5.77

B635	NRC	22.0	RIF	B	unheated	0	1.62	6.83
B635	NRC	22.0	RIF	B	unheated	2	1.91	
B635	NRC	22.0	RIF	B	unheated	5	2.96	
B635	NRC	22.0	RIF	B	unheated	7	3.62	
B635	NRC	22.0	RIF	B	unheated	8	3.90	
B635	NRC	22.0	RIF	B	unheated	10	4.83	
B635	NRC	22.0	RIF	B	unheated	12	5.20	
B635	NRC	22.0	RIF	B	unheated	24	7.73	6.26
B635	NRC	22.0	RIF	B	unheated	30	8.10	
B635	NRC	22.0	RIF	B	unheated	48	8.16	6.08
B635	NRC	12.4	RIF	B	unheated	0	1.79	6.84
B635	NRC	12.4	RIF	B	unheated	12	2.13	
B635	NRC	12.4	RIF	B	unheated	24	3.08	
B635	NRC	12.4	RIF	B	unheated	30	3.72	
B635	NRC	12.4	RIF	B	unheated	48	5.46	6.75
B635	NRC	12.4	RIF	B	unheated	54	5.72	
B635	NRC	12.4	RIF	B	unheated	72	6.61	
B635	NRC	12.4	RIF	B	unheated	144	8.10	
B635	NRC	12.4	RIF	B	unheated	167	8.21	5.78
B635	NRC	14.8	RIF	B	unheated	0	1.78	6.84
B635	NRC	14.8	RIF	B	unheated	12	2.60	
B635	NRC	14.8	RIF	B	unheated	24	4.41	
B635	NRC	14.8	RIF	B	unheated	30	5.23	
B635	NRC	14.8	RIF	B	unheated	48	6.89	6.82
B635	NRC	14.8	RIF	B	unheated	54	7.09	
B635	NRC	14.8	RIF	B	unheated	72	7.61	

B635	NRC	14.8	RIF	B	unheated	144	8.27	5.72
B635	NRC	14.8	RIF	B	unheated	0	1.83	6.84
B635	NRC	18.0	RIF	B	unheated	7	2.85	
B635	NRC	18.0	RIF	B	unheated	10	3.63	
B635	NRC	18.0	RIF	B	unheated	12	6.34	
B635	NRC	18.0	RIF	B	unheated	24	6.96	
B635	NRC	18.0	RIF	B	unheated	30	8.10	
B635	NRC	18.0	RIF	B	unheated	48	7.99	6.55
B635	NRC	18.0	RIF	B	unheated	54	8.16	5.86
B626	NRC	29.9	BHI	A	unheated	0	1.83	7.2
B626	NRC	29.9	BHI	A	unheated	2	2.10	
B626	NRC	29.9	BHI	A	unheated	4	3.40	7.22
B626	NRC	29.9	BHI	A	unheated	5	4.67	
B626	NRC	29.9	BHI	A	unheated	7	6.20	
B626	NRC	29.9	BHI	A	unheated	8	7.12	7.08
B626	NRC	29.9	BHI	A	unheated	10	7.32	
B626	NRC	29.9	BHI	A	unheated	12	7.67	
B626	NRC	29.9	BHI	A	unheated	24	8.21	
B626	NRC	29.9	BHI	A	unheated	30	8.16	6.4
B626	NRC	24.7	BHI	A	unheated	0	1.84	7.2
B626	NRC	24.7	BHI	A	unheated	2	2.04	
B626	NRC	24.7	BHI	A	unheated	5	4.10	
B626	NRC	24.7	BHI	A	unheated	7	4.57	
B626	NRC	24.7	BHI	A	unheated	8	5.16	7.22
B626	NRC	24.7	BHI	A	unheated	10	6.15	

B626	NRC	24.7	BHI	A	unheated	12	7.01	
B626	NRC	24.7	BHI	A	unheated	24	7.82	
B626	NRC	24.7	BHI	A	unheated	30	7.91	
B626	NRC	24.7	BHI	A	unheated	48	8.25	6.19
B626	NRC	22.0	BHI	A	unheated	0	1.82	7.2
B626	NRC	22.0	BHI	A	unheated	2	1.92	
B626	NRC	22.0	BHI	A	unheated	5	2.21	
B626	NRC	22.0	BHI	A	unheated	7	3.81	
B626	NRC	22.0	BHI	A	unheated	8	4.31	7.23
B626	NRC	22.0	BHI	A	unheated	10	4.89	
B626	NRC	22.0	BHI	A	unheated	12	5.61	
B626	NRC	22.0	BHI	A	unheated	24	6.90	
B626	NRC	22.0	BHI	A	unheated	30	7.30	
B626	NRC	22.0	BHI	A	unheated	48	8.01	6.1
B626	NRC	18.0	BHI	A	unheated	0	1.78	7.2
B626	NRC	18.0	BHI	A	unheated	5	2.20	
B626	NRC	18.0	BHI	A	unheated	8	2.35	7.23
B626	NRC	18.0	BHI	A	unheated	12	2.98	
B626	NRC	18.0	BHI	A	unheated	24	6.68	
B626	NRC	18.0	BHI	A	unheated	30	7.12	
B626	NRC	18.0	BHI	A	unheated	48	7.04	6.78
B626	NRC	18.0	BHI	A	unheated	54	7.29	
B626	NRC	18.0	BHI	A	unheated	72	7.77	6.1
B626	NRC	14.8	BHI	A	unheated	0	1.88	7.2
B626	NRC	14.8	BHI	A	unheated	12	2.03	
B626	NRC	14.8	BHI	A	unheated	24	3.54	

B626	NRC	14.8	BHI	A	unheated	30	4.53	
B626	NRC	14.8	BHI	A	unheated	48	6.73	7.11
B626	NRC	14.8	BHI	A	unheated	54	6.88	
B626	NRC	14.8	BHI	A	unheated	72	5.75	6.91
B626	NRC	14.8	BHI	A	unheated	96	5.52	7.02
B626	NRC	12.3	BHI	A	unheated	0	1.77	7.2
B626	NRC	12.3	BHI	A	unheated	24	1.85	
B626	NRC	12.3	BHI	A	unheated	48	3.70	
B626	NRC	12.3	BHI	A	unheated	72	5.49	7.14
B626	NRC	12.3	BHI	A	unheated	96	6.62	7.06
B626	NRC	12.3	BHI	A	unheated	167	6.48	6.91
B626	NRC	12.3	BHI	A	unheated	192	6.96	
B626	NRC	12.3	BHI	A	unheated	216	7.44	6.38
B626	NRC	12.3	BHI	A	unheated	240	7.68	
B626	NRC	12.3	BHI	A	unheated	264	7.71	6.23
B626	NRC	29.9	RIF	A	unheated	0	1.75	6.79
B626	NRC	29.9	RIF	A	unheated	2	2.11	
B626	NRC	29.9	RIF	A	unheated	4	3.20	6.81
B626	NRC	29.9	RIF	A	unheated	5	4.51	
B626	NRC	29.9	RIF	A	unheated	7	5.83	
B626	NRC	29.9	RIF	A	unheated	8	6.61	6.73
B626	NRC	29.9	RIF	A	unheated	10	6.99	
B626	NRC	29.9	RIF	A	unheated	12	7.27	
B626	NRC	29.9	RIF	A	unheated	24	7.79	
B626	NRC	29.9	RIF	A	unheated	30	7.79	4.21

B626	NRC	24.7	RIF	A	unheated	0	1.81	6.79
B626	NRC	24.7	RIF	A	unheated	2	2.07	
B626	NRC	24.7	RIF	A	unheated	5	3.54	
B626	NRC	24.7	RIF	A	unheated	7	4.46	
B626	NRC	24.7	RIF	A	unheated	8	5.12	6.82
B626	NRC	24.7	RIF	A	unheated	10	5.88	
B626	NRC	24.7	RIF	A	unheated	12	6.61	
B626	NRC	24.7	RIF	A	unheated	24	8.14	
B626	NRC	24.7	RIF	A	unheated	30	8.13	
B626	NRC	24.7	RIF	A	unheated	48	8.08	6.1
B626	NRC	22.0	RIF	A	unheated	0	1.92	6.79
B626	NRC	22.0	RIF	A	unheated	2	2.05	
B626	NRC	22.0	RIF	A	unheated	5	2.41	
B626	NRC	22.0	RIF	A	unheated	7	3.71	
B626	NRC	22.0	RIF	A	unheated	8	4.21	6.84
B626	NRC	22.0	RIF	A	unheated	10	4.85	
B626	NRC	22.0	RIF	A	unheated	12	5.56	
B626	NRC	22.0	RIF	A	unheated	24	7.91	
B626	NRC	22.0	RIF	A	unheated	30	8.12	
B626	NRC	22.0	RIF	A	unheated	48	7.96	6.28
B626	NRC	18.0	RIF	A	unheated	0	1.91	6.79
B626	NRC	18.0	RIF	A	unheated	5	2.12	
B626	NRC	18.0	RIF	A	unheated	8	2.53	6.85
B626	NRC	18.0	RIF	A	unheated	12	3.67	
B626	NRC	18.0	RIF	A	unheated	24	6.26	
B626	NRC	18.0	RIF	A	unheated	30	7.07	

B626	NRC	18.0	RIF	A	unheated	48	8.12	6.33
B626	NRC	18.0	RIF	A	unheated	54	8.19	
B626	NRC	18.0	RIF	A	unheated	72	8.40	6.23
B626	NRC	14.8	RIF	A	unheated	0	1.94	6.79
B626	NRC	14.8	RIF	A	unheated	12	2.00	
B626	NRC	14.8	RIF	A	unheated	24	3.86	
B626	NRC	14.8	RIF	A	unheated	30	4.53	
B626	NRC	14.8	RIF	A	unheated	48	6.36	6.75
B626	NRC	14.8	RIF	A	unheated	54	6.79	
B626	NRC	14.8	RIF	A	unheated	72	7.51	6.39
B626	NRC	14.8	RIF	A	unheated	96	7.96	6.32
B626	NRC	12.3	RIF	A	unheated	0	1.88	6.79
B626	NRC	12.3	RIF	A	unheated	24	2.08	
B626	NRC	12.3	RIF	A	unheated	48	3.36	
B626	NRC	12.3	RIF	A	unheated	72	4.46	6.77
B626	NRC	12.3	RIF	A	unheated	96	5.44	6.83
B626	NRC	12.3	RIF	A	unheated	167	6.17	5.49
B626	NRC	12.3	RIF	A	unheated	192	6.07	
B626	NRC	12.3	RIF	A	unheated	216	5.87	5.16
B626	NRC	12.3	RIF	A	unheated	240	5.53	
B626	NRC	12.3	RIF	A	unheated	264	5.31	5.16
B626	NRC	30.0	BHI	B	unheated	0	1.91	7.38
B626	NRC	30.0	BHI	B	unheated	2	1.98	
B626	NRC	30.0	BHI	B	unheated	4	3.32	
B626	NRC	30.0	BHI	B	unheated	5	3.95	

B626	NRC	30.0	BHI	B	unheated	7	5.83	
B626	NRC	30.0	BHI	B	unheated	8	6.99	
B626	NRC	30.0	BHI	B	unheated	10	7.45	6.7
B626	NRC	30.0	BHI	B	unheated	12	7.51	
B626	NRC	30.0	BHI	B	unheated	24	8.19	
B626	NRC	30.0	BHI	B	unheated	30	8.07	
B626	NRC	30.0	BHI	B	unheated	48	8.08	6.12
B626	NRC	24.7	BHI	B	unheated	0	1.82	7.38
B626	NRC	24.7	BHI	B	unheated	2	1.75	
B626	NRC	24.7	BHI	B	unheated	5	2.20	
B626	NRC	24.7	BHI	B	unheated	7	4.01	
B626	NRC	24.7	BHI	B	unheated	8	4.66	
B626	NRC	24.7	BHI	B	unheated	10	5.88	7.38
B626	NRC	24.7	BHI	B	unheated	12	6.46	
B626	NRC	24.7	BHI	B	unheated	24	7.59	
B626	NRC	24.7	BHI	B	unheated	30	7.75	
B626	NRC	24.7	BHI	B	unheated	48	8.27	6.88
B626	NRC	22.0	BHI	B	unheated	0	1.70	7.38
B626	NRC	22.0	BHI	B	unheated	2	1.92	
B626	NRC	22.0	BHI	B	unheated	5	2.40	
B626	NRC	22.0	BHI	B	unheated	7	3.52	
B626	NRC	22.0	BHI	B	unheated	8	3.96	
B626	NRC	22.0	BHI	B	unheated	10	4.89	7.37
B626	NRC	22.0	BHI	B	unheated	12	5.48	
B626	NRC	22.0	BHI	B	unheated	24	6.86	
B626	NRC	22.0	BHI	B	unheated	30	7.18	

B626	NRC	22.0	BHI	B	unheated	48	7.53	7.11
B626	NRC	18.0	BHI	B	unheated	0	1.64	7.38
B626	NRC	18.0	BHI	B	unheated	5	1.90	
B626	NRC	18.0	BHI	B	unheated	8	2.02	7.36
B626	NRC	18.0	BHI	B	unheated	12	2.46	
B626	NRC	18.0	BHI	B	unheated	24	6.36	
B626	NRC	18.0	BHI	B	unheated	30	7.40	
B626	NRC	18.0	BHI	B	unheated	48	6.00	
B626	NRC	18.0	BHI	B	unheated	54	6.30	
B626	NRC	18.0	BHI	B	unheated	72	6.30	6.8
B626	NRC	14.8	BHI	B	unheated	0	1.60	7.38
B626	NRC	14.8	BHI	B	unheated	7	1.56	
B626	NRC	14.8	BHI	B	unheated	12	1.81	
B626	NRC	14.8	BHI	B	unheated	24	3.00	
B626	NRC	14.8	BHI	B	unheated	30	3.90	
B626	NRC	14.8	BHI	B	unheated	48	6.65	7.18
B626	NRC	14.8	BHI	B	unheated	54	7.05	
B626	NRC	14.8	BHI	B	unheated	72	6.08	6.94
B626	NRC	14.8	BHI	B	unheated	144	6.12	6.36
B626	NRC	12.4	BHI	B	unheated	0	1.75	7.38
B626	NRC	12.4	BHI	B	unheated	12	1.56	
B626	NRC	12.4	BHI	B	unheated	24	1.58	
B626	NRC	12.4	BHI	B	unheated	30	1.70	
B626	NRC	12.4	BHI	B	unheated	48	2.98	
B626	NRC	12.4	BHI	B	unheated	54	3.64	

B626	NRC	12.4	BHI	B	unheated	72	4.84	7.4
B626	NRC	12.4	BHI	B	unheated	144	5.72	
B626	NRC	12.4	BHI	B	unheated	167	5.80	
B626	NRC	12.4	BHI	B	unheated	192	5.48	
B626	NRC	12.4	BHI	B	unheated	216	5.04	7.09
B626	NRC	12.4	BHI	B	unheated	240	5.15	
B626	NRC	12.4	BHI	B	unheated	312	5.49	
B626	NRC	12.4	BHI	B	unheated	335	5.43	6.12
B626	NRC	30.0	RIF	B	unheated	0	1.70	6.8
B626	NRC	30.0	RIF	B	unheated	2	2.13	
B626	NRC	30.0	RIF	B	unheated	4	3.00	
B626	NRC	30.0	RIF	B	unheated	5	4.15	
B626	NRC	30.0	RIF	B	unheated	7	5.61	
B626	NRC	30.0	RIF	B	unheated	8	6.08	
B626	NRC	30.0	RIF	B	unheated	10	6.52	6.65
B626	NRC	30.0	RIF	B	unheated	12	6.83	
B626	NRC	30.0	RIF	B	unheated	24	8.13	
B626	NRC	30.0	RIF	B	unheated	30	8.01	
B626	NRC	30.0	RIF	B	unheated	48	7.04	5.72
B626	NRC	24.7	RIF	B	unheated	0	1.66	6.8
B626	NRC	24.7	RIF	B	unheated	2	2.16	
B626	NRC	24.7	RIF	B	unheated	5	2.86	
B626	NRC	24.7	RIF	B	unheated	7	4.22	
B626	NRC	24.7	RIF	B	unheated	8	4.60	
B626	NRC	24.7	RIF	B	unheated	10	5.64	6.87
B626	NRC	24.7	RIF	B	unheated	12	6.11	

B626	NRC	24.7	RIF	B	unheated	24	8.00	
B626	NRC	24.7	RIF	B	unheated	30	8.26	
B626	NRC	24.7	RIF	B	unheated	48	8.17	6.21
B626	NRC	22.0	RIF	B	unheated	0	1.82	6.8
B626	NRC	22.0	RIF	B	unheated	2	2.11	
B626	NRC	22.0	RIF	B	unheated	5	2.23	
B626	NRC	22.0	RIF	B	unheated	7	3.20	
B626	NRC	22.0	RIF	B	unheated	8	3.87	
B626	NRC	22.0	RIF	B	unheated	10	4.62	6.9
B626	NRC	22.0	RIF	B	unheated	12	5.20	
B626	NRC	22.0	RIF	B	unheated	24	7.49	
B626	NRC	22.0	RIF	B	unheated	30	8.04	
B626	NRC	22.0	RIF	B	unheated	48	8.37	6.67
B626	NRC	18.0	RIF	B	unheated	0	1.73	6.8
B626	NRC	18.0	RIF	B	unheated	5	2.03	
B626	NRC	18.0	RIF	B	unheated	8	2.06	
B626	NRC	18.0	RIF	B	unheated	12	2.63	6.76
B626	NRC	18.0	RIF	B	unheated	24	5.78	
B626	NRC	18.0	RIF	B	unheated	30	6.43	
B626	NRC	18.0	RIF	B	unheated	48	7.79	
B626	NRC	18.0	RIF	B	unheated	54	7.87	
B626	NRC	18.0	RIF	B	unheated	72	7.95	5.99
B626	NRC	14.8	RIF	B	unheated	0	1.68	6.8
B626	NRC	14.8	RIF	B	unheated	7	1.76	
B626	NRC	14.8	RIF	B	unheated	12	1.76	6.82

B626	NRC	14.8	RIF	B	unheated	24	3.38	
B626	NRC	14.8	RIF	B	unheated	30	3.95	
B626	NRC	14.8	RIF	B	unheated	48	5.91	
B626	NRC	14.8	RIF	B	unheated	54	6.51	
B626	NRC	14.8	RIF	B	unheated	72	7.10	6.57
B626	NRC	14.8	RIF	B	unheated	144	8.00	4.98
B626	NRC	12.4	RIF	B	unheated	0	1.85	6.8
B626	NRC	12.4	RIF	B	unheated	12	1.81	
B626	NRC	12.4	RIF	B	unheated	24	1.87	
B626	NRC	12.4	RIF	B	unheated	30	1.98	
B626	NRC	12.4	RIF	B	unheated	48	3.18	
B626	NRC	12.4	RIF	B	unheated	54	3.48	
B626	NRC	12.4	RIF	B	unheated	72	4.38	6.86
B626	NRC	12.4	RIF	B	unheated	144	5.64	
B626	NRC	12.4	RIF	B	unheated	167	5.69	
B626	NRC	12.4	RIF	B	unheated	192	5.63	
B626	NRC	12.4	RIF	B	unheated	216	5.72	5.75
B626	NRC	12.4	RIF	B	unheated	240	5.61	
B626	NRC	12.4	RIF	B	unheated	312	5.38	
B626	NRC	12.4	RIF	B	unheated	335	5.32	4.92
B596	NRC	29.8	BHI	A	unheated	0	1.59	7.16
B596	NRC	29.8	BHI	A	unheated	2	1.88	
B596	NRC	29.8	BHI	A	unheated	4	2.61	
B596	NRC	29.8	BHI	A	unheated	5	4.37	
B596	NRC	29.8	BHI	A	unheated	7	5.79	7.18
B596	NRC	29.8	BHI	A	unheated	8	6.43	

B596	NRC	29.8	BHI	A	unheated	10	7.21	6.91
B596	NRC	29.8	BHI	A	unheated	12	7.45	
B596	NRC	29.8	BHI	A	unheated	24	8.02	
B596	NRC	29.8	BHI	A	unheated	30	7.90	5.88
B596	NRC	24.7	BHI	A	unheated	0	1.68	7.16
B596	NRC	24.7	BHI	A	unheated	2	1.84	
B596	NRC	24.7	BHI	A	unheated	5	2.43	
B596	NRC	24.7	BHI	A	unheated	7	4.71	7.2
B596	NRC	24.7	BHI	A	unheated	8	4.68	
B596	NRC	24.7	BHI	A	unheated	10	5.68	7.18
B596	NRC	24.7	BHI	A	unheated	12	6.38	
B596	NRC	24.7	BHI	A	unheated	24	7.66	
B596	NRC	24.7	BHI	A	unheated	30	7.78	5.79
B596	NRC	22.0	BHI	A	unheated	0	1.73	7.16
B596	NRC	22.0	BHI	A	unheated	2	1.81	
B596	NRC	22.0	BHI	A	unheated	5	1.85	
B596	NRC	22.0	BHI	A	unheated	7	2.92	7.21
B596	NRC	22.0	BHI	A	unheated	8	3.32	
B596	NRC	22.0	BHI	A	unheated	10	3.95	7.18
B596	NRC	22.0	BHI	A	unheated	12	4.81	
B596	NRC	22.0	BHI	A	unheated	24	6.96	
B596	NRC	22.0	BHI	A	unheated	30	7.21	6.33
B596	NRC	18.0	BHI	A	unheated	0	1.69	7.16
B596	NRC	18.0	BHI	A	unheated	5	1.73	
B596	NRC	18.0	BHI	A	unheated	8	1.99	

B596	NRC	18.0	BHI	A	unheated	12	2.60	7.18
B596	NRC	18.0	BHI	A	unheated	24	5.72	
B596	NRC	18.0	BHI	A	unheated	30	6.91	6.77
B596	NRC	18.0	BHI	A	unheated	48	6.22	
B596	NRC	18.0	BHI	A	unheated	54	6.70	6.77
B596	NRC	18.0	BHI	A	unheated	72	6.90	6.53
B596	NRC	14.8	BHI	A	unheated	0	1.60	7.16
B596	NRC	14.8	BHI	A	unheated	12	2.21	7.17
B596	NRC	14.8	BHI	A	unheated	24	3.19	
B596	NRC	14.8	BHI	A	unheated	30	4.19	7.17
B596	NRC	14.8	BHI	A	unheated	48	6.82	
B596	NRC	14.8	BHI	A	unheated	54	7.01	6.99
B596	NRC	14.8	BHI	A	unheated	72	5.73	6.92
B596	NRC	14.8	BHI	A	unheated	96	6.06	6.93
B596	NRC	12.3	BHI	A	unheated	0	1.46	7.16
B596	NRC	12.3	BHI	A	unheated	24	1.74	
B596	NRC	12.3	BHI	A	unheated	48	3.21	
B596	NRC	12.3	BHI	A	unheated	72	5.18	7.18
B596	NRC	12.3	BHI	A	unheated	96	6.64	
B596	NRC	12.3	BHI	A	unheated	167	5.88	6.18
B596	NRC	12.3	BHI	A	unheated	192	5.32	5.79
B596	NRC	12.3	BHI	A	unheated	216	5.11	5.72
B596	NRC	12.3	BHI	A	unheated	240	5.29	5.58
B596	NRC	12.3	BHI	A	unheated	264	5.26	5.69
B596	NRC	12.3	BHI	A	unheated	335	5.05	5.66
B596	NRC	29.8	RIF	A	unheated	0	1.79	6.8

B596	NRC	29.8	RIF	A	unheated	2	1.89	
B596	NRC	29.8	RIF	A	unheated	4	2.65	
B596	NRC	29.8	RIF	A	unheated	5	3.58	
B596	NRC	29.8	RIF	A	unheated	7	5.09	
B596	NRC	29.8	RIF	A	unheated	10	6.48	6.65
B596	NRC	29.8	RIF	A	unheated	12	6.98	
B596	NRC	29.8	RIF	A	unheated	24	7.76	
B596	NRC	29.8	RIF	A	unheated	30	6.90	5.72
B596	NRC	24.7	RIF	A	unheated	0	1.78	6.8
B596	NRC	24.7	RIF	A	unheated	2	1.91	
B596	NRC	24.7	RIF	A	unheated	5	2.81	
B596	NRC	24.7	RIF	A	unheated	7	3.68	
B596	NRC	24.7	RIF	A	unheated	8	4.28	
B596	NRC	24.7	RIF	A	unheated	10	5.01	6.87
B596	NRC	24.7	RIF	A	unheated	12	5.56	
B596	NRC	24.7	RIF	A	unheated	24	8.07	
B596	NRC	24.7	RIF	A	unheated	30	7.85	6.21
B596	NRC	22.0	RIF	A	unheated	0	1.66	6.8
B596	NRC	22.0	RIF	A	unheated	2	1.87	
B596	NRC	22.0	RIF	A	unheated	5	2.10	
B596	NRC	22.0	RIF	A	unheated	7	3.09	
B596	NRC	22.0	RIF	A	unheated	8	3.29	
B596	NRC	22.0	RIF	A	unheated	10	4.01	6.9
B596	NRC	22.0	RIF	A	unheated	12	4.44	
B596	NRC	22.0	RIF	A	unheated	24	7.64	

B596	NRC	22.0	RIF	A	unheated	30	7.74	6.67
B596	NRC	18.0	RIF	A	unheated	0	1.78	6.8
B596	NRC	18.0	RIF	A	unheated	5	1.91	
B596	NRC	18.0	RIF	A	unheated	8	2.04	
B596	NRC	18.0	RIF	A	unheated	12	2.48	6.76
B596	NRC	18.0	RIF	A	unheated	24	5.26	
B596	NRC	18.0	RIF	A	unheated	30	6.26	
B596	NRC	18.0	RIF	A	unheated	48	8.01	
B596	NRC	18.0	RIF	A	unheated	54	7.79	
B596	NRC	18.0	RIF	A	unheated	72	7.99	5.99
B596	NRC	14.8	RIF	A	unheated	0	1.74	6.8
B596	NRC	14.8	RIF	A	unheated	12	1.78	6.82
B596	NRC	14.8	RIF	A	unheated	24	2.87	
B596	NRC	14.8	RIF	A	unheated	30	3.64	
B596	NRC	14.8	RIF	A	unheated	48	5.37	
B596	NRC	14.8	RIF	A	unheated	54	6.09	
B596	NRC	14.8	RIF	A	unheated	72	6.95	6.57
B596	NRC	14.8	RIF	A	unheated	96	7.44	
B596	NRC	12.3	RIF	A	unheated	0	1.73	6.8
B596	NRC	12.3	RIF	A	unheated	24	1.82	
B596	NRC	12.3	RIF	A	unheated	48	3.01	
B596	NRC	12.3	RIF	A	unheated	72	4.25	6.86
B596	NRC	12.3	RIF	A	unheated	96	5.22	
B596	NRC	12.3	RIF	A	unheated	167	7.99	
B596	NRC	12.3	RIF	A	unheated	192	7.67	
B596	NRC	12.3	RIF	A	unheated	216	7.09	5.75

B596	NRC	12.3	RIF	A	unheated	240	6.39	
B596	NRC	12.3	RIF	A	unheated	264	5.94	
B596	NRC	12.3	RIF	A	unheated	335	5.97	4.92
B594	IFR	9.0	RIF	A	heated	0	2.32	
B594	IFR	9.0	RIF	A	heated	24	2.52	
B594	IFR	9.0	RIF	A	heated	36	2.46	
B594	IFR	9.0	RIF	A	heated	48	2.56	
B594	IFR	9.0	RIF	A	heated	72	2.46	
B594	IFR	9.0	RIF	A	heated	96	2.56	
B594	IFR	9.0	RIF	A	heated	120	2.47	
B594	IFR	9.0	RIF	A	heated	144	2.45	
B594	IFR	9.0	RIF	A	heated	168	2.52	
B594	IFR	9.0	RIF	A	heated	264	2.51	
B594	IFR	9.0	RIF	A	heated	480	2.52	
B594	IFR	12.1	RIF	A	heated	0	2.40	
B594	IFR	12.1	RIF	A	heated	6	2.50	
B594	IFR	12.1	RIF	A	heated	12	2.47	
B594	IFR	12.1	RIF	A	heated	24	2.48	
B594	IFR	12.1	RIF	A	heated	36	2.51	
B594	IFR	12.1	RIF	A	heated	48	2.51	
B594	IFR	12.1	RIF	A	heated	60	2.62	
B594	IFR	12.1	RIF	A	heated	72	2.56	
B594	IFR	12.1	RIF	A	heated	84	2.69	
B594	IFR	12.1	RIF	A	heated	96	2.51	
B594	IFR	12.1	RIF	A	heated	120	2.58	

B594	IFR	12.1	RIF	A	heated	144	2.63	
B594	IFR	12.1	RIF	A	heated	168	2.66	
B594	IFR	12.1	RIF	A	heated	264	3.03	
B594	IFR	12.1	RIF	A	heated	360	3.09	
B594	IFR	12.1	RIF	A	heated	480	3.10	
B594	IFR	15.1	RIF	A	heated	0	2.41	
B594	IFR	15.1	RIF	A	heated	2	2.53	
B594	IFR	15.1	RIF	A	heated	4	2.48	
B594	IFR	15.1	RIF	A	heated	6	2.54	
B594	IFR	15.1	RIF	A	heated	8	2.49	
B594	IFR	15.1	RIF	A	heated	10	2.50	
B594	IFR	15.1	RIF	A	heated	12	2.39	
B594	IFR	15.1	RIF	A	heated	24	2.70	
B594	IFR	15.1	RIF	A	heated	30	2.88	
B594	IFR	15.1	RIF	A	heated	48	4.17	
B594	IFR	15.1	RIF	A	heated	60	4.96	
B594	IFR	15.1	RIF	A	heated	72	5.76	
B594	IFR	15.1	RIF	A	heated	96	6.82	
B594	IFR	15.1	RIF	A	heated	120	7.19	
B594	IFR	15.1	RIF	A	heated	144	7.39	
B594	IFR	15.1	RIF	A	heated	168	7.31	
B594	IFR	18.1	RIF	A	heated	0	2.42	
B594	IFR	18.1	RIF	A	heated	2	2.50	
B594	IFR	18.1	RIF	A	heated	4	2.61	
B594	IFR	18.1	RIF	A	heated	8	2.48	
B594	IFR	18.1	RIF	A	heated	10	2.49	

B594	IFR	18.1	RIF	A	heated	12	2.57	
B594	IFR	18.1	RIF	A	heated	24	4.45	
B594	IFR	18.1	RIF	A	heated	30	5.48	
B594	IFR	18.1	RIF	A	heated	48	7.57	
B594	IFR	18.1	RIF	A	heated	60	7.94	
B594	IFR	18.1	RIF	A	heated	72	8.12	
B594	IFR	18.1	RIF	A	heated	96	8.31	
B594	IFR	18.1	RIF	A	heated	120	8.30	
B594	IFR	18.1	RIF	A	heated	144	8.22	
B594	IFR	22.1	RIF	A	heated	0	2.37	
B594	IFR	22.1	RIF	A	heated	2	2.36	
B594	IFR	22.1	RIF	A	heated	3	2.44	
B594	IFR	22.1	RIF	A	heated	4	2.53	
B594	IFR	22.1	RIF	A	heated	6	2.41	
B594	IFR	22.1	RIF	A	heated	8	2.80	
B594	IFR	22.1	RIF	A	heated	10	3.04	
B594	IFR	22.1	RIF	A	heated	12	3.60	
B594	IFR	22.1	RIF	A	heated	24	6.99	
B594	IFR	22.1	RIF	A	heated	30	7.21	
B594	IFR	22.1	RIF	A	heated	36	7.62	
B594	IFR	22.1	RIF	A	heated	48	8.16	
B594	IFR	22.1	RIF	A	heated	60	8.40	
B594	IFR	22.1	RIF	A	heated	72	8.50	
B594	IFR	9.0	RIF	B	heated	0	2.09	
B594	IFR	9.0	RIF	B	heated	24	2.03	

B594	IFR	9.0	RIF	B	heated	72	2.01	
B594	IFR	9.0	RIF	B	heated	96	2.03	
B594	IFR	9.0	RIF	B	heated	144	1.97	
B594	IFR	9.0	RIF	B	heated	168	1.89	
B594	IFR	9.0	RIF	B	heated	264	1.98	
B594	IFR	9.0	RIF	B	heated	360	1.94	
B594	IFR	9.0	RIF	B	heated	480	1.98	
B594	IFR	12.1	RIF	B	heated	0	2.03	
B594	IFR	12.1	RIF	B	heated	24	2.06	
B594	IFR	12.1	RIF	B	heated	72	2.10	
B594	IFR	12.1	RIF	B	heated	96	2.02	
B594	IFR	12.1	RIF	B	heated	144	2.00	
B594	IFR	12.1	RIF	B	heated	168	1.88	
B594	IFR	12.1	RIF	B	heated	264	2.00	
B594	IFR	12.1	RIF	B	heated	360	1.98	
B594	IFR	12.1	RIF	B	heated	480	1.96	
B594	IFR	15.0	RIF	B	heated	0	2.09	
B594	IFR	15.0	RIF	B	heated	2	2.01	
B594	IFR	15.0	RIF	B	heated	4	1.95	
B594	IFR	15.0	RIF	B	heated	8	2.07	
B594	IFR	15.0	RIF	B	heated	12	2.10	
B594	IFR	15.0	RIF	B	heated	24	2.53	
B594	IFR	15.0	RIF	B	heated	30	2.96	
B594	IFR	15.0	RIF	B	heated	48	4.19	
B594	IFR	15.0	RIF	B	heated	72	5.72	
B594	IFR	15.0	RIF	B	heated	96	6.64	

B594	IFR	15.0	RIF	B	heated	120	7.32	
B594	IFR	15.0	RIF	B	heated	144	7.80	
B594	IFR	15.0	RIF	B	heated	168	7.98	
B594	IFR	18.1	RIF	B	heated	0	2.08	
B594	IFR	18.1	RIF	B	heated	2	2.04	
B594	IFR	18.1	RIF	B	heated	4	2.08	
B594	IFR	18.1	RIF	B	heated	8	2.10	
B594	IFR	18.1	RIF	B	heated	12	2.25	
B594	IFR	18.1	RIF	B	heated	24	4.44	
B594	IFR	18.1	RIF	B	heated	30	5.52	
B594	IFR	18.1	RIF	B	heated	48	7.21	
B594	IFR	18.1	RIF	B	heated	72	8.16	
B594	IFR	18.1	RIF	B	heated	96	8.27	
B594	IFR	18.1	RIF	B	heated	120	8.29	
B594	IFR	22.0	RIF	B	heated	0	2.06	
B594	IFR	22.0	RIF	B	heated	2	2.13	
B594	IFR	22.0	RIF	B	heated	3	2.10	
B594	IFR	22.0	RIF	B	heated	4	2.18	
B594	IFR	22.0	RIF	B	heated	6	2.19	
B594	IFR	22.0	RIF	B	heated	8	2.55	
B594	IFR	22.0	RIF	B	heated	10	3.43	
B594	IFR	22.0	RIF	B	heated	12	3.88	
B594	IFR	22.0	RIF	B	heated	24	7.00	
B594	IFR	22.0	RIF	B	heated	30	7.59	
B594	IFR	22.0	RIF	B	heated	48	8.03	

B594	IFR	22.0	RIF	B	heated	72	7.64	
B594	IFR	22.0	RIF	B	unheated	0	2.75	
B594	IFR	22.0	RIF	B	unheated	2	3.02	
B594	IFR	22.0	RIF	B	unheated	3	3.14	
B594	IFR	22.0	RIF	B	unheated	4	3.22	
B594	IFR	22.0	RIF	B	unheated	6	4.03	
B594	IFR	22.0	RIF	B	unheated	24	7.73	
B594	IFR	22.0	RIF	B	unheated	30	7.89	
B594	IFR	22.0	RIF	B	unheated	48	8.21	
B594	IFR	9.0	RIF	C	heated	0	2.01	
B594	IFR	9.0	RIF	C	heated	24	2.03	
B594	IFR	9.0	RIF	C	heated	72	2.07	
B594	IFR	9.0	RIF	C	heated	144	2.02	
B594	IFR	9.0	RIF	C	heated	168	1.92	
B594	IFR	9.0	RIF	C	heated	264	1.94	
B594	IFR	9.0	RIF	C	heated	360	1.89	
B594	IFR	12.1	RIF	C	heated	0	2.06	
B594	IFR	12.1	RIF	C	heated	24	2.03	
B594	IFR	12.1	RIF	C	heated	72	2.14	
B594	IFR	12.1	RIF	C	heated	144	2.57	
B594	IFR	12.1	RIF	C	heated	168	3.16	
B594	IFR	12.1	RIF	C	heated	264	3.12	
B594	IFR	12.1	RIF	C	heated	360	2.59	
B594	IFR	15.0	RIF	C	heated	0	2.03	
B594	IFR	15.0	RIF	C	heated	8	2.00	
B594	IFR	15.0	RIF	C	heated	12	2.14	

B594	IFR	15.0	RIF	C	heated	24	2.46	
B594	IFR	15.0	RIF	C	heated	30	3.02	
B594	IFR	15.0	RIF	C	heated	48	4.20	
B594	IFR	15.0	RIF	C	heated	72	5.54	
B594	IFR	15.0	RIF	C	heated	96	6.66	
B594	IFR	15.0	RIF	C	heated	120	7.27	
B594	IFR	15.0	RIF	C	heated	144	7.45	
B594	IFR	15.0	RIF	C	heated	168	7.00	
B594	IFR	18.1	RIF	C	heated	0	2.03	
B594	IFR	18.1	RIF	C	heated	4	2.05	
B594	IFR	18.1	RIF	C	heated	8	2.09	
B594	IFR	18.1	RIF	C	heated	12	2.34	
B594	IFR	18.1	RIF	C	heated	24	4.63	
B594	IFR	18.1	RIF	C	heated	30	5.73	
B594	IFR	18.1	RIF	C	heated	48	7.61	
B594	IFR	18.1	RIF	C	heated	72	8.17	
B594	IFR	18.1	RIF	C	heated	96	8.34	
B594	IFR	18.1	RIF	C	heated	120	8.48	
B594	IFR	18.1	RIF	C	heated	144	8.41	
B594	IFR	22.0	RIF	C	heated	0	1.99	
B594	IFR	22.0	RIF	C	heated	2	2.03	
B594	IFR	22.0	RIF	C	heated	3	2.01	
B594	IFR	22.0	RIF	C	heated	4	2.14	
B594	IFR	22.0	RIF	C	heated	6	2.14	
B594	IFR	22.0	RIF	C	heated	8	2.40	

B594	IFR	22.0	RIF	C	heated	10	3.08	
B594	IFR	22.0	RIF	C	heated	12	3.80	
B594	IFR	22.0	RIF	C	heated	24	6.90	
B594	IFR	22.0	RIF	C	heated	30	7.38	
B594	IFR	22.0	RIF	C	heated	48	8.15	
B594	IFR	22.0	RIF	C	heated	72	8.23	
B594	IFR	22.0	RIF	C	heated	96	8.08	
B594	IFR	22.0	RIF	C	unheated	0	2.89	
B594	IFR	22.0	RIF	C	unheated	2	3.18	
B594	IFR	22.0	RIF	C	unheated	3	3.17	
B594	IFR	22.0	RIF	C	unheated	4	3.14	
B594	IFR	22.0	RIF	C	unheated	6	4.06	
B594	IFR	22.0	RIF	C	unheated	8	4.85	
B594	IFR	22.0	RIF	C	unheated	10	5.59	
B594	IFR	22.0	RIF	C	unheated	12	6.21	
B594	IFR	22.0	RIF	C	unheated	24	7.88	
B594	IFR	22.0	RIF	C	unheated	30	8.05	
B594	IFR	22.0	RIF	C	unheated	48	8.34	
B596	IFR	9.0	RIF	A	heated	0	1.92	
B596	IFR	9.0	RIF	A	heated	24	1.86	
B596	IFR	9.0	RIF	A	heated	72	1.90	
B596	IFR	9.0	RIF	A	heated	96	1.98	
B596	IFR	9.0	RIF	A	heated	144	2.04	
B596	IFR	9.0	RIF	A	heated	168	1.88	
B596	IFR	9.0	RIF	A	heated	264	1.85	
B596	IFR	9.0	RIF	A	heated	360	1.98	

B596	IFR	9.0	RIF	A	heated	480	1.95	
B596	IFR	9.0	RIF	B	heated	0	1.67	
B596	IFR	9.0	RIF	B	heated	24	1.72	
B596	IFR	9.0	RIF	B	heated	72	1.66	
B596	IFR	9.0	RIF	B	heated	96	1.74	
B596	IFR	9.0	RIF	B	heated	144	1.70	
B596	IFR	9.0	RIF	B	heated	168	1.83	
B596	IFR	12.0	RIF	A	heated	0	1.92	
B596	IFR	12.0	RIF	A	heated	24	1.94	
B596	IFR	12.0	RIF	A	heated	72	2.37	
B596	IFR	12.0	RIF	A	heated	96	2.63	
B596	IFR	12.0	RIF	A	heated	144	3.37	
B596	IFR	12.0	RIF	A	heated	168	3.97	
B596	IFR	12.0	RIF	A	heated	216	5.29	
B596	IFR	12.0	RIF	A	heated	264	6.37	
B596	IFR	12.0	RIF	A	heated	312	6.84	
B596	IFR	12.0	RIF	A	heated	360	7.04	
B596	IFR	12.0	RIF	A	heated	480	7.08	
B596	IFR	12.1	RIF	B	heated	0	1.77	
B596	IFR	12.1	RIF	B	heated	24	1.69	
B596	IFR	12.1	RIF	B	heated	72	1.94	
B596	IFR	12.1	RIF	B	heated	96	2.39	
B596	IFR	12.1	RIF	B	heated	144	3.04	
B596	IFR	12.1	RIF	B	heated	168	3.36	
B596	IFR	12.1	RIF	B	heated	216	5.36	

B596	IFR	12.1	RIF	B	heated	264	6.25	
B596	IFR	15.0	RIF	A	heated	0	1.86	
B596	IFR	15.0	RIF	A	heated	2	1.91	
B596	IFR	15.0	RIF	A	heated	3	1.95	
B596	IFR	15.0	RIF	A	heated	8	2.15	
B596	IFR	15.0	RIF	A	heated	12	2.08	
B596	IFR	15.0	RIF	A	heated	24	2.33	
B596	IFR	15.0	RIF	A	heated	30	2.78	
B596	IFR	15.0	RIF	A	heated	48	4.54	
B596	IFR	15.0	RIF	A	heated	72	6.56	
B596	IFR	15.0	RIF	A	heated	96	7.38	
B596	IFR	15.0	RIF	A	heated	120	7.64	
B596	IFR	15.0	RIF	A	heated	144	7.56	
B596	IFR	15.0	RIF	A	heated	168	7.46	
B596	IFR	15.0	RIF	B	heated	0	1.68	
B596	IFR	15.0	RIF	B	heated	2	1.79	
B596	IFR	15.0	RIF	B	heated	4	1.78	
B596	IFR	15.0	RIF	B	heated	8	1.82	
B596	IFR	15.0	RIF	B	heated	12	1.95	
B596	IFR	15.0	RIF	B	heated	24	1.94	
B596	IFR	15.0	RIF	B	heated	30	2.50	
B596	IFR	15.0	RIF	B	heated	48	4.23	
B596	IFR	15.0	RIF	B	heated	72	6.46	
B596	IFR	15.0	RIF	B	heated	96	7.26	
B596	IFR	15.0	RIF	B	heated	120	7.48	
B596	IFR	15.0	RIF	B	heated	144	7.57	

B596	IFR	15.0	RIF	B	heated	168	7.72	
B596	IFR	18.1	RIF	A	heated	0	1.98	
B596	IFR	18.1	RIF	A	heated	2	1.90	
B596	IFR	18.1	RIF	A	heated	3	1.95	
B596	IFR	18.1	RIF	A	heated	8	2.17	
B596	IFR	18.1	RIF	A	heated	12	2.67	
B596	IFR	18.1	RIF	A	heated	24	4.01	
B596	IFR	18.1	RIF	A	heated	30	5.20	
B596	IFR	18.1	RIF	A	heated	48	7.04	
B596	IFR	18.1	RIF	A	heated	72	7.68	
B596	IFR	18.1	RIF	A	heated	96	7.83	
B596	IFR	18.1	RIF	A	heated	120	7.86	
B596	IFR	18.1	RIF	B	heated	0	1.73	
B596	IFR	18.1	RIF	B	heated	2	1.74	
B596	IFR	18.1	RIF	B	heated	4	1.81	
B596	IFR	18.1	RIF	B	heated	8	1.80	
B596	IFR	18.1	RIF	B	heated	12	1.99	
B596	IFR	18.1	RIF	B	heated	24	3.67	
B596	IFR	18.1	RIF	B	heated	30	4.83	
B596	IFR	18.1	RIF	B	heated	48	6.92	
B596	IFR	18.1	RIF	B	heated	72	7.90	
B596	IFR	18.1	RIF	B	heated	96	8.06	
B596	IFR	18.1	RIF	B	heated	120	8.01	
B596	IFR	23.0	RIF	A	heated	0	1.91	

B596	IFR	23.0	RIF	A	heated	2	1.88	
B596	IFR	23.0	RIF	A	heated	3	2.18	
B596	IFR	23.0	RIF	A	heated	4	1.97	
B596	IFR	23.0	RIF	A	heated	6	2.72	
B596	IFR	23.0	RIF	A	heated	8	2.56	
B596	IFR	23.0	RIF	A	heated	10	2.90	
B596	IFR	23.0	RIF	A	heated	12	3.30	
B596	IFR	23.0	RIF	A	heated	24	6.67	
B596	IFR	23.0	RIF	A	heated	30	7.43	
B596	IFR	23.0	RIF	A	heated	48	7.62	
B596	IFR	23.0	RIF	A	heated	72	7.14	
B596	IFR	23.0	RIF	A	heated	96	6.75	
B596	IFR	21.9	RIF	B	heated	0	1.74	
B596	IFR	21.9	RIF	B	heated	2	1.71	
B596	IFR	21.9	RIF	B	heated	3	1.68	
B596	IFR	21.9	RIF	B	heated	4	1.74	
B596	IFR	21.9	RIF	B	heated	6	1.82	
B596	IFR	21.9	RIF	B	heated	8	2.00	
B596	IFR	21.9	RIF	B	heated	10	2.21	
B596	IFR	21.9	RIF	B	heated	12	2.76	
B596	IFR	21.9	RIF	B	heated	24	6.33	
B596	IFR	21.9	RIF	B	heated	30	7.29	
B596	IFR	21.9	RIF	B	heated	48	7.60	
B596	IFR	21.9	RIF	B	heated	72	7.40	
B596	IFR	21.9	RIF	B	heated	96	7.00	
B596	IFR	23.0	RIF	A	unheated	0	2.10	

B596	IFR	23.0	RIF	A	unheated	2	2.62	
B596	IFR	23.0	RIF	A	unheated	3	2.77	
B596	IFR	23.0	RIF	A	unheated	4	2.97	
B596	IFR	23.0	RIF	A	unheated	6	3.37	
B596	IFR	23.0	RIF	A	unheated	8	3.87	
B596	IFR	23.0	RIF	A	unheated	10	4.48	
B596	IFR	23.0	RIF	A	unheated	24	7.30	
B596	IFR	23.0	RIF	A	unheated	30	7.60	
B596	IFR	23.0	RIF	A	unheated	48	7.67	
B596	IFR	23.0	RIF	A	unheated	72	7.37	
B596	IFR	23.0	RIF	A	unheated	96	7.22	
B596	IFR	21.9	RIF	B	unheated	0	2.21	
B596	IFR	21.9	RIF	B	unheated	2	2.69	
B596	IFR	21.9	RIF	B	unheated	3	2.68	
B596	IFR	21.9	RIF	B	unheated	4	2.87	
B596	IFR	21.9	RIF	B	unheated	6	3.15	
B596	IFR	21.9	RIF	B	unheated	8	4.11	
B596	IFR	21.9	RIF	B	unheated	10	4.37	
B596	IFR	21.9	RIF	B	unheated	12	5.07	
B596	IFR	21.9	RIF	B	unheated	24	7.05	
B596	IFR	21.9	RIF	B	unheated	30	7.51	
B596	IFR	21.9	RIF	B	unheated	48	7.76	
B596	IFR	9.0	RIF	C	heated	0	1.82	
B596	IFR	9.0	RIF	C	heated	24	1.87	
B596	IFR	9.0	RIF	C	heated	72	1.81	

B596	IFR	9.0	RIF	C	heated	96	1.86	
B596	IFR	9.0	RIF	C	heated	144	1.84	
B596	IFR	9.0	RIF	C	heated	216	1.76	
B596	IFR	9.0	RIF	C	heated	264	1.81	
B596	IFR	9.0	RIF	C	heated	480	1.98	
B596	IFR	12.1	RIF	C	heated	0	1.80	
B596	IFR	12.1	RIF	C	heated	24	1.91	
B596	IFR	12.1	RIF	C	heated	72	2.35	
B596	IFR	12.1	RIF	C	heated	96	2.85	
B596	IFR	12.1	RIF	C	heated	144	3.69	
B596	IFR	12.1	RIF	C	heated	168	4.03	
B596	IFR	12.1	RIF	C	heated	216	4.48	
B596	IFR	12.1	RIF	C	heated	264	4.83	
B596	IFR	12.1	RIF	C	heated	312	5.13	
B596	IFR	12.1	RIF	C	heated	360	5.45	
B596	IFR	12.1	RIF	C	heated	480	5.44	
B596	IFR	15.1	RIF	C	heated	0	1.80	
B596	IFR	15.1	RIF	C	heated	2	1.82	
B596	IFR	15.1	RIF	C	heated	4	1.78	
B596	IFR	15.1	RIF	C	heated	8	1.86	
B596	IFR	15.1	RIF	C	heated	12	1.67	
B596	IFR	15.1	RIF	C	heated	24	2.11	
B596	IFR	15.1	RIF	C	heated	30	2.53	
B596	IFR	15.1	RIF	C	heated	48	4.33	
B596	IFR	15.1	RIF	C	heated	72	6.64	
B596	IFR	15.1	RIF	C	heated	96	7.30	

B596	IFR	15.1	RIF	C	heated	120	7.58	
B596	IFR	15.1	RIF	C	heated	144	7.71	
B596	IFR	18.1	RIF	C	heated	0	1.79	
B596	IFR	18.1	RIF	C	heated	2	1.82	
B596	IFR	18.1	RIF	C	heated	4	1.69	
B596	IFR	18.1	RIF	C	heated	8	1.85	
B596	IFR	18.1	RIF	C	heated	12	2.01	
B596	IFR	18.1	RIF	C	heated	24	3.80	
B596	IFR	18.1	RIF	C	heated	30	4.92	
B596	IFR	18.1	RIF	C	heated	48	7.18	
B596	IFR	18.1	RIF	C	heated	72	7.94	
B596	IFR	18.1	RIF	C	heated	96	8.10	
B596	IFR	18.1	RIF	C	heated	120	8.22	
B596	IFR	22.1	RIF	C	heated	0	1.82	
B596	IFR	22.1	RIF	C	heated	2	1.91	
B596	IFR	22.1	RIF	C	heated	3	1.73	
B596	IFR	22.1	RIF	C	heated	4	1.76	
B596	IFR	22.1	RIF	C	heated	6	1.90	
B596	IFR	22.1	RIF	C	heated	8	2.03	
B596	IFR	22.1	RIF	C	heated	10	2.26	
B596	IFR	22.1	RIF	C	heated	12	3.03	
B596	IFR	22.1	RIF	C	heated	24	6.69	
B596	IFR	22.1	RIF	C	heated	30	7.36	
B596	IFR	22.1	RIF	C	heated	48	7.74	
B596	IFR	22.1	RIF	C	heated	72	8.10	

B596	IFR	22.1	RIF	C	heated	96	7.62	
B596	IFR	22.1	RIF	C	unheated	0	2.08	
B596	IFR	22.1	RIF	C	unheated	2	2.53	
B596	IFR	22.1	RIF	C	unheated	3	2.59	
B596	IFR	22.1	RIF	C	unheated	4	2.68	
B596	IFR	22.1	RIF	C	unheated	6	3.07	
B596	IFR	22.1	RIF	C	unheated	8	3.84	
B596	IFR	22.1	RIF	C	unheated	10	4.41	
B596	IFR	22.1	RIF	C	unheated	12	5.05	
B596	IFR	22.1	RIF	C	unheated	24	7.43	
B596	IFR	22.1	RIF	C	unheated	30	7.79	
B596	IFR	22.1	RIF	C	unheated	48	7.87	
B577	IFR	11.9	BHI	C	heated	0	1.50	
B577	IFR	11.9	BHI	C	heated	24	1.64	
B577	IFR	11.9	BHI	C	heated	72	3.32	
B577	IFR	11.9	BHI	C	heated	96	4.18	7.3
B577	IFR	11.9	BHI	C	heated	144	6.77	
B577	IFR	11.9	BHI	C	heated	168	6.62	6.95
B577	IFR	11.9	BHI	C	heated	216	6.28	
B577	IFR	11.9	BHI	C	heated	264	6.38	6.69
B577	IFR	11.9	BHI	C	heated	312	5.30	6.8
B577	IFR	11.9	BHI	C	heated	360	5.41	
B577	IFR	11.9	BHI	C	heated	480	5.29	6.27
B577	IFR	15.1	BHI	C	heated	0	1.66	
B577	IFR	15.1	BHI	C	heated	4	1.56	
B577	IFR	15.1	BHI	C	heated	12	1.87	

B577	IFR	15.1	BHI	C	heated	24	2.20	
B577	IFR	15.1	BHI	C	heated	30	2.63	7.38
B577	IFR	15.1	BHI	C	heated	49	4.95	
B577	IFR	15.1	BHI	C	heated	72	7.13	7.05
B577	IFR	15.1	BHI	C	heated	120	7.46	
B577	IFR	15.1	BHI	C	heated	144	7.76	6.68
B577	IFR	15.1	BHI	C	heated	168	5.13	6.33
B577	IFR	18.1	BHI	C	heated	0	1.50	
B577	IFR	18.1	BHI	C	heated	4	1.66	
B577	IFR	18.1	BHI	C	heated	12	1.87	
B577	IFR	18.1	BHI	C	heated	24	4.69	7.36
B577	IFR	18.1	BHI	C	heated	30	6.05	
B577	IFR	18.1	BHI	C	heated	49	6.25	6.8
B577	IFR	18.1	BHI	C	heated	72	6.34	6.68
B577	IFR	18.1	BHI	C	heated	96	7.30	6.37
B577	IFR	18.1	BHI	C	heated	120	7.76	6
B577	IFR	22.0	BHI	C	heated	0	1.55	
B577	IFR	22.0	BHI	C	heated	2	1.45	
B577	IFR	22.0	BHI	C	heated	4	1.60	
B577	IFR	22.0	BHI	C	heated	8	1.75	
B577	IFR	22.0	BHI	C	heated	10	3.03	
B577	IFR	22.0	BHI	C	heated	12	3.84	7.39
B577	IFR	22.0	BHI	C	heated	24	7.24	6.79
B577	IFR	22.0	BHI	C	heated	30	7.30	
B577	IFR	22.0	BHI	C	heated	49	7.57	6.09

B577	IFR	22.0	BHI	C	heated	72	7.76	
B577	IFR	22.0	BHI	C	heated	96	8.09	6.25
B577	IFR	22.0	BHI	C	unheated	0	2.76	
B577	IFR	22.0	BHI	C	unheated	2	3.15	
B577	IFR	22.0	BHI	C	unheated	4	3.30	
B577	IFR	22.0	BHI	C	unheated	6	3.58	
B577	IFR	22.0	BHI	C	unheated	8	4.64	
B577	IFR	22.0	BHI	C	unheated	10	5.60	
B577	IFR	22.0	BHI	C	unheated	12	5.93	7.35
B577	IFR	22.0	BHI	C	unheated	24	7.30	6.47
B577	IFR	22.0	BHI	C	unheated	30	7.37	
B577	IFR	22.0	BHI	C	unheated	49	7.51	5.94
B577	IFR	22.0	BHI	C	unheated	72	7.68	6.15
B577	IFR	25.0	BHI	C	heated	0	1.46	
B577	IFR	25.0	BHI	C	heated	2	1.72	
B577	IFR	25.0	BHI	C	heated	4	1.78	
B577	IFR	25.0	BHI	C	heated	6	2.00	
B577	IFR	25.0	BHI	C	heated	8	3.12	
B577	IFR	25.0	BHI	C	heated	10	3.85	
B577	IFR	25.0	BHI	C	heated	12	5.00	7.41
B577	IFR	25.0	BHI	C	heated	24	7.74	6.28
B577	IFR	25.0	BHI	C	heated	30	7.75	
B577	IFR	25.0	BHI	C	heated	49	7.80	6.08
B577	IFR	25.0	BHI	C	heated	72	7.74	6.65
B577	IFR	12.1	RIF	A	heated	0	1.80	
B577	IFR	12.1	RIF	A	heated	21	1.82	

B577	IFR	12.1	RIF	A	heated	24	1.95	
B577	IFR	12.1	RIF	A	heated	72	2.48	
B577	IFR	12.1	RIF	A	heated	96	3.12	
B577	IFR	12.1	RIF	A	heated	144	4.83	
B577	IFR	12.1	RIF	A	heated	168	5.46	
B577	IFR	12.1	RIF	A	heated	216	5.87	
B577	IFR	12.1	RIF	A	heated	264	6.18	
B577	IFR	12.1	RIF	A	heated	312	6.28	
B577	IFR	12.1	RIF	A	heated	360	6.47	
B577	IFR	15.1	RIF	A	heated	0	1.82	
B577	IFR	15.1	RIF	A	heated	4	1.89	
B577	IFR	15.1	RIF	A	heated	12	1.88	
B577	IFR	15.1	RIF	A	heated	21	2.11	
B577	IFR	15.1	RIF	A	heated	24	2.10	
B577	IFR	15.1	RIF	A	heated	30	2.53	
B577	IFR	15.1	RIF	A	heated	49	4.64	
B577	IFR	15.1	RIF	A	heated	72	6.51	
B577	IFR	15.1	RIF	A	heated	96	7.33	
B577	IFR	15.1	RIF	A	heated	120	7.86	
B577	IFR	15.1	RIF	A	heated	144	8.17	
B577	IFR	15.1	RIF	A	heated	168	8.36	
B577	IFR	18.2	RIF	A	heated	0	1.81	
B577	IFR	18.2	RIF	A	heated	4	1.91	
B577	IFR	18.2	RIF	A	heated	12	1.99	
B577	IFR	18.2	RIF	A	heated	21	3.66	

B577	IFR	18.2	RIF	A	heated	24	4.26	
B577	IFR	18.2	RIF	A	heated	30	5.14	
B577	IFR	18.2	RIF	A	heated	49	7.26	
B577	IFR	18.2	RIF	A	heated	72	8.07	
B577	IFR	18.2	RIF	A	heated	96	7.88	
B577	IFR	18.2	RIF	A	heated	120	7.56	
B577	IFR	22.0	RIF	A	heated	0	1.87	
B577	IFR	22.0	RIF	A	heated	2	1.87	
B577	IFR	22.0	RIF	A	heated	4	1.90	
B577	IFR	22.0	RIF	A	heated	8	2.08	
B577	IFR	22.0	RIF	A	heated	10	2.68	
B577	IFR	22.0	RIF	A	heated	12	3.31	
B577	IFR	22.0	RIF	A	heated	21	6.46	
B577	IFR	22.0	RIF	A	heated	24	6.71	
B577	IFR	22.0	RIF	A	heated	30	7.25	
B577	IFR	22.0	RIF	A	heated	49	8.23	
B577	IFR	22.0	RIF	A	heated	72	8.41	
B577	IFR	22.0	RIF	A	heated	96	7.86	
B577	IFR	22.0	RIF	A	unheated	0	1.20	
B577	IFR	22.0	RIF	A	unheated	2	1.67	
B577	IFR	22.0	RIF	A	unheated	3	1.56	
B577	IFR	22.0	RIF	A	unheated	4	1.78	
B577	IFR	22.0	RIF	A	unheated	6	2.43	
B577	IFR	22.0	RIF	A	unheated	8	3.26	
B577	IFR	22.0	RIF	A	unheated	10	3.88	
B577	IFR	22.0	RIF	A	unheated	12	4.67	

B577	IFR	22.0	RIF	A	unheated	21	6.90	
B577	IFR	22.0	RIF	A	unheated	24	7.29	
B577	IFR	22.0	RIF	A	unheated	30	7.86	
B577	IFR	22.0	RIF	A	unheated	49	8.47	
B577	IFR	22.0	RIF	A	unheated	72	8.64	
B577	IFR	24.9	RIF	A	heated	0	1.80	
B577	IFR	24.9	RIF	A	heated	2	1.80	
B577	IFR	24.9	RIF	A	heated	3	1.85	
B577	IFR	24.9	RIF	A	heated	4	1.67	
B577	IFR	24.9	RIF	A	heated	6	2.22	
B577	IFR	24.9	RIF	A	heated	8	3.12	
B577	IFR	24.9	RIF	A	heated	12	4.52	
B577	IFR	24.9	RIF	A	heated	21	7.03	
B577	IFR	24.9	RIF	A	heated	24	7.60	
B577	IFR	24.9	RIF	A	heated	49	8.62	
B577	IFR	24.9	RIF	A	heated	72	8.70	
B577	IFR	11.9	RIF	B	heated	0	1.82	
B577	IFR	11.9	RIF	B	heated	21	1.79	
B577	IFR	11.9	RIF	B	heated	24	1.74	
B577	IFR	11.9	RIF	B	heated	72	2.41	
B577	IFR	11.9	RIF	B	heated	96	3.04	
B577	IFR	15.1	RIF	B	heated	0	1.84	
B577	IFR	15.1	RIF	B	heated	4	1.75	
B577	IFR	15.1	RIF	B	heated	12	1.79	
B577	IFR	15.1	RIF	B	heated	21	1.90	

B577	IFR	15.1	RIF	B	heated	24	2.04	
B577	IFR	15.1	RIF	B	heated	30	2.51	
B577	IFR	15.1	RIF	B	heated	49	4.40	
B577	IFR	15.1	RIF	B	heated	72	6.70	
B577	IFR	15.1	RIF	B	heated	96	7.36	
B577	IFR	15.1	RIF	B	heated	120	7.88	
B577	IFR	18.2	RIF	B	heated	0	1.80	
B577	IFR	18.2	RIF	B	heated	4	1.69	
B577	IFR	18.2	RIF	B	heated	12	1.93	
B577	IFR	18.2	RIF	B	heated	21	3.53	
B577	IFR	18.2	RIF	B	heated	24	4.02	
B577	IFR	18.2	RIF	B	heated	30	5.16	
B577	IFR	18.2	RIF	B	heated	49	7.18	
B577	IFR	18.2	RIF	B	heated	72	8.29	
B577	IFR	18.2	RIF	B	heated	96	8.63	
B577	IFR	18.2	RIF	B	heated	120	8.70	
B577	IFR	22.0	RIF	B	heated	0	1.68	
B577	IFR	22.0	RIF	B	heated	2	1.87	
B577	IFR	22.0	RIF	B	heated	4	1.80	
B577	IFR	22.0	RIF	B	heated	8	1.99	
B577	IFR	22.0	RIF	B	heated	10	2.74	
B577	IFR	22.0	RIF	B	heated	12	3.31	
B577	IFR	22.0	RIF	B	heated	21	6.64	
B577	IFR	22.0	RIF	B	heated	24	7.07	
B577	IFR	22.0	RIF	B	heated	30	7.68	
B577	IFR	22.0	RIF	B	heated	49	8.48	

B577	IFR	22.0	RIF	B	heated	72	8.34	
B577	IFR	22.0	RIF	B	heated	96	8.59	
B577	IFR	22.0	RIF	B	heated	0	1.53	
B577	IFR	22.0	RIF	B	heated	2	2.25	
B577	IFR	22.0	RIF	B	heated	6	3.34	
B577	IFR	22.0	RIF	B	heated	8	4.14	
B577	IFR	22.0	RIF	B	heated	10	4.81	
B577	IFR	22.0	RIF	B	heated	12	5.46	
B577	IFR	22.0	RIF	B	heated	21	7.32	
B577	IFR	22.0	RIF	B	heated	24	7.61	
B577	IFR	22.0	RIF	B	heated	30	8.14	
B577	IFR	22.0	RIF	B	heated	49	8.67	
B577	IFR	22.0	RIF	B	heated	72	8.52	
B577	IFR	24.9	RIF	B	heated	0	1.82	
B577	IFR	24.9	RIF	B	heated	2	1.71	
B577	IFR	24.9	RIF	B	heated	4	1.91	
B577	IFR	24.9	RIF	B	heated	6	2.08	
B577	IFR	24.9	RIF	B	heated	8	2.69	
B577	IFR	24.9	RIF	B	heated	10	3.42	
B577	IFR	24.9	RIF	B	heated	12	4.20	
B577	IFR	24.9	RIF	B	heated	21	7.14	
B577	IFR	24.9	RIF	B	heated	24	7.65	
B577	IFR	24.9	RIF	B	heated	30	8.25	
B577	IFR	24.9	RIF	B	heated	49	8.27	
B577	IFR	24.9	RIF	B	heated	72	8.73	

B577	IFR	24.9	RIF	B	heated	96	8.22	
B577	IFR	11.9	RIF	C	heated	0	1.64	6.81
B577	IFR	11.9	RIF	C	heated	24	1.58	
B577	IFR	11.9	RIF	C	heated	72	2.17	
B577	IFR	11.9	RIF	C	heated	96	3.09	6.78
B577	IFR	11.9	RIF	C	heated	144	3.99	
B577	IFR	11.9	RIF	C	heated	168	4.40	6.92
B577	IFR	11.9	RIF	C	heated	216	5.19	
B577	IFR	11.9	RIF	C	heated	264	5.37	7.28
B577	IFR	11.9	RIF	C	heated	312	5.51	7.55
B577	IFR	11.9	RIF	C	heated	360	5.85	
B577	IFR	11.9	RIF	C	heated	480	5.64	6.58
B577	IFR	15.1	RIF	C	heated	0	1.51	6.81
B577	IFR	15.1	RIF	C	heated	4	1.45	
B577	IFR	15.1	RIF	C	heated	12	1.66	
B577	IFR	15.1	RIF	C	heated	24	1.79	
B577	IFR	15.1	RIF	C	heated	30	2.36	6.92
B577	IFR	15.1	RIF	C	heated	49	4.26	
B577	IFR	15.1	RIF	C	heated	72	6.47	6.8
B577	IFR	15.1	RIF	C	heated	96	7.21	6.33
B577	IFR	15.1	RIF	C	heated	120	7.68	
B577	IFR	15.1	RIF	C	heated	144	7.82	6.28
B577	IFR	15.1	RIF	C	heated	168	7.12	6.55
B577	IFR	18.1	RIF	C	heated	0	1.39	6.81
B577	IFR	18.1	RIF	C	heated	4	1.51	
B577	IFR	18.1	RIF	C	heated	12	1.65	

B577	IFR	18.1	RIF	C	heated	24	3.86	6.9
B577	IFR	18.1	RIF	C	heated	30	4.92	
B577	IFR	18.1	RIF	C	heated	49	6.92	6.5
B577	IFR	18.1	RIF	C	heated	72	8.03	6.37
B577	IFR	18.1	RIF	C	heated	96	8.12	6.6
B577	IFR	18.1	RIF	C	heated	120	8.15	
B577	IFR	22.0	RIF	C	heated	0	1.56	6.81
B577	IFR	22.0	RIF	C	heated	2	1.56	
B577	IFR	22.0	RIF	C	heated	4	1.49	
B577	IFR	22.0	RIF	C	heated	8	1.95	
B577	IFR	22.0	RIF	C	heated	10	2.45	
B577	IFR	22.0	RIF	C	heated	12	2.90	6.98
B577	IFR	22.0	RIF	C	heated	24	6.55	6.84
B577	IFR	22.0	RIF	C	heated	30	6.48	
B577	IFR	22.0	RIF	C	heated	49	7.88	6.48
B577	IFR	22.0	RIF	C	heated	72	8.07	
B577	IFR	22.0	RIF	C	heated	96	8.13	5.1
B577	IFR	22.0	RIF	C	unheated	0	2.92	6.81
B577	IFR	22.0	RIF	C	unheated	2	3.23	
B577	IFR	22.0	RIF	C	unheated	4	3.30	
B577	IFR	22.0	RIF	C	unheated	6	4.11	
B577	IFR	22.0	RIF	C	unheated	8	4.90	
B577	IFR	22.0	RIF	C	unheated	10	5.48	
B577	IFR	22.0	RIF	C	unheated	12	6.15	6.87
B577	IFR	22.0	RIF	C	unheated	24	7.64	6.33

B577	IFR	22.0	RIF	C	unheated	30	7.75	
B577	IFR	22.0	RIF	C	unheated	49	8.27	6.6
B577	IFR	22.0	RIF	C	unheated	72	8.30	
B577	IFR	25.0	RIF	C	heated	0	1.66	6.81
B577	IFR	25.0	RIF	C	heated	2	1.60	
B577	IFR	25.0	RIF	C	heated	4	1.62	
B577	IFR	25.0	RIF	C	heated	6	1.80	
B577	IFR	25.0	RIF	C	heated	8	2.50	
B577	IFR	25.0	RIF	C	heated	10	3.49	
B577	IFR	25.0	RIF	C	heated	12	4.16	6.98
B577	IFR	25.0	RIF	C	heated	24	7.16	6.52
B577	IFR	25.0	RIF	C	heated	30	7.68	
B577	IFR	25.0	RIF	C	heated	49	8.03	6.65
B577	IFR	25.0	RIF	C	heated	72	8.59	

ANNEX B – Kinetic parameters estimated from viable counts measurements.

UH=unheated; HT=heated.

Strain	T (°C)	LAB	Treatment	Medium	replicate	μ_{max} (h ⁻¹)	lag (h)	h ₀	N_{max} (log CFU/mL)	se(μ_{max})	se(lag)	se(N_{max})	se(fit)	R ²
B577	12	NRC	UH	BHI	A	0.080	0.000	0.000	5.398	0.008		0.230	0.561	0.864
B577	25	NRC	UH	BHI	B	1.383	0.000	0.000	7.983	0.078		0.337	0.611	0.940
B577	30	NRC	UH	RIF	B	1.147	0.000	0.000	7.947	0.051		0.267	0.465	0.961
B577	30	NRC	UH	RIF	A	1.291	0.000	0.000	7.664	0.047		0.248	0.374	0.971
B577	22	NRC	UH	RIF	A	0.728	0.000	0.000	8.194	0.023		0.164	0.254	0.990
B577	22	IFR	UH	RIF	C	0.640	0.000	0.000	8.012	0.028		0.151	0.293	0.981
B577	22	IFR	UH	RIF	B	0.647	0.000	0.000	8.396	0.017		0.155	0.264	0.990
B577	18	NRC	UH	RIF	A	0.400	0.000	0.000	8.144	0.010		0.122	0.236	0.993
B577	22	IFR	HT	RIF	C	0.558	5.484	1.330	7.993	0.040	3.281	0.230	0.398	0.981

B577	15	IFR	HT	BHI	C	0.313	24.290	3.300	6.871	0.092	14.310	0.406	0.784	0.906
B577	18	NRC	UH	BHI	A	0.636	7.021	1.941	6.657	0.091	4.067	0.215	0.470	0.956
B577	18	IFR	HT	RIF	C	0.322	7.216	1.009	8.093	0.021	4.114	0.175	0.297	0.990
B577	18	IFR	HT	BHI	C	0.617	12.340	3.311	6.911	0.117	6.123	0.263	0.527	0.956
B577	15	NRC	UH	BHI	B	0.374	14.160	2.302	6.160	0.078	6.862	0.178	0.322	0.976
B577	18	IFR	HT	RIF	B	0.316	8.394	1.154	8.554	0.020	3.929	0.190	0.319	0.988
B577	18	IFR	HT	RIF	A	0.354	8.239	1.267	7.810	0.025	3.852	0.159	0.278	0.989
B577	12	IFR	HT	RIF	C	0.048	36.370	0.763	5.611	0.003	16.100	0.098	0.185	0.988
B577	25	IFR	HT	RIF	C	0.660	4.703	1.349	8.211	0.044	1.972	0.239	0.365	0.984
B577	15	NRC	UH	RIF	A	0.239	5.773	0.600	7.781	0.005	2.368	0.069	0.106	0.998
B577	22	NRC	UH	BHI	A	1.012	3.558	1.565	7.164	0.087	1.438	0.161	0.279	0.983
B577	25	NRC	UH	RIF	A	1.154	2.042	1.024	8.054	0.048	0.818	0.128	0.181	0.994
B577	15	IFR	HT	RIF	A	0.207	19.530	1.756	8.039	0.013	6.993	0.166	0.295	0.989
B577	22	NRC	UH	BHI	B	1.224	3.234	1.721	7.266	0.087	1.150	0.180	0.312	0.980
B577	25	IFR	HT	RIF	A	0.718	4.353	1.359	8.650	0.033	1.503	0.197	0.279	0.991

B577	22	IFR	UH	BHI	C	0.923	3.877	1.555	7.464	0.070	1.243	0.104	0.208	0.989
B577	30	NRC	UH	BHI	A	2.212	2.909	2.797	7.806	0.196	0.881	0.235	0.438	0.966
B577	22	IFR	HT	RIF	A	0.716	7.197	2.239	8.015	0.044	2.121	0.186	0.344	0.985
B577	22	IFR	HT	BHI	C	0.824	6.006	2.151	7.680	0.067	1.747	0.169	0.332	0.987
B577	12	NRC	UH	BHI	B	0.392	32.340	5.508	5.518	0.064	8.207	0.188	0.301	0.965
B577	22	IFR	HT	RIF	B	0.791	7.425	2.554	8.328	0.037	1.542	0.149	0.281	0.991
B577	15	NRC	UH	BHI	A	0.549	21.280	5.082	6.257	0.126	4.414	0.141	0.314	0.975
B577	15	IFR	HT	RIF	C	0.245	23.680	2.526	7.470	0.013	4.834	0.121	0.236	0.993
B577	12	NRC	UH	RIF	A	0.117	53.680	2.736	7.753	0.008	10.700	0.128	0.269	0.990
B577	25	IFR	HT	RIF	B	0.798	5.070	1.760	8.368	0.023	0.953	0.098	0.191	0.996
B577	25	NRC	UH	BHI	A	1.523	3.783	2.504	7.357	0.083	0.709	0.175	0.253	0.987
B577	12	IFR	HT	RIF	A	0.077	56.660	1.898	6.224	0.003	9.372	0.084	0.160	0.993
B577	15	IFR	HT	RIF	B	0.252	25.230	2.765	7.641	0.010	3.198	0.119	0.161	0.996
B577	25	IFR	HT	BHI	C	1.225	5.575	2.970	7.758	0.054	0.583	0.058	0.115	0.998

B577	12	IFR	HT	RIF	B	0.061	48.260	1.271		0.003	3.767		0.041	0.995
B577	22	IFR	UH	RIF	A	0.624	0.000	0.000	8.435	0.026		0.178	0.272	0.991
B577	12	IFR	HT	BHI	C	0.129	43.280	2.420	6.571	0.016	13.310	0.195	0.279	0.985
B594	22	IFR	UH	RIF	B	0.519	0.000	0.000	8.103	0.016		0.140	0.179	0.995
B594	15	IFR	HT	RIF	B	0.130	14.040	0.796	7.852	0.007	7.244	0.164	0.225	0.992
B594	15	IFR	HT	RIF	C	0.143	12.750	0.790	7.245	0.006	5.950	0.108	0.177	0.994
B594	18	IFR	HT	RIF	B	0.336	9.008	1.315	8.188	0.023	3.867	0.170	0.293	0.989
B594	18	IFR	HT	RIF	C	0.363	8.566	1.351	8.328	0.024	3.512	0.135	0.270	0.991
B594	22	IFR	HT	RIF	A	0.560	6.631	1.614	8.175	0.035	2.497	0.165	0.314	0.986
B594	22	IFR	UH	RIF	C	0.902	3.217	1.262	8.091	0.061	1.210	0.105	0.182	0.993
B594	22	IFR	HT	RIF	C	0.611	5.591	1.484	8.094	0.024	1.455	0.123	0.218	0.994
B594	18	IFR	HT	RIF	A	0.348	10.420	1.575	8.182	0.017	2.620	0.087	0.190	0.995
B594	12	IFR	HT	RIF	A	0.009	126.700	0.484	3.096	0.001	31.590	0.049	0.069	0.905
B594	22	IFR	HT	RIF	B	0.659	5.761	1.650	7.788	0.025	1.108	0.115	0.183	0.995
B594	15	IFR	HT	RIF	A	0.156	23.400	1.584	7.282	0.005	2.925	0.062	0.106	0.997

B596	15	NRC	UH	BHI	A	0.257	0.000	0.000	0.000	6.369	0.027		0.429	0.690	0.893
B596	22	IFR	UH	RIF	B	0.517	0.000	0.000	0.000	7.643	0.014		0.147	0.194	0.991
B596	22	IFR	UH	RIF	C	0.570	0.000	0.000	0.000	7.855	0.013		0.126	0.171	0.994
B596	22	IFR	UH	RIF	A	0.548	0.000	0.000	0.000	7.479	0.013		0.070	0.140	0.996
B596	25	NRC	UH	RIF	A	0.925	1.900	0.764	0.764	7.962	0.051	1.141	0.121	0.169	0.995
B596	25	NRC	UH	BHI	A	1.213	2.515	1.326	1.326	7.711	0.103	1.310	0.276	0.390	0.973
B596	12	NRC	UH	BHI	A	0.212	29.040	2.680	2.680	5.506	0.047	14.200	0.186	0.492	0.914
B596	22	NRC	UH	RIF	A	0.788	3.478	1.191	1.191	7.750	0.057	1.396	0.153	0.168	0.995
B596	30	NRC	UH	BHI	A	2.004	2.219	1.933	1.933	7.730	0.140	0.851	0.198	0.353	0.981
B596	12	NRC	UH	RIF	A	0.124	28.210	1.521	1.521	7.853	0.010	10.560	0.169	0.212	0.993
B596	15	NRC	UH	RIF	A	0.244	11.730	1.244	1.244	7.309	0.011	4.063	0.169	0.197	0.993
B596	18	IFR	HT	RIF	A	0.309	6.795	0.913	0.913	7.784	0.011	2.339	0.085	0.146	0.997
B596	30	NRC	UH	RIF	A	1.522	2.467	1.633	1.633	7.253	0.116	0.840	0.206	0.324	0.981
B596	18	NRC	UH	BHI	A	0.659	9.447	2.707	2.707	6.686	0.051	2.403	0.142	0.269	0.988

B596	18	IFR	HT	RIF	B	0.333	9.535	1.380	7.989	0.013	2.424	0.101	0.173	0.996
B596	22	NRC	UH	BHI	A	0.977	4.516	1.919	7.088	0.071	1.102	0.135	0.190	0.992
B596	18	IFR	HT	RIF	C	0.354	9.949	1.531	8.083	0.014	2.319	0.101	0.174	0.996
B596	22	IFR	HT	RIF	A	0.688	7.761	2.321	7.237	0.048	1.794	0.149	0.289	0.986
B596	18	NRC	UH	RIF	A	0.520	9.254	2.094	7.933	0.022	1.815	0.079	0.136	0.998
B596	12	IFR	HT	RIF	B	0.065	103.600	2.930		0.003	14.470		0.264	0.976
B596	22	IFR	HT	RIF	C	0.756	8.920	2.933	7.752	0.029	1.139	0.098	0.183	0.996
B596	15	IFR	HT	RIF	B	0.235	24.820	2.537	7.523	0.008	2.804	0.072	0.140	0.997
B596	22	IFR	HT	RIF	B	0.743	9.321	3.012	7.341	0.025	0.949	0.078	0.148	0.997
B596	15	IFR	HT	RIF	A	0.222	22.460	2.172	7.520	0.006	2.170	0.055	0.106	0.998
B596	15	IFR	HT	RIF	C	0.245	24.570	2.615	7.542	0.007	2.356	0.074	0.125	0.998
B596	12	IFR	HT	RIF	A	0.059	89.580	2.292	7.039	0.001	7.667	0.071	0.108	0.997
B596	12	IFR	HT	RIF	C	0.030	9.779	0.126	5.399	0.002	21.610	0.114	0.159	0.987
B626	25	NRC	UH	BHI	A	1.055	0.000	0.000	7.995	0.027		0.152	0.263	0.988
B626	25	NRC	UH	RIF	A	0.994	0.000	0.000	8.115	0.018		0.106	0.183	0.994

B626	15	NRC	UH	RIF	A	0.256	8.510	0.948	7.780	0.016	4.872	0.236	0.304	0.984
B626	22	NRC	UH	BHI	A	1.044	3.271	1.485	7.403	0.126	1.833	0.233	0.403	0.969
B626	12	NRC	UH	RIF	A	0.118	21.760	1.119	5.788	0.013	12.150	0.127	0.286	0.969
B626	12	NRC	UH	BHI	A	0.171	23.900	1.775	7.242	0.020	12.500	0.193	0.433	0.965
B626	25	NRC	UH	RIF	B	1.064	1.849	0.855	7.998	0.057	0.940	0.216	0.215	0.990
B626	30	NRC	UH	RIF	A	1.829	1.747	1.389	7.541	0.115	0.814	0.162	0.294	0.984
B626	22	NRC	UH	RIF	A	0.988	2.983	1.281	7.998	0.069	1.285	0.126	0.217	0.992
B626	22	NRC	UH	BHI	B	1.025	3.089	1.377	7.187	0.072	1.248	0.139	0.241	0.988
B626	18	NRC	UH	RIF	B	0.527	7.757	1.777	7.866	0.032	2.832	0.138	0.238	0.993
B626	30	NRC	UH	BHI	A	2.085	1.997	1.811	7.895	0.127	0.728	0.163	0.306	0.985
B626	15	NRC	UH	BHI	B	0.443	17.680	3.409	6.613	0.097	6.055	0.250	0.365	0.976
B626	25	NRC	UH	BHI	B	1.426	3.477	2.156	7.858	0.106	1.170	0.212	0.367	0.979
B626	18	NRC	UH	BHI	B	0.919	11.000	4.395	6.499	0.223	3.630	0.244	0.487	0.959
B626	22	NRC	UH	RIF	B	1.006	3.918	1.713	7.770	0.088	1.272	0.176	0.247	0.988

B626	18	NRC	UH	BHI	A	0.761	9.322	3.085	7.318	0.056	2.149	0.143	0.279	0.988
B626	12	NRC	UH	RIF	B	0.138	26.070	1.562	5.572	0.009	5.831	0.057	0.151	0.992
B626	30	NRC	UH	BHI	B	2.161	2.648	2.487	7.909	0.113	0.568	0.127	0.266	0.989
B626	30	NRC	UH	RIF	B	1.784	2.128	1.651	8.127	0.078	0.455	0.179	0.179	0.994
B626	15	NRC	UH	RIF	B	0.275	11.560	1.381	7.106	0.010	2.382	0.185	0.174	0.994
B626	12	NRC	UH	BHI	B	0.191	30.770	2.553	5.759	0.009	3.589	0.102	0.144	0.994
B626	18	NRC	UH	RIF	A	0.504	5.044	1.106	8.233	0.021	1.822	0.115	0.198	0.995
B626	15	NRC	UH	RIF	A	0.256	8.510	0.948	7.780	0.016	4.872	0.236	0.304	0.984
B626	15	NRC	UH	BHI	A	0.386	14.070	2.363	6.877	0.012	1.076	0.054	0.052	0.999
B635	15	NRC	UH	BHI	B	0.255	0.000	0.000		0.012			0.576	0.942
B635	18	NRC	UH	RIF	B	0.595	0.000	0.000	8.027	0.070		0.513	0.851	0.891
B635	12	NRC	UH	BHI	A	0.216	0.000	0.000	6.881	0.016		0.248	0.632	0.902
B635	22	NRC	UH	BHI	A	0.783	0.000	0.000	7.166	0.041		0.243	0.416	0.964
B635	15	NRC	UH	BHI	A	0.326	0.000	0.000	6.140	0.019		0.194	0.387	0.955
B635	12	NRC	UH	RIF	A	0.172	0.000	0.000	7.866	0.005		0.227	0.279	0.986

B635	18	NRC	UH	BHI	A	0.539	0.000	0.000	0.000	7.102	0.030		0.201	0.384	0.974
B635	30	NRC	UH	BHI	A	1.549	0.000	0.000	0.000	7.888	0.062		0.221	0.427	0.970
B635	30	NRC	UH	RIF	A	1.223	0.000	0.000	0.000	7.698	0.039		0.211	0.313	0.980
B635	12	NRC	UH	RIF	B	0.173	0.000	0.000	0.000	8.147	0.005		0.186	0.263	0.988
B635	15	NRC	UH	RIF	A	0.253	0.000	0.000	0.000	8.077	0.007		0.184	0.249	0.989
B635	22	NRC	UH	BHI	B	0.849	0.000	0.000	0.000	7.586	0.022		0.163	0.224	0.991
B635	22	NRC	UH	RIF	A	0.730	0.000	0.000	0.000	7.724	0.017		0.137	0.180	0.993
B635	25	NRC	UH	RIF	B	1.016	0.000	0.000	0.000	7.964	0.019		0.136	0.192	0.994
B635	30	NRC	UH	RIF	B	1.208	0.000	0.000	0.000	8.006	0.021		0.130	0.187	0.994
B635	22	NRC	UH	RIF	B	0.724	0.000	0.000	0.000	8.001	0.015		0.130	0.159	0.995
B635	25	NRC	UH	RIF	A	0.929	0.000	0.000	0.000	7.873	0.016		0.112	0.158	0.995
B635	25	NRC	UH	BHI	A	1.085	0.000	0.000	0.000	7.693	0.019		0.103	0.178	0.994
B635	18	NRC	UH	RIF	A	0.423	0.000	0.000	0.000	7.955	0.006		0.098	0.136	0.997
B635	18	NRC	UH	BHI	B	0.734	4.742	1.513	7.465	0.044	1.587		0.182	0.244	0.991

B635	30	NRC	UH	BHI	B	1.899	1.632	1.347	7.842	0.064	0.468	0.099	0.173	0.995
B635	25	NRC	UH	BHI	B	1.361	2.254	1.334	7.732	0.046	0.596	0.118	0.168	0.995
B635	12	NRC	UH	BHI	B	0.284	11.110	1.371	7.453	0.004	1.189	0.053	0.067	0.999

ANNEX C – Estimated specific growth rates by means of turbidity measurements.

*In bold, parameter taken as variable to assess cardinal values.

Strain	T (°C)	standard deviation (T)	pH	a_w	μ_{\max} (h ⁻¹)	n° points	R ²
B594	13.00	0.02	7.40	0.997	0.13	8	0.9746
B594	13.00	0.02	7.40	0.997	0.10	7	0.9728
B594	13.00	0.02	7.40	0.997	0.11	8	0.9648
B594	15.00	0.01	7.40	0.997	0.29	7	0.9945
B594	15.00	0.01	7.40	0.997	0.33	8	0.9933
B594	15.00	0.01	7.40	0.997	0.32	7	0.9973
B594	15.00	0.01	7.40	0.997	0.35	7	0.9982
B594	14.99	0.03	7.40	0.997	0.32	10	0.9857
B594	14.99	0.03	7.40	0.997	0.34	10	0.9670
B594	14.99	0.03	7.40	0.997	0.27	7	0.9890
B594	14.99	0.03	7.40	0.997	0.32	10	0.9703
B594	18.01	0.02	7.40	0.997	0.55	10	0.9935
B594	18.01	0.02	7.40	0.997	0.54	10	0.9912
B594	18.01	0.02	7.40	0.997	0.55	10	0.9978
B594	18.01	0.02	7.40	0.997	0.56	10	0.9928
B594	20.00	0.02	7.40	0.997	0.71	10	0.9937
B594	20.00	0.02	7.40	0.997	0.78	10	0.9840
B594	20.00	0.02	7.40	0.997	0.76	10	0.9831
B594	20.00	0.02	7.40	0.997	0.76	10	0.9969

B594	25.00	0.04	7.40	0.997	1.44	10	0.9904
B594	25.00	0.04	7.40	0.997	1.49	10	0.9898
B594	25.00	0.04	7.40	0.997	1.52	10	0.9934
B594	25.00	0.04	7.40	0.997	1.48	10	0.9891
B594	30.00	0.00	7.40	0.997	2.13	10	0.9961
B594	30.00	0.00	7.40	0.997	2.22	10	0.9963
B594	30.00	0.00	7.40	0.997	2.22	10	0.9879
B594	30.00	0.00	7.40	0.997	2.25	10	0.9834
B594	30.00	0.00	7.40	0.997	2.19	10	0.9940
B594	30.00	0.00	7.40	0.997	2.14	10	0.9964
B594	30.00	0.00	7.40	0.997	2.33	10	0.9888
B594	30.00	0.00	7.40	0.997	2.17	10	0.9897
B594	35.00	0.00	7.40	0.997	2.64	10	0.9824
B594	35.00	0.00	7.40	0.997	2.66	9	0.9900
B594	35.00	0.00	7.40	0.997	2.76	10	0.9873
B594	35.00	0.00	7.40	0.997	2.68	9	0.9912
B594	35.00	0.00	7.40	0.997	2.84	10	0.9892
B594	35.00	0.00	7.40	0.997	3.18	10	0.9901
B594	35.00	0.00	7.40	0.997	2.93	10	0.9916
B594	35.00	0.00	7.40	0.997	2.91	10	0.9906
B594	37.00	0.00	7.40	0.997	2.67	7	0.9865
B594	37.00	0.00	7.40	0.997	2.79	10	0.9911
B594	37.00	0.00	7.40	0.997	2.77	10	0.9929
B594	37.00	0.00	7.40	0.997	2.59	10	0.9922

B594	37.00	0.00	7.40	0.997	2.76	10	0.9955
B594	37.00	0.00	7.40	0.997	2.79	10	0.9950
B594	40.00	0.01	7.40	0.997	2.64	10	0.9873
B594	40.00	0.01	7.40	0.997	2.47	10	0.9937
B594	40.00	0.01	7.40	0.997	2.56	10	0.9959
B594	40.00	0.01	7.40	0.997	2.69	10	0.9879
B594	40.00	0.01	7.40	0.997	2.69	10	0.9940
B594	40.00	0.01	7.40	0.997	2.67	10	0.9953
B594	41.00	0.00	7.40	0.997	2.35	10	0.9943
B594	41.00	0.00	7.40	0.997	2.33	10	0.9976
B594	41.00	0.00	7.40	0.997	2.31	10	0.9957
B594	41.00	0.00	7.40	0.997	2.47	10	0.9969
B594	43.00	0.01	7.40	0.997	1.54	8	0.9968
B594	43.00	0.01	7.40	0.997	1.68	10	0.9922
B594	43.00	0.01	7.40	0.997	1.74	10	0.9957
B594	45.00	0.01	7.40	0.997	1.30	10	0.9912
B594	45.00	0.01	7.40	0.997	1.31	10	0.9930
B594	45.00	0.01	7.40	0.997	1.53	9	0.9894
B594	46.00	0.01	7.40	0.997	1.08	8	0.9941
B594	46.00	0.01	7.40	0.997	1.03	9	0.9836
B594	46.00	0.01	7.40	0.997	0.97	7	0.9822
B594	46.50	0.01	7.40	0.997	0.51	8	0.9881
B594	46.50	0.01	7.40	0.997	0.48	8	0.9853
B594	46.50	0.01	7.40	0.997	0.51	8	0.9803

B594	47.00	0.01	7.40	0.997	0.41	9	0.9794
B596	13.00	0.02	7.40	0.997	0.26	9	0.9872
B596	13.00	0.02	7.40	0.997	0.24	7	0.9823
B596	13.00	0.02	7.40	0.997	0.29	10	0.9569
B596	15.00	0.01	7.40	0.997	0.34	9	0.9757
B596	15.00	0.01	7.40	0.997	0.32	10	0.9738
B596	15.00	0.01	7.40	0.997	0.28	10	0.9645
B596	15.00	0.01	7.40	0.997	0.31	9	0.9646
B596	14.99	0.03	7.40	0.997	0.22	9	0.9874
B596	14.99	0.03	7.40	0.997	0.21	7	0.9766
B596	18.00	0.03	7.40	0.997	0.53	10	0.9947
B596	18.00	0.03	7.40	0.997	0.50	8	0.9936
B596	18.00	0.03	7.40	0.997	0.63	10	0.9939
B596	18.00	0.03	7.40	0.997	0.53	10	0.9865
B596	18.00	0.03	7.40	0.997	0.60	10	0.9906
B596	18.00	0.03	7.40	0.997	0.53	10	0.9925
B596	18.00	0.03	7.40	0.997	0.55	10	0.9956
B596	18.00	0.03	7.40	0.997	0.55	10	0.9965
B596	18.00	0.03	7.40	0.997	0.56	10	0.9916
B596	20.00	0.00	7.40	0.997	0.91	10	0.9870
B596	20.00	0.00	7.40	0.997	0.89	10	0.9870
B596	20.00	0.00	7.40	0.997	0.80	10	0.9913
B596	20.00	0.00	7.40	0.997	0.87	10	0.9982
B596	20.00	0.00	7.40	0.997	0.87	10	0.9989

B596	20.00	0.00	7.40	0.997	0.88	10	0.9909
B596	20.00	0.00	7.40	0.997	0.88	10	0.9944
B596	20.00	0.00	7.40	0.997	0.89	10	0.9924
B596	20.00	0.00	7.40	0.997	0.97	10	0.9873
B596	25.00	0.04	7.40	0.997	1.33	10	0.9852
B596	25.00	0.04	7.40	0.997	1.26	8	0.9957
B596	25.00	0.06	7.40	0.997	1.42	10	0.9870
B596	25.00	0.06	7.40	0.997	1.46	10	0.9937
B596	25.00	0.06	7.40	0.997	1.47	10	0.9924
B596	25.00	0.06	7.40	0.997	1.49	10	0.9984
B596	25.00	0.06	7.40	0.997	1.40	10	0.9927
B596	25.00	0.06	7.40	0.997	1.51	10	0.9953
B596	25.00	0.06	7.40	0.997	1.57	10	0.9938
B596	25.00	0.06	7.40	0.997	1.57	10	0.9944
B596	25.00	0.06	7.40	0.997	1.56	10	0.9933
B596	25.00	0.06	7.40	0.997	1.72	10	0.9931
B596	30.00	0.00	7.40	0.997	2.37	10	0.9865
B596	30.00	0.00	7.40	0.997	2.61	9	0.9926
B596	30.00	0.00	7.40	0.997	2.48	9	0.9938
B596	30.00	0.00	7.40	0.997	2.14	8	0.9805
B596	30.00	0.00	7.40	0.997	1.86	8	0.9902
B596	30.00	0.00	7.40	0.997	1.89	10	0.9956
B596	30.00	0.00	7.40	0.997	1.90	10	0.9860
B596	30.00	0.00	7.40	0.997	1.90	10	0.9968

B596	30.00	0.00	7.40	0.997	1.93	10	0.9892
B596	35.00	x	7.40	0.997	3.02	10	0.9957
B596	35.00	x	7.40	0.997	3.06	10	0.9978
B596	35.00	x	7.40	0.997	3.05	10	0.9936
B596	35.00	x	7.40	0.997	2.84	8	0.9991
B596	35.00	x	7.40	0.997	3.00	9	0.9966
B596	40.00	0.02	7.40	0.997	3.49	10	0.9827
B596	40.00	0.02	7.40	0.997	3.76	8	0.9822
B596	40.00	0.02	7.40	0.997	3.56	10	0.9802
B596	40.00	0.02	7.40	0.997	4.14	10	0.9914
B596	40.00	0.02	7.40	0.997	3.82	10	0.9920
B596	40.00	0.02	7.40	0.997	3.47	10	0.9970
B596	40.00	0.02	7.40	0.997	3.85	10	0.9871
B596	40.00	0.02	7.40	0.997	3.80	10	0.9868
B596	40.00	0.02	7.40	0.997	3.94	10	0.9925
B596	40.00	0.01	7.40	0.997	4.15	7	0.9995
B596	40.00	0.01	7.40	0.997	4.21	9	0.9898
B596	41.00	0.00	7.40	0.997	3.50	8	0.9918
B596	41.00	0.00	7.40	0.997	4.24	8	0.9920
B596	41.00	0.00	7.40	0.997	4.38	8	0.9817
B596	43.00	0.05	7.40	0.997	3.96	9	0.9815
B596	43.00	0.05	7.40	0.997	3.57	10	0.9829
B596	43.00	0.05	7.40	0.997	3.69	10	0.9770
B596	45.00	0.01	7.40	0.997	2.82	10	0.9802

B596	45.00	0.01	7.40	0.997	2.49	8	0.9852
B596	45.00	0.01	7.40	0.997	2.53	8	0.9954
B596	45.00	0.01	7.40	0.997	3.10	10	0.9847
B596	46.00	0.01	7.40	0.997	2.40	10	0.9886
B596	46.00	0.01	7.40	0.997	2.36	10	0.9931
B596	46.00	0.01	7.40	0.997	2.26	10	0.9969
B596	46.00	0.01	7.40	0.997	2.45	10	0.9937
B596	47.00	0.01	7.40	0.997	1.60	10	0.9806
B596	47.00	0.01	7.40	0.997	1.60	8	0.9893
B596	47.00	0.01	7.40	0.997	1.63	10	0.9980
B596	47.50	0.01	7.40	0.997	1.08	8	0.9886
B596	47.50	0.01	7.40	0.997	1.11	8	0.9854
B596	47.50	0.01	7.40	0.997	1.51	8	0.9894
B596	47.50	0.01	7.40	0.997	1.23	9	0.9884
B596	47.50	0.01	7.40	0.997	1.32	9	0.9908
B596	47.50	0.01	7.40	0.997	1.40	8	0.9883
B596	47.50	0.01	7.40	0.997	1.43	8	0.9936
B626	15.00	0.01	7.40	0.997	0.27	9	0.9828
B626	15.00	0.01	7.40	0.997	0.29	10	0.9860
B626	15.00	0.01	7.40	0.997	0.32	10	0.9840
B626	15.00	0.01	7.40	0.997	0.31	10	0.9775
B626	15.00	0.01	7.40	0.997	0.35	10	0.9840
B626	14.99	0.03	7.40	0.997	0.30	10	0.9867
B626	14.99	0.03	7.40	0.997	0.30	8	0.9834

B626	18.01	0.02	7.40	0.997	0.55	10	0.9899
B626	18.01	0.02	7.40	0.997	0.56	10	0.9849
B626	18.01	0.02	7.40	0.997	0.55	10	0.9918
B626	20.00	0.02	7.40	0.997	0.86	10	0.9935
B626	20.00	0.02	7.40	0.997	0.83	10	0.9917
B626	20.00	0.02	7.40	0.997	0.80	10	0.9970
B626	20.00	0.01	7.40	0.997	0.87	10	0.9943
B626	20.00	0.01	7.40	0.997	0.85	10	0.9981
B626	20.00	0.01	7.40	0.997	0.87	10	0.9923
B626	25.00	0.04	7.40	0.997	1.41	10	0.9966
B626	25.00	0.04	7.40	0.997	1.40	10	0.9946
B626	25.00	0.04	7.40	0.997	1.46	10	0.9934
B626	30.00	0.00	7.40	0.997	2.07	10	0.9962
B626	30.00	0.00	7.40	0.997	1.91	10	0.9899
B626	30.00	0.00	7.40	0.997	1.92	10	0.9904
B626	30.00	0.00	7.40	0.997	1.84	10	0.9815
B626	30.00	0.00	7.40	0.997	1.87	10	0.9963
B626	30.00	0.00	7.40	0.997	1.82	10	0.9930
B626	35.00	0.00	7.40	0.997	2.71	10	0.9860
B626	35.00	x	7.40	0.997	2.88	10	0.9986
B626	35.00	x	7.40	0.997	2.90	10	0.9979
B626	35.00	x	7.40	0.997	2.91	8	0.9977
B626	35.00	x	7.40	0.997	2.78	10	0.9968
B626	35.00	x	7.40	0.997	2.75	10	0.9986

B626	37.00	0.00	7.40	0.997	3.12	10	0.9959
B626	40.00	0.01	7.40	0.997	3.37	10	0.9935
B626	40.00	0.01	7.40	0.997	3.26	10	0.9922
B626	40.00	0.01	7.40	0.997	3.58	10	0.9966
B626	40.00	0.01	7.40	0.997	3.77	10	0.9870
B626	40.00	0.01	7.40	0.997	3.65	10	0.9985
B626	41.00	0.00	7.40	0.997	3.43	10	0.9918
B626	41.00	0.00	7.40	0.997	3.47	10	0.9945
B626	41.00	0.00	7.40	0.997	3.38	10	0.9955
B626	43.00	0.01	7.40	0.997	3.51	10	0.9984
B626	43.00	0.01	7.40	0.997	3.45	10	0.9976
B626	43.00	0.01	7.40	0.997	3.55	10	0.9904
B626	45.00	0.01	7.40	0.997	2.80	10	0.9976
B626	45.00	0.01	7.40	0.997	2.82	10	0.9982
B626	45.00	0.01	7.40	0.997	2.82	10	0.9982
B626	46.00	0.01	7.40	0.997	2.42	10	0.9910
B626	46.00	0.01	7.40	0.997	2.40	10	0.9912
B626	46.00	0.01	7.40	0.997	2.40	10	0.9948
B626	47.00	0.01	7.40	0.997	1.86	10	0.9909
B626	47.00	0.01	7.40	0.997	1.92	10	0.9954
B626	47.00	0.01	7.40	0.997	1.80	10	0.9972
B626	47.50	0.01	7.40	0.997	1.48	9	0.9851
B626	47.50	0.01	7.40	0.997	1.18	8	0.9954
B626	47.50	0.01	7.40	0.997	1.70	7	0.9825

B626	47.50	0.01	7.40	0.997	0.99	9	0.9936
B626	47.50	0.01	7.40	0.997	1.18	9	0.9800
B626	47.50	0.01	7.40	0.997	1.53	10	0.9819
B594	37.00	0.00	7.40	0.955	0.15	7	0.9627
B594	37.00	0.00	7.40	0.959	0.08	3	0.9998
B594	37.00	0.00	7.40	0.959	0.18	3	0.9788
B594	37.00	0.00	7.40	0.959	0.17	4	0.9674
B594	37.00	0.00	7.40	0.971	1.64	4	0.9990
B594	37.00	0.00	7.40	0.971	1.79	5	0.9984
B594	37.00	0.00	7.40	0.971	1.38	4	0.9915
B594	37.00	0.00	7.40	0.980	2.04	5	0.9967
B594	37.00	0.00	7.40	0.980	1.88	5	0.9968
B594	37.00	0.00	7.40	0.980	2.14	5	0.9905
B594	37.00	0.00	7.40	0.990	2.74	5	0.9995
B594	37.00	0.00	7.40	0.990	2.49	5	0.9960
B594	37.00	0.00	7.40	0.990	2.38	5	0.9911
B594	37.00	0.00	7.40	0.997	2.19	5	0.9995
B594	37.00	0.00	7.40	0.997	2.44	5	0.9974
B594	37.00	0.00	7.40	0.997	2.33	5	0.9867
B594	37.00	0.00	7.40	0.959	0.30	5	0.9588
B594	37.00	0.00	7.40	0.970	1.40	5	0.9862
B594	37.00	0.00	7.40	0.971	1.35	5	0.9853
B594	37.00	0.00	7.40	0.971	1.28	4	0.9743
B594	37.00	0.00	7.40	0.971	1.68	5	0.9721

B594	37.00	0.00	7.40	0.971	1.55	4	0.9632
B594	37.00	0.00	7.40	0.971	1.57	5	0.9595
B594	37.00	0.00	7.40	0.959	0.10	4	0.9551
B594	37.00	0.00	7.40	0.959	0.07	4	0.9507
B596	37.00	0.00	7.40	0.948	0.45	4	0.9583
B596	37.00	0.00	7.40	0.955	0.51	7	0.9590
B596	37.00	0.00	7.40	0.959	0.97	5	0.9585
B596	37.00	0.00	7.40	0.959	0.88	5	0.9560
B596	37.00	0.00	7.40	0.959	1.03	5	0.9553
B596	37.00	0.00	7.40	0.971	1.70	5	0.9898
B596	37.00	0.00	7.40	0.971	1.56	5	0.9873
B596	37.00	0.00	7.40	0.971	1.51	5	0.9575
B596	37.00	0.00	7.40	0.980	2.45	5	0.9933
B596	37.00	0.00	7.40	0.980	2.55	5	0.9926
B596	37.00	0.00	7.40	0.980	2.70	5	0.9913
B596	37.00	0.00	7.40	0.990	2.75	5	0.9994
B596	37.00	0.00	7.40	0.990	2.92	5	0.9852
B596	37.00	0.00	7.40	0.990	2.84	5	0.9808
B596	37.00	0.00	7.40	0.997	2.77	5	0.9983
B596	37.00	0.00	7.40	0.997	2.44	4	0.9972
B596	37.00	0.00	7.40	0.997	2.30	4	0.9939
B596	37.00	0.00	7.40	0.997	2.26	4	0.9863
B596	37.00	0.00	7.40	0.980	2.73	5	0.9844
B596	37.00	0.00	7.40	0.980	2.09	5	0.9837

B596	37.00	0.00	7.40	0.997	2.14	5	0.9831
B596	37.00	0.00	7.40	0.997	2.50	5	0.9792
B596	37.00	0.00	7.40	0.980	2.17	5	0.9756
B596	37.00	0.00	7.40	0.980	2.73	5	0.9662
B596	37.00	0.00	7.40	0.997	2.17	5	0.9630
B596	37.00	0.00	7.40	0.971	1.34	5	0.9570
B596	37.00	0.00	7.40	0.959	0.76	4	0.9517
B626	37.00	0.00	7.40	0.948	0.33	4	0.9962
B626	37.00	0.00	7.40	0.955	0.76	8	0.9649
B626	37.00	0.00	7.40	0.959	1.04	5	0.9967
B626	37.00	0.00	7.40	0.959	1.19	4	0.9934
B626	37.00	0.00	7.40	0.959	0.88	5	0.9931
B626	37.00	0.00	7.40	0.971	1.57	5	0.9948
B626	37.00	0.00	7.40	0.971	1.90	5	0.9931
B626	37.00	0.00	7.40	0.971	1.39	5	0.9871
B626	37.00	0.00	7.40	0.980	2.94	5	0.9861
B626	37.00	0.00	7.40	0.980	2.76	5	0.9809
B626	37.00	0.00	7.40	0.990	3.46	5	0.9760
B626	37.00	0.00	7.40	0.990	3.32	5	0.9586
B626	37.00	0.00	7.40	0.997	2.61	5	0.9902
B626	37.00	0.00	7.40	0.997	2.75	5	0.9876
B626	37.00	0.00	7.40	0.997	2.50	5	0.9824
B626	37.00	0.00	7.40	0.971	1.70	5	0.9834
B626	37.00	0.00	7.40	0.959	0.78	4	0.9920

B626	37.00	0.00	7.40	0.971	1.57	5	0.9865
B626	37.00	0.00	7.40	0.980	2.89	5	0.9807
B626	37.00	0.00	7.40	0.971	1.40	5	0.9798
B626	37.00	0.00	7.40	0.997	2.79	5	0.9780
B626	37.00	0.00	7.40	0.997	2.54	5	0.9754
B626	37.00	0.00	7.40	0.959	0.96	5	0.9738
B626	37.00	0.00	7.40	0.971	2.08	5	0.9704
B626	37.00	0.00	7.40	0.971	2.05	4	0.9662
B626	37.00	0.00	7.40	0.959	1.03	5	0.9624
B626	37.00	0.00	7.40	0.959	0.83	5	0.9615
B626	37.00	0.00	7.40	0.971	1.74	5	0.9545
B626	37.00	0.00	7.40	0.971	1.41	5	0.9536
B594	37.00	0.00	4.60	0.997	0.04	5	0.9956
B594	37.00	0.00	4.60	0.997	0.07	6	0.9867
B594	37.00	0.00	4.70	0.997	0.05	5	0.9822
B594	37.00	0.00	4.80	0.997	0.07	5	0.9926
B594	37.00	0.00	4.96	0.997	0.15	5	0.9920
B594	37.00	0.00	5.00	0.997	0.44	10	0.9686
B594	37.00	0.00	5.00	0.997	0.56	6	0.9652
B594	37.00	0.00	5.27	0.997	0.65	5	0.9990
B594	37.00	0.00	5.27	0.997	0.50	5	0.9693
B594	37.00	0.00	5.27	0.997	0.48	5	0.9620
B594	37.00	0.00	5.51	0.997	1.85	5	0.9940
B594	37.00	0.00	5.51	0.997	1.71	5	0.9910

B594	37.00	0.00	5.51	0.997	1.78	5	0.9850
B594	37.00	0.00	6.15	0.997	2.03	5	0.9980
B594	37.00	0.00	6.15	0.997	2.20	5	0.9940
B594	37.00	0.00	6.15	0.997	2.03	5	0.9920
B594	37.00	0.00	6.61	0.997	2.14	5	0.9940
B594	37.00	0.00	6.61	0.997	2.54	5	0.9730
B594	37.00	0.00	6.61	0.997	2.57	5	0.9690
B594	37.00	0.00	7.02	0.997	2.22	5	0.9940
B594	37.00	0.00	7.02	0.997	2.39	5	0.9880
B594	37.00	0.00	7.02	0.997	2.48	5	0.9640
B594	37.00	0.00	7.85	0.997	2.87	5	0.9890
B594	37.00	0.00	7.85	0.997	2.40	5	0.9880
B594	37.00	0.00	7.85	0.997	2.73	5	0.9540
B594	37.00	0.00	8.42	0.997	2.51	5	0.9930
B594	37.00	0.00	8.42	0.997	2.37	5	0.9770
B594	37.00	0.00	8.42	0.997	2.59	5	0.9730
B594	37.00	0.00	8.92	0.997	0.43	5	0.9970
B594	37.00	0.00	8.92	0.997	0.44	5	0.9920
B594	37.00	0.00	8.92	0.997	0.46	5	0.9850
B594	37.00	0.00	9.22	0.997	0.49	5	0.9965
B594	37.00	0.00	9.22	0.997	0.65	5	0.9850
B594	37.00	0.00	9.22	0.997	0.61	5	0.9690
B596	37.00	0.00	4.60	0.997	0.08	5	0.9824
B596	37.00	0.00	4.70	0.997	0.03	5	0.9655

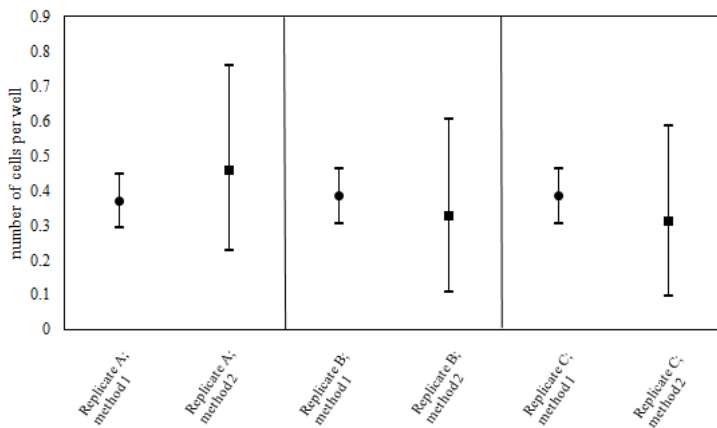
B596	37.00	0.00	4.80	0.997	0.04	6	0.9945
B596	37.00	0.00	4.89	0.997	0.22	8	0.9831
B596	37.00	0.00	4.96	0.997	0.21	5	0.9846
B596	37.00	0.00	4.96	0.997	0.19	5	0.9723
B596	37.00	0.00	5.00	0.997	0.55	7	0.9940
B596	37.00	0.00	5.00	0.997	0.79	8	0.9891
B596	37.00	0.00	5.27	0.997	0.50	5	0.9693
B596	37.00	0.00	5.51	0.997	1.15	5	0.9972
B596	37.00	0.00	5.51	0.997	1.70	5	0.9949
B596	37.00	0.00	6.15	0.997	1.73	5	0.9810
B596	37.00	0.00	6.15	0.997	1.54	4	0.9872
B596	37.00	0.00	7.02	0.997	2.33	5	0.9997
B596	37.00	0.00	7.85	0.997	2.36	5	0.9910
B596	37.00	0.00	7.85	0.997	2.60	5	0.9736
B596	37.00	0.00	8.42	0.997	2.91	5	0.9973
B596	37.00	0.00	8.42	0.997	2.28	5	0.9954
B596	37.00	0.00	8.92	0.997	0.35	5	0.9644
B596	37.00	0.00	8.92	0.997	0.38	5	0.9612
B596	37.00	0.00	9.22	0.997	0.49	5	0.9965
B596	37.00	0.00	9.22	0.997	0.45	5	0.9594
B626	37.00	0.00	4.60	0.997	0.07	7	0.9819
B626	37.00	0.00	4.70	0.997	0.08	7	0.9775
B626	37.00	0.00	4.80	0.997	0.06	5	0.9812
B626	37.00	0.00	4.89	0.997	0.08	5	0.9698

B626	37.00	0.00	4.89	0.997	0.24	6	0.9499
B626	37.00	0.00	4.96	0.997	0.11	5	0.9920
B626	37.00	0.00	4.96	0.997	0.15	5	0.9900
B626	37.00	0.00	4.96	0.997	0.27	5	0.9635
B626	37.00	0.00	5.00	0.997	0.78	6	0.9963
B626	37.00	0.00	5.00	0.997	0.54	5	0.9797
B626	37.00	0.00	5.27	0.997	0.49	5	0.9940
B626	37.00	0.00	5.27	0.997	0.55	5	0.9880
B626	37.00	0.00	5.27	0.997	0.40	5	0.9660
B626	37.00	0.00	5.51	0.997	2.04	5	0.9980
B626	37.00	0.00	5.51	0.997	2.15	5	0.9870
B626	37.00	0.00	6.15	0.997	2.04	5	0.9940
B626	37.00	0.00	6.15	0.997	2.19	5	0.9770
B626	37.00	0.00	6.15	0.997	2.37	5	0.9580
B626	37.00	0.00	6.61	0.997	2.13	5	0.9960
B626	37.00	0.00	6.61	0.997	2.72	5	0.9900
B626	37.00	0.00	6.61	0.997	2.64	5	0.9700
B626	37.00	0.00	7.02	0.997	2.80	5	0.9980
B626	37.00	0.00	7.02	0.997	2.79	5	0.9940
B626	37.00	0.00	7.02	0.997	2.42	5	0.9910
B626	37.00	0.00	7.85	0.997	2.72	5	0.9970
B626	37.00	0.00	7.85	0.997	2.95	5	0.9780
B626	37.00	0.00	7.85	0.997	2.71	5	0.9580
B626	37.00	0.00	8.42	0.997	2.55	5	0.9880

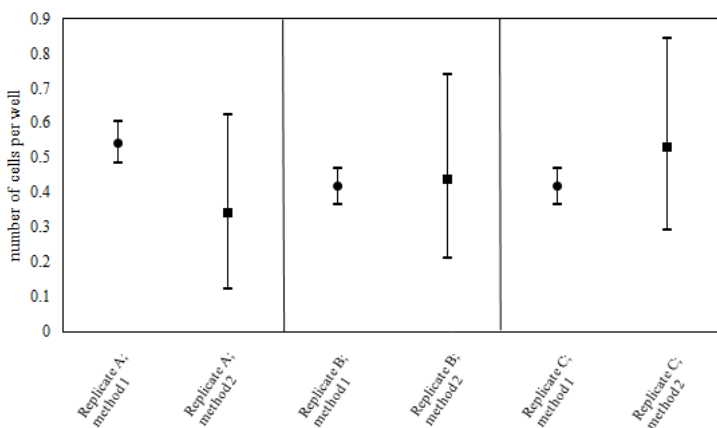
B626	37.00	0.00	8.42	0.997	2.67	5	0.9830
B626	37.00	0.00	8.42	0.997	2.94	5	0.9790
B626	37.00	0.00	8.92	0.997	0.38	5	0.9770
B626	37.00	0.00	8.92	0.997	0.34	5	0.9700
B626	37.00	0.00	8.92	0.997	0.39	5	0.9690
B626	37.00	0.00	9.22	0.997	0.46	5	0.9950
B626	37.00	0.00	9.22	0.997	0.44	5	0.9870
B626	37.00	0.00	9.22	0.997	0.53	5	0.9780
B626	37.00	0.00	8.92	0.997	0.32	5	0.9560
B626	37.00	0.00	9.22	0.997	0.55	5	0.9750
B626	37.00	0.00	9.22	0.997	0.50	5	0.9730
B626	37.00	0.00	9.22	0.997	0.47	5	0.9640
B626	37.00	0.00	4.96	0.997	0.15	5	0.9550

ANNEX D – Plots comparing average number of cells per well for heated and unheated cells, according to method 1 and method 2 for all tested temperatures.

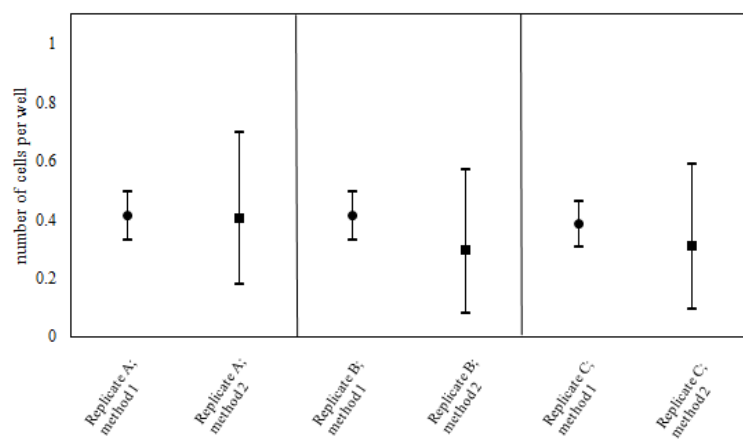
15 °C HEATED



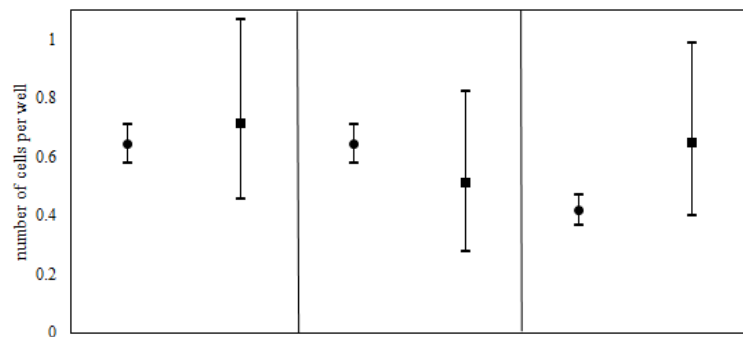
15 °C UNHEATED



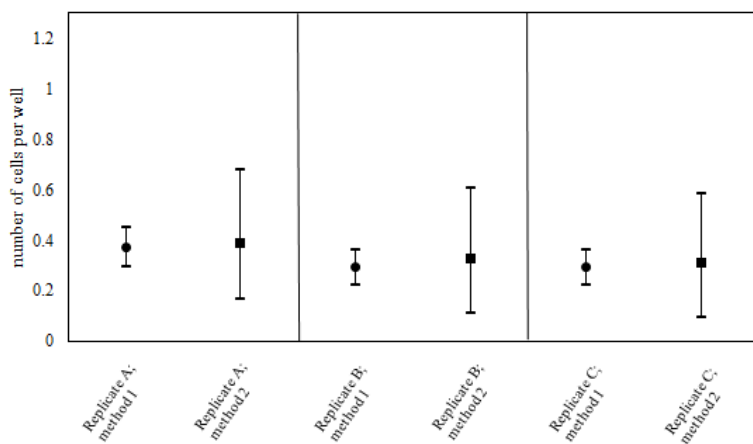
22 °C HEATED



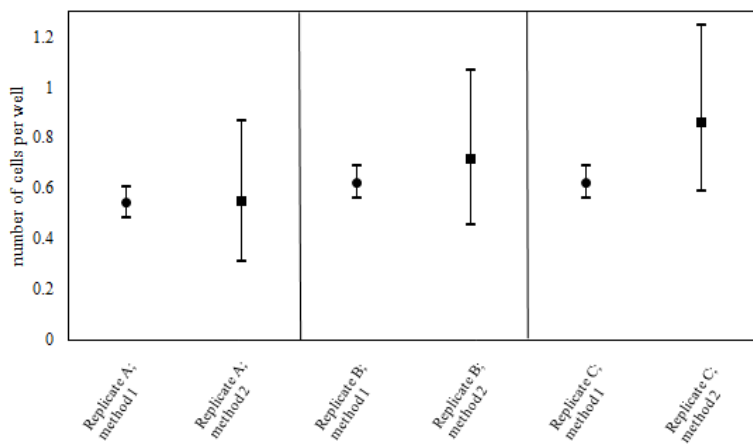
22 °C UNHEATED



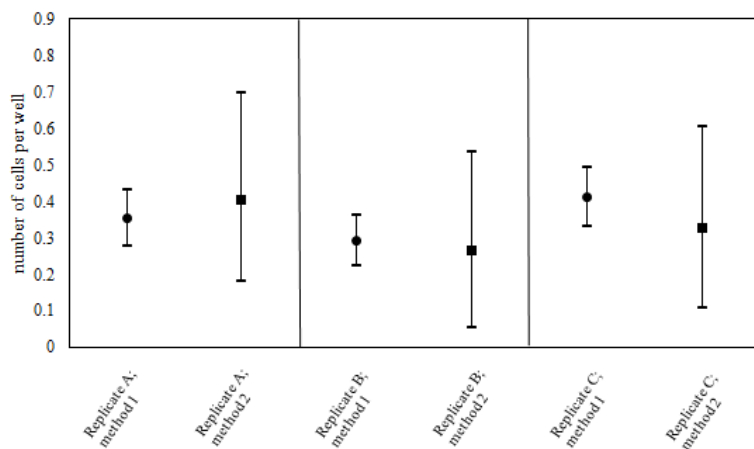
25 °C HEATED



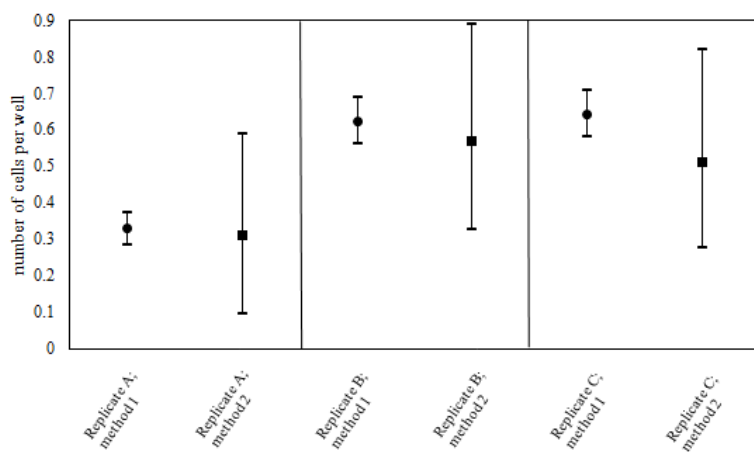
25 °C UNHEATED



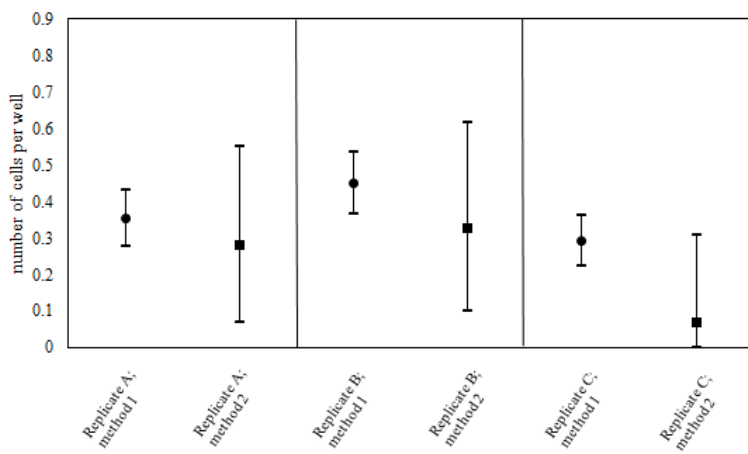
40 °C HEATED



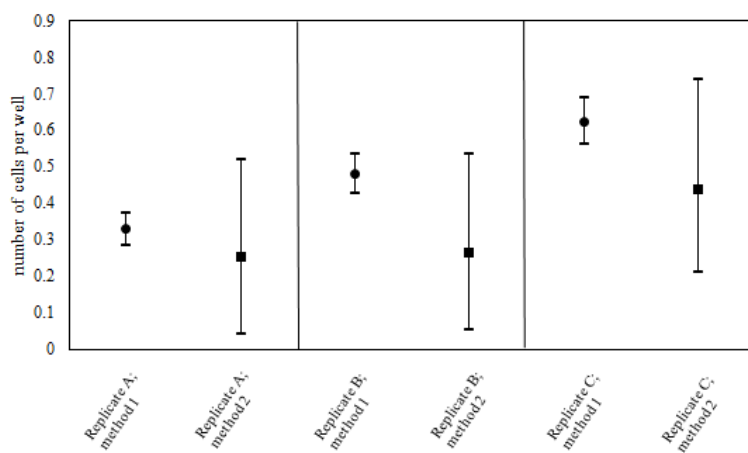
40 °C UNHEATED



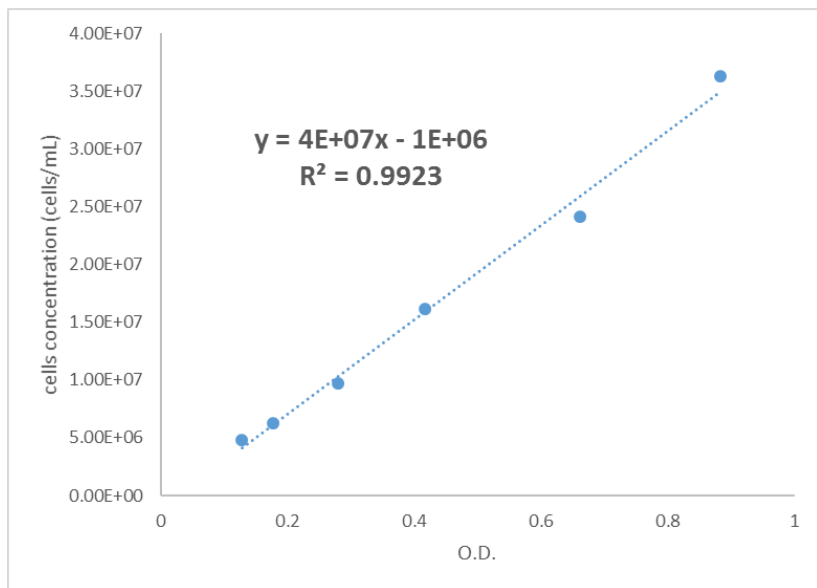
47 °C HEATED



47 °C UNHEATED



ANNEX E – Calibration curve for B577 (F4810/72) strain.



ANNEX F – Paper published at Frontiers for Microbiology in 2017 as part of this thesis.



From Culture-Medium-Based Models to Applications to Food: Predicting the Growth of *B. cereus* in Reconstituted Infant Formulae

Nathália Buss de Silva^{1,2}, József Baranyi³, Bruno A. M. Carcioff¹ and Marlon Elouze^{2*}

¹ Department of Chemical and Food Engineering, Federal University of Santa Catarina, Florianópolis, Brazil; ² Nestlé Research Center, Lausanne, Switzerland; ³ Institute of Nutrition, University of Debrecen, Debrecen, Hungary

OPEN ACCESS

Edited by:

Jean-Christophe Augustin,
Ecole Nationale Supérieure d'Alimentation,
France

Reviewed by:

Olivier Couvert,
Laboratoire Universitaire de
Biodiversité Ecologie Microbiens
(LEEM), France
Mette Gauguier,
Parsons College, American Farm
School, Greece

*Correspondence:

Marlon Elouze
marlon.elouze@rdc.nestle.com

Specialty section:

This article was submitted to
Food Microbiology,
a section of the journal
Frontiers in Microbiology

Received: 03 May 2017

Accepted: 05 September 2017

Published: 27 September 2017

Citation:
Buss de Silva N, Baranyi J,
Carcioff BAM and Elouze M (2017)
From Culture-Medium-Based Models
to Applications to Food: Predicting the
Growth of *B. cereus* in Reconstituted
Infant Formulae.
Front. Microbiol. 8:1799.
doi: 10.3389/fmicb.2017.01799

Predictive models of the growth of foodborne organisms are commonly based on data generated in laboratory medium. It is a crucial question how to apply the predictions to realistic food scenarios. A simple approach is to assume that the bias factor, i.e., the ratio between the maximum specific growth rate in culture medium and the food in question is constant in the region of interest of the studied environmental variables. In this study, we investigate the validity of this assumption using two well-known link functions, the square-root and the natural logarithm, both having advantageous properties when modeling the variation of the maximum specific growth rate with temperature. The main difference between the two approaches appears in terms of the respective residuals as the temperature decreases to its minimum. The model organism was *Bacillus cereus*. Three strains (B594, B596, and F4810/72) were grown in Reconstituted Infant Formulae, while one of them (F4810/72) was grown also in culture medium to calculate the bias factor. Their growth parameters were estimated using viable count measurements at temperatures ranging from 12 to 25°C. We utilized the fact that, if the bias factor is independent of the temperature, then the minimum growth temperature parameter of the square-root model of Ratkowsky et al. (1962) is the same for culture medium and food. We concluded, supported also by mathematical analysis, that the Ratkowsky model works well but its rearrangement for the natural logarithm of the specific growth rate is more appropriate for practical regression. On the other hand, when analyzing mixed culture data, available in the ComBase database, we observed a trend different from the one generated by pure cultures. This suggests that the identity of the strains dominating the growth of mixed cultures depends on the temperature. Such analysis can increase the accuracy of predictive models, based on culture medium, to food scenarios, bringing significant saving for the food industry.

Keywords: *Bacillus cereus*, predictive microbiology, bias factor, reconstituted infant formulae, Ratkowsky model

INTRODUCTION

Bacillus cereus is a Gram positive, spore-forming, facultative anaerobic, rod-shaped pathogen (Kotiranta et al., 2000). *Bacillus cereus* strains are ubiquitous in the environment and can be isolated from soil, water and vegetables (Althayer and Sutherland, 2006; El-Arabi and Griffiths, 2013). They are commonly found in raw materials and processed foods, such as rice, milk and dairy products,

meat and meat products, pasteurized liquid egg, ready-to-eat vegetables, and spices (Ceuppens et al., 2011). *Bacillus cereus* can be responsible for food poisoning illnesses in two ways: by heat labile, diarrhea-causing enterotoxins produced in the small intestine, and by heat stable cereulide toxin produced in the food before ingestion (Ceuppens et al., 2011), causing emetic syndromes. Emetic strains are, therefore, a concern to the food industry since it is not possible to eliminate the cereulide once performed in the food. Growth and toxin production must be strictly controlled, especially in food targeted to sensitive populations.

Bacillus cereus can endure ultrahigh-temperature (UHT) pasteurization, resist spray drying and survive in final products (McCauley et al., 2014). Moreover, according to a review published by the European Food Safety Agency (EFSA, 2005), *B. cereus* strains are highly variable in terms of their tolerance to high temperatures and their ability to grow. This is mainly dependent on their phylogenetic group (Carlin et al., 2013). Mathematical modeling can be a valuable tool to assess and quantify this variability. It is widely accepted that temperature is the most important external environmental factor affecting microbial response. Among the available predictive models, the model of Ratkowsky et al. (1982) is commonly used to predict the maximum specific growth rate in the suboptimal region of temperature.

However, developing and validating a new model to predict microbial behavior during the manufacturing or the shelf life of a food commodity require extensive experimental work. It is a good practice to use readily available published data and models in the literature or in user-friendly predictive microbiology tools. For example, ComBase (<https://www.combase.cc>) provides culture-medium-based predictive models for a large collection of micro-organisms including *B. cereus*. To establish a "correction factor" that could be used to predict the behavior of the organism in food from culture-medium based models would be valuable for the food industry. To quantify the similarity between prediction and observation, the accuracy and bias factors, A_f and B_f , respectively, of ILOM (1996) is commonly used for practical applications. The indicators $\ln(A_f)$ and $\ln(B_f)$ are certain average differences between the natural logarithm of the predicted and observed $\ln(\mu)$ values of the organism in the studied range of environmental conditions, where μ denotes the maximum specific growth rate under a given condition. In the case of A_f , the difference is meant as an absolute value, while in the case of B_f it is meant with its sign. Consequently, a bias factor $B_f = 1$ means that, in a studied region, on average, the model predictions are neither over-estimating nor under-estimating the growth rate compared to the observations. However, this could happen in such a way, too, that the predictions are underestimations in one part of the region while they are overestimations in the other part. It would be desirable that, for a given food matrix, the bias factor is independent of the environmental conditions, primarily of the temperature, at least in the normal physiological growth region of the organism. In this case, culture-medium-based predictions, available from public software tools such as ComBase, could be readily applied to the food in question. Since culture medium broths provide optimal substrate

for the organism, the bias factor $B_{f(opt)/H_{min}}$ should normally be < 1 .

The main objectives of this paper are (i) to provide a numerical analysis for the connection between bias and the two most frequently used transformations of the maximum specific growth rate parameter, the square-root and the logarithm functions, and (ii) to test whether the bias factor for *B. cereus* in reconstituted Infant Formulae (RIF) can be considered constant, at least in a sub-optimal region of the temperature.

MATERIALS AND METHODS

Samples Preparation

In laminar flow cabinet, infant formulae milk powder was weighted into sterile bottles, warm ($\sim 50^\circ\text{C}$) sterile water was aseptically added and then mixed to dissolve, according to manufacturer's instructions to obtain 50 ml of RIF samples.

Strains Preparation

Three emetic strains of *Bacillus cereus* were used in this study: B594 and B596 isolated from cereals and filed in the Nestlé culture collection and F4810/72 a reference strain from the DSMZ culture collection isolated during an outbreak investigation and also referred to as DSMZ4312 as reported in Carlin et al. (2013). Stock cultures were formed using subcultures of each strain supplemented with glycerol and stored at -80°C until used. For each strain, one tube of frozen stock culture was used to inoculate 100 ml of BHI (Sigma-Aldrich) and stored for 24 h at 30°C . Then 100 μl of this culture was put into another 10 ml of BHI and incubated for 18 h at 30°C . The subculture was then enumerated both on selective (Bacara, BioMérieux) and a non-selective (TSAYE, Sigma-Aldrich) media, diluted to a target level of 10^6 CFU/ml before applying a thermal stress during 25 s at 72°C . The plates were incubated for 24 h at 30°C . The stressed culture was also enumerated both on the selective and non-selective media to assess the stress intensity. This protocol allowed to mimic the processing conditions that influences the physiological state of naturally contaminating *B. cereus* cells.

Experimental Design

Prior to inoculation, RIF bottles were equilibrated at the targeted temperatures (9, 12, 15, 18, 22, 25°C for F4810/72 strain and 9, 12, 15, 18, and 22°C for B594 and B596 strains). Appropriate dilution of the inoculum was then added to 50 ml of RIF to reach an initial concentration of $2.5 \log$ CFU/ml. Inoculated bottles were sampled for viable counts on Bacara medium at appropriate sampling times to describe the different phases of the growth curves. Three independent replicates were performed for each experiment. For the reference strain F4810/72, additional experiments were performed in BHI following the same protocol to calculate the bias factor. All experiments were performed with pure culture.

Data Analysis

Primary and Secondary Modeling

For each temperature, each curve was fitted by the primary model of Baranyi and Roberts (1994) using the DMFit Excel

Add-in, downloadable from <http://www.combase.cc/index.php/en/locks>. As a second step, the effects of the environment, history and strain were studied and modeled on the maximum specific growth rate (μ), duration of lag phase (λ), and the natural logarithm of the maximum population density ($\log_{10} N_{max}$).

The maximum population density and the $\lambda_0 = \mu \cdot \lambda$ parameters were taken as constant, as the simplest (zero-order) model, obtained via taking the multiplicative average of their estimates from the primary model.

The model of Ratkowsky et al. (1982),

$$\sqrt{\mu} = a + bT \quad (1)$$

in the reparameterized version

$$\sqrt{\mu} = b(T - T_{min}) \quad (2)$$

was fitted to the square root of the specific growth rates to describe the effect of temperature, where a and b are constants and $T_{min} = -b/a$ is a nominal minimum growth temperature, at which the extrapolated maximum specific growth rate would be zero.

We use the above well-established model in its second form, Equation (2), so (though it leads to non-linear regression), the important T_{min} parameter and its standard error can directly be obtained. To carry out the non-linear fitting, the method of Levenberg-Marquardt (Press et al., 1986) was programmed in Visual Basic for Applications assigned to MS Excel.

We also tested the Ratkowsky model in a rearranged form, with the natural logarithm link function applied to the observed maximum specific growth rates:

$$\ln \mu = \ln b^2 + \ln(T - T_{min})^2 \quad (3)$$

Bias Factor

A measure of the deviation between observed and predicted growth, called the "bias factor" was introduced by Ross (1996). As per definition, its natural logarithm, $\ln(B_f)$ is the average value between the observed and predicted $\ln(\mu)$ values where μ denotes the maximum specific growth rate of the organism. It is of common sense to expect the conditions (here the temperature), under which the μ -values were generated, randomly distributed in the modeled region, in which case

$$\ln(B_f) = E[\ln(\mu_{obs}) - \ln(\mu_{pred})] \quad (4)$$

where E denotes the "expected value" operator. Since the μ_{pred} predictions produced by commonly used software packages are often based on experiments carried out in culture medium broth, while practical observations (μ_{obs}) refer to food, the above expectation can be translated to

$$\ln(B_f) = E[\ln(\mu_{food}) - \ln(\mu_{broth})]. \quad (5)$$

In our case, the studied food matrix is RIF; for which a bias factor can be derived via the above formula from the growth rate in broth.

RESULTS

Primary and Secondary Modeling

Examples for fitting the primary model can be seen in Figure 1.

The parameter estimates from the primary modeling are given in the Supplementary Information. Figure 2 shows all specific rate estimates for the three studied strains at the different temperatures in broth and in RIF.

The estimates for the b and T_{min} parameters, when the Ratkowsky model was fitted to the maximum specific growth rates, are shown in Table 1. The T_{min} -estimate for the strain B594 was significantly higher than the respective estimates for the other two strains.

The Ratkowsky model claims two major benefits: the linear model structure for the " $\sqrt{\mu}$ vs. temperature" relationship, and the constant variance of the measured $\sqrt{\mu}$ values, independently of the temperature. In our case, because of biological replicates

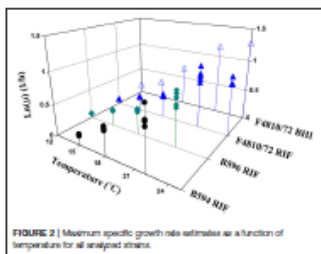
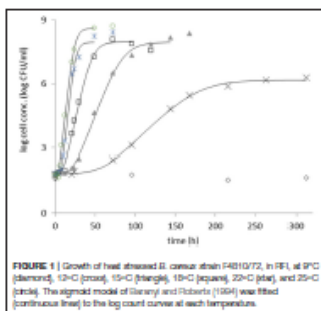


TABLE 1 | Estimated parameters and their standard errors for the square root model in RIF (3 strains) and BHI (one strain).

Strain and medium	T_{min} (°C)	b ($\mu^{-1} \sqrt{R^2 C}$)
BS94, RIF	5.43 ± 0.06	0.0643 ± 0.006
BS94, BHI	5.52 ± 0.72	0.0505 ± 0.009
F4810/72, RIF	5.40 ± 0.08	0.0510 ± 0.009
F4810/72, BHI	5.13 ± 1.12	0.0601 ± 0.006

(broth), it was possible to study the relative deviations of the specific growth rates (standard deviation divided by the mean) within the replicate curve-triplets. These showed no correlation with the temperature ($p = 0.65$), see **Figure 3**.

This suggests that the natural logarithm could also be a suitable link function for the maximum specific growth rate when modeling its dependence on the temperature. This comes from the relationships:

$$\frac{\mu_{obs} - \mu}{\mu} = \epsilon \quad (6)$$

$$\mu_{obs} = \mu(1 + \epsilon) \quad (7)$$

$$\ln(\mu_{obs}) = \ln(\mu) + \ln(1 + \epsilon) \approx \ln(\mu) + \epsilon \quad (8)$$

where the approximation is accurate at least for one digit if the relative error ϵ is less than 0.3. For ϵ -values over 0.3, the approximation in Equation (8) would have worse than one digit accuracy. From this, it also follows that, since our average relative errors are less than 10%, the standard error of fit of the secondary model for $\ln(\mu)$ will be ca 0.1 (or possibly higher, if the secondary model describes the "a vs. T" relationship inaccurately).

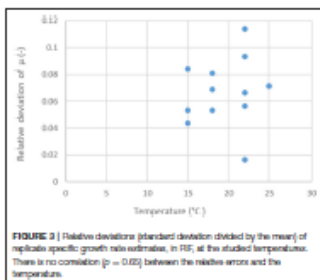
It can be readily seen that if the ϵ random error in the Equations (6–8) is constant, independently of the temperature, then the same cannot hold for the square-root model and vice versa. Revisiting Equation (7), one can obtain, by first order approximation:

$$\sqrt{\mu_{obs}} = \sqrt{\mu} \cdot \sqrt{1 + \epsilon} \approx \sqrt{\mu} + \frac{\sqrt{\mu}}{2} \cdot \epsilon \quad (9)$$

This means that, if the natural logarithm transformation makes the deviation of the observed specific rates constant, then the deviation generated by the square-root function should tend to be smaller with temperature decreasing to T_{min} . That is, the absolute residuals should show a decreasing trend with the temperature (and, therefore, with the μ -values) - as indeed we will see it later. On the other hand, if the square-root was the correct transformation to stabilize the variance still the natural logarithm of the μ -values is regressed in the secondary model, then the residuals should show increasing trend as the temperature decreases to T_{min} :

$$\sqrt{\mu_{obs}} = \sqrt{\mu} + \delta \quad (10)$$

$$\ln \mu_{obs} \approx \ln \mu + \ln \left(1 + \frac{\delta}{\sqrt{\mu}} \right)^2 \quad (11)$$

**FIGURE 3** | Relative deviations (standard deviation divided by the mean) of replicate specific growth rate substrates, in RIF, at the studied temperatures. There is no correlation ($p = 0.65$) between the relative errors and the temperature.

Bias Factor

The maximum specific growth rate of the strain F4810/72 was measured in both RIF and BHI, providing a good opportunity to investigate the bias factor. Notice that, if this is independent of the temperature, then the secondary model for $\ln(\mu)$ for the two media (Equation 3) differ only by an additive constant (Equation 5). This is equivalent to the assumption that the T_{min} parameter is the same for the BHI and RIF. Our investigations showed that the T_{min} of this same strain in BHI was 5.13 ± 1.12 which is not significantly different ($p = 0.35$) from the T_{min} -value in RIF 5.40 ± 0.88 (**Table 1**).

Then we use the formulae

$$\sqrt{\mu_{broth}} = b_{broth} (T - T_{min}) \quad (12)$$

$$\sqrt{\mu_{food}} = b_{food} (T - T_{min}) \quad (13)$$

from which the ratio $B_f = (b_{food}/b_{broth})^2$ is constant, so the secondary models for $\ln(\mu)$, for broth and food, should be parallel and differ from each other by the

$$\ln(B_f) = 2 \ln(b_{food}/b_{broth}) \quad (14)$$

constant additive term. The opposite direction of this conclusion can be proven similarly, therefore, the assumption that T_{min} is the same for culture medium and food is equivalent to the one that the ratio between maximum specific growth rates in culture medium broth and food is constant, independently of the temperature. In our situation, we showed, by F -test, that the strain F4810/72 has the same $T_{min} = 5.26$ value for BHI and RIF ($p = 0.35$). Therefore, their model can be written as

$$\sqrt{\mu_{BHI}} = 0.050 (T - 5.26)$$

$$\sqrt{\mu_{RIF}} = 0.061 (T - 5.26)$$

Substituting the coefficients above in Equation (14), it can be calculated that, for this strain, the ratio between the maximum specific growth rates in RIF and culture medium broth is $B_f = (0.050/0.061)^2 = 0.67$. That is, this strain grows at one third slower in RIF compared to BH1.

Figure 4 demonstrates well the equivalence between the two assumptions: common T_{min} value for the square-root and parallel models for the logarithm link functions. The model (3) fitted to the $\ln(\mu)$ values of the strain F4810/72 in BH1 and RIF are parallel because they have similar T_{min} estimates. As follows from Equation (9), the deviation from the parallel behavior would be apparent at low temperatures only.

The shown equivalence is independent of the question whether the square-root or the logarithm transformation stabilizes the variance of the μ -values. According to the Equations (7) and (9), both cannot be valid at the same time. Comparing the absolute residuals for both the square-root and logarithm link function, on all the data, the Figure 5 emerges.

The residuals with the square-root link function show a decreasing trend as the temperature decreases to T_{min} ($p = 0.004$), while in the case of logarithm link function, it does not show correlation with the temperature ($p = 0.37$). Therefore, based on our data, while the Ratkowsky model accurately describes how the maximum specific growth rate depends on temperature, the logarithm link function is more suitable to be applied to the observed maximum specific growth rates when regressing them against temperature. The difficulty is that this difference between the two link functions can be detected at low temperatures only, where it is not easy to keep the environment constant for the required long time to reach the stationary phase, therefore, the environmental effects (e.g., pH decrease in the medium) rather than biological ones (linked to strain variability for example) can dominate the variability of the observed maximum specific growth rates.

DISCUSSION

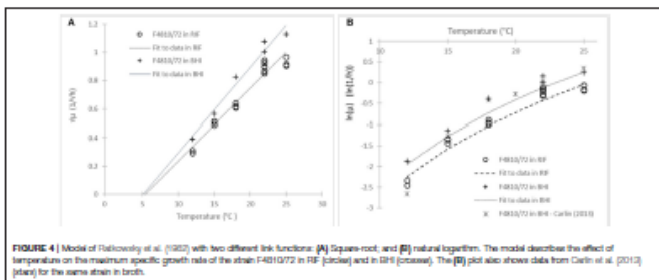
The paper of Carlini et al. (2013) gives an opportunity to compare the kinetic parameters of the reference strain F4810/72 in broth as shown in Figure 4. Fitting the square-root model to the 12–25°C data for the same strain in that paper, the estimated parameters were not different at 5% significance level ($p = 0.12$).

In the same way, we can validate our rate estimates by the Combase Predictor available from <http://www.combase.cc>. In Figure 6, the square root values of our specific growth rates can be compared with results from Combase Predictor, in broth and milk, assuming a bias factor of $B_f = 0.67$ for the food scenario.

The validation plot in Figure 6 is a convincing proof of the diversity of the kinetic behavior of *B. cereus* strains. The Combase Predictor is based on growth curves generated by a cocktail of six strains (Sutherland et al., 1996). A plausible explanation for the seemingly unexpected non-linear behavior of the $\sqrt{\mu}$ predictions is that different strains were the dominant ones at different temperatures, while the same parameter of a pure culture show a constant linear pattern with temperature.

For quantitative validation, we made an extensive use of the Bias and Accuracy factors of Roos (1996). We point out here that while acknowledging the useful applicability of these indicators, their definition needs some refinement, in agreement with Baranyi et al. (1999). When the average of the $\ln(\mu_{max})$

$\ln(\mu_{max})$ values is taken, it is implicitly assumed that the probability distribution of this difference is independent of the temperature and possibly other environmental factors (Gill and Phillips, 1985; Buchanan and Baig, 1997; Neumeier et al., 1997; Mellefont et al., 2003). The constant bias-factor is a reasonable assumption in case of the temperature, with the rationale that all affecting biochemical reactions speed up or slow down when temperature changes. It is less obvious with other environmental factors, like pH or water activity; nonetheless the assumption provides a convenient approximation that is easy to build in predictive packages.



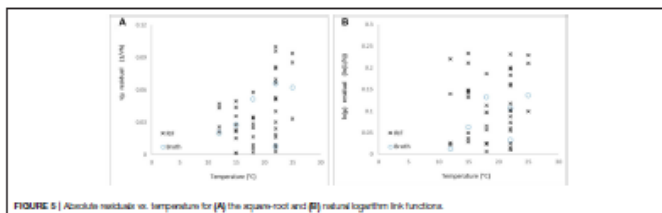


FIGURE 5 | Absolute residuals vs. temperature for (A) the square root and (B) natural logarithm link functions.

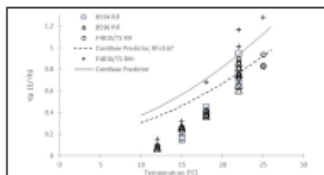


FIGURE 6 | Square root of maximum specific growth rate of *S. cerevisiae* vs. temperature from different sources. Our EG24, EG26, and F4810/72 strains in RIF (open diamonds, circle and triangle, resp.). Our data for F4810/72 in broth (blue square) and CorniBase Predictor results (continuous line). The dashed line below the CorniBase Predictor curve is the prediction obtained by using the $\theta = 0.67$ bias factor.

The assumption of the temperature-independent bias factor is equivalent to the existence of a minimum growth temperature that is the same for the model and for the food matrix on which the model is tested. Indeed, this latter condition has been assumed by quite a few authors (Miles et al., 1997; Carlin et al., 2013; Aryani et al., 2015, 2016), and was observed in our situation, too, when comparing the temperature-dependent maximum specific growth rates in RIF and culture medium. The CorniBase database (<http://www.combase.cc>) also provides a good opportunity to check how much the temperature-independence of the bias factor is tenable.

In conclusion, we agree with many authors (Bernaerts et al., 2000; Ross et al., 2003; Powell et al., 2015; Den Bostan et al., 2017) that, at sub-optimal temperatures, the Ratkowsky model is a good

representation of the effect of temperature on the maximum specific growth rate measured in a pure culture, in both laboratory medium and food. However, the constant variance assumption does not necessarily hold at low temperatures. Besides, we established that the minimum growth temperature can be taken as the same T_{min} value for culture medium and food, therefore, the bias factor is, indeed, independent of the temperature. In mixed cultures, however none of the above holds, and more complex developments (data and mathematical considerations) are needed for an accurate model; see Baranyi et al. (2017), which is, in a sense, a continuation of this paper.

AUTHOR CONTRIBUTIONS

NBds: experiments and writing up. JB: Experimental design, data analysis and writing up. BAMC: Consultation. ME: conception, experimental design and writing up.

ACKNOWLEDGMENTS

The experiments were carried out at the Institute of Food Research, Norwich, UK. The authors wish to express their thanks to Suste George and Amanda Demter for their help in the laboratory. NBds thankfully acknowledges the scholarship from the Brazilian Coordination for the Improvement of Higher Education Personnel (CAPES).

SUPPLEMENTARY MATERIAL

The Supplementary Material for this article can be found online at: <http://journal.frontiersin.org/article/10.3389/fmicb.2017.01799/full#supplementary-material>

REFERENCES

Alkayy, M., and Sallerbund, A. D. (2006). Bacterial urease is common in the environment but creck kists producing isolates are rare. *J. Appl. Microbiol.* 100, 7–14. doi: 10.1111/j.1365-2672.2005.02764.x

Aryani, D. C., Den Bostan, H. M. W., Hantzer, W. C., and Zwickerling, M. H. (2015). Quantifying strain variability in modeling growth of *Listeria monocytogenes*. *Int. J. Food Microbiol.* 208, 19–29. doi: 10.1016/j.ijfoodmicro.2015.05.006

Aryani, D. C., Zwickerling, M. H., and Den Bostan, H. M. W. (2016). The effect of different matrices on the growth kinetics and heat resistance of

- Lactaria monocorymbes* and *Lactofactus plantarum*. *Int. J. Food Microbiol.* 236, 326–337. doi: 10.1016/j.ijfoodmicro.2016.09.012
- Hanayci, J., and Roberts, T. A. (1994). A dynamic approach to predicting bacterial growth in food. *Int. J. Food Microbiol.* 23, 277–286. doi: 10.1016/0168-1605(94)90157-0
- Hanayci, J., Dias da Silva, N., and Elouaz, M. (2017). Relationships between the parameters of temperature-dependent growth models for *Bacillus cereus* strains. *Food Microbiol.* 6:1090. doi: 10.3389/food.2017.01090
- Hanayci, J., Piu, C., and Ross, T. (1999). Validating and comparing predictive models. *Int. J. Food Microbiol.* 48, 159–166. doi: 10.1016/S0168-1605(99)00035-5
- Hernandez, K., Vercyck, K. J., and Van Impe, J. F. (2005). On the design of optimal dynamic experiments for parameter estimation of a Ratkowsky-type growth kinetics at suboptimal temperatures. *Int. J. Food Microbiol.* 54, 27–38. doi: 10.1016/S0168-1605(99)01460-3
- Huchman, R. L., and Ingh, L. K. (1997). Effect of water activity and humectant identity on the growth kinetics of *Escherichia coli* O157:H7. *Food Microbiol.* 14, 413–425. doi: 10.1006/food.1997.0101
- Carlin, F., Abagrac, C., Bida, A., Galandriestre, M. H., Couvert, O., and Nguyen-The, C. (2012). Variation of cardinal growth parameters and growth limits according to phylogenetic affiliation in the *Bacillus cereus* Group: consequences for risk assessment. *Food Microbiol.* 33, 69–76. doi: 10.1016/j.fm.2012.08.014
- Czappea, S., Rajkovic, A., Heyndrickx, M., Tella, V., Van De Wiele, T., Ross, T., et al. (2011). Regulation of toxin production by *Bacillus cereus* and its food safety implications. *Crit. Rev. Microbiol.* 37, 189–213. doi: 10.1081/1040841X.2011.598832
- Den Besten, H. M. W., Arysni, D. C., Metelaar, K. L., and Zwietering, M. H. (2017). Microbial variability in growth and heat resistance of a pathogen and a spoiler: all variables are equal but some are more equal than others. *Int. J. Food Microbiol.* 240, 24–31. doi: 10.1016/j.ijfoodmicro.2016.04.025
- ISPA (2005). Opinion of the scientific panel on biological hazards on *Bacillus cereus* and other *Bacillus* spp. in foodstuffs. *EFSA J.* 175, 1–48. doi: 10.2835/efsa.2005.175
- El-Anabi, T. F., and Corliss, M. W. (2013). “*Bacillus cereus*,” in *Foodborne Pathogens and Zoonoses*, 4th Edn, eds G. J. Morris, and M. Peller (London: Academic Press), 401–407.
- Gill, C. O., and Phillips, D. M. (1985). The effect of media composition on the relationship between temperature and growth rate of *Escherichia coli*. *Food Microbiol.* 2, 285–290. doi: 10.1016/0740-0020(85)90010-5
- Kottranta, A., Loukkanen, K., and Hapanen, M. (2000). Epidemiology and pathogenesis of *Bacillus cereus* infections. *Microb. Drug Resist.* 2, 189–196. doi: 10.1016/S1526-679X(00)00269-0
- Mansley, C. M., McMeekin, K., Moore, S. C., Pagan, N., and Pei, Z. M. (2014). Prevalence and characterization of foodborne pathogens from Australian dairy farm environments. *J. Dairy Sci.* 97, 7402–7412. doi: 10.3168/jds.2014-8735
- Melchior, L. A., McMeekin, T. A., and Ross, T. (2003). Performance evaluation of a model describing the effects of temperature, water activity, pH and lactic acid concentration on the growth of *Escherichia coli*. *Int. J. Food Microbiol.* 82, 45–58. doi: 10.1016/S0168-1605(02)00252-2
- Miles, D. W., Ross, T., Olley, J., and McMeekin, T. A. (1997). Development and evaluation of a predictive model for the effect of temperature and water activity on the growth rate of *Vibrio parahaemolyticus*. *Int. J. Food Microbiol.* 38, 133–142. doi: 10.1016/S0168-1605(97)00100-1
- Nunayen, K., Ross, T., Thomann, G., and McMeekin, T. A. (1997). Validation of a model describing the effects of temperature and water activity on the growth of psychrotrophic pseudomonads. *Int. J. Food Microbiol.* 36, 55–63. doi: 10.1016/S0168-1605(97)00090-1
- Prowel, S. M., Ratkowsky, D. A., and Tamplin, M. L. (2015). Predictive model for the growth of spoilage bacteria on modified atmosphere packaged Atlantic salmon produced in Australia. *Food Microbiol.* 47, 111–115. doi: 10.1016/j.fm.2014.12.001
- Preso, W. H., Toulouky, S. A., Vetterling, W. T., and Flannery, B. P. (1986). *Numerical Recipes: The Art of Scientific Computing*. New York, NY: Cambridge University Press.
- Ratkowsky, D., Olley, J., McMeekin, T. A., and Ball, A. (1982). Relationship between temperature and growth rate of bacterial cultures. *J. Bacteriol.* 149, 1–5.
- Ross, T. (1996). Indices for performance evaluation of predictive models in food microbiology. *J. Appl. Microbiol.* 81, 501–508. doi: 10.1111/j.1365-2672.1996.tb01946.x
- Ross, T., Ratkowsky, D. A., Melchior, L. A., and McMeekin, T. A. (2003). Modelling the effects of temperature, water activity, pH and lactic acid concentration on the growth rate of *Escherichia coli*. *Int. J. Food Microbiol.* 82, 33–43. doi: 10.1016/S0168-1605(02)00252-0
- Sutherland, J. P., Ahme, A., and Beaumont, A. L. (1996). Preparation and validation of a growth model for *Bacillus cereus*: the effects of temperature, pH, sodium chloride and carbon dioxide. *Int. J. Food Microbiol.* 36, 319–372. doi: 10.1016/0168-1605(96)00962-2

Conflict of Interest Statement: The authors declare that the research was conducted in the absence of any commercial or financial relationships that could be construed as a potential conflict of interest.

Copyright © 2017 Dias da Silva, Hanayci, Corliss and Elouaz. This is an open-access article distributed under the terms of the Creative Commons Attribution License (CC BY). The use, distribution or reproduction in other forums is permitted, provided the original author(s) or licensor are credited and that the original publication in this journal is cited, in accordance with accepted academic practice. No use, distribution or reproduction is permitted which does not comply with these terms.